Université de Montréal

Étude du mécanisme d'augmentation de la relâche virale par la protéine Vpu du VIH-1

par
Mathieu Dubé

Département de microbiologie et immunologie
Faculté de Médecine

Thèse présentée à la Faculté des Études Supérieures
En vue de l'obtention du grade de Philosophiae (Ph.D.)
En Virologie et Immunologie

Juin 2011

Université de Montréal
Faculté des Études Supérieures

Cette thèse intitulée :

Étude du mécanisme d'augmentation de la relâche virale par la protéine Vpu du VIH-1

Présentée par :
Mathieu Dubé

A été évaluée par un jury composé des personnes suivantes :

Petronela Ancuta, Ph.D.
Président-rapporteur

Éric A. Cohen, Ph.D.
Directeur de recherche

Michel Desjardins, Ph.D.
Membre du jury

Markus Thali, Ph.D.
Examinateur externe

Jacques Archambault, Ph.D.
Représentant du doyen

SOMMAIRE

Les différentes protéines accessoires du VIH-1, l'agent étiologique du SIDA, optimisent la réplication et la propagation du virus *in vivo*. Parmi ces dernières figure Vpu, l'antagoniste du facteur de restriction nommé Tetherin qui prévient la relâche des particules virales à partir de la surface de cellules infectées. En diminuant son expression de surface, Vpu prévient l'incorporation de ce facteur de restriction dans la particule virale en formation et conséquemment, empêche la formation d'une ancre protéique reliant le virus mature à la membrane plasmique de la cellule infectée. La mécanistique sous-jacente n'était cependant pas connue.

Cette présente thèse relate nos travaux exécutés afin d'élucider la dynamique des mécanismes cellulaires responsables de cet antagonisme. Une approche de mutagénèse dirigée a d'abord permis d'identifier deux régions contenant des déterminants de la localisation de Vpu dans le réseau *trans*-Golgi (RTG), puis de démontrer la relation existante entre cette distribution et l'augmentation de la relâche des particules virales. Des expériences subséquentes de marquage métabolique suivi d'une chasse exécutées dans des systèmes cellulaires où Tetherin est exprimée de façon endogène ont suggéré le caractère dispensable de l'induction par Vpu de la dégradation du facteur de restriction lors de son antagonisme. En revanche, une approche de réexpression de Tetherin conduite en cytométrie en flux, confirmée en microscopie confocale, a mis en évidence une séquestration de Tetherin dans le RTG en présence de Vpu, phénomène qui s'est avéré nécessiter l'interaction entre les deux protéines. L'usage d'un système d'expression de Vpu inductible conjugué à des techniques de cytométrie en flux nous a permis d'apprécier l'effet majeur de Vpu sur la Tetherin néo-synthétisée et plus mineur sur la Tetherin de surface. En présence de Vpu, la séquestration intracellulaire de la Tetherin néo-synthétisée et la légère accélération de l'internalisation naturelle de celle en surface se sont avérées suffisantes à la réduction de son expression globale à la membrane plasmique et ce, à temps pour l'initiation du processus de relâche virale.

À la lumière de nos résultats, nous proposons un modèle où la séquestration de la Tetherin néo-synthétisée dans le RTG préviendrait le réapprovisionnement de Tetherin en surface qui, combinée avec l'internalisation naturelle de Tetherin à partir de la membrane plasmique, imposerait l'établissement d'un nouvel équilibre de Tetherin incompatible avec une restriction de la relâche des particules virales. Cette thèse nous a donc permis d'identifier un processus par lequel Vpu augmente la sécrétion de virus matures et établit une base mécanistique nécessaire à la compréhension de la contribution de Vpu à la propagation et à la pathogénèse du virus, ce qui pourrait mener à l'élaboration d'une stratégie visant à contrer l'effet de cette protéine virale.

Mots clés : Virus, VIH-1, protéines accessoires, Vpu, Tetherin, relâche des particules virales, restriction, trafic et séquestration.

ABSTRACT

All accessory proteins of HIV-1, the ethiologic agent of AIDS, are thought to optimize viral replication and propagation *in vivo*. Among them, Vpu antagonizes Tetherin, a cellular factor that inhibits viral particle release. Downregulation of cell-surface Tetherin by Vpu is believed to prevent incorporation of this restriction factor into nascent viral particles, which would impede the formation of a Tetherin-derived protein anchor that bridges the virus to the plasma membrane of the infected cell. This thesis presents our studies on cellular mechanisms governing Tetherin antagonism by Vpu. A directed mutagenesis approach first identified two regions encompassing determinants of the localization of Vpu in the *trans*-Golgi network, and it correlated this intracellular distribution with enhanced release viral particle. Pulse-chase experiments in cellular systems wherein Tetherin was endogenously expressed showed that Vpu-induced Tetherin degradation is dispensable for restriction. In contrast, both a flow cytometry-based Tetherin re-expression assay and confocal microscopy analyses demonstrated that Vpu-mediated sequestration of Tetherin in the *trans*-Golgi network, a phenomenon that appeared to be triggered by the transmembrane association of the two proteins, was necessary for release inhibition. Vpu inducible expression in flow cytometry-based experiments provided evidence for an optimal antagonism of Tetherin at 6h after Vpu expression, following the interruption of Tetherin re-supply and a ~~to the~~ modest acceleration of the natural clearance of surface-localized Tetherin. Our work supports a model in which Tetherin sequestration in the *trans*-Golgi network prevents its re-supply, which, combined with its clearance from the surface, imposes a new equilibrium at the plasma membrane that is incompatible with the restriction of viral particle release. Overall, this thesis sheds light on the processes by which Vpu enhances the secretion of mature viruses and it establishes a mechanistic basis that could serve as starting point for the development of strategies aimed at interfering with Tetherin functions.

Keywords : Virus, HIV-1, accessory protein, Vpu, Tetherin, viral particle release, restriction, traffic and sequestration.

.

TABLE DES MATIÈRES

ABBRÉVIATIONS

ADN	Acide désoxyribonucléique
AP-1	Protéine adaptatrice-1
AP-2	Protéine adaptatrice-2
APOBEC3F	«Apolipoprotein B mRNA-editing catalytic polypeptide 3F» Polypeptide 3F d'apolipoprotéine B catalytique à l'activité d'édition de l'ARNm
APOBEC3G	«Apolipoprotein B mRNA-editing catalytic polypeptide 3G» Polypeptide 3G d'apolipoprotéine B catalytique à l'activité d'édition de l'ARNm
ARN	Acide ribonucléique
ARNi	ARN d'interférence
ARNm	ARN messager
ATF-4	Facteur de transcription 4
ATR	(«Ataxia telangiectasia-mutated and Rad3-related» Relié à Rad3 et à l'ataxia telangiectasia muté
Brd4	Protéine contenant un bromodomaine 4
BST-2	«Bone marrow stromal antigen-2» Antigène-2 de la moëlle épinière stromale
β-TrCP	«β-transducin repeat-containing protein» Protéine contenant des répétitions de la β-transducin
CA	Capside
CD	«Cluster of differentiation» Cluster de différenciation
CPD	Carboxypeptidase D
Cdc25A	Cycle de division cellulaire 25A
CDK9	«Cyclin-dependent kinase 9» Kinase dépendante d'une cyclin 9
CPZ	Chimpanzé
CMH-I	Complexe majeur d'histocompatibilité de type 1
CMH-II	Complexe majeur d'histocompatibilité de type 2
CMV	Corps multivésiculaires
CPI	Complexe de pré-intégration
CTI	Complexe de transcription inverse
CypA	Cyclophilin A
DDB1	«DNA damage-binding protein 1» Protéine 1 liant les dommages à l'ADN
EGFR	«Epidermal growth factor receptor» Récepteur du facteur de croissance épidermique
Emi1	Inhibiteur mitotique précoce 1
Env	Protéine de l'enveloppe
EPS15	Substrat-15 du récepteur de l'hormone de croissance épidermale

ERR	Élément de réponse à Rev
ESCRT-I	«Endosomal sorting complex I required for transport» Complexe de triage endosomal I requis pour le transport
ESCRT-III	«Endosomal sorting complex III required for transport» Complexe de triage endosomal III requis pour le transport
Gag	«Group specific antigen» Antigène spécifique au groupe
gp41	Glycoprotéine de 41kDa
gp120	Glycoprotéine de 120kDa
gp160	Glycoprotéine de 160kDa
HAART	«Highly active antiretroviral therapy» Thérapie antirétrovirale très active
HLA	Antigène de leucocyte humain
HTLV	Virus T-lymphotropique humain
ICAM	Molécule d'adhésion intercellulaire
ILT-7	«Immunoglobulin-like transcript-7» Transcrit 7 similaire aux immunoglobulines
Ii	Chaîne invariante
IN	Intégrase
IFN	Interféron
KSHV	Virus de l'herpès associé au sarcome de Kaposi
LDLR	«Low density lipoprotein receptor» Récepteur de lipoprotéine de faible densité
LEDGF/p75	«Lens epithelium-derived growth factor/75 kDa protein» Facteur de croissance dérivé du cristallin /protéine de 75kDa
LTR	«Long terminal repeats» Longues répétitions terminales
MA	Matrice
MAC	Macaque
MARCH	Protéines associées aux membranes RING-CH
MICA	Polypeptide relié à la séquence A du CMH de classe 1
MLV	«Murine leukemia virus» Virus de leucémie murine
Nef	Facteur négatif
NC	Nucléocapside
NF-κB	«Nuclear factor kappa-light chain enhancer of activated B cells» or «Nuclear factor kappa B» Facteur nucléaire kappa B
NK	«Natural killer cells» Cellules tueuses naturelles
NKT	«Natural killer T-cells» Cellules T tueuses naturelles
NRTI	«Nucleoside reverse transcriptase inhibitor» Inhibiteur de la transcription inverse analogue aux nucléosides
NNRTI	«Non-nucleoside reverse transcriptase inhibitor»

	Inhibiteur de la transcription inverse non-analogue aux nucléosides
NTB-A	Antigène des cellules NK,T et B
ONUSIDA	Programme commun des Nations Unis sur le SIDA
PAM	Protéine associée à Myc
PC6B	Proprotéine convertase 6B
PI	«Protease inhibitor» Inhibiteur de protéase
PI(4,5)P2	Phosphatidylinositol-(4,5)-bisphosphate
Pol	Polymérase virale
$Pr55^{Gag}$	Précurseur de Gag de 55 kDa
Pro	Protéase virale
P-TEFb	Facteur B de l'élongation de la transcription positive
Rab	Protéine reliée à Ras dans le cerveau
RE	Réticulum endoplasmique
Rev	Régulateur de l'expression des gènes viraux
RING	«Really interesting new gene» Nouveau gène très intéressant
RTG	Réseau *trans*-Golgi
SIDA	Syndrome de l'immunodéficience humaine acquise
SMM	Macaque mangabey
SP1	«Specificity protein-1» Protéine de spécificité-1
TAR	Élément de réponse à Tat
TAN	Singe tantalus
Tat	Transactivateur transriptionnel
TI	Transcriptase inverse
TIP47	«Tail-interacting protein of 47 kDA» Protéine de 47 kDA interagissant avec une queue
TRIM5α	«TRIpartite interaction motif 5 alpha» Motif d'interaction tripartite 5 alpha
VAMP4	Protéine transmembranaire associée aux vésicules-4
VIH-1	Virus de l'immunodéficience humaine de type 1
VIH-2	Virus de l'immunodéficience humaine de type 2
VIS	Virus de l'immunodéficience simienne
VIScpz	Virus de l'immunodéficience simienne du chimpanzé
VISmac	Virus de l'immunodéficience simienne du macaque
VIStan	Virus de l'immunodéficience simienne du singe tantalus
VISsmm	Virus de l'immunodéficience simienne du macaque mangabey
VISH	Virus de l'immunodéficience simienne humaine
Vif	«Viral infectivity factor» Facteur viral d'infectivité
VMAT1	Transporteur vésiculaire de monoamine-1
VMAT2	Transporteur vésiculaire de monoamine-2
Vpr	Protéine virale R
VprBP	Protéine liant Vpr

Vpu	Protéine virale U
VSV	Virus de la stomatite vésiculaire

TABLE DES FIGURES

À ma mère, qui en regardant les étoiles, a reconnu ma voie,

À mon père, qui ne m'en a jamais éloigné,

À mes sœurs, qui ont semé en moi le goût de débattre,

Et à mon amour, qui m'a donné un deuxième souffle.

REMERCIEMENTS

J'aurai finalement passé sept années au laboratoire de rétrovirologie humaine. J'y ai fait mes premières armes en recherche, j'y ai grandi et j'y ai vieilli. Mes souvenirs de ma vie de jeune adulte seront étroitement reliés à ce que j'y ai vécu. Permettez-moi de remercier les acteurs de ma réussite ayant brillés durant ce chapitre déterminant de ma vie.

J'aimerais d'abord remercier mon directeur de laboratoire, Dr. Éric Cohen. Je me souviens encore de notre première rencontre, à l'aurore de mon stage d'été. J'étais fort intimidé; avec du recul je ne suis pas sûr si je me serais moi-même donné une bonne impression. Néanmoins, Éric m'a pris sous sa tutelle et a toujours cru en moi. Merci de votre soutien! Merci aussi aux organismes financiers tels que les Instituts de recherche en santé du Canada (IRSC), l'Institut de recherche clinique de Montréal (IRCM) et l'université de Montréal pour leur soutient financier tout au long de mon doctorat.

Merci de tout cœur à Julie Binette. Sa patience, son dévouement et surtout son amitié me furent essentiels. Merci à Jean-Philippe Belzile, dont la gentillesse et le talent ont été une grande source d'inspiration. Que de problèmes insolubles ont trouvé leurs réponses grâce à son savoir encyclopédique! Merci, Catherine Paquay pour son sourire et son enthousiasme. Ce fût une joie et un honneur de guider ses premiers pas dans notre domaine!

Merci à Bibhuti Bhusan Roy, Pierre Guiot-Guillain, Grace Leung et Antoine Chiasson pour leur remarquable travail. Bien sûr, un gros merci à Johanne Mercier qui m'a si souvent épaulé et sauvé (au figuré et au sens propre). Merci de m'avoir enduré durant les moments difficiles!

Merci à Jonathan Richard, avec qui il fût toujours fort agréable de rire et pleurer face à l'hasardeuse destinée des Canadiens. Sa camaraderie ne sera jamais oubliée. J'ai toujours apprécié son esprit vif et ses prédispositions au cabotinage! Merci à Nicole, qui a été d'une grande aide durant toutes ces années! Mes remerciements à Francine Gérard

qui, avec Catherine et Jonathan, m'a généreusement fait part de son opinion sur ma thèse. Et merci à tous mes ex- ou futurs ex-collègues qui ont croisé mon chemin; les Mélanie Welman, Geneviève St-Onge, Philippe Courtemanche-Asselin, Rachel Bourgeois, Andrès Finzi, Nathalye Belzile, Mariana Bego, Tram Pham, Levon Abrahamyan, Amélie Fradette-Turcotte et j'en passe. Merci à l'IRCM et aux IRSC qui m'ont économiquement supporté durant ces dernières années.

J'ai beaucoup investi dans mon doctorat ces dernières années. Le seul regret que j'entretiens, c'est de l'avoir parfois fait au détriment de ma famille. Néanmoins, mes parents et mes sœurs ont été le ciment ayant permis de bâtir ma carrière scientifique. Que de fois ils m'ont revigoré, peut-être même sans le savoir. J'ai tiré beaucoup de mon énergie grâce à leur indéfectible support. Je remercie mon père Claude; grâce à lui, j'ai appris la vigueur au travail et développé mon esprit logique. Je remercie ma mère Marie-France; grâce à qui j'ai développé ma volubilité (oui oui, Marie-France, c'est grâce à toi!) et ma curiosité. Merci à Martine d'avoir été mon modèle de débrouillardise et d'entrepreneurship. Et merci à Amélie, qui a toujours fait preuve d'une salutaire compréhension à ma réalité, parfois difficile. Son propre parcours m'a souvent inspiré.

Il me reste une personne importante à remercier. Cette dernière détient les clés de mon cœur, de mon âme et de mon avenir. Merci Geneviève d'avoir partagé ma vie malgré le dévouement que j'ai porté à mon doctorat. Tu m'as fourni l'énergie nécessaire à la complétion de mes études. Merci de m'attendre patiemment à New York … Maintenant, je puis te rejoindre.

INTRODUCTION

1. Incidence du SIDA

Le syndrome de l'immunodéficience humaine acquise (SIDA) est une maladie chronique caractérisée par une lente dégénérescence du système immunitaire dont l'agent étiologique est le virus de l'immunodéficience humaine (VIH). Plus de 33 millions d'individus seraient actuellement infectés par ce virus dans le monde selon le programme commun des Nations Unis sur le SIDA (ONUSIDA) (247). La prépondérance de ce virus dans la population n'est pas homogène. Un premier degré de diversité est imputable au passage chez l'homme de deux souches virales non-apparentées. Ainsi, le VIH de type 1 (VIH-1), principal responsable de l'épidémie planétaire, aurait pour précurseur le virus de l'immunodéficience simienne (VIS) du chimpanzé (cpz) alors que le VIH-2 serait plutôt une adaptation d'une souche de VIS de macaque mangabey (smm) (128). Quatre transferts inter-espèces indépendant auraient mené à l'émergence chez le VIH-1 du groupe M, largement répandu, et des groupes N, O et P, beaucoup plus rares (57, 128). En raison de l'importante dérive génétique du virus, le groupe M peut même être sous-divisé en plusieurs sous-types (A-J,K) dont la distribution dans la population varie géographiquement (247).

L'infection de certaines cellules du système immunitaire, principalement les macrophages et les lymphocytes T exprimant le cluster de différenciation-4 (CD4) mène à une réplication rapide du virus et à une déplétion modérée des lymphocytes T CD4 durant les premières semaines. Cette phase aigüe est suivie d'un rétablissement partiel du nombre de lymphocytes T CD4 et d'une diminution marquée de la charge virale (233). La persistance du virus causée principalement par l'infection de cellules réservoir à longue vie explique le lent déclin des lymphocytes T CD4 s'échelonnant potentiellement sur plusieurs années (phase chronique). Il s'ensuit la phase SIDA où le faible niveau des lymphocytes T CD4 ne permet plus de contrôler les pathogènes opportunistes, menant éventuellement à la mort de l'individu. De nos jours, la thérapie antirétrovirale très active(HAART), communément appellée trithérapie, permet d'augmenter considérablement l'espérance de vie des patients infectés. ONUSIDA

rapportait en 2010 un recul d'environ 14% de la mortalité due à la maladie par rapport à 2004 (247). Les efforts déployés à la prévention ont aussi permis de réduire de près de 19% le nombre de nouvelles infections en comparaison de 1999. Malgré ces signes encourageants, plus de gens vivent infectés par le VIH-1 en 2009 qu'une décennie auparavant, démontrant la limite des présentes approches thérapeutiques ou prophylactiques. Le besoin de développer de nouvelles stratégies visant l'éradication du virus chez le patient explique donc la poursuite de la recherche fondamentale sur le virus.

2. Nature du virus

Le VIH-1 est un membre du genre *lentiviridae* de la famille des *retroviridae*. Il s'agit d'un virus pouvant atteindre 80-120 nm enveloppé d'une bicouche lipidique (23). Ce virus cible les cellules du système immunitaire exprimant le récepteur de surface CD4 et l'un, l'autre ou les deux corécepteurs CCR5 et CXCR4. Les lymphocytes T CD4+ naïfs, activés ou mémoires ainsi que les macrophages représentent les principaux types cellulaires susceptibles à l'infection productive par le VIH-1 (résumé dans (89, 111)). L'infection des lymphocytes Th17, des cellules de Langerhans, des macrophages du cerveau et des cellules microgliales a aussi été démontrée (4, 82, 90). Quoique les cellules dendritiques soient plutôt associées à un modèle de transfert passif (cheval de Troie, résumé dans (112)), certaines évidences suggèrent qu'elles pourraient aussi être productivement infectées (13).

Structurellement, ce virus est composé d'une matrice hexagonale sous-jacente à la membrane virale, de trimères formant le récepteur viral et d'une capside conique (Figure 1A). La capside virale protège le génome viral d'environ 10 kilobases composé de deux brins d'acide ribonucléique (ARN) monocaténaires. Le génome du virus code pour neuf gènes (Figure 1B) et plusieurs ARN régulateurs non codants à partir de ses trois cadres de lecture distincts (14, 186). Comme tout rétrovirus, le VIH-1 possède les gènes *gag* (« group-specific antigen »), *env* (protéine de l'enveloppe; le récepteur) et *pol* (polymérase) ainsi que de longues répétitions terminales (LTR) homologues non-codantes en 5' et en 3' flanquant les régions codantes. Chacun de ces gènes code pour

une poly-protéine qui, suite à des processus de maturation et de clivage, produit les protéines essentielles au cycle viral. La maturation du précurseur Gag ($Pr55^{Gag}$) produit les protéines structurelles de la

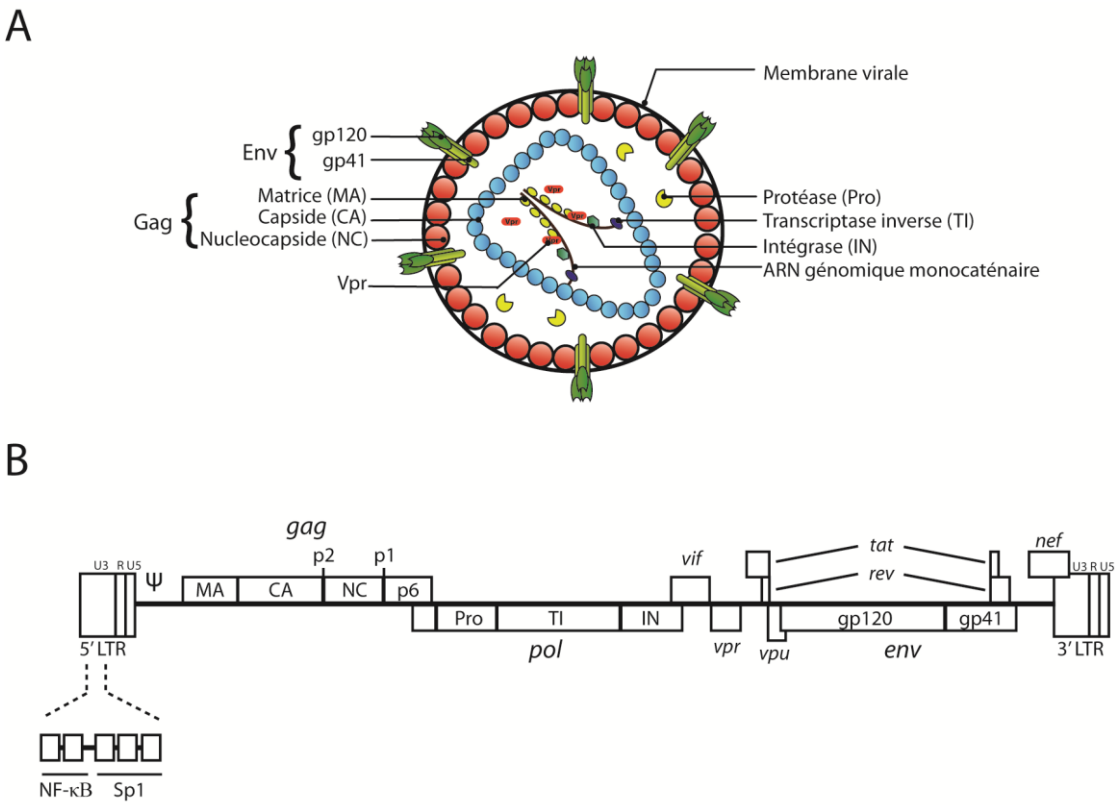

Figure 1: Structures du virus et du génome du VIH-1
(A) Schéma représentant une particule virale mature du VIH-1 de 80-120 nm. (B) Organisation d'ADN génomique du virus. Les trois cadres de lecture sont représentés. Les noms des gènes sont en italique alors que les noms des protéines sont en caractères romans. Les différents éléments des LTR sont représentés: les éléments U3 et U5 dérivés respectivement des séquences uniques en 3' et en 5' de l'ARN viral, ainsi que l'élément R dérivé de la séquence répétée à ses deux extrémités. La présence des sites de liaison aux facteurs de transcription, soit du facteur nucléaire kappaB (NF-κB) et de la protéine de spécificité-1 (Sp1), sont illustrés au niveau de l'élément U3. MA: matrice, CA: capside, NC: nucléocapside, Pro: protéase, TI:transcriptase inverse, IN: intégrase, LTR: longues répétitions terminales.

matrice (MA, p17), de la capside (CA, p24) et de la nucléocapside (NC, p7); la maturation du précurseur de la protéine de l'enveloppe (Env, gp160) dans le réseau *trans*-Golgi (RTG) donne le récepteur viral composé de trois copies de l'hétérodimère gp120 et gp41; celle du précurseur Pol procure les protéines enzymatiques telles que la

transcriptase inverse (TI), l'intégrase (IN) et la protéase virale (Pro). De plus, le génome du VIH-1 contient aussi les gènes *tat* et *rev* codant pour les protéines régulatrices Tat et Rev, respectivement. Étant nécessaires à la réplication virale *in vivo* et *in vitro*, ces protéines sont dites « essentielles ». Le génome du VIH-1 est aussi caractérisé par la présence de gènes additionnels qui ne sont pas absolument nécessaires à la réplication *in vitro*. Ces gènes, soit *vif*, *vpr*, *vpu* et *nef* codent pour des protéines non-enzymatiques « accessoires » qui façonnent l'environnement cellulaire et favorise la persistance du virus *in vivo*. Ces facteurs agissent à différentes étapes du cycle de réplication du virus.

3. Cycle réplicatif du virus

Un cycle réplicatif viral peut être défini par la synchronisation des processus nécessaires à la genèse de nouvelles particules virales infectieuses. Dans le cas du VIH-1, il comporte six grandes étapes : 1) l'entrée, 2) la transcription inverse, 3) l'intégration, 4) la production des protéines virales, 5) l'assemblage et 6) la relâche (Figure 2). L'**entrée** est le processus par lequel le matériel génétique du virus accède au milieu cytosolique. Le modèle traditionnel d'entrée suggère une fusion des membranes plasmiques d'origine virales et cellulaires. Ce dogme a récemment été remis en question par une étude suggèrant plutôt que la fusion surviendrait au niveau des endosomes, suite à l'internalisation, par un processus indépendant du pH alors que la fusion en surface, quoique observable, ne serait pas productive (177). Dans tous les cas, l'entrée implique la reconnaissance du récepteur cellulaire CD4 par la gp120 (131), menant à un premier changement conformationnel du récepteur viral qui expose sa boucle V3, site de liaison des corécepteurs CCR5 (chez les macrophages et lymphocytes T CD4 périphériques) ou CXCR4 (chez les lymphocytes T CD4), selon le tropisme du virus (51, 200). L'engagement du récepteur viral à l'un ou l'autre de ces co-récepteurs entraîne une seconde réorganisation du récepteur viral et permet l'insertion de la gp41 à la membrane cellulaire, puis la fusion pH-indépendante de la membrane virale et endosomale (168). La capside, ainsi délivrée dans le cytoplasme, est sujette à l'action de protéases cellulaires, libérant ainsi le complexe de transcription inverse (CTI) composé des deux brins d'ARN génomique monocaténaires, d'IN, de TI, de NC, et peut-être de Tat, Vpr,

MA et CA (2, 260). Dans le cytoplasme, l'ARN monocaténaire est converti au cœur du CTI en ADN bicaténaire proviral par la TI, un processus nommé **transcription inverse** (260). La composition du CTI varie durant tout ce processus pour devenir un complexe de pré-intégration (CPI), composé de l'ADN génomique bicaténaire, TI, IN, Vpr, MA et d'un rabat d'ADN résiduel de la transcription inverse. La dynéine, un moteur protéique responsable du transport de cargos sur les microtubules, assure la migration du CPI vers le noyau (165). Vpr, IN, MA et le rabat d'ADN permettraient quant à eux l'importation du CPI dans le nucléoplasme via des pores nucléaires (240). IN catalyse par la suite l'insertion des extrémités du provirus à la chromatine de la cellule. Cette intégration provoque des bris doubles brins d'ADN dans le génome de l'hôte qui sont réparés par des enzymes cellulaires, achevant ainsi le processus d'**intégration** (102). Ce sont les polymérases cellulaires qui assurent la réplication du génome viral alors intégré ainsi que sa transcription. La transcription virale est modulée par des éléments transcriptionnels au niveau des LTR, dont l'élément de réponse à Tat (TAR). En se liant à cet élément, Tat prévient l'interruption précoce de la transcription causée par la boucle TAR et permet ainsi la transcription d'ARN messager (ARNm) de pleine longueur (122, 197). L'expression chronologique des différentes protéines précoces et tardives est contrôlée par Rev. L'association de cette protéine à l'élément répondant à Rev (ERR) accélère l'exportation des ARNm vers le cytoplasme et prévient l'épissage alternatif des zones codantes pour les protéines tardives telles que Gag, Pol, Env, Vif, Vpr et Vpu. Elle permet aussi la transcription du génome viral complet, prêt à être encapsidé. La traduction des protéines virales permet **l'expression des protéines virales**, puis l'**assemblage** d'une nouvelle particule virale. Le précurseur de l'enveloppe (gp160) est traduit dans le réticulum endoplasmique (RE) et trafique par la voie classique de sécrétion (98, 164). Dans le RTG, la furine cellulaire clive la gp160, étape préalable à la formation d'hétérodimères gp120/gp41 (98). La protéine cellulaire TIP47 (« Protéine de

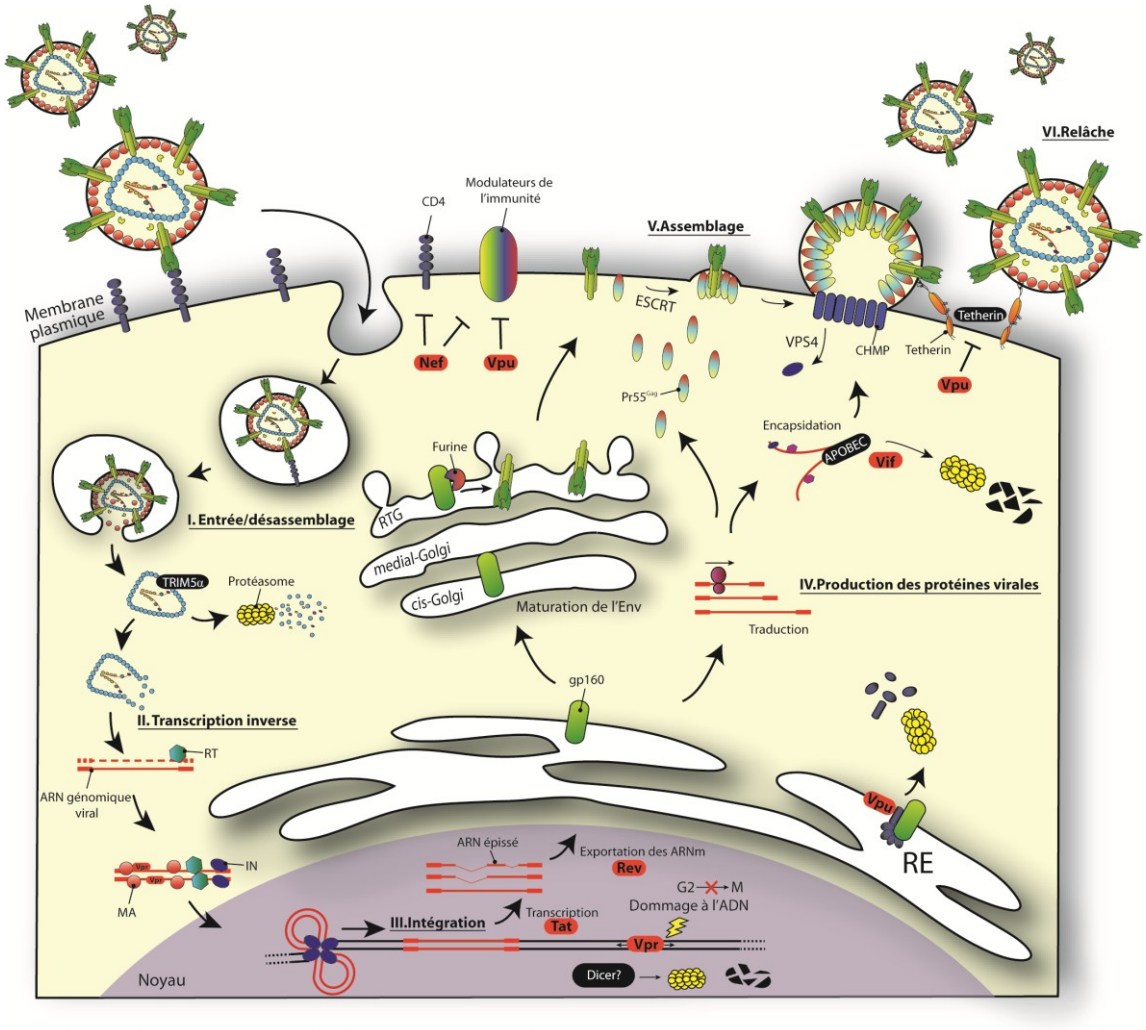

Figure 2: Le cycle de réplication du VIH-1
Schéma allégé illustrant un cycle réplicatif complet du VIH-1. Par souci de simplicité, le cycle est divisé en cinq grandes étapes. Les différentes protéines accessoires et régulatrices sont illustrées par les capsules rouges. Les facteurs de restriction sont indiqués par les capsules noires.

47 kDA interagissant avec une queue») connecterait les trimères gp120/gp41 à Gag au niveau des sites d'assemblage, assurant ainsi leur incorporation aux particules virales naissantes *(148). Ces sites d'assemblage constituent des* microenvironnements cellulaires spécialisés où les précurseurs Gag ($Pr55^{Gag}$) lient la membrane et s'y accumulent. L'association de $Pr55^{Gag}$ à la membrane plasmique implique l'association du domaine MA myristoylé à un lipide enrichi à la membrane plasmique, le phosphatidylinositol-(4,5)-bisphosphate (PI(4,5)P2) (25, 187, 189). La subséquente accumulation d'unités $Pr55^{Gag}$ force la multimérisation du précurseur et la formation du

site d'assemblage (16). L'encombrement stérique qui en résulte emprisonnerait certains constituants de la membrane plasmique tels que les tétraspanines (CD81, CD82, CD63 et CD9) et le cholestérol, créant un microenvironnement similaire aux radeaux lipidiques propice à l'assemblage et à la relâche (135). L'ARN génomique viral et les facteurs viraux associés (RT, IN et Vpr) sont incorporés à la particule virale en formation grâce au motif ψ situé près du 5'LTR par le domaine NC du précurseur (88, 205). Le domaine L (« late »; tardif) de p6 renferme un motif PTAP responsable du recrutement de Tsg101 par $Pr55^{Gag}$ (252). Il s'agit d'une composante d'ESCRT-I (complexe de triage endosomal I requis pour le transport), un complexe normalement impliqué dans le triage de cargos transmembranaires vers les compartiments lysosomaux, l'invagination des membranes endosomales dans les corps multivésiculaires (CMV) et la scission des vésicules intra-CMV par fusion des cols d'invagination (123). Le recrutement de Tsg101 par p6 mènerait à l'accumulation d'unités CHMP2 et CHMP4 d'ESCRT-III (complexe de triage endosomal III requis pour le transport) à la naissance du col d'invagination (16, 179, 238, 269). L'ATPase VPS4 catalyse le désassemblage de ce multimère unité par unité, causant ainsi la constriction graduelle du col et son éventuelle fusion (16, 238). Parallèlement à ce processus, $Pr55^{Gag}$ est graduellement clivé par Pro en CA, MA et NC, donnant ainsi naissance respectivement à la capside, à la matrice et au CTI (46, 134, 169). La particule virale mature infectieuse dont le col a fusionné grâce à VPS4 n'a plus de jonction avec la membrane plasmique; avec ce processus de **relâche** se termine donc le cycle réplicatif du virus.

4. Interactions entre facteurs de l'hôte et protéines accessoires

Les interrelations entre les protéines virales et les facteurs de l'hôte ont suscité beaucoup d'intérêt au cours des dernières années. Des criblages génomiques ont en effet permis de mettre en évidence un impressionnant nombre de facteurs cellulaires nécessaires à la réplication du virus (22, 83, 274). Par exemple, Tat recrute le complexe pTEFb et la cyclin T1 afin de permettre l'élongation des transcrits viraux alors que l'interaction entre Rev et la nucléoporine hRIP/Rab en accélère l'exportation (37, 261, 275). Gag recrute les complexes ESCRT afin de compléter l'assemblage et la relâche

des virions (252). La furine clive la gp160 en gp120/gp41 (98). Le facteur de croissance LEDGF/p75 est un important cofacteur d'IN durant l'intégration (37). Néanmoins, le cytoplasme représente tout de même un environnement hostile au virus dans la mesure où nombre de protéines cellulaires semblent nuire à sa réplication. De ce constat est né le concept de « facteur de restriction » qui s'est largement développé au cours de la dernière décennie. Ces facteurs de restriction sont particuliers : ils semblent suffire à bloquer l'une ou l'autre des étapes du cycle de réplication virale (Figure 2) et représentent une sorte d'extension au niveau cellulaire de la réponse immunitaire innée, étant généralement induits par les interférons (IFN). TRIM5α (« TRIpartite interaction motif-5 ») fut le premier facteur de restriction anti-VIH-1 identifié. Il s'agit d'une protéine cellulaire induite par l'IFN contenant un domaine RING aussi retrouvé chezles E3 ligases (53, 208). TRIM5α restreint l'infection à une étape entre l'entrée et la transcription inverse en provoquant le désassemblage prématuré et la dégradation protéasomale de la capside du VIH-1 (32, 237). Originellement, le tropisme interespèce des lentivirus a en partie été attribué à TRIM5α. En effet, la variante humaine peut restreindre le MLV (« murin leukemia virus »), mais pas le VIH-1 ou le VIS de macaque (mac). Inversement, TRIM5α simien restreint le VIH-1 et le MLV mais pas le VISmac (212, 236). L'activité restrictive de TRIM5α est intimement reliée à la cyclophilin A (CypA), une autre protéine cellulaire ayant une forte affinité pour CA. Chez l'humain, l'association entre CA et CypA protège la capside du VIH-1 de l'action de TRIM5α humaine (212, 244). Alors que la résistance du VIH-1 à TRIM5α est conférée par la protéine CypA cellulaire, la négation des processus cellulaires nuisibles à la réplication est généralement assurée par les protéines accessoires du VIH-1.

Nef

Bien que Nef ne semble pas contrer formellement un facteur de restriction, du moins dans le cadre de l'infection de cellules humaines, ses différentes fonctions n'en demeurent pas moins nécessaires à la réplication et à la propagation du virus (48, 65, 151). Il s'agit d'une protéine myristoylée de 27 acides aminés exprimée précocement durant l'infection (65). Nef agit principalement comme protéine adaptatrice modulant

l'expression de surface de plusieurs protéines impliquées dans la réponse immunitaire. Nef induit l'endocytose de CD4 par la voie clathrine-dépendante via un mécanisme requérant la protéine adaptatrice-2 (AP-2), menant ultimement à la dégradation lysosomale du récepteur (33, 117). Cette activité, en combinaison avec l'effet de Vpu sur les molécules de CD4 néo-synthétisées (voir revue), prévient à la fois la surinfection et les phénomènes d'interférence entre CD4 et l'Env dans la voie de sécrétion qui diminuent l'infectivité du virus (140, 203). Nef accélère aussi l'internalisation des complexes majeurs d'histocompatibilité de type-I et -II (CMH-I et -II) en recrutant plutôt AP-1, une protéine adaptatrice impliquée dans l'endocytose (17, 201, 263). L'effet de Nef sur le CMH-I ne provoque pas leur destruction par les cellules tueuses naturelles (NK) puisque cette protéine virale affecte spécifiquement les antigènes humains de leucocyte (HLA) -A et -B du CMH-I et non pas HLA-C et -E, les ligands reconnus par ces cellules du système immunitaire inné (3, 40). Cette protection est de plus favorisée par la séquestration intracellulaire par Nef de NKp44L, un autre ligand des cellules NK (67). Le rôle de Nef dans la modulation de la réponse immunitaire est complété par sa modulation négative de l'expression de surface de CMH-II et de la chaîne invariante (Ii), ce qui empêche la présentation d'antigènes viraux à la surface des cellules infectées (239). Outre ces effets, Nef favorise une étape précoce de l'infection indépendamment de son effet sur CD4 (36, 170, 220). Le(s) mécanisme(s) est(sont) mal compris, mais pourrait impliquer la perturbation du réseau d'actine cortical qui représente une barrière physique à l'entrée du virus et/ou la diminution du niveau de surface d'un facteur cellulaire nuisant à l'infectivité du virus (27, 195).

Vif et APOBEC3F/G

L'activité de Vif est étroitement reliée aux protéines d'**APOBEC3** (« apolipoprotein B mRNA-editing catalytic polypeptide 3 ») qui ont un important rôle dans l'immunité innée contre les rétrovirus, transposons, hepadnavirus, foamy virus et autres pathogènes intracellulaires (87). Induites par l'IFN, ces protéines possèdent une activité cytidine déaminase (35, 192). Durant la réplication d'un virus défectif pour l'expression de Vif, leur antagoniste, les variantes APOBEC3F/3G sont encapsidées

dans les particules virales en formation (100, 125, 126, 160, 258). Suite à l'entrée d'un tel virus dans une nouvelle cellule cible, les molécules d'APOBEC3F/3G associées au virus convertissent les nucléotides guanosine en adénosine lors de la transcription inverse (24, 157, 175, 219). L'hypermutation de l'ADN viral génomique qui en découle provoque une infection abortive (157). Contrairement à TRIM5α qui cible une composante structurelle du virus susceptible de devenir résistante suite à l'accumulation de mutations, APOBEC3F/3G vise non-spécifiquement une composante virale beaucoup plus fondamentale en l'ADN viral génomique généré lors de la transcription inverse, ce qui explique probablement l'émergence du gène *vif*. . L'expression de cette protéine est nécessaire à l'infection productive par VIH-1 de lymphocytes T CD4 périphériques et de macrophages (66, 76, 77). C'est une protéine de 23 acides aminés exprimée tardivement durant l'infection qui prévient l'encapsidation d'APOBEC3F/3G (70, 234). Vif connecte APOBEC3F/3G à l'elongine C et à la Cullin5, toutes deux composantes du complexe E3 ubiquitine ligase Cullin 5 RING (nouveau gène très intéressant), ce qui résulte en la poly-ubiquitination et la dégradation par le protéasome de ce facteur de restriction (43, 161, 167, 232). Vif aurait aussi un impact marqué au niveau du cycle cellulaire. Dans un premier temps, elle accélèrerait la transition entre les phases G1 à S en recrutant Brd4 et Cdk9, deux importants modulateurs du cycle cellulaire (256). Puis, par un mécanisme requérant le recrutement du complexe E3 ubiquitine ligase Cullin 5 RING, Vif ralentirait le cycle cellulaire en phase G2 sans toutefois la bloquer complètement (49, 207, 257). La dégradation d'un facteur inconnu autre qu'APOBEC serait responsable de ce phénomène. L'importance de la modulation globale du cycle cellulaire par Vif sur la réplication du virus reste cependant à être établie.

Vpr et son facteur de restriction

Vpr est une petite protéine soluble de 96 acides aminés exprimée tardivement durant l'infection (39, 78). Son incorporation aux particules virales via le domaine p6 de $Pr55^{Gag}$ et sa sécrétion sous forme soluble à partir de cellules infectées (103, 146, 264) lui permettrait tout de même d'exercer des activités biologiques très précocement durant le cycle de réplication (150). Vpr contre un **facteur de restriction lié aux macrophages** qui interfère, dans ces cellules, avec une étape du cycle de réplication située entre la

transcription inverse et la transcription des gènes viraux (42, 61, 224). L'identité de ce facteur demeure encore spéculative, mais de récentes données suggèrent qu'il pourrait s'agir de Dicer, une protéine impliquée dans la genèse des ARN d'interférence (ARNi) (41). Bien qu'il ne soit pas clair comment cette protéine parviendrait à restreindre l'infection dans les macrophages, sa dégradation protéasomale catalysée par le recrutement de la E3 ligase DDB1-CUL4A^{VPRBP} par Vpr suffirait à surmonter cette activité restrictive (31). L'effet de Vpr sur Dicer semble restreint aux macrophages puisque cette protéine accessoire n'a pas d'effet significatif sur la réplication virale dans les lymphocytes T CD4. Néanmoins, elle y interagit tout de même avec le complexe DDB1-CUL4A^{VPRBP} (11, 50, 106, 141, 214). Ce complexe Vpr-DDB1-CUL4A^{VPRBP}, associé à la chromatine de ces cellules T CD4 au niveau de foyers mobiles, balaierait le génome de l'hôte à la recherche d'un substrat associé aux sites de bris d'ADN doubles brins. L'ubiquitination et la dégradation protéasomale de ce substrat mènent à l'activation d'ATR (relié à Rad3 et à l'ataxia telangiectasia muté), une protéine kinase responsable de la détection de dommages à l'ADN, et à l'arrêt du cycle cellulaire en phase G2/M (10, 12, 50). L'identité de ce substrat demeure inconnnue; Dicer demeure une possibilité quoiqu'aucune donnée ne la supporte à l'heure actuelle. Il n'est pas clair si cette dernière activité de Vpr favorise la pathogénèse virale. La conservation de l'arrêt de cycle chez les différentes souches de lentivirus de primates lui suggère tout de même un rôle important (196, 231).

Vpr pourrait représenter un modulateur du système immunitaire au cours de l'infection. D'une part, la sécrétion de Vpr soluble par la cellule infectée préviendrait la maturation des cellules dendritiques, l'activation des cellules T CD4 et les fonctions des cellules NK, contribuant possiblement à la dysfonction immunitaire observée chez les patients infectés (153, 154, 251). De plus, l'activation d'ATR par Vpr mène à l'expression des ligands NKG2D reconnus par les cellules NK, engendrait conséquemment la lyse des cellules infectées par ces médiateurs de l'immunité innée (199, 259). Par contre, comment la reconnaissance des cellules infectées par les cellules NK et la promotion de la dysfonction des médiateurs de la réponse immunitaire grâce à Vpr contribueraient à la pathogénèse et/ou à la persistance virale n'est pas clair.

Vpu et Tetherin

Tetherin/BST2/CD317 est le dernier facteur de restriction découvert à ce jour. L'activité restrictive de Tetherin implique la reconnaissance non pas d'une protéine virale spécifique, mais plutôt de la membrane lipidique virale, qui n'est pas sujette à la dérive génétique. L'incapacité du virus à sélectionner une variante résistante à la Tetherin explique probablement l'émergence de l'activité antagoniste de la protéine **Vpu**.

Nous avons récemment publié en 2010 dans le journal *Retrovirology* une revue exhaustive sur cet antagoniste viral (ci-joint) (57). Mariana Bego, Ph.D., y a décrit la biologie cellulaire de la Tetherin dans la section «Role of Vpu in HIV-1 release and transmission»; Catherine Paquay, M.D., s'est occupée de la section «Role of Vpu in primate lentivirus cross-species transmission and the emergence of pandemic HIV-1 strains»; Éric Cohen, Ph.D., a pris en charge l'introduction et les sections «The Vpu gene product» et «Role of Vpu in HIV-1-induced CD4 receptor downregulation» alors que j'ai écrit les sections «HIV-1 riposte to Tetherin-mediated restriction», «Vpu, a versatile Tetherin antagonist» et «Tetherin, a common enemy».

Modulation of HIV-1-host interaction: role of the Vpu accessory protein

Mathieu Dubé*, Mariana Bego*, Catherine Paquay*

and Éric A. Cohen [1,2]

Laboratory of Human Retrovirology, Institut de Recherches Cliniques de Montréal (IRCM) and [1]Department of Microbiology and Immunology, Université de Montréal, Montreal, Quebec, Canada.

Running Title: HIV-1 Vpu accessory protein functions

* These authors contributed equally to this work.

[2]Corresponding author:

Manuscript information: 71 pages, 6 figures

Word and character counts: abstract = 139 words; text word count = 10382 words

Abstract

Viral protein U (Vpu) is a type 1 membrane-associated accessory protein that is unique to human immunodeficiency virus type 1 (HIV-1) and a subset of related simian immunodeficiency virus (SIV). The Vpu protein encoded by HIV-1 is associated with two primary functions during the viral life cycle. First, it contributes to HIV-1-induced CD4 receptor downregulation by mediating the proteasomal degradation of newly synthesized CD4 molecules in the endoplasmic reticulum (ER). Second, it enhances the release of progeny virions from infected cells by antagonizing Tetherin, an interferon (IFN)-regulated host restriction factor that directly cross-links virions on host cell-surface. This review will mostly focus on recent advances on the role of Vpu in CD4 downregulation and Tetherin antagonism and will discuss how these two functions may have impacted primate immunodeficiency virus cross-species transmission and the emergence of pandemic strain of HIV-1.

Introduction

HIV-1 interaction with host target cells is complex with nearly every step of the virus infection cycle relying on the recruitment of cellular proteins and basic machineries by viral proteins [1]. For instance, the Tat regulatory protein recruits the pTEFb complex during viral transcription to enhance host RNA polymerase II processivity and promote efficient elongation of viral transcripts (reviewed in [2]). Similarly, the p6 domain of the Gag structural protein interacts with the ESCRT complex during viral assembly to direct the budding of progeny virions (reviewed in [3]). Recent discoveries have shed light on an additional level of complexity involving host proteins that provide considerable resistance to infection by HIV-1 and other viruses via cell-autonomous mechanisms that are likely part of the antiviral innate immune response. As a virus inducing a persistent infection, HIV-1 has evolved countermeasures to overcome the antiviral activity of these host factors, also called restriction factors, mainly through the activities of a set of viral accessory proteins that include the Vif, Vpr, Vpu and Nef proteins. These accessory proteins, which have been recently the subject of intense research and progress, represent one of the defining features of primate immunodeficiency viruses. They are not commonly found in other retroviruses and as such are likely to play a key role in HIV-1 pathogenesis. Overall, it is becoming increasingly clear that the function of these non-enzymatic viral proteins is to modulate the cellular environment within infected cells to promote efficient viral replication, transmission and evasion from innate and acquired immunity (for recent

reviews [4, 5]). In this review, we will focus on the recent progress made in our understanding of the functions and mode of action of the HIV-1 Vpu accessory protein and relate these to the pathogenesis of the virus as well as the emergence of pandemic HIV-1 strains. Furthermore, we will highlight along the way some important questions for the future.

The vpu gene product

Vpu was initially identified as the product of an open reading frame (ORF), referred as the U ORF (initially all HIV-1 ORFs were designated by alphabetical letters) located between the first exon of the *tat* and *env* genes of HIV-1 [6, 7]. The *vpu* gene is present in the genome of HIV-1 but is absent from HIV-2 and other related SIVs, such as SIV from sooty mangabey (SIVsmm) and SIV from rhesus macaques (SIVmac) [6, 7]. Structural homologues have been detected in SIV from chimpanzee (SIVcpz), the precursor of HIV-1, and in SIV's from the mona monkey (*Cervicopithecus mona*; SIVmon), the greater spot-nosed monkey (Cercopithecus nictitans; SIVgsn), the mustached monkey (*Cercopithecus cephus*; SIVmus) and more recently in Dent's mona monkey (*Cercopitheus mona denti*; SIVden) and gorilla (*Gorilla gorilla*; SIVgor) [8-13].

The Vpu protein encoded by HIV-1 is a 77-86 amino-acids membrane-associated protein capable of homooligomerization [14]. The protein is translated from a Rev-dependent bicistronic mRNA, which also encodes the viral envelope glycoprotein (Env),

suggesting that expression of Vpu and Env are coordinated during HIV-1 infection [15]. The protein is predicted to have a short luminal N-terminal domain (3-12 amino acids), a single transmembrane (TM) spanning domain that also serves as an uncleaved signal peptide (23 amino acids) and a charged C-terminal hydrophilic domain of 47-59 residues that extends into the cytoplasm [14, 16] (Figure 1A). While the crystal structure of the entire Vpu protein has yet to be solved, the molecular structure of the N-terminal domain (residues 2-30) has been determined by nuclear magnetic resonance (NMR) and found to contain a TM α-helix spanning residues 8 to 25 with an average tilt angle of 13 degrees [17, 18]. Interestingly, modeling as well as biochemical and genetic evidence have suggested that the TM domain is critical for Vpu oligomerization and that a pentameric structure for the TM domain would be optimal for the formation of an ion channel [19, 20]. In that regard, several studies have suggested that Vpu, like the M2 protein of influenza, may have an ion channel activity (for a recent review: [21]). However, whether the ion channel activity of Vpu is required for Vpu function is still controversial. NMR analysis of the cytosolic domain, on the other hand, revealed that this part of the protein comprises two α-helical regions interconnected by a flexible loop containing a highly conserved sequence (DSGNES) [16, 22, 23], which includes a pair of serine residues (S52 and S56) that are phosphorylated by casein kinase II [24-27] (Figure 1).

HIV-1 Vpu proteins encoded by subtype B strains appear to be largely expressed on intracellular membranes, which correspond to the ER, the *trans* Golgi network (TGN) as well as endosomal compartments, but no accumulation of the protein is

readily detected at the cell surface [28-30]. Unlike the better-studied HIV-1 subtype B Vpu proteins, subtype C and SIVcpz Vpu alleles fused to EGFP were reported to be transported to the plasma membrane [31-33]. Interestingly, as depicted in figure 1B, amino acid sequence analysis of the cytosolic domain of HIV-1 Vpu reveals the presence of putative trafficking signals that harbor a degree of amino acid variation among Vpu alleles from different subtypes [34]. These trafficking signals include: 1) an overlapping tyrosine (YXXΦ where Φ designs a hydrophobic residue) and an acidic/dileucine based ([D/E]XXXL[L/I/V]) sorting motifs in the hinge region between the TM anchor and the cytosolic domain, normally implicated in endocytosis as well as in the targeting of TM proteins to lysosomes and lysosome-related organelles [35]; 2) another acidic/dileucine sorting signal, [D/E]XXXL[L/I/V], in the second α-helix of the Vpu cytoplasmic tail [32] (Figure 1B). The fact that several laboratory-adapted strains and primary isolates of HIV-1 harbor *vpu* genes with polymorphism at the level of these putative trafficking signals [29, 34], raises the possibility that regulation of Vpu subcellular localization and perhaps biological activities may indeed confer the virus a selective advantage in some physiological conditions.

Studies mostly performed with Vpu originating from subgroup B laboratory-adapted strains (NL4-3, BH10) have established two main functions during infection of HIV-1 target cells in tissue culture systems. First, Vpu induces a rapid degradation of newly synthesized CD4 receptor molecules in the ER via the ubiquitin-proteasome system [36, 37]. In addition to its effect on CD4 catabolism, Vpu promotes the release of progeny virions from HIV-1-infected human cells [7, 26, 28, 38-40] by counteracting

Tetherin (also designated BST2, CD317 and HM1.24), a host restriction factor that strongly inhibits the release of virions from the host cell surface [41, 42].

Role of Vpu in HIV-1-induced CD4 receptor downregulation

Expression of CD4 molecules at the surface of HIV-1 infected cells is detrimental to efficient viral replication and spread

The process of HIV-1 entry into target cells begins with the binding of the viral envelope glycoprotein gp120 to both the CD4 receptor and one of the chemokine co-receptors, CXCR4 or CCR5 [43]. Despite the critical role played by the CD4 receptor during viral entry, it is well established that an early and lasting effect of infection is the downregulation of the CD4 receptor from the host cell surface. In fact, it appears that once viral entry has occurred, continuous expression of the CD4 receptor may be detrimental to efficient viral replication and spread. Early work on this issue has shown that newly synthesized CD4 molecules are capable of retaining the Env precursor proteins in the ER through their high Env binding affinity, therefore preventing transport and processing of mature Env products, gp120 and gp41, to the site of virus assembly [44-47]. Additionally, expression of CD4 at the cell surface promotes superinfection of cells by cell-free and cell-associated viruses [48] and can interfere with the efficient release of infectious progeny virions from the cell surface [49-54]. While the disadvantageous effect of CD4 on the release and infectivity of cell-free virus is well established, it is unclear whether the expression of CD4 at the cell surface of infected

cells also impedes cell-to-cell viral transmission through virological synapses, a mode of propagation that is believed to promote efficient viral dissemination [55, 56]. Despite its compact genome, HIV-1 devotes two accessory proteins, Nef and Vpu, to the task of suppressing expression of its primary receptor. Early in infection, Nef removes mature CD4 molecules that are already present at the cell surface by enhancing their endocytosis by a pathway involving clathrin and AP2 [57-59] followed by delivery of internalized CD4 to the multivesicular body pathway for eventual degradation in the lysosomes [60, 61]. In contrast, Vpu, which is expressed late during the virus life cycle, acts on newly synthesized CD4 molecules in the ER and as such counteracts their effects in the early biosynthetic pathway [62]. This functional convergence, involving two viral proteins acting on CD4 molecules located in different cellular compartments and operating by distinct mechanisms, implies that cell surface CD4 downregulation must play an important role for HIV-1 replication and propagation.

Vpu hijacks the host ubiquitin machinery to target CD4 for proteasomal degradation

The degradation of CD4 mediated by Vpu involves multiple steps that are thought to be initiated by the physical binding of Vpu to the cytoplasmic tail of CD4 in the ER. Mutational and deletion analyses of CD4 have delineated a domain of the molecule, encompassing residues 414 and 419 (LSEKKT) as well as an α-helix located in the membrane proximal region of the viral receptor cytosolic region, that are required for Vpu binding and CD4 degradation [63-67] (Figure 2). The domain of Vpu that is interacting with the cytosolic region of CD4 is still not precisely defined but previous

studies have shown that these binding determinants are likely to be present in the cytoplasmic region of the protein [68]. In support of this finding, a mutant of Vpu that harbored a TM domain with a randomized primary sequence was still able to bind CD4 and mediate its degradation as well as its wild-type (WT) counterpart [69]. Furthermore, mutational analysis of the Vpu cytoplasmic domain revealed that the first α-helix was structurally important for CD4 binding and degradation [70, 71]. Although the binding of Vpu to CD4 is necessary to induce CD4 degradation, it is not sufficient. Phosphorylation-deficient mutants of Vpu were shown to be unable to induce CD4 degradation while interacting with CD4 as efficiently as their WT counterpart [26, 63, 68, 72, 73]. A major finding in the mechanism underlying Vpu-mediated CD4 degradation was the discovery that phosphorylated Vpu proteins interacted with β-TrCP-1 [73] and β-TrCP-2 [74], two paralogous F-box adaptor proteins that are part of the cytosolic Skp1-Cullin1-F-Box (SCF) E3 ubiquitin (Ub) ligase complex [73]. β-TrCP functions as a substrate specificity receptor for the $SCF^{\beta\text{-}TrCP}$ E3 Ub ligase and recognizes substrates, such as Vpu, upon phosphorylation of the two serine residues present within a conserved $DS^{P}G\Phi XS^{P}$ β-TrCP recognition motif [75] (Figure 1B). By directly interacting with the WD-repeat β-propeller of β-TrCP, Vpu is able to form a CD4-Vpu-β-TrCP ternary complex and as such brings CD4 and the other components of the E3 Ub ligase in close proximity so that *trans*-ubiquitination of CD4 could occur (Figure 2). In fact, biochemical and functional evidence in human cells as well as in yeast *S. cerevisiae* expressing Vpu and CD4 revealed that $SCF^{\beta\text{-}TrCP}$ recruitment by Vpu results in polyubiquitination of the cytosolic tail of CD4 [76, 77], thus marking the viral receptor for degradation by the cytosolic proteasome [37, 78]. The function of Vpu in

CD4 degradation is therefore very similar to that of E3 Ub ligase adaptors, which link substrates to Ub ligases. Both β-TrCP1 and β-TrCP2 appear to be involved in the formation of a functional Vpu-$SCF^{\beta\text{-TrCP}}$ E3 Ub ligase complex since small interfering (si) RNA silencing of both genes simultaneously was required to fully reverse Vpu-mediated CD4 degradation [74].

While the first helix of Vpu appears important for CD4 binding, the role of the second helix remains unclear. Deletion of the C-terminal 23 amino-acid residues or substitution of residues Val 64 to Met 70 abrogated Vpu-mediated CD4 degradation without, however, affecting CD4 binding [31, 71]. A more recent study analyzed systematically the importance of each amino-acid within this region by alanine scan mutagenesis and identified Leu 63 and Val 68 as residues required for CD4 downregulation. Interestingly, in the case of Leu 63, substitution of this residue with Ala or Val, which maintain the predicted secondary structure of the helix, did not affect binding to CD4 or β-TrCP, but did abolish CD4 downregulation [70], suggesting that binding of Vpu to CD4 and recruitment of β-TrCP might not be sufficient to induce CD4 degradation and consequently that other process and/or interactions might be involved in this mechanism. It is interesting to note that the conserved Leu 63 and Val 68 are part of a conserved acidic/dileucine sorting signal, [D/E]XXXL[L/I/V] (Figure 1B), usually involved in the trafficking of membrane proteins between the endosomes and the TGN. The role of this sorting motif on Vpu exit from the ER as well as on its trafficking in general still remains undefined.

ERAD-ication of CD4 by Vpu

The process of Vpu-mediated CD4 degradation is reminiscent of a cellular quality control process called ER-associated protein degradation (ERAD) that eliminates misfolded or unassembled proteins from the ER [79, 80]. Abnormal proteins targeted by the ERAD pathway are usually recognized by a quality control system within the ER lumen and ultimately degraded by the cytoplasmic ubiquitin-proteasome system following transport across the ER membrane by a process called dislocation. However, unlike typical ERAD, which uses several membrane-bound E3 Ub ligases, including the HRD1-SEL1L complex [81], TEB4/MARCH-VI [82], and the GP78-RMA1 complex [83], Vpu-mediated CD4 degradation relies on the cytosolic $SCF^{\beta\text{-}TrCP}$ E3 Ub ligase complex that is responsible for ubiquitination and degradation of non-ERAD substrates such as IκBα [84] and β-catenin [85]. Consistent with these findings, genetic evidence in *S. cerevisiae* yeast expressing human CD4 and HIV-1 Vpu revealed that CD4 degradation induced by Vpu did not require HRD1 (E3), SEL1L and the E2 Ub conjugating enzyme UBC7, which are key components of the machinery responsible for ubiquitination of most ERAD substrates [76].

Recent studies have dissected in molecular terms the process of CD4 degradation mediated by Vpu and found that although the mechanism is distinct from typical ERAD it still shares similar features and, importantly, involves late stages components of the ERAD pathway. As a first step, Vpu was found to target CD4 for degradation by a process involving polyubiquitination of the CD4 cytosolic tail by $SCF^{\beta\text{-}TrCP}$ [76, 77] (Figure 2). Interestingly, replacement of cytosolic Ub acceptor lysine residues reduced

but did not abolish Vpu-mediated CD4 ubiquitination and degradation, raising the possibility that the CD4 degradation induced by Vpu is not entirely dependent on the ubiquitination of cytosolic lysines [77]. Indeed, recent evidence revealed that more profound inhibition of degradation could be achieved by mutation of all lysine, serine and threonine residues in the CD4 cytosolic tail ([86] and our unpublished results). The ubiquitination process involved in Vpu-mediated CD4 degradation, therefore, resembles that involved in MHC-I downregulation induced by the mouse gamma herpesvirus (Gamma-HSV) mK3 E3 Ub ligase, which mediates ubiquitination of nascent MHC-I heavy chain (HC) cytosolic tail via serine, threonine or lysine residues to target MHC-I heavy chain for degradation by ERAD [87]. As a second step, although Vpu uses a non-ERAD E3 Ub ligase to induce CD4 degradation, it is co-opting downstream components of the ERAD pathway. In fact, the VCP-UFD1L-NPL4 complex, a key component of the ERAD dislocation machinery [88, 89], was shown to be involved in CD4 degradation by Vpu (Figure 2). Using siRNA, a recent study reported a requirement of the valosin-containing protein (VCP) AAA ATPase p97 and its associated co-factors UFD1L and NPL4 in Vpu-mediated CD4 degradation [86]. Furthermore, the fact that mutants of p97 that are unable to bind ATP or to catalyze ATP hydrolysis exerted a potent dominant negative (DN) effect on Vpu-mediated CD4 degradation indicated that the ATPase activity of p97 was required for this process [77, 86]. Further dissection of the role of the UFD1L and NPL4 cofactors in Vpu-mediated CD4 degradation revealed that while p97 appears to energize the dislocation process through ATP binding and hydolysis, UFD1L binds ubiquitinated CD4 through recognition of K-48 chains and NPL4 stabilizes the complex [86]. A role of the VCP-UFD1L-NPL4 complex in

mediating the extraction of CD4 from the ER membrane, as observed for ERAD substrates [76] is consistent with data showing that Vpu was promoting the dislocation of ubiquitinated CD4 intermediates across the ER membrane [76, 77]. Vpu, therefore, appears to bypass the early stages of ERAD including substrate recognition and ubiquitination by ERAD machinery components, but joins in the later stages beginning with dislocation by the VCP-UFD1L-NPL4 complex (Figure 2).

Retention of CD4 molecules in the ER by Vpu?

Besides its role in CD4 ubiquitination and dislocation across the ER membrane so that receptor molecules be accessible to the cytosolic proteasome, a recent study provided evidence that Vpu plays also a role in the retention of CD4 in the ER [86]. It was initially found that Vpu was targeting CD4 molecules that were retained in the ER through formation of a complex with Env [62]. However, Magadan and colleagues found that even in absence of Env, large amounts of CD4 are retained in the ER in the presence of Vpu when ERAD is blocked [86]. Unexpectedly, these authors further showed that this retention was independent of the only interaction of Vpu and CD4 reported to date, which involves the cytosolic domain of both proteins. Rather, CD4 ER retention appeared primarily dependent on direct or indirect interactions involving the TM domains of both CD4 and Vpu. Indeed, a Vpu mutant containing a heterologous TM domain from the G glycoprotein of vesicular stomatitis virus (VSV) failed to retain CD4 in the ER. Although these results support a role of TM domain interactions in the retention of CD4 in the ER by Vpu, this interaction does not appear to rely on Vpu TM primary sequences since a Vpu mutant containing a scrambled TM domain was still

competent at binding CD4 and at mediating CD4 degradation [69]. Vpu-mediated ubiquitination appears also to contribute to CD4 retention in the ER, but the mechanism remains unclear. Therefore, it appears that Vpu retains CD4 in the ER by the additive effects of two distinct mechanisms: assignment of ER residency through the TM domain and ubiquitination of the cytosolic tail. The findings of Magadan and colleagues supporting a role of Vpu in the retention of CD4 in the ER are not entirely consistent with those of a previous report, which showed that CD4 can efficiently traffic to the Golgi complex in presence of Vpu when CD4 is not retained in the ER by Env [36]. Indeed, using a subviral construct expressing Vpu and a mutant of gp160 defective for CD4 binding, Willey and colleagues found that despite the presence of Vpu the majority of CD4 acquired Endo H-resistant complex carbohydrates in the Golgi apparatus within 60 min after synthesis. Whether this discrepancy results from a difference in Vpu expression levels (Willey et al. expressed Vpu from a subviral vector while Magadan et al. used a codon-optimized Vpu construct that expresses much higher levels of the protein) or from differences in the assays used (prevention of CD4 degradation by blocking ERAD vs allowing trafficking of CD4 by not blocking the receptor exit from the ER with Env) remains unclear. Clearly, more studies will be required to fully understand the mechanism through which Vpu confers on CD4 an intrinsic propensity to reside in the ER. Importantly, it will be critical to assess its relevance and contribution in the context of HIV infection where large amounts of CD4 are already complexed to Env gp160 in the ER.

Overall, based on previous findings and more recent evidence, a model of Vpu-mediated CD4 degradation emerges whereby Vpu might exert two distinct separable

activities in the process of downregulating CD4: retention in the ER followed by targeting to a variant ERAD pathway (Figure 2).

Role of Vpu in HIV-1 release and transmission

Vpu promotes efficient release of HIV-1 particles in a cell-type specific manner

In addition to its effect on CD4 catabolism, Vpu was reported to promote the efficient release of virus particles from HIV-1-infected cells [7, 38]. This finding was supported by electron microscopy (EM) studies, which revealed an accumulation of mature virions still tethered to the plasma membrane of infected T cells in the absence of Vpu [28, 90]. Early studies demonstrated that the need of Vpu for efficient HIV-1 particle release was only observed in certain cell types. Notably, while Vpu-deficient HIV-1 release was drastically reduced in HeLa cells, monocyte-derived macrophages, and to a smaller extent in primary CD4+ T cells, normal viral particle release was observed in HEK293T, COS, CV-1, and Vero cells [39, 91, 92]. Importantly, the fact that Vpu could significantly enhance viral particle production by Gag proteins from HIV-2 or retroviruses distantly related to HIV-1, such as Visna and murine leukemia virus (MLV), suggested that the effect of Vpu was unlikely to require highly specific interactions with Gag proteins, but rather was more consistent with a model where Vpu enhanced retroviral release indirectly through modification of the cellular environment [40].

Tetherin, the last obstacle to enveloped virus release

The notion that a cellular inhibitor of HIV-1 particle release antagonized by Vpu could be responsible for the inefficient release of Vpu-deficient HIV-1 in restrictive cells was suggested by the observation that heterokaryons between restrictive HeLa and permissive COS cells exhibited a restrictive phenotype similar to that displayed by HeLa cells [93]. Importantly, the fact that virions retained at the cell surface could be released by protease treatment suggested that a protein expressed at the cell surface was involved in the "tethering" of virions to the cell surface as opposed to a budding defect that prevented membrane separation [94]. Interestingly, cell types that allowed efficient release of Vpu-deficient HIV-1 viruses could become restrictive for viral release after type 1 IFN treatment, thus suggesting that the putative cellular protein that efficiently tethered virions on host cell surface was induced by type I IFN [95].

Almost simultaneously, the Bieniasz and Guatelli groups identified Tetherin as the cellular factor responsible for the inhibition of HIV-1 particle release and counteracted by the Vpu accessory protein [41, 42]. Both groups found Tetherin to be constitutively expressed in cell lines that required Vpu for efficient particle release, like HeLa cells but not in permissive HEK293T and HT1080 cells. Likewise, expression of Tetherin and its associated restrictive phenotype could be induced by IFN-α in permissive HEK293T and HT1080 cells and enhanced in Jurkat and primary CD4+ T cells. Furthermore, while introduction of Tetherin into HEK293T and HT1080 cells inhibited HIV-1 particle release in absence of Vpu, siRNA-directed depletion of Tetherin in HeLa cells led to efficient release of Vpu-deficient HIV-1 particles [41, 42]. In addition to HIV-1, Tetherin has been shown to exert its antiviral activity against a

broad range of enveloped viruses, including many retroviruses (alpharetrovirus, betaretrovirus, deltaretrovirus, lentivirus, and spumaretrovirus), filoviruses (Ebola and Marburg viruses), arenaviruses (Lassa virus), paramyxoviruses (Nipah virus) as well as Kaposi Sarcoma Herpes Virus (KSHV) [41, 42, 94, 96-99], thus indicating that the process of restriction is unlikely to involve specific interactions with virion protein components.

Tetherin: expression, structure and trafficking

Tetherin is a protein highly expressed in plasmacytoid dendritic cells (pDCs), the major producers of type I IFN, and in some cancer cells, while lower basal levels of expression are detected in bone marrow stromal cells, terminally differentiated B cells, macrophages, and T cells [100-104]. Its expression is strongly induced by type I IFNs in virtually all cell types [99, 101, 105-107], indicating that it is likely part of the innate defense response to virus infections.

Tetherin is a glycosylated type II integral membrane protein of between 28 and 36 kDa with an unusual topology in that it harbors two completely different types of membrane anchor at the N- and C-terminus. It is composed of a short N-terminal cytoplasmic tail linked to a TM anchor that is predicted to be a single α-helix, a central extracellular domain predicted to form a coiled-coil structural motif, and a putative C-terminal glycophosphatidyl-inositol (GPI)-linked lipid anchor [105, 108, 109] (Figure 3A). This rather atypical topology is only observed in one isoform of the prion protein [110]. As a GPI-anchored protein, Tetherin is found within the cholesterol-enriched

lipid domains from which HIV-1 and other enveloped viruses preferentially assemble and bud [108, 111-113]. The protein is localized not only at the plasma membrane but also within several endosomal membrane compartments, including the TGN as well as early and recycling endosomes [29, 108, 112, 114]. Clathrin-mediated internalization of human Tetherin is dependent upon a non-canonical tyrosine-based motif present in the cytoplasmic tail of the protein (Figure 3B), which appears recognized by α-adaptin but not the μ2-subunit of the AP-2 complex as it was initially reported for the rat Tetherin [109, 112]. Moreover, after endocytosis, Tetherin delivered to early endosomes is subsequently transported to the TGN through recognition of the cytoplasmic domain by the μ1-subunit of the AP-1 complex [109], suggesting the involvement of the sequential action of AP-2 and AP-1 complexes in internalization and delivery back of Tetherin to the TGN. Although the current data is consistent with a model whereby Tetherin continually cycles between the plasma membrane and the TGN with a fraction targeted for degradation, it still remains to be determined whether the protein is indeed recycling from the TGN to the cell surface. Interestingly, recent findings from Rollason and colleagues revealed that Tetherin localizes at the apical surface of polarized epithelial cells, where it interacts indirectly with the underlying actin cytoskeleton, thus providing a physical link between lipid rafts and the apical actin network in these cells [111]. Whether or not this property of Tetherin relates to its activity as an inhibitor of HIV-1 release remains unknown.

Tetherin ectodomain contains two N-linked glycosylation sites, three cysteine residues and a coiled-coil motif that mediates homodimerization (Figure 3B). Tetherin

glycosylation was shown to be important for proper transport and perhaps folding of the protein [115] but, however appeared dispensable for its activity as a restriction factor [97, 115, 116]. In contrast, the presence of cysteine residues in the extracellular domain of Tetherin was found required for the anti-HIV-1 function of the protein, as mutation of all three cysteine residues to alanine abrogated the antiviral activity without affecting Tetherin's expression at the cell surface [115, 116]. In that regard, it has been proposed that Tetherin forms a parallel dimeric coiled-coil that is stabilized by C53-C53, C63-C63 and C91-C91 disulfide bonds. Interactions within the coiled-coil domain and at least one disulfide bond formation are required for dimer stability and antiviral function [115, 116]. Recently, a partial structure of the extracellular domain of Tetherin has been solved by X-ray crystallography by three different groups [117-119]. All these studies support a model in which the primary functional state of Tetherin is a parallel dimeric disulfide-bound coiled-coil that displays flexibility at the N-terminus.

Tetherin directly cross-links HIV-1 virions on infected cell surface

Accumulating evidence suggest that Tetherin prevents viral release by directly cross-linking virions to host cell membranes. Additionally, restricted mature virus particles can also be found within intracellular endosomal structures [94], suggesting that following retention at the plasma membrane, tethered particles could be internalized and perhaps targeted for degradation in late endosomal compartments [120]. Consistent with a direct tethering mechanism, immuno-EM studies revealed that Tetherin is detected in the physical bridge between nascent virions and the plasma membrane as well as between virions tethered to each other [121, 122]. In fact, both biochemical and

immuno-EM evidence indicate that Tetherin is incorporated into virions [114, 115, 121, 122]. Importantly, the view that Tetherin itself, without the need of any specific cellular cofactor, is responsible for tethering virions on host cell surface, is supported by evidence from the Bieniasz group. They elegantly showed that protein configuration rather than primary sequences is critical for the tethering phenotype. Indeed, an entirely artificial Tetherin-like protein consisting of structurally similar domains from three unrelated proteins (TM from transferrin receptor, coiled-coil from distrophia myotonica protein kinase and GPI anchor from urokinase plasminogen activator receptor), inhibited the release of HIV-1 and Ebola virus-like-particles in a manner strikingly similar to Tetherin [115].

Although strong evidence for a direct tethering mechanism exists, the precise topology of the Tetherin dimers and the definition of the molecular interfaces retaining nascent virions at the cell surface remain open questions. For instance, it is not clear whether both membrane anchors remain in a single membrane surface and virions are retained by interaction between two Tetherin ectodomains (Figure 4A) or, if both Tetherin anchors can be incorporated in different membrane surfaces (Figure 4B). The fact that removal of either the cytoplasmic tail or the GPI anchor abrogates the antiviral activity of Tetherin [41, 115] supports a model whereby Tetherin is a parallel homodimer with one set of anchors in the host membrane and the other in the virion membrane (Figure 4B). This data also suggests that anti-parallel dimers with monomeric links to membranes (Figure 4C) do not exist or cannot effectively tether. It remains unclear whether the parallel dimers of Tetherin that span the plasma and viral

membranes have a preference for which membrane anchor ends up in the cell membrane or in the virion although there is some evidence that the TM anchor is favored in the virus membrane and the TM anchor in the cell [115]. While this membrane spanning model is consistent with the structural properties of Tetherin, there is, however two caveats to this model. First, treatment of tethered virions with the GPI anchor-cleaving enzyme, phosphatidyl inositol-specific phospholipase C (Pi-PLC), did not effectively release virions from the cell surface [122]. Second, based on the structural data, the maximum distance that can be bridged by Tetherin in the configuration outlined in figure 4 is about 17 nm [117-119]. However, the distance between the plasma membrane and tethered viral membranes observed in EM studies is frequently significantly larger than that [121, 122]. One alternative model to the membrane spanning domain model is that .individual Tetherin monomers are anchored at both end to the viral or plasma membranes but associates with each other through dimers or higher order structures (Figure 4A). Although this model explains a requirement for dimerization it does not explain why Tetherin requires both of its membrane anchor domains for its antiviral activity [41, 115]. Moreover, in this model, Tetherin would tether virus particles quite close to the plasma membrane (3-5 nm), a distance not supported by EM analysis [41, 115, 121, 122]. Clearly more studies are required to fully understand how Tetherin dimers tether newly formed virions to host cell surface.

Effect of Tetherin on HIV-1 cell-to-cell transmission

Increasing evidence suggests that HIV-1 can spread directly between T cells by forming a polarized supra-molecular structure termed a virological synapse, whereby

nascent virions are recruited to intimate adhesive contacts between infected and uninfected cells [55, 56]. Since Vpu-deficient HIV-1 particles accumulate at the cell surface as a result of Tetherin-mediated restriction, it is unclear whether these restricted virions can undergo cell-to-cell transfer or whether Tetherin restricts spread via virological synapses in addition to inhibiting the release of cell-free virions. Tetherin was recently reported to inhibit productive cell-to-cell transmission from Tetherin-positive donor cells (HEK 293T, HeLa and T-cells) to target lymphocytes without, however, preventing formation of virological synapses [123]. Interestingly, in presence of Tetherin, Vpu-deficient viruses accumulated at the synapses and were essentially transferred to target cells as large abnormal aggregates. These viral aggregates were found to be impaired in their ability to fuse to target cells and as such did not efficiently promote productive infection after transfer. These findings contrast with results recently reported by Jolly and colleagues, which indeed showed that Tetherin does not restrict virological synapse-mediated T-cell to T-cell transfer of Vpu-deficient HIV-1 [124]. In fact, this study showed that in some circumstances Tetherin might promote cell-to-cell transfer either by mediating the accumulation of virions at the cell surface or by regulating the integrity of the virological synapse. These latter findings are indeed consistent with a previous study that reported that *in vitro* selection of HIV-1 to spread via cell-to-cell contact in T-cell lines led to the emergence of viral variants with mutations in both the Env protein and in Vpu [125]. Likewise, earlier observations showed that WT and Vpu-deficient HIV-1 production usually peak at the same time during a spreading infection even though less Vpu-deficient virus is released in the extracellular milieu [28, 38]. The contrasting results obtained by Jolly and colleagues

[124] and Casartelli and colleagues [123] might reflect cell type dependent variations in the levels of Tetherin expression since the two studies used distinct Tetherin-expressing cell donor systems. It is indeed possible that under high Tetherin expression conditions such as those prevailing in macrophages and dendritic cells (DCs), HIV-1 cell-to-cell transmission might be impaired, whereas at lower levels, such as in T-lymphocytes, Tetherin may not restrict or may even contribute to cell-to-cell transmission. In that regard, Schindler and colleagues recently showed that a Vpu mutant (S52A) that displayed an impaired Tetherin antagonism, was unable to replicate efficiently in macrophages, while it spread as well as the wild type virus in *ex vivo* lymphoid tissue (HLT) or peripheral blood lymphocytes [103]. Therefore, one role of Vpu would be to maintain a balance between cell-free and cell-to-cell HIV-1 spread in the face of antiviral immune responses.

Potential roles of Tetherin in innate immunity

HIV-1 infection induces pDCs to produce a broad range of type I IFN through the activation of Toll-like receptors 7 and 9 (TLR7 and TLR9) [126, 127]. Type I IFN activates natural killer (NK) cells, myeloid DCs, T cells, B cells, and macrophages and induces expression of several hundreds of different IFN-stimulated genes, including Tetherin. In turn, it was recently reported that human Tetherin is the natural ligand for ILT7, a protein that is expressed exclusively on pDCs [107]. Binding of Tetherin to ILT7 was found to trigger a signaling pathway that negatively modulates TLR7- or TLR9-mediated type I IFN and proinflammatory cytokine secretion, thus establishing a negative feedback loop in which IFN-induced Tetherin binding to the ILT7-FcεRIγ

complex signals the inhibition of additional IFN production [107]. Therefore, in addition to its anti-viral function, Tetherin might also have a role in modulating pDC's IFN responses as well as inflammatory responses to virus infection. Whether or not Vpu interferes with this Tetherin immunomodulatory function during HIV-1 infection remains an open question.

HIV-1 riposte to Tetherin-mediated restriction

How Vpu counteracts the antiviral activity of Tetherin has attracted considerable attention since the discovery of the restriction factor. A key observation made early on was that Vpu downregulated Tetherin from the cell-surface [42]. This reduction of Tetherin levels at the cell surface correlated with the enhancement of HIV-1 particle release observed upon Vpu expression. Since Tetherin restricts HIV-1 virus particle release at the plasma membrane, removal of Tetherin from its site of tethering action represents an intuitive model through which Vpu could counteract this cellular restriction, although this model has been challenged [102]. Reduction of Tetherin at the cell-surface is likely to prevent cross-linking of cellular and viral membranes, which implies that virions released from Vpu-expressing cells would be devoid of Tetherin molecules. Although this notion is supported by the decreased co-localization between Tetherin and Gag in presence of Vpu [41, 96, 128], biochemical analyses revealed that Vpu expression decreases only partially Tetherin accumulation in released virus particles [115, 121, 122]. Furthermore, immuno-EM studies showed that virions produced from Vpu-expressing cells still incorporate Tetherin albeit at a lower density

[114, 122]. These results suggest that either a threshold level of virion-associated Tetherin is required to mediate the restriction or alternatively removal of Tetherin from specific plasma membrane microdomains could underlie the mechanism by which Vpu antagonizes Tetherin. In that regard, Habermann and colleagues reported that Vpu would be more efficient at downregulating Tetherin outside HIV-1 assembly sites [114], thus reducing the ability of the plasma membrane to retain fully released Tetherin-containing virions. Interestingly, a recent study provided evidence that partitioning of Vpu in lipid rafts would be required to promote virus particle release [129]. It will be important to determine whether Vpu targets a pool of Tetherin located in specific microdomains of the plasma membrane or whether the viral antagonist targets the restriction factor independently of its distribution at the plasma membrane.

Vpu, a versatile Tetherin antagonist

Several mechanisms have been proposed to explain how Vpu can downregulate Tetherin from the cell surface and as a result antagonize its antiviral activity on HIV-1 release. These include proteasomal or endo-lysosomal degradation of the restriction factor and/or alteration of its trafficking toward the cell surface, resulting in intracellular sequestration. Although mechanistically distinct, these modes of antagonism all rely on the ability of Vpu to bind Tetherin since the restriction imposed by Tetherin on viral particle release can be restored by mutations disrupting their mutual association [130-134]. Such mutations have been all mapped so far to either Vpu or Tetherin TM domains, thus strongly suggesting that the two proteins associate through their

respective TM regions [131, 132, 135-137]. Evidence for each of the proposed Vpu anti-Tetherin mechanisms are reviewed and discussed below.

i) Vpu-mediated degradation of Tetherin. Vpu expression was found to decrease the total steady-state levels of Tetherin [128, 130, 134, 138, 139]. This depletion occurs at a post-transcriptional step since levels of Tetherin transcript are not affected by Vpu [130, 134]. Importantly, pulse-chase experiments revealed that Vpu accelerates the turnover of endogenous Tetherin [130, 131, 139]. As observed with Vpu-mediated CD4 degradation, recruitment of β-TrCP was found to be required for Vpu-mediated Tetherin degradation since phosphorylation-deficient Vpu mutants did not alter Tetherin turnover [130, 131]. Likewise, siRNA-mediated depletion of β-TrCP or inactivation of the $SCF^{\beta\text{-}TrCP}$ E3 Ub ligase by overexpression of a DN mutant of β-TrCP, β-TrCPΔF, which binds Vpu but is unable to link it to the $SCF^{\beta\text{-}TrCP}$ E3 ligase complex, abolished Vpu-mediated Tetherin degradation, indicating that recruitment of the $SCF^{\beta\text{-}TrCP}$ complex is critical for Vpu-mediated Tetherin degradation [128, 130, 133, 134]. In that regard, siRNA depletion experiments revealed that Vpu takes specifically advantage of the cytoplasmic β-TrCP-2 isoform, but not the nuclear β-TrCP-1, to achieve Tetherin degradation [128, 130, 133]. Finally, complementing this set of functional evidence, β-TrCP was found in a ternary complex together with Vpu and Tetherin [133, 134], but was not critical for the association of Vpu to Tetherin [130].

This degradative process was initially thought to be proteasomal in nature since long treatment with proteasomal inhibitors prevented exogenously-expressed Tetherin degradation in presence of Vpu in HEK 293T cells [134, 138-140]. Furthermore, overexpression of Ub K48R, a DN mutant of Ub, which interferes with

polyubiquitination, prevented Tetherin degradation [134]. Consistently, Vpu was found to promote the β-TrCP-mediated ubiquitination of Tetherin cytoplasmic tail on serine, threonine, lysine and cysteine residues at least in HEK293T [141] (Figure 3B). Interestingly, depletion of the ERAD component, AAA ATPase p97, affected Vpu-mediated Tetherin degradation [134], suggesting that Vpu could mediate Tetherin proteasomal degradation in the ER through an ERAD-like process. However, there are several caveats with the data supporting proteosomal degradation. First, the results were often obtained by overexpression of epitope tagged-Tetherin in non restrictive HEK 293T cells, an experimental setting which results in the accumulation of immature Tetherin molecule within the endoplasmic reticulum [116]. Second, long exposure with proteasome inhibitors or Ub K48R overexpression are not always an unambiguous evidence of ubiquitin–proteasome degradation since these processes can deplete free Ub, thus affecting indirectly Ub-dependent trafficking and/or lysosomal degradation [142, 143]. Accordingly, inhibitors of lysosomal sorting and acidification, such as bafilomycin A and concanamycin were found to inhibit Vpu-mediated Tetherin degradation and could interfere with Tetherin downregulation from the cell-surface [128, 130]. This type of degradation is indeed consistent with the recent observation that Tetherin undergoes monoubiquitination on cytoplasmic lysines 18 and/or 21 in presence of Vpu [144]. Taken together, these findings support a model whereby Tetherin undergoes degradation in lysosomes in presence of Vpu. However, proteasomal degradation cannot be completely excluded, at this point.

ii) Vpu-mediated intracellular sequestration of Tetherin. Although Vpu expression induces Tetherin degradation in most cellular systems studied to date, several lines of

evidence suggest that degradation of Tetherin *per se* cannot entirely account for Vpu-mediated Tetherin antagonism. For instance, Vpu was found to decrease total cellular Tetherin to a lesser extent than cell-surface Tetherin in HeLa cells [128]. Furthermore, Vpu mutants that contain mutations in the $DS^{P}G\Phi XS^{P}$ β-TrCP recognition motif that render them deficient for directing β-TrCP-dependent degradation of Tetherin are still able to partially [39, 42, 128, 130, 134] or in some instances to totally [24, 102, 103] overcome the Tetherin-mediated particle release restriction. Moreover, Vpu-mediated Tetherin degradation is a relatively slow process [130, 131] (half-life of ~8h is decreased by ~2-fold in presence of Vpu) as compared to the efficient CD4 receptor degradation induced by Vpu (half-life of ~6h is decreased by ~25-fold in presence of Vpu [36]). There is now increasing evidence for the existence of an anti-Tetherin mechanism that is distinct from degradation of the restriction factor. In that regard, recent evidence showed that Vpu did not promote Tetherin endocytosis [128, 131], but rather induced a re-localization of the antiviral factor to a perinuclear compartment that extensively overlapped with the TGN marker, TGN46, and Vpu itself, thus leading to a specific removal of cell-surface Tetherin [131, 144, 145]. These findings are indeed consistent with previous data showing that proper distribution of Vpu in the TGN is critical to overcome Tetherin restriction on HIV-1 release [29]. Overall, it appears that Vpu may antagonize Tetherin, at least in part, by sequestering the protein intracellularly through alteration of its normal anterograde trafficking. Importantly, mutations of the putative Ub-acceptor lysine residues, K18 and K21, in the cytosolic tail of Tetherin (Figure 1B), completely abolished Vpu-mediated monoubiquitination [144] and degradation [140] of the restriction factor without, however, affecting its antagonism by

Vpu. These findings provide genetic evidence that Tetherin ubiquitination/degradation and Tetherin antagonism may be two separable Vpu activities. Moreover, since the lysine-less Tetherin mutant was still found to be downregulated at the cell surface in presence of Vpu, it appears that Tetherin downregulation and ubiquitination/degradation may not be as strictly linked during Vpu-mediated antagonism [140, 144]. These unexpected results contrast, however, with previous data showing that Vpu mutants that are unable to recruit β-TrCP (and as such are predicted to be unable to mediate Tetherin ubiquitination/degradation), such as phosphorylation-deficient Vpu mutants, display an attenuated Tetherin antagonism (~ 50% of WT Vpu) [128, 131, 134, 146]. Likewise, depletion of β-TrCP-2 or expression of a DN mutant of β-TrCP, β-TrCPΔF, could partially inhibit Vpu-mediated Tetherin antagonism [128, 130, 134]. The recent results of Tokarev and colleagues indicating that β-TrCP-mediated polyubiquitination of the Tetherin cytoplasmic tail specifically on serine and threonine residues is critical for Vpu-mediated Tetherin antagonism, while having little effect on the stability of the restriction factor in presence of Vpu, might provide some clues on the role β-TrCP on Tetherin antagonism. Based on these results, it is indeed possible that Vpu-mediated polyubiquitination of Tetherin via β-TrCP, might enhance the sequestration of the restriction factor without necessarily leading to Tetherin degradation [141]. Taken together, these recent findings suggest that Tetherin antagonism by Vpu precedes and may not be dependent on degradation of the restriction factor, but rather results in the sequestration of Tetherin away from budding virions (Figure 5). Clearly more studies are needed to evaluate the contribution of Tetherin ubiquitination and degradation in the

mechanism through which Vpu antagonizes the restriction on HIV-1 particle release especially in cells that are natural target for infection.

Although current evidence is consistent with a model whereby antagonism of Tetherin by Vpu involves sequestration of the restriction factor in a perinuclear compartment, it is unclear whether Vpu subverts recycling and/or other intracellular sorting steps of Tetherin. Mutation of the overlapping Tyrosine (Tyr6 and Tyr8) trafficking signals in the Tetherin cytoplasmic tail (Figure 1B), which blocks the protein natural pathway of endocytosis, did not abolish the sensitivity to Vpu in non-restrictive cells (HEK 293T, HT1080) transiently [131, 133, 145] or stably expressing the Tetherin mutant [140]. Thus, it appears that Tetherin intracellular sequestration may occur before endocytosis of the restriction factor from the cell surface and as such involve newly synthesized Tetherin en route to the PM [131, 133]. However, it cannot completely be ruled-out that Vpu could interact with endocytosed Tetherin and prevent its recycling back to the cell surface since previous data demonstrated a requirement for the recycling endosomes in Vpu function [30] and recent studies reported that AP2 depletion [128] or over-expression of dominant DN mutant of Dynamin [133] could partially interfere with Vpu-mediated downregulation of Tetherin from the cell surface. Moreover, Tetherin is accumulating in presence of Vpu in structures just beneath the plasma membrane that could correspond to early and/or recycling endosomes [114]. Indeed, since Vpu is produced from a Rev-regulated gene expressed late during the virus life cycle, the direct removal of Tetherin from the plasma membrane via endosomal trafficking may be critical to ensure a rapid and efficient neutralization of Tetherin antiviral activity.

Tetherin, a common enemy

While HIV-1 Vpu was the first anti-Tetherin factor discovered, there is now a growing list of virus-encoded proteins harboring anti-Tetherin activities. Namely, KSHV K5, HIV-2 Env, and Ebola gp were found to overcome human Tetherin antiviral activity apparently through distinct mechanisms [98, 99, 144, 147-149] (Table 1). Nef from SIVcpz, SIVgor, SIVagm and SIVsmm, Env from SIVtan (SIV from Tantalus monkey) and Vpu from SIVgsn, SIVmon and SIVmus were also reported to antagonize Tetherin from their corresponding host [150-153]. Their strategies differ, though. The KSHV K5 protein, which is a membrane associated Ring-CH (MARCH) Ub ligase, induces a species-specific downregulation of human Tetherin from the cell surface by inducing ubiquitination of Tetherin cytoplasmic lysines and targeting the restriction factor to lysosomes for degradation [99, 144]. In contrast, HIV-2 Env or SIVtan Env do not display any ability to induce Tetherin degradation [145, 147-149]. Instead, these envelope proteins redistribute Tetherin from the plasma membrane to a perinuclear compartment that appears to correspond to the TGN most probably by a sequestration mechanism [145, 148, 149]. However, in contrast to Vpu, the determinants controlling Tetherin sensitivity to HIV-2 and SIVtan Env proteins are located in the restriction factor ectodomain [148, 149]. Studies on HIV-2, SIVtan Env and KSHV K5 indicate that both sequestration and degradation represent potent mechanisms by which Tetherin antiviral activity can be overcomed. The fact that HIV-1 Vpu can exploit both mechanisms confirms its great versatility and might perhaps explain the efficient

counteraction that it displays against human Tetherin. Although the precise mechanism underlying Tetherin antagonism by Nef remains to be determined, it was found that SIVmac Nef downregulates rhesus Tetherin from the cell surface and as shown for Vpu-mediated Tetherin antagonism, this downregulation correlated with enhanced SIVmac particle release [150, 152]. Finally, the antagonism of human Tetherin by Ebola gp is still not entirely understood. The case of Ebola gp is particularly interesting since it is the only known anti-Tetherin factor that does not appear to downregulate Tetherin from the cell surface to promote the release of Ebola virus-like particle [147]. Even more surprising, interaction between Tetherin and Ebola gp would not require any specific sequence, a feature that is unique among Tetherin antagonists identified to date [147]. Therefore, it appears that Ebola virus gp might use a novel mechanism to neutralize Tetherin restriction. Clearly, comparative studies of these anti-Tetherin viral factors will not only further our understanding of their mechanisms of action but will also provide key information on host cell processes involved in Tetherin antagonism.

Role of Vpu in primate lentivirus cross-species transmission and the emergence of pandemic HIV-1 strains

Genes encoding for restriction factor, such as TRIM5-α, APOBEC3G and Tetherin undergo rapid evolution, a process also known as positive selection, most likely

as the result of the selective pressure imposed by new emerging viral pathogens or to escape from viral antagonists during the millions of years of virus-host co-evolution [154-156]. Consequently, these restriction factors display a high degree of sequence divergence and constitute potent limiting barriers to virus cross-species transmission because viral antagonists usually function in a species-specific manner. In fact, sequence alignment of Tetherin from different primate species reveals important selective genetic changes that lead to amino-acid substitution or deletion primarily in the cytoplasmic and TM domains of the protein, regions that are now known to be targeted by Tetherin antagonists [138, 156, 157] (Figure 3B).

These genetic changes in Tetherin sequence have shaped the evolution of primate lentiviruses and influenced at least in part their ability to transmit across species. There is evidence suggesting that SIVcpz, the precursor of HIV-1, results from recombination events between the precursors of the SIVgsn/mon/mus and the SIV from red capped mangabeys (SIVrcm) lineages [158] (Figure 6). The precursor of SIVgsn/mon/mus that contributed to the 3'-half of the SIVcpz/HIV-1 genome, most likely harbored a *vpu* gene product able to both induce CD4 degradation and antagonize Tetherin since all descendants do. Since it is believed that the ancestor of the SIVrcm lineage used Nef to antagonize Tetherin, given that this lineage does not encode a *vpu* gene, the chimeric virus that gave rise to SIVcpz contained two potential Tetherin antagonists. However, the SIVcpz Vpu protein inherited from the SIVgsn/mon/mus lineage is devoid of any activity against the chimpanzee and human Tetherin [151, 153, 157].

The resistance displayed by the chimpanzee Tetherin to the Vpu protein originating from the SIVgsn/mon/mus lineage results from the high sequence variability in the TM domain of Tetherin reported between non-hominoid primates (monkeys such as rhesus or African green monkey) and hominoid primates (such as chimpanzees, gorillas and humans) [151, 156, 157] (Figure 1B). Indeed, this TM domain was demonstrated to be the site conferring Vpu susceptibility and binding [131, 132, 136, 138, 156]. As a result Nef, and not Vpu, evolved to become an effective Tetherin antagonist in SIVcpz-infected chimpanzee, most likely because the cytoplasmic domain sequence DDIWK targeted by Nef is somewhat less divergent between chimpanzee and monkey than the TM domain targeted by Vpu [150-153, 157]. The deletion of sequences, highly subjected to adaptation and recognized by Nef, in human Tetherin is hypothesized to be the result of a previous encounter with a viral pathogen during human evolution that used a Nef-like protein, if not Nef itself, to antagonize Tetherin [157]. Conversely, few differences were observed in the TM domain of Tetherin between chimpanzee and human Tetherin, suggesting that Vpu has not driven Tetherin adaptation for a long period in primate evolution and accounting for the ability of the HIV-1 Vpu to counteract the chimpanzee Tetherin [157] (Figure 3B).

The inability to use Nef as a human Tetherin antagonist following SIVcpz cross-species transmission to human has likely led SIVcpz to proceed to a "neofunctionalization" of its initially incompetent Vpu protein in order to efficiently overcome the restriction imposed by human Tetherin (Figure 6). In support of this adaptation mechanism, it was recently reported that the differential ability of HIV-1 and SIVcpz Vpu to antagonize human Tetherin could be mapped to two regions of the TM

domain of Vpu (amino-acid residues 1-8 and 14-22). Importantly, SIVcpz Vpu was completely able to overcome the human Tetherin restriction when these two regions were substituted for those from HIV-1 Vpu [157]. Furthermore, analysis of a SIVcpz strain (LB7) that represents the closest relative to HIV-1 group M revealed that the LB7 Vpu allele is predicted to need 7 minimal adaptations within these two critical regions of the TM domain to gain the ability to antagonize human Tetherin [157]. Consistent with these findings, mutagenesis of the prototypical NL4.3 Vpu TM domain identified three amino acid positions A14, W22 and, to a lesser extent A18, as Vpu residues critical for Tetherin binding and antagonism [135] (Figure 1B). Interestingly, these residues are predicted to align on the same face of the Vpu TM α-helix and as such might potentially be part of the interface that directly or indirectly interacts with the TM domain of human Tetherin.

The adaptation towards Vpu specifically shaped to counteract the hominoid Tetherin is at the center of the lineage-specific anti-Tetherin activity harbored by HIV-1 Vpu [138, 151, 156]. In line with this observation, substituting the TM domain of the human Tetherin with that from African green monkey or rhesus monkey Tetherin abrogated the chimeric protein sensitivity and binding to HIV-1 Vpu [131, 132, 156]. Indeed, analysis of the residues within the TM domain of human Tetherin, which determines the susceptibility to HIV-1 Vpu-mediated antagonism, revealed that one single substitution mutation for a residue found in the monkey Tetherin (T45I) combined to a deletion of two amino acids (G25,I26), absent from agm Tetherin, resulted in an efficient restriction of wild-type HIV-1 [156]. More recently, using a live cell based assay to monitor interaction, Kobayashi and colleagues performed a detailed

analysis of the amino-acid residues within the TM domain of human Tetherin that are involved in Vpu binding [136]. This study identified three amino acid residues (I34, L37 and L41) as critical determinants for Vpu interaction and susceptibility [136] (Figure 3B). Furthermore, consistent with previous studies [132, 138, 156, 159], they found that the integrity of the $_{22}$L-L-L-G-I$_{26}$ amino acid sequence, which is indeed altered by a deletion of two amino acids in agm/rhesus Tetherins (deletion of L22,L23 or L24,G25 or G25,I26, depending on the alignment), and/or conservation of a threonine at position 45 are required for the antagonism by Vpu (Figure 3B). On the basis of computer-assisted structural modeling and mutagenesis data, this study proposes that alignment of amino-acids of I34, I37, L41 and T45 on the same helical face in the TM domain, a positioning apparently governed by the presence of L22 and L23 (or perhaps the integrity of the $_{22}$L-L-L-G-I$_{26}$ amino-acid sequence), is crucial for human Tetherin antagonism by Vpu. Intriguingly, while mutation at position T45 affected the sensitivity of human Tetherin to Vpu, it did not significantly affect the formation of a Tetherin-Vpu complex, suggesting that interaction of Vpu to Tetherin alone is not sufficient to mediate Tetherin antagonism. Further studies will be necessary to address this potentially important issue.

Phylogenetic analyses indicate that at least three independent cross-species transmissions of SIVcpz gave rise to HIV-1 group M (main), N (non-M, non-O) and O (outlier) [160]. The functional properties acquired by Vpu proteins during these three independent transmissions of SIVcpz to humans have been recently analyzed and showed to have perhaps determined the propensity of these different groups to spread efficiently [151]. The Vpu protein of the HIV-1 M group responsible for the global

HIV-1 pandemic was found to efficiently antagonize human Tetherin and to induce CD4 degradation. In contrast, the non-pandemic HIV-1 group O Vpu was found to have preserved its ability to mediate CD4 degradation but displayed a very weak activity against human Tetherin, while the rare HIV-1 group N gained some anti-human Tetherin activity but lost its ability to degrade CD4 (Figure 6). These observations have led Kirchhoff and colleagues to propose that the acquisition of a fully competent Vpu protein able to antagonize Tetherin and mediate CD4 degradation may have facilitated the global spread of the HIV-1 M group, as opposed to the N and O groups whose distribution has remained very limited and focused to West Africa [151]. Nevertheless, the fact that HIV-1 from the N and O groups are still able to cause AIDS in infected individuals suggests that Vpu-mediated CD4 degradation and Tetherin antagonism may not be biological activities required for HIV-1 dissemination within an infected individual but rather functions that are critical for efficient transmission between individuals. A similar parallel can also be established with HIV-2, whose geographical distribution has been limited in comparison to HIV-1 [161]. As discussed previously, HIV-2 antagonizes human Tetherin using its Env glycoprotein since its genome does not encode a Vpu protein and its Nef protein cannot counteract human Tetherin [145, 148]. Interestingly, HIV-2 Env was found to antagonize Tetherin less efficiently than HIV-1 Vpu, perhaps, because its mode of action solely involves a trapping of the restriction factor in the TGN [148]. However, the fact that this virus uses a structural protein to both downregulate CD4 (through complex formation in the ER) and Tetherin, could have also entailed a greater fitness cost to the virus than the use of accessory proteins such as Vpu or Nef, thus explaining in part its attenuated virulence in comparison to

HIV-1 [161]. Therefore, it will be interesting to assess in the future whether Tetherin antagonism and/or CD4 degradation promote human-to-human HIV-1 transmission, perhaps by increasing the secretion of infectious virions into the genital fluids.

Conclusions and perspectives

As molecular and cellular details about the mechanisms through which Vpu mediates CD4 degradation and antagonizes Tetherin emerge, it is becoming increasingly clear that the acquisition of a multifunctional Vpu protein by HIV-1 has played a crucial role in the virulence of this virus. Although the role of Vpu as an antagonist of Tetherin has obvious implications on virus secretion and potentially on the transmission efficiency from human to human, its effect on the dissemination of HIV-1 following establishment of infection is less clear, especially since the potential restricting effect of Tetherin imposed on cell-to-cell viral transmission does not appear to significantly interfere with viral spread at least in T lymphocytes [124]. It is possible that once infection is established in lymphoid tissue, such as the gut-associated lymphoid tissue (GALT), a major site of HIV-1 replication, cell-to-cell transfer may be an important mode of HIV-1 dissemination as opposed to a transmission via cell-free virus. One might speculate that Tetherin antagonism by Vpu may be less critical at this point. More studies will be required in the future to address this issue and to assess whether enhanced cell-to-cell transmission might not be a way for HIV-1 to escape or even tolerate Tetherin restriction. The contribution of Vpu-mediated CD4 degradation to

HIV-1 spread remains unclear and will need to be further addressed. As discusses above, previous studies have suggested that this function would facilitate virion assembly by releasing Env precursor gp160 trapped with newly synthesized CD4 in the ER and maintain the release of fully infectious virions (reviewed in [21]). In that regard, experiments using the simian-human immunodeficiency virus (SHIV) model in pigtail macaques, a host that does not express a Tetherin protein susceptible to HIV-1 Vpu, suggested that the ability of Vpu to downregulation CD4 expression directly correlated with the progression of disease in this animal model [162, 163]. Macaques inoculated with SHIV expressing a Vpu protein with mutations of the two phosphoserines involved in the recruitment of β-TrCP did not show any evidence of CD4+ T cell depletion and maintained significantly lower viral loads than macaques inoculated with parental SHIV. These findings obtained in *vivo* suggest that Vpu-mediated CD4 degradation may have an important role in disease progression. However, we cannot rule-out that Vpu may have additional functions that are important for viral pathogenesis. In that regard, it is interesting to note that a recent study reported a novel activity of Vpu, that is the downregulation of CD1d at the cell surface of infected DCs and the impairment of CD1d-mediated natural killer T (NKT) cell activation [164]. CD1d is a membrane-associated protein that is expressed at the cell surface of antigen presenting cells (APCs), such as monocytes, macrophages and DCs. This protein is responsible for the presentation of exogenous pathogen-induced lipid antigens to NKT cells expressing an invariant αβT cell receptor and in doing so triggers the mutual activation of both APCs and NKT cells and the subsequent induction of cellular immune responses. Analysis of the mechanism of Vpu-mediated CD1d downregulation revealed that Vpu does not

enhance constitutive endocytosis of CD1d nor induces its degradation. Rather, Vpu was found to interact with CD1d and inhibit its recycling from endosomal compartments to the plasma membrane by sequestering CD1d in an intracellular compartment. Targeting of membrane-associated surface proteins by Vpu does not appear to be limited to CD4, Tetherin and CD1d since recent evidence indicates that Vpu can also downregulate the NK-T and B cell antigen (NTB-A) co-activator at the surface of infected cells and as a result interferes with the degranulation of NK cells [165]. NTB-A is type 1 membrane-associated protein that belongs to the signaling lymphocytic activation molecules (SLAM) family of receptors that functions as a homotypic ligand-activation NK receptor pair in the induction of NK cell responses. Interestingly, NTB-A downregulation by Vpu was found to be distinct from CD4 and Tetherin downregulation since Vpu did not alter the steady-state levels of NTB-A and did not rely on the recruitment of β-TrCP to reduce cell surface NTB-A. Like with CD1d and Tetherin, Vpu did not enhance NTB-A endocytosis but rather appeared to interact with co-activator molecules through its TM domain. These findings suggest that Vpu might also downregulate NTB-A through alteration of the protein trafficking and/or recycling, which would lead to the sequestration of the molecule in an intracellular compartment. Importantly, Vpu-mediated downregulation of NTB-A was found to interfere specifically with NK cell degranulation, thus ultimately protecting infected cells from NK cell-mediated lysis.

The fact that Vpu is now reported to target, in addition to CD4, three membrane-associated cell surface proteins involved in various aspects of the innate immune response raises the possibility that Vpu may be a key factor used by HIV-1 to evade

innate immunity. While it may be too soon to call Vpu a virulence factor, the recent discoveries presented in this review tend to suggest that this accessory protein provides HIV-1 with unique properties at the level of virus transmission and escape from host defenses. Further research in these areas will not only provide exciting new insight into the role of Vpu in HIV-1 pathogenesis but may also lead to new therapeutic intervention for treating HIV-1 infection.

Acknowledgments

We apologize to the authors of many interesting studies that could not be cited due to space limitations. EAC is recipient of the Canada Research Chair in Human Retrovirology and is supported by grants from the Canadian Institute of Health Research (CIHR) and the Fonds de Recherches en Santé du Québec (FRSQ).

Authors' contributions

MD, MB, CP, EAC drafted sections of the text, edited each other's contributions, read and approved the final manuscript.

Competing interests

The authors declare that they have no competing interests.

References

1. Goff SP: Host factors exploited by retroviruses. *Nat Rev Microbiol* 2007, 5:253-263.

2. Peterlin BM, Price DH: Controlling the elongation phase of transcription with P-TEFb. *Mol Cell* 2006, 23:297-305.

3. Morita E, Sundquist WI: Retrovirus budding. *Annu Rev Cell Dev Biol* 2004, 20:395-425.

4. Kirchhoff F: Immune evasion and counteraction of restriction factors by HIV-1 and other primate lentiviruses. *Cell Host Microbe* 2010, 8:55-67.

5. Malim MH, Emerman M: HIV-1 accessory proteins--ensuring viral survival in a hostile environment. *Cell Host Microbe* 2008, 3:388-398.

6. Cohen EA, Terwilliger EF, Sodroski JG, Haseltine WA: Identification of a protein encoded by the vpu gene of HIV-1. *Nature* 1988, 334:532-534.

7. Strebel K, Klimkait T, Martin MA: A novel gene of HIV-1, vpu, and its 16-kilodalton product. *Science* 1988, 241:1221-1223.

8. Barlow KL, Ajao AO, Clewley JP: Characterization of a novel simian immunodeficiency virus (SIVmonNG1) genome sequence from a mona monkey (Cercopithecus mona). *J Virol* 2003, 77:6879-6888.

9. Courgnaud V, Salemi M, Pourrut X, Mpoudi-Ngole E, Abela B, Auzel P, Bibollet-Ruche F, Hahn B, Vandamme AM, Delaporte E, Peeters M: Characterization of a novel simian immunodeficiency virus with a vpu gene from greater spot-nosed monkeys (Cercopithecus nictitans) provides new insights into simian/human immunodeficiency virus phylogeny. *J Virol* 2002, 76:8298-8309.

10. Courgnaud V, Abela B, Pourrut X, Mpoudi-Ngole E, Loul S, Delaporte E, Peeters M: Identification of a new simian immunodeficiency virus lineage with a vpu gene present among different cercopithecus monkeys (C. mona, C. cephus, and C. nictitans) from Cameroon. *J Virol* 2003, 77:12523-12534.

11. Dazza MC, Ekwalanga M, Nende M, Shamamba KB, Bitshi P, Paraskevis D, Saragosti S: Characterization of a novel vpu-harboring simian immunodeficiency virus from a Dent's Mona monkey (Cercopithecus mona denti). *J Virol* 2005, 79:8560-8571.

12. Takehisa J, Kraus MH, Ayouba A, Bailes E, Van Heuverswyn F, Decker JM, Li Y, Rudicell RS, Learn GH, Neel C, et al: Origin and biology of simian immunodeficiency virus in wild-living western gorillas. *J Virol* 2009, 83:1635-1648.

13. Huet T, Cheynier R, Meyerhans A, Roelants G, Wain-Hobson S: Genetic organization of a chimpanzee lentivirus related to HIV-1. *Nature* 1990, 345:356-359.

14. Maldarelli F, Chen MY, Willey RL, Strebel K: Human immunodeficiency virus type 1 Vpu protein is an oligomeric type I integral membrane protein. *J Virol* 1993, 67:5056-5061.

15. Schwartz S, Felber BK, Fenyo EM, Pavlakis GN: Env and Vpu proteins of human immunodeficiency virus type 1 are produced from multiple bicistronic mRNAs. *J Virol* 1990, 64:5448-5456.

16. Wray V, Federau T, Henklein P, Klabunde S, Kunert O, Schomburg D, Schubert U: Solution structure of the hydrophilic region of HIV-1 encoded virus protein U (Vpu) by CD and 1H NMR spectroscopy. *Int J Pept Protein Res* 1995, 45:35-43.

17. Park SH, Opella SJ: Tilt angle of a trans-membrane helix is determined by hydrophobic mismatch. *J Mol Biol* 2005, 350:310-318.

18. Park SH, Mrse AA, Nevzorov AA, Mesleh MF, Oblatt-Montal M, Montal M, Opella SJ: Three-dimensional structure of the channel-forming trans-membrane domain of virus protein "u" (Vpu) from HIV-1. *J Mol Biol* 2003, 333:409-424.

19. Hussain A, Das SR, Tanwar C, Jameel S: Oligomerization of the human immunodeficiency virus type 1 (HIV-1) Vpu protein--a genetic, biochemical and biophysical analysis. *Virol J* 2007, 4:81.

20. Lopez CF, Montal M, Blasie JK, Klein ML, Moore PB: Molecular dynamics investigation of membrane-bound bundles of the channel-forming transmembrane domain of viral protein U from the human immunodeficiency virus HIV-1. *Biophys J* 2002, 83:1259-1267.

21. Ruiz A, Guatelli JC, Stephens EB: The Vpu protein: new concepts in virus release and CD4 down-modulation. *Curr HIV Res* 2010, 8:240-252.

22. Federau T, Schubert U, Flossdorf J, Henklein P, Schomburg D, Wray V: Solution structure of the cytoplasmic domain of the human immunodeficiency virus type 1 encoded virus protein U (Vpu). *Int J Pept Protein Res* 1996, 47:297-310.

23. Henklein P, Schubert U, Kunert O, Klabunde S, Wray V, Kloppel KD, Kiess M, Portsmann T, Schomburg D: Synthesis and characterization of the hydrophilic C-terminal domain of the human immunodeficiency virus type 1-encoded virus protein U (Vpu). *Pept Res* 1993, 6:79-87.

24. Friborg J, Ladha A, Gottlinger H, Haseltine WA, Cohen EA: Functional analysis of the phosphorylation sites on the human immunodeficiency virus type 1 Vpu protein. *J Acquir Immune Defic Syndr Hum Retrovirol* 1995, 8:10-22.

25. Schubert U, Schneider T, Henklein P, Hoffmann K, Berthold E, Hauser H, Pauli G, Porstmann T: Human-immunodeficiency-virus-type-1-encoded Vpu protein is phosphorylated by casein kinase II. *Eur J Biochem* 1992, 204:875-883.

26. Schubert U, Strebel K: Differential activities of the human immunodeficiency virus type 1-encoded Vpu protein are regulated by phosphorylation and occur in different cellular compartments. *J Virol* 1994, 68:2260-2271.

27. Schubert U, Henklein P, Boldyreff B, Wingender E, Strebel K, Porstmann T: The human immunodeficiency virus type 1 encoded Vpu protein is phosphorylated by casein kinase-2 (CK-2) at positions Ser52 and Ser56 within a predicted alpha-helix-turn-alpha-helix-motif. *J Mol Biol* 1994, 236:16-25.

28. Klimkait T, Strebel K, Hoggan MD, Martin MA, Orenstein JM: The human immunodeficiency virus type 1-specific protein vpu is required for efficient virus maturation and release. *J Virol* 1990, 64:621-629.

29. Dube M, Roy BB, Guiot-Guillain P, Mercier J, Binette J, Leung G, Cohen EA: Suppression of Tetherin-restricting activity upon human immunodeficiency virus type 1 particle release correlates with localization of Vpu in the trans-Golgi network. *J Virol* 2009, 83:4574-4590.

30. Varthakavi V, Smith RM, Martin KL, Derdowski A, Lapierre LA, Goldenring JR, Spearman P: The pericentriolar recycling endosome plays a key role in Vpu-mediated enhancement of HIV-1 particle release. *Traffic* 2006, 7:298-307.

31. Pacyniak E, Gomez ML, Gomez LM, Mulcahy ER, Jackson M, Hout DR, Wisdom BJ, Stephens EB: Identification of a region within the cytoplasmic domain of the subtype B Vpu protein of human immunodeficiency virus type 1 (HIV-1) that is responsible for retention in the golgi complex and its absence in the Vpu protein from a subtype C HIV-1. *AIDS Res Hum Retroviruses* 2005, 21:379-394.

32. Ruiz A, Hill MS, Schmitt K, Guatelli J, Stephens EB: Requirements of the membrane proximal tyrosine and dileucine-based sorting signals for efficient transport of the subtype C Vpu protein to the plasma membrane and in virus release. *Virology* 2008, 378:58-68.

33. Gomez LM, Pacyniak E, Flick M, Hout DR, Gomez ML, Nerrienet E, Ayouba A, Santiago ML, Hahn BH, Stephens EB: Vpu-mediated CD4 down-regulation and degradation is conserved among highly divergent SIV(cpz) strains. *Virology* 2005, 335:46-60.

34. McCormick-Davis C, Dalton SB, Singh DK, Stephens EB: Comparison of Vpu sequences from diverse geographical isolates of HIV type 1 identifies the presence of highly variable domains, additional invariant amino acids, and a signature sequence motif common to subtype C isolates. *AIDS Res Hum Retroviruses* 2000, 16:1089-1095.

35. Bonifacino JS, Traub LM: Signals for sorting of transmembrane proteins to endosomes and lysosomes. *Annu Rev Biochem* 2003, 72:395-447.

36. Willey RL, Maldarelli F, Martin MA, Strebel K: Human immunodeficiency virus type 1 Vpu protein induces rapid degradation of CD4. *J Virol* 1992, 66:7193-7200.

37. Schubert U, Anton LC, Bacik I, Cox JH, Bour S, Bennink JR, Orlowski M, Strebel K, Yewdell JW: CD4 glycoprotein degradation induced by human immunodeficiency virus type 1 Vpu protein requires the function of proteasomes and the ubiquitin-conjugating pathway. *J Virol* 1998, 72:2280-2288.

38. Terwilliger EF, Cohen EA, Lu YC, Sodroski JG, Haseltine WA: Functional role of human immunodeficiency virus type 1 vpu. *Proc Natl Acad Sci U S A* 1989, 86:5163-5167.

39. Schubert U, Clouse KA, Strebel K: Augmentation of virus secretion by the human immunodeficiency virus type 1 Vpu protein is cell type independent and occurs in cultured human primary macrophages and lymphocytes. *J Virol* 1995, 69:7699-7711.

40. Gottlinger HG, Dorfman T, Cohen EA, Haseltine WA: Vpu protein of human immunodeficiency virus type 1 enhances the release of capsids produced by gag gene constructs of widely divergent retroviruses. *Proc Natl Acad Sci U S A* 1993, 90:7381-7385.

41. Neil SJ, Zang T, Bieniasz PD: Tetherin inhibits retrovirus release and is antagonized by HIV-1 Vpu. *Nature* 2008, 451:425-430.

42. Van Damme N, Goff D, Katsura C, Jorgenson RL, Mitchell R, Johnson MC, Stephens EB, Guatelli J: The interferon-induced protein BST-2 restricts HIV-1 release and is downregulated from the cell surface by the viral Vpu protein. *Cell Host Microbe* 2008, 3:245-252.

43. Ray N, Doms RW: HIV-1 coreceptors and their inhibitors. *Curr Top Microbiol Immunol* 2006, 303:97-120.

44. Buonocore L, Rose JK: Blockade of human immunodeficiency virus type 1 production in CD4+ T cells by an intracellular CD4 expressed under control of the viral long terminal repeat. *Proc Natl Acad Sci U S A* 1993, 90:2695-2699.

45. Crise B, Buonocore L, Rose JK: CD4 is retained in the endoplasmic reticulum by the human immunodeficiency virus type 1 glycoprotein precursor. *J Virol* 1990, 64:5585-5593.

46. Jabbar MA, Nayak DP: Intracellular interaction of human immunodeficiency virus type 1 (ARV-2) envelope glycoprotein gp160 with CD4 blocks the movement and maturation of CD4 to the plasma membrane. *J Virol* 1990, 64:6297-6304.

47. Stevenson M, Meier C, Mann AM, Chapman N, Wasiak A: Envelope glycoprotein of HIV induces interference and cytolysis resistance in CD4+ cells: mechanism for persistence in AIDS. *Cell* 1988, 53:483-496.

48. Wildum S, Schindler M, Munch J, Kirchhoff F: Contribution of Vpu, Env, and Nef to CD4 down-modulation and resistance of human immunodeficiency virus type 1-infected T cells to superinfection. *J Virol* 2006, 80:8047-8059.

49. Lama J, Mangasarian A, Trono D: Cell-surface expression of CD4 reduces HIV-1 infectivity by blocking Env incorporation in a Nef- and Vpu-inhibitable manner. *Curr Biol* 1999, 9:622-631.

50. Ross TM, Oran AE, Cullen BR: Inhibition of HIV-1 progeny virion release by cell-surface CD4 is relieved by expression of the viral Nef protein. *Curr Biol* 1999, 9:613-621.

51. Cortes MJ, Wong-Staal F, Lama J: Cell surface CD4 interferes with the infectivity of HIV-1 particles released from T cells. *J Biol Chem* 2002, 277:1770-1779.

52. Levesque K, Zhao YS, Cohen EA: Vpu exerts a positive effect on HIV-1 infectivity by down-modulating CD4 receptor molecules at the surface of HIV-1-producing cells. *J Biol Chem* 2003, 278:28346-28353.

53. Tanaka M, Ueno T, Nakahara T, Sasaki K, Ishimoto A, Sakai H: Downregulation of CD4 is required for maintenance of viral infectivity of HIV-1. *Virology* 2003, 311:316-325.

54. Bour S, Perrin C, Strebel K: Cell surface CD4 inhibits HIV-1 particle release by interfering with Vpu activity. *J Biol Chem* 1999, 274:33800-33806.

55. Jolly C, Sattentau QJ: Retroviral spread by induction of virological synapses. *Traffic* 2004, 5:643-650.

56. Mothes W, Sherer NM, Jin J, Zhong P: Virus cell-to-cell transmission. *J Virol* 2010, 84:8360-8368.

57. Aiken C, Konner J, Landau NR, Lenburg ME, Trono D: Nef induces CD4 endocytosis: requirement for a critical dileucine motif in the membrane-proximal CD4 cytoplasmic domain. *Cell* 1994, 76:853-864.

58. Rhee SS, Marsh JW: Human immunodeficiency virus type 1 Nef-induced down-modulation of CD4 is due to rapid internalization and degradation of surface CD4. *J Virol* 1994, 68:5156-5163.

59. Chaudhuri R, Lindwasser OW, Smith WJ, Hurley JH, Bonifacino JS: Downregulation of CD4 by human immunodeficiency virus type 1 Nef is dependent on clathrin and involves direct interaction of Nef with the AP2 clathrin adaptor. *J Virol* 2007, 81:3877-3890.

60. daSilva LL, Sougrat R, Burgos PV, Janvier K, Mattera R, Bonifacino JS: Human immunodeficiency virus type 1 Nef protein targets CD4 to the multivesicular body pathway. *J Virol* 2009, 83:6578-6590.

61. Lindwasser OW, Chaudhuri R, Bonifacino JS: Mechanisms of CD4 downregulation by the Nef and Vpu proteins of primate immunodeficiency viruses. *Curr Mol Med* 2007, 7:171-184.

62. Willey RL, Maldarelli F, Martin MA, Strebel K: Human immunodeficiency virus type 1 Vpu protein regulates the formation of intracellular gp160-CD4 complexes. *J Virol* 1992, 66:226-234.

63. Bour S, Schubert U, Strebel K: The human immunodeficiency virus type 1 Vpu protein specifically binds to the cytoplasmic domain of CD4: implications for the mechanism of degradation. *J Virol* 1995, 69:1510-1520.

64. Lenburg ME, Landau NR: Vpu-induced degradation of CD4: requirement for specific amino acid residues in the cytoplasmic domain of CD4. *J Virol* 1993, 67:7238-7245.

65. Vincent MJ, Raja NU, Jabbar MA: Human immunodeficiency virus type 1 Vpu protein induces degradation of chimeric envelope glycoproteins bearing the cytoplasmic and anchor domains of CD4: role of the cytoplasmic domain in Vpu-induced degradation in the endoplasmic reticulum. *J Virol* 1993, 67:5538-5549.

66. Willey RL, Buckler-White A, Strebel K: Sequences present in the cytoplasmic domain of CD4 are necessary and sufficient to confer sensitivity to the human immunodeficiency virus type 1 Vpu protein. *J Virol* 1994, 68:1207-1212.

67. Yao XJ, Friborg J, Checroune F, Gratton S, Boisvert F, Sekaly RP, Cohen EA: Degradation of CD4 induced by human immunodeficiency virus type 1 Vpu protein: a predicted alpha-helix structure in the proximal cytoplasmic region of CD4 contributes to Vpu sensitivity. *Virology* 1995, 209:615-623.

68. Margottin F, Benichou S, Durand H, Richard V, Liu LX, Gomas E, Benarous R: Interaction between the cytoplasmic domains of HIV-1 Vpu and CD4: role of Vpu residues involved in CD4 interaction and in vitro CD4 degradation. *Virology* 1996, 223:381-386.

69. Schubert U, Bour S, Ferrer-Montiel AV, Montal M, Maldarell F, Strebel K: The two biological activities of human immunodeficiency virus type 1 Vpu protein involve two separable structural domains. *J Virol* 1996, 70:809-819.

70. Hill MS, Ruiz A, Schmitt K, Stephens EB: Identification of amino acids within the second alpha helical domain of the human immunodeficiency virus type 1 Vpu that are critical for preventing CD4 cell surface expression. *Virology* 2010, 397:104-112.

71. Tiganos E, Yao XJ, Friborg J, Daniel N, Cohen EA: Putative alpha-helical structures in the human immunodeficiency virus type 1 Vpu protein and CD4 are involved in binding and degradation of the CD4 molecule. *J Virol* 1997, 71:4452-4460.

72. Paul M, Jabbar MA: Phosphorylation of both phosphoacceptor sites in the HIV-1 Vpu cytoplasmic domain is essential for Vpu-mediated ER degradation of CD4. *Virology* 1997, 232:207-216.

73. Margottin F, Bour SP, Durand H, Selig L, Benichou S, Richard V, Thomas D, Strebel K, Benarous R: A novel human WD protein, h-beta TrCp, that interacts with HIV-1 Vpu connects CD4 to the ER degradation pathway through an F-box motif. *Mol Cell* 1998, 1:565-574.

74. Butticaz C, Michielin O, Wyniger J, Telenti A, Rothenberger S: Silencing of both beta-TrCP1 and HOS (beta-TrCP2) is required to suppress human immunodeficiency virus type 1 Vpu-mediated CD4 down-modulation. *J Virol* 2007, 81:1502-1505.

75. Nakayama KI, Nakayama K: Ubiquitin ligases: cell-cycle control and cancer. *Nat Rev Cancer* 2006, 6:369-381.

76. Meusser B, Sommer T: Vpu-mediated degradation of CD4 reconstituted in yeast reveals mechanistic differences to cellular ER-associated protein degradation. *Mol Cell* 2004, 14:247-258.

77. Binette J, Dube M, Mercier J, Cohen EA: Requirements for the selective degradation of CD4 receptor molecules by the human immunodeficiency virus type 1 Vpu protein in the endoplasmic reticulum. *Retrovirology* 2007, 4:75.

78. Fujita K, Omura S, Silver J: Rapid degradation of CD4 in cells expressing human immunodeficiency virus type 1 Env and Vpu is blocked by proteasome inhibitors. *J Gen Virol* 1997, 78 (Pt 3):619-625.

79. Meusser B, Hirsch C, Jarosch E, Sommer T: ERAD: the long road to destruction. *Nat Cell Biol* 2005, 7:766-772.

80. Vembar SS, Brodsky JL: One step at a time: endoplasmic reticulum-associated degradation. *Nat Rev Mol Cell Biol* 2008, 9:944-957.

81. Kikkert M, Doolman R, Dai M, Avner R, Hassink G, van Voorden S, Thanedar S, Roitelman J, Chau V, Wiertz E: Human HRD1 is an E3 ubiquitin ligase involved in degradation of proteins from the endoplasmic reticulum. *J Biol Chem* 2004, 279:3525-3534.

82. Hassink G, Kikkert M, van Voorden S, Lee SJ, Spaapen R, van Laar T, Coleman CS, Bartee E, Fruh K, Chau V, Wiertz E: TEB4 is a C4HC3 RING finger-containing ubiquitin ligase of the endoplasmic reticulum. *Biochem J* 2005, 388:647-655.

83. Fang S, Ferrone M, Yang C, Jensen JP, Tiwari S, Weissman AM: The tumor autocrine motility factor receptor, gp78, is a ubiquitin protein ligase implicated in degradation from the endoplasmic reticulum. *Proc Natl Acad Sci U S A* 2001, 98:14422-14427.

84. Spencer E, Jiang J, Chen ZJ: Signal-induced ubiquitination of IkappaBalpha by the F-box protein Slimb/beta-TrCP. *Genes Dev* 1999, 13:284-294.

85. Latres E, Chiaur DS, Pagano M: The human F box protein beta-Trcp associates with the Cul1/Skp1 complex and regulates the stability of beta-catenin. *Oncogene* 1999, 18:849-854.

86. Magadan JG, Perez-Victoria FJ, Sougrat R, Ye Y, Strebel K, Bonifacino JS: Multilayered mechanism of CD4 downregulation by HIV-1 Vpu involving distinct ER retention and ERAD targeting steps. *PLoS Pathog* 2010, 6:e1000869.

87. Wang X, Herr RA, Chua WJ, Lybarger L, Wiertz EJ, Hansen TH: Ubiquitination of serine, threonine, or lysine residues on the cytoplasmic tail can induce ERAD of MHC-I by viral E3 ligase mK3. *J Cell Biol* 2007, 177:613-624.

88. Ye Y, Meyer HH, Rapoport TA: The AAA ATPase Cdc48/p97 and its partners transport proteins from the ER into the cytosol. *Nature* 2001, 414:652-656.

89. Ye Y, Meyer HH, Rapoport TA: Function of the p97-Ufd1-Npl4 complex in retrotranslocation from the ER to the cytosol: dual recognition of nonubiquitinated polypeptide segments and polyubiquitin chains. *J Cell Biol* 2003, 162:71-84.

90. Yao XJ, Garzon S, Boisvert F, Haseltine WA, Cohen EA: The effect of vpu on HIV-1-induced syncytia formation. *J Acquir Immune Defic Syndr* 1993, 6:135-141.

91. Sakai H, Tokunaga K, Kawamura M, Adachi A: Function of human immunodeficiency virus type 1 Vpu protein in various cell types. *J Gen Virol* 1995, 76 (Pt 11):2717-2722.

92. Geraghty RJ, Talbot KJ, Callahan M, Harper W, Panganiban AT: Cell type-dependence for Vpu function. *J Med Primatol* 1994, 23:146-150.

93. Varthakavi V, Smith RM, Bour SP, Strebel K, Spearman P: Viral protein U counteracts a human host cell restriction that inhibits HIV-1 particle production. *Proc Natl Acad Sci U S A* 2003, 100:15154-15159.

94. Neil SJ, Eastman SW, Jouvenet N, Bieniasz PD: HIV-1 Vpu promotes release and prevents endocytosis of nascent retrovirus particles from the plasma membrane. *PLoS Pathog* 2006, 2:e39.

95. Neil SJ, Sandrin V, Sundquist WI, Bieniasz PD: An interferon-alpha-induced tethering mechanism inhibits HIV-1 and Ebola virus particle release but is counteracted by the HIV-1 Vpu protein. *Cell Host Microbe* 2007, 2:193-203.

96. Jouvenet N, Neil SJ, Zhadina M, Zang T, Kratovac Z, Lee Y, McNatt M, Hatziioannou T, Bieniasz PD: Broad-spectrum inhibition of retroviral and filoviral particle release by tetherin. *J Virol* 2009, 83:1837-1844.

97. Sakuma T, Noda T, Urata S, Kawaoka Y, Yasuda J: Inhibition of Lassa and Marburg virus production by tetherin. *J Virol* 2009, 83:2382-2385.

98. Kaletsky RL, Francica JR, Agrawal-Gamse C, Bates P: Tetherin-mediated restriction of filovirus budding is antagonized by the Ebola glycoprotein. *Proc Natl Acad Sci U S A* 2009, 106:2886-2891.

99. Mansouri M, Viswanathan K, Douglas JL, Hines J, Gustin J, Moses AV, Fruh K: Molecular mechanism of BST2/tetherin downregulation by K5/MIR2 of Kaposi's sarcoma-associated herpesvirus. *J Virol* 2009, 83:9672-9681.

100. Goto T, Nakano T, Kohno T, Morimatsu S, Morita C, Hong W, Kiso Y, Nakai M, Sano K: Targets of a protease inhibitor, KNI-272, in HIV-1-infected cells. *J Med Virol* 2001, 63:203-209.

101. Blasius AL, Giurisato E, Cella M, Schreiber RD, Shaw AS, Colonna M: Bone marrow stromal cell antigen 2 is a specific marker of type I IFN-producing cells in the naive mouse, but a promiscuous cell surface antigen following IFN stimulation. *J Immunol* 2006, 177:3260-3265.

102. Miyagi E, Andrew AJ, Kao S, Strebel K: Vpu enhances HIV-1 virus release in the absence of Bst-2 cell surface down-modulation and intracellular depletion. *Proc Natl Acad Sci U S A* 2009, 106:2868-2873.

103. Schindler M, Rajan D, Banning C, Wimmer P, Koppensteiner H, Iwanski A, Specht A, Sauter D, Dobner T, Kirchhoff F: Vpu serine 52 dependent counteraction of tetherin is required for HIV-1 replication in macrophages, but not in ex vivo human lymphoid tissue. *Retrovirology* 2010, 7:1.

104. Sato K, Yamamoto SP, Misawa N, Yoshida T, Miyazawa T, Koyanagi Y: Comparative study on the effect of human BST-2/Tetherin on HIV-1 release in cells of various species. *Retrovirology* 2009, 6:53.

105. Ishikawa J, Kaisho T, Tomizawa H, Lee BO, Kobune Y, Inazawa J, Oritani K, Itoh M, Ochi T, Ishihara K, et al.: Molecular cloning and chromosomal mapping of a bone marrow stromal cell surface gene, BST2, that may be involved in pre-B-cell growth. *Genomics* 1995, 26:527-534.

106. Tsukamoto N, Okada S, Onami Y, Sasaki Y, Umezawa K, Kawakami Y: Impairment of plasmacytoid dendritic cells for IFN production by the ligand for immunoglobulin-like transcript 7 expressed on human cancer cells. *Clin Cancer Res* 2009, 15:5733-5743.

107. Cao W, Bover L, Cho M, Wen X, Hanabuchi S, Bao M, Rosen DB, Wang YH, Shaw JL, Du Q, et al: Regulation of TLR7/9 responses in plasmacytoid dendritic cells by BST2 and ILT7 receptor interaction. *J Exp Med* 2009, 206:1603-1614.

108. Kupzig S, Korolchuk V, Rollason R, Sugden A, Wilde A, Banting G: Bst-2/HM1.24 is a raft-associated apical membrane protein with an unusual topology. *Traffic* 2003, 4:694-709.

109. Rollason R, Korolchuk V, Hamilton C, Schu P, Banting G: Clathrin-mediated endocytosis of a lipid-raft-associated protein is mediated through a dual tyrosine motif. *J Cell Sci* 2007, 120:3850-3858.

110. Moore RC, Lee IY, Silverman GL, Harrison PM, Strome R, Heinrich C, Karunaratne A, Pasternak SH, Chishti MA, Liang Y, et al: Ataxia in prion protein (PrP)-deficient mice is associated with upregulation of the novel PrP-like protein doppel. *J Mol Biol* 1999, 292:797-817.

111. Rollason R, Korolchuk V, Hamilton C, Jepson M, Banting G: A CD317/tetherin-RICH2 complex plays a critical role in the organization of the subapical actin cytoskeleton in polarized epithelial cells. *J Cell Biol* 2009, 184:721-736.

112. Masuyama N, Kuronita T, Tanaka R, Muto T, Hirota Y, Takigawa A, Fujita H, Aso Y, Amano J, Tanaka Y: HM1.24 is internalized from lipid rafts by clathrin-mediated endocytosis through interaction with alpha-adaptin. *J Biol Chem* 2009, 284:15927-15941.

113. Waheed AA, Freed EO: Lipids and membrane microdomains in HIV-1 replication. *Virus Res* 2009, 143:162-176.

114. Habermann A, Krijnse-Locker J, Oberwinkler H, Eckhardt M, Homann S, Andrew A, Strebel K, Krausslich HG: CD317/tetherin is enriched in the HIV-1 envelope and downregulated from the plasma membrane upon virus infection. *J Virol* 2010, 84:4646-4658.

115. Perez-Caballero D, Zang T, Ebrahimi A, McNatt MW, Gregory DA, Johnson MC, Bieniasz PD: Tetherin inhibits HIV-1 release by directly tethering virions to cells. *Cell* 2009, 139:499-511.

116. Andrew AJ, Miyagi E, Kao S, Strebel K: The formation of cysteine-linked dimers of BST-2/tetherin is important for inhibition of HIV-1 virus release but not for sensitivity to Vpu. *Retrovirology* 2009, 6:80.

117. Hinz A, Miguet N, Natrajan G, Usami Y, Yamanaka H, Renesto P, Hartlieb B, McCarthy AA, Simorre JP, Gottlinger H, Weissenhorn W: Structural basis of HIV-1 tethering to membranes by the BST-2/tetherin ectodomain. *Cell Host Microbe* 2010, 7:314-323.

118. Schubert HL, Zhai Q, Sandrin V, Eckert DM, Garcia-Maya M, Saul L, Sundquist WI, Steiner RA, Hill CP: Structural and functional studies on the extracellular domain of BST2/tetherin in reduced and oxidized conformations. *Proc Natl Acad Sci U S A* 2010, 107:17951-17956.

119. Yang H, Wang J, Jia X, McNatt MW, Zang T, Pan B, Meng W, Wang HW, Bieniasz PD, Xiong Y: Structural insight into the mechanisms of enveloped virus tethering by tetherin. *Proc Natl Acad Sci U S A* 2010, 107:18428-18432.

120. Miyakawa K, Ryo A, Murakami T, Ohba K, Yamaoka S, Fukuda M, Guatelli J, Yamamoto N: BCA2/Rabring7 promotes tetherin-dependent HIV-1 restriction. *PLoS Pathog* 2009, 5:e1000700.

121. Hammonds J, Wang JJ, Yi H, Spearman P: Immunoelectron microscopic evidence for Tetherin/BST2 as the physical bridge between HIV-1 virions and the plasma membrane. *PLoS Pathog* 2010, 6:e1000749.

122. Fitzpatrick K, Skasko M, Deerinck TJ, Crum J, Ellisman MH, Guatelli J: Direct restriction of virus release and incorporation of the interferon-induced protein BST-2 into HIV-1 particles. *PLoS Pathog* 2010, 6:e1000701.

123. Casartelli N, Sourisseau M, Feldmann J, Guivel-Benhassine F, Mallet A, Marcelin AG, Guatelli J, Schwartz O: Tetherin restricts productive HIV-1 cell-to-cell transmission. *PLoS Pathog* 2010, 6:e1000955.

124. Jolly C, Booth NJ, Neil SJ: Cell-Cell Spread of Human Immunodeficiency Virus Type 1 Overcomes Tetherin/BST-2-Mediated Restriction in T cells. *J Virol* 2010, 84:12185-12199.

125. Gummuluru S, Kinsey CM, Emerman M: An in vitro rapid-turnover assay for human immunodeficiency virus type 1 replication selects for cell-to-cell spread of virus. *J Virol* 2000, 74:10882-10891.

126. Fitzgerald-Bocarsly P, Jacobs ES: Plasmacytoid dendritic cells in HIV infection: striking a delicate balance. *J Leukoc Biol* 2010, 87:609-620.

127. Beignon AS, McKenna K, Skoberne M, Manches O, DaSilva I, Kavanagh DG, Larsson M, Gorelick RJ, Lifson JD, Bhardwaj N: Endocytosis of HIV-1 activates plasmacytoid dendritic cells via Toll-like receptor-viral RNA interactions. *J Clin Invest* 2005, 115:3265-3275.

128. Mitchell RS, Katsura C, Skasko MA, Fitzpatrick K, Lau D, Ruiz A, Stephens EB, Margottin-Goguet F, Benarous R, Guatelli JC: Vpu antagonizes BST-2-mediated restriction of HIV-1 release via beta-TrCP and endo-lysosomal trafficking. *PLoS Pathog* 2009, 5:e1000450.

129. Ruiz A, Hill MS, Schmitt K, Stephens EB: Membrane raft association of the Vpu protein of human immunodeficiency virus type 1 correlates with enhanced virus release. *Virology* 2010, 408:89-102.

130. Douglas JL, Viswanathan K, McCarroll MN, Gustin JK, Fruh K, Moses AV: Vpu directs the degradation of the human immunodeficiency virus restriction factor BST-2/Tetherin via a {beta}TrCP-dependent mechanism. *J Virol* 2009, 83:7931-7947.

131. Dube M, Roy BB, Guiot-Guillain P, Binette J, Mercier J, Chiasson A, Cohen EA: Antagonism of tetherin restriction of HIV-1 release by Vpu involves binding and sequestration of the restriction factor in a perinuclear compartment. *PLoS Pathog* 2010, 6:e1000856.

132. Rong L, Zhang J, Lu J, Pan Q, Lorgeoux RP, Aloysius C, Guo F, Liu SL, Wainberg MA, Liang C: The transmembrane domain of BST-2 determines its sensitivity to down-modulation by human immunodeficiency virus type 1 Vpu. *J Virol* 2009, 83:7536-7546.

133. Iwabu Y, Fujita H, Kinomoto M, Kaneko K, Ishizaka Y, Tanaka Y, Sata T, Tokunaga K: HIV-1 accessory protein Vpu internalizes cell-surface BST-2/tetherin through transmembrane interactions leading to lysosomes. *J Biol Chem* 2009, 284:35060-35072.

134. Mangeat B, Gers-Huber G, Lehmann M, Zufferey M, Luban J, Piguet V: HIV-1 Vpu neutralizes the antiviral factor Tetherin/BST-2 by binding it and directing its beta-TrCP2-dependent degradation. *PLoS Pathog* 2009, 5:e1000574.

135. Vigan R, Neil SJ: Determinants of tetherin antagonism in the transmembrane domain of the human immunodeficiency virus type 1 vpu protein. *J Virol* 2010, 84:12958-12970.

136. Kobayashi T, Ode H, Yoshida T, Sato K, Gee P, Yanamato S, Ebina H, Strebel K, Sato H, Koyanagi Y: Identification of amino acids in the human tetherin transmembrane domain responsible for HIV-1 Vpu interaction and susceptibility. *J Virol* 2010, Published online Nov 10, 2010.

137. Banning C, Votteler J, Hoffmann D, Koppensteiner H, Warmer M, Reimer R, Kirchhoff F, Schubert U, Hauber J, Schindler M: A flow cytometry-based FRET assay to identify and analyse protein-protein interactions in living cells. *PLoS One* 2010, 5:e9344.

138. Gupta RK, Hue S, Schaller T, Verschoor E, Pillay D, Towers GJ: Mutation of a single residue renders human tetherin resistant to HIV-1 Vpu-mediated depletion. *PLoS Pathog* 2009, 5:e1000443.

139. Goffinet C, Allespach I, Homann S, Tervo HM, Habermann A, Rupp D, Oberbremer L, Kern C, Tibroni N, Welsch S, et al: HIV-1 antagonism of CD317 is species specific and involves Vpu-mediated proteasomal degradation of the restriction factor. *Cell Host Microbe* 2009, 5:285-297.

140. Goffinet C, Homann S, Ambiel I, Tibroni N, Rupp D, Keppler OT, Fackler OT: Antagonism of CD317 restriction of HIV-1 particle release and depletion of CD317 are separable activities of HIV-1 Vpu. *J Virol* 2010, 84:4089-4094.

141. Tokarev AA, Munguia J, Guatelli JC: Serine-threonine ubiquitination mediates downregulation of BST-2/tetherin and relief of restricted virion release by HIV-1 Vpu. *J Virol* 2010.

142. Douglas JL, Gustin JK, Viswanathan K, Mansouri M, Moses AV, Fruh K: The great escape: viral strategies to counter BST-2/tetherin. *PLoS Pathog* 2010, 6:e1000913.

143. Melikova MS, Kondratov KA, Kornilova ES: Two different stages of epidermal growth factor (EGF) receptor endocytosis are sensitive to free ubiquitin depletion produced by proteasome inhibitor MG132. *Cell Biol Int* 2006, 30:31-43.

144. Pardieu C, Vigan R, Wilson SJ, Calvi A, Zang T, Bieniasz P, Kellam P, Towers GJ, Neil SJ: The RING-CH ligase K5 antagonizes restriction of KSHV and HIV-1 particle release by mediating ubiquitin-dependent endosomal degradation of tetherin. *PLoS Pathog* 2010, 6:e1000843.

145. Hauser H, Lopez LA, Yang SJ, Oldenburg JE, Exline CM, Guatelli JC, Cannon PM: HIV-1 Vpu and HIV-2 Env counteract BST-2/tetherin by sequestration in a perinuclear compartment. *Retrovirology* 2010, 7:51.

146. Douglas CC, Thomas D, Lanman J, Prevelige PE, Jr.: Investigation of N-terminal domain charged residues on the assembly and stability of HIV-1 CA. *Biochemistry* 2004, 43:10435-10441.

147. Lopez LA, Yang SJ, Hauser H, Exline CM, Haworth KG, Oldenburg J, Cannon PM: Ebola virus glycoprotein counteracts BST-2/Tetherin restriction in a sequence-independent manner that does not require tetherin surface removal. *J Virol* 2010, 84:7243-7255.

148. Le Tortorec A, Neil SJ: Antagonism to and intracellular sequestration of human tetherin by the human immunodeficiency virus type 2 envelope glycoprotein. *J Virol* 2009, 83:11966-11978.

149. Gupta RK, Mlcochova P, Pelchen-Matthews A, Petit SJ, Mattiuzzo G, Pillay D, Takeuchi Y, Marsh M, Towers GJ: Simian immunodeficiency virus envelope glycoprotein counteracts tetherin/BST-2/CD317 by intracellular sequestration. *Proc Natl Acad Sci U S A* 2009, 106:20889-20894.

150. Zhang F, Wilson SJ, Landford WC, Virgen B, Gregory D, Johnson MC, Munch J, Kirchhoff F, Bieniasz PD, Hatziioannou T: Nef proteins from simian immunodeficiency viruses are tetherin antagonists. *Cell Host Microbe* 2009, 6:54-67.

151. Sauter D, Schindler M, Specht A, Landford WN, Munch J, Kim KA, Votteler J, Schubert U, Bibollet-Ruche F, Keele BF, et al: Tetherin-driven adaptation of Vpu and Nef function and the evolution of pandemic and nonpandemic HIV-1 strains. *Cell Host Microbe* 2009, 6:409-421.

152. Jia B, Serra-Moreno R, Neidermyer W, Rahmberg A, Mackey J, Fofana IB, Johnson WE, Westmoreland S, Evans DT: Species-specific activity of SIV Nef and HIV-1 Vpu in overcoming restriction by tetherin/BST2. *PLoS Pathog* 2009, 5:e1000429.

153. Yang SJ, Lopez LA, Hauser H, Exline CM, Haworth KG, Cannon PM: Anti-tetherin activities in Vpu-expressing primate lentiviruses. *Retrovirology* 2010, 7:13.

154. Sawyer SL, Wu LI, Emerman M, Malik HS: Positive selection of primate TRIM5alpha identifies a critical species-specific retroviral restriction domain. *Proc Natl Acad Sci U S A* 2005, 102:2832-2837.

155. Sawyer SL, Emerman M, Malik HS: Ancient adaptive evolution of the primate antiviral DNA-editing enzyme APOBEC3G. *PLoS Biol* 2004, 2:E275.

156. McNatt MW, Zang T, Hatziioannou T, Bartlett M, Fofana IB, Johnson WE, Neil SJ, Bieniasz PD: Species-specific activity of HIV-1 Vpu and positive selection of tetherin transmembrane domain variants. *PLoS Pathog* 2009, 5:e1000300.

157. Lim ES, Malik HS, Emerman M: Ancient adaptive evolution of tetherin shaped the functions of Vpu and Nef in human immunodeficiency virus and primate lentiviruses. *J Virol* 2010, 84:7124-7134.

158. Bailes E, Gao F, Bibollet-Ruche F, Courgnaud V, Peeters M, Marx PA, Hahn BH, Sharp PM: Hybrid origin of SIV in chimpanzees. *Science* 2003, 300:1713.

159. Ruiz A, Lau D, Mitchell RS, Hill MS, Schmitt K, Guatelli JC, Stephens EB: BST-2 mediated restriction of simian-human immunodeficiency virus. *Virology* 2010, 406:312-321.

160. Hahn BH, Shaw GM, De Cock KM, Sharp PM: AIDS as a zoonosis: scientific and public health implications. *Science* 2000, 287:607-614.

161. de Silva TI, Cotten M, Rowland-Jones SL: HIV-2: the forgotten AIDS virus. *Trends Microbiol* 2008, 16:588-595.

162. Singh DK, McCormick C, Pacyniak E, Lawrence K, Dalton SB, Pinson DM, Sun F, Berman NE, Calvert M, Gunderson RS, et al: A simian human immunodeficiency virus with a nonfunctional Vpu (deltavpuSHIV(KU-1bMC33)) isolated from a macaque with neuroAIDS has selected for mutations in env and nef that contributed to its pathogenic phenotype. *Virology* 2001, 282:123-140.

163. Singh DK, Griffin DM, Pacyniak E, Jackson M, Werle MJ, Wisdom B, Sun F, Hout DR, Pinson DM, Gunderson RS, et al: The presence of the casein kinase II phosphorylation sites of Vpu enhances the CD4(+) T cell loss caused by the simian-human immunodeficiency virus SHIV(KU-lbMC33) in pig-tailed macaques. *Virology* 2003, 313:435-451.

164. Moll M, Andersson SK, Smed-Sorensen A, Sandberg JK: Inhibition of lipid antigen presentation in dendritic cells by HIV-1 Vpu interference with CD1d recycling from endosomal compartments. *Blood* 2010, 116:1876-1884.

165. Shah AH, Sowrirajan B, Davis ZB, Ward JP, Campbell EM, Planelles V, Barker E: Degranulation of natural killer cells following interaction with HIV-1-infected cells is hindered by downmodulation of NTB-A by Vpu. *Cell Host Microbe* 2010, 8:397-409.

Table

Table 1: Anti-Tetherin mechanisms reported for the known Tetherin antagonists

Tetherin antagonists	Binding	Mechanisms	References
HIV-1 Vpu	Yes	Proteosomal degradation	(84, 94, 156)
		Lysosomal degradation	(55, 172)
		Sequestration in TGN and/or endosomes	(58, 101)
HIV-2 Env	Yes	Intracellular sequestration	(101, 142)
SIV Nef	?	Increased internalization from the cell-surface?	(115, 211, 271)
SIVtan Env	?	Intracellular sequestration	(95)
KSHV K5	?	Lysosomal degradation	(158, 191)
Ebola gp	Yes	?	(121, 149)

Figure 1: Schematic representations of Vpu

Predicted secondary and tertiary structure of Vpu showing the N-terminal transmembrane domain (TM) and the two α-helices of the cytoplasmic (CYTO) domain. The numbers indicate amino acids position of the NL4.3 prototypical Vpu allele. In both panels, yellow circles represent phosphorylated serine residues (S52 and S56) sites. The 13° tilt angle of the TM domain is indicated. (B) Vpu topology with the corresponding HIV-1/SIVcpz *Ptt* Vpu consensus sequences (HIV sequence database, www.hiv.lanl.gov). Question marks indicate residues with no consensus available. The red box indicates the conserved sequences recognized by β-TrCP. The blue boxes highlight areas containing putative trafficking signals shown below. X and Φ correspond to variable and hydrophobic amino-acid residues, respectively. αH: α-helix.

A

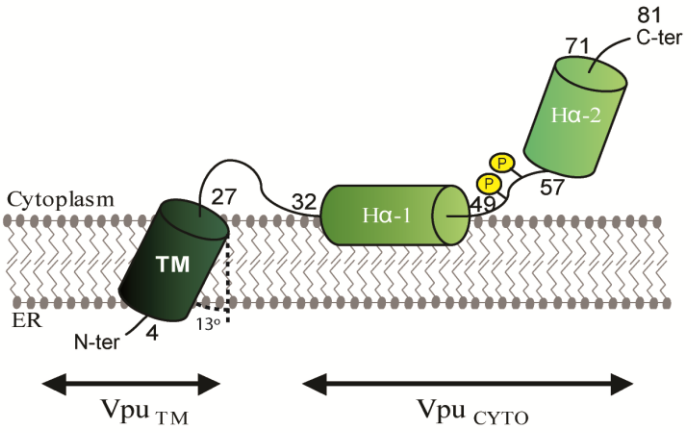
81
C-ter
71
Hα-2
57
P
P
49
32
Hα-1
27
Cytoplasm
TM
ER
N-ter
4
13°
Vpu TM
Vpu CYTO

B

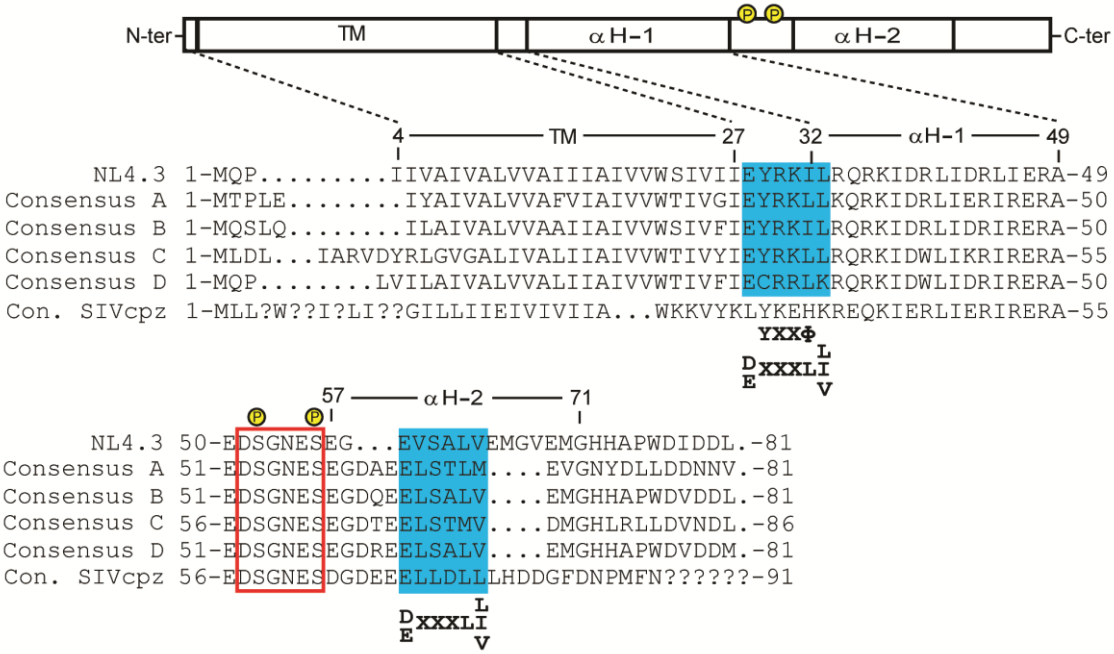
N-ter
TM
αH-1
αH-2
C-ter
4
TM
27
32
αH-1
49
NL4.3 1-MQP.....IIVAIVALVVAIIIAIVVWSIVIIEYRKILRQRKIDRLIDRLIERA-49
Consensus A 1-MTPLE.....IYAIVALVVAFVIAIVVWTIVGIEYRKLLKQRKIDRLIERIRERA-50
Consensus B 1-MQSLQ.....ILAIVALVVAAIIAIVVWSIVFIEYRKILRQRKIDRLIDRIRERA-50
Consensus C 1-MLDL...IARVDYRLGVGALIVALIIAIVVWTIVYIEYRKLLRQRKIDWLIKRIRERA-55
Consensus D 1-MQP.....LVILAIVALVVALIIAIVVWTIVFIECRRLKRQRKIDWLIDRIRERA-50
Con. SIVcpz 1-MLL?W??I?LI??GILLIIEIVIVIIA...WKKVYKLYKEHKREQKIERLIERIRERA-55
YXXΦ
DE XXXLIV
57
αH-2
71
NL4.3 50-EDSGNESEG...EVSALVEMGVEMGHHAPWDIDDL.-81
Consensus A 51-EDSGNESEGDAEELSTLM....EVGNYDLLDDNNV.-81
Consensus B 51-EDSGNESEGDQEELSALV....EMGHHAPWDVDDL.-81
Consensus C 56-EDSGNESEGDTEELSTMV....DMGHLRLLDVNDL.-86
Consensus D 51-EDSGNESEGDREELSALV....EMGHHAPWDVDDM.-81
Con. SIVcpz 56-EDSGNESDGDEEELLDLLLHDDGFDNPMFN??????-91
DE XXXLIV

Figure 2: Model of Vpu-mediated CD4 degradation

First, Vpu retains CD4 in the ER through TM domains interactions; formation of Env/CD4 complexes could contribute to this retention. In addition, CD4 and Vpu also interact through their cytosolic domains. The minimal region of the CD4 cytoplasmic tail conferring Vpu sensitivity was mapped to the region 414-LSEKKT-419. Recruitment of the $SCF^{\beta\text{-}TrCP}$ E3 ubiquitin ligase complex by Vpu is mediated by interactions of phosphoserines in Vpu and the WD boxes of β-TrCP. Interactions between Vpu and CD4 result in the *trans*-ubiquination of the cytosolic tail of CD4 on lysine, serine and threonine residues. These ubiquitination events might further contribute to CD4 retention in the ER but, importantly, target CD4 for degradation by the cytosolic proteasome. This targeting involves a dislocation step mediated by the p97-UFD1L-NPL4 complex, a critical component of ERAD. This complex recognizes K48-linked polyubiquitinated chains on the cytosolic tail of CD4 through the UFD1L co-factor. The p97 protein via its ATPase activity subsequently directs the dislocation of CD4 across the ER membrane where the receptor becomes readily accessible for proteasomal degradation.

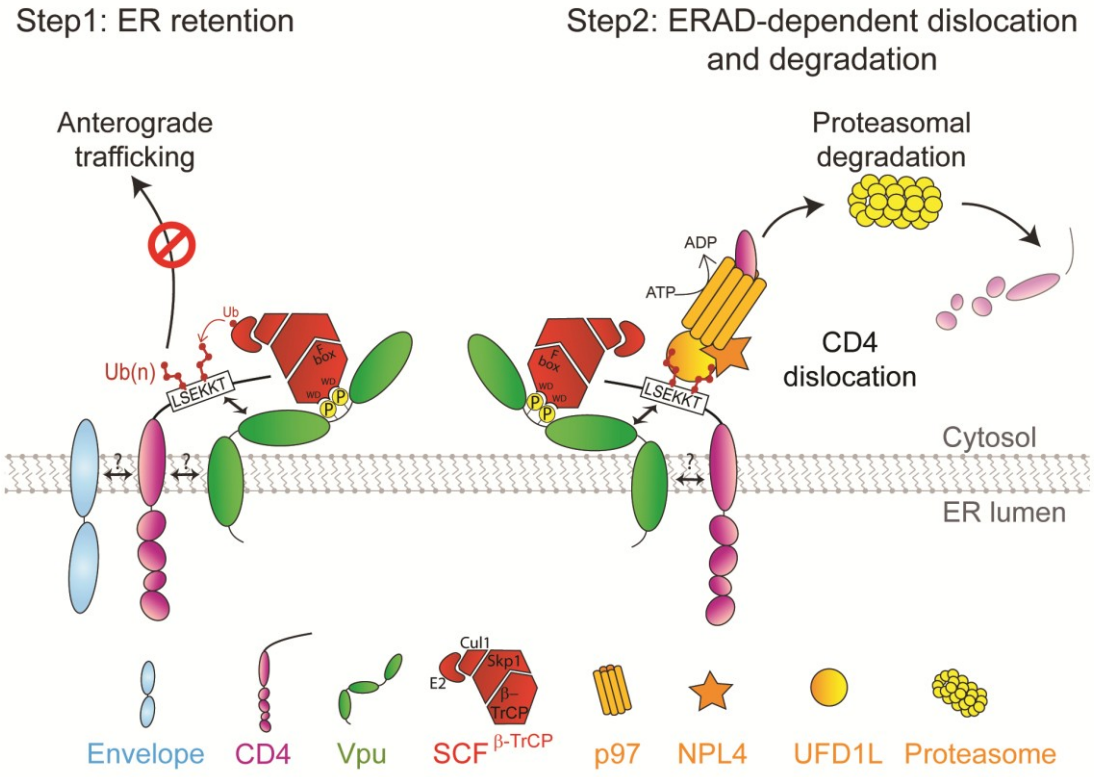
Step1: ER retention
Step2: ERAD-dependent dislocation and degradation
Anterograde trafficking
Proteasomal degradation
ADP
ATP
Ub
Ub(n)
F-box
WD
P
LSEKKT
CD4 dislocation
Cytosol
ER lumen
?
Cul1
Skp1
E2
β-TrCP
Envelope
CD4
Vpu
SCF β-TrCP
p97
NPL4
UFD1L
Proteasome

Figure 3: Schematic representations of Tetherin

Secondary and tertiary model structure of human Tetherin. Glycosylation sites at position 65 and 92 are shown as well as the GPI-anchor and the cytoplasmic, transmembrane (TM) and extracellular coiled-coil domains. The functional parallel dimeric state is shown here. (B) Tetherin topology. An amino-acid sequence alignment of human, chimpanzee, rhesus and African green monkey (agm) Tetherin alleles is shown below. Hyphens and bold letters represent respectively deletions and residues in human Tetherin under positive selection. Putative Ub-acceptor residues, cysteine residues involved in dimerization as well as N-glycosylation sites are labelled in orange, pink and red, respectively. Putative trafficking signals, the predicted transmembrane domain and the coiled-coil domain are highlighted in blue, green and yellow. The sites of interaction mapped for SIV Nef and HIV-1 Vpu are boxed in dark blue and dark green, respectively. Note that the SIV Nef-interacting region is deleted in human Tetherin. The site of cleavage prior to addition of the GPI lipid anchor is represented by the dashed line.

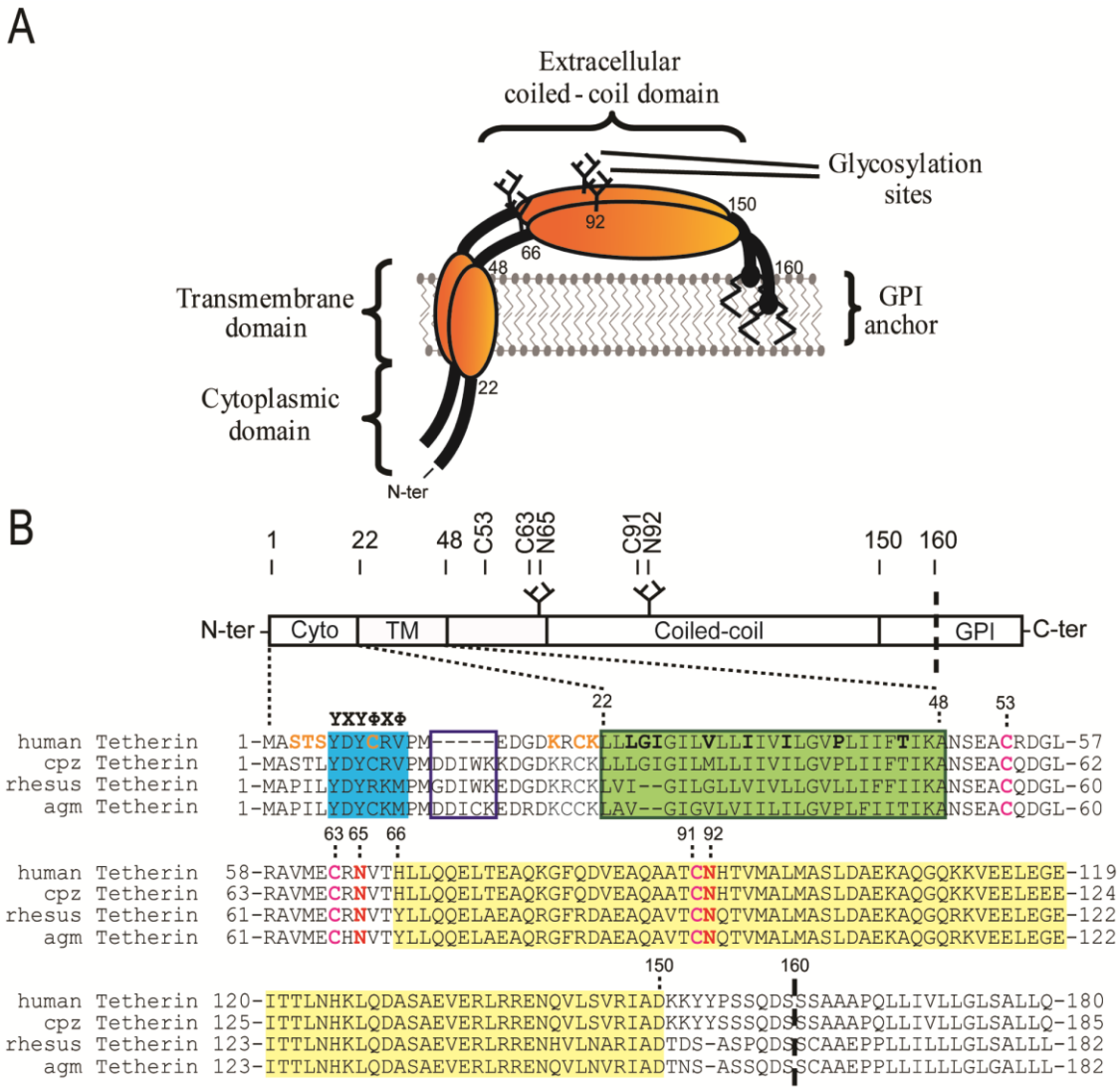
A
Extracellular
coiled-coil domain
Glycosylation
sites
92
150
66
48
160
Transmembrane
domain
GPI
anchor
Cytoplasmic
domain
22
N-ter
B
1
22
48
C53
C63
N65
C91
N92
150
160
N-ter
Cyto
TM
Coiled-coil
GPI
C-ter
YXYΦXΦ
22
48
53
human Tetherin 1-MASTSYDYCRVPM-----EDGDKRCKLLLGIGILVLLIIVILGVPLIIFTIKANSEACRDGL-57
cpz Tetherin 1-MASTLYDYCRVPMDDIWKKDGDKRCKLLLGIGILMLLIIVILGVPLIIFTIKANSEACQDGL-62
rhesus Tetherin 1-MAPILYDYRKMPMGDIWKEDGDKRCKLVI--GILGLLVIVLLGVLLIFFIIKANSEACQDGL-60
agm Tetherin 1-MAPILYDYCKMPMDDICKEDRDKCCKLAV--GIGVLVIILILGVPLFIITIKANSEACQDGL-60
63 65 66
91 92
human Tetherin 58-RAVMECRNVTHLLQQELTEAQKGFQDVEAQAATCNHTVMALMASLDAEKAQGQKKVEELEGE-119
cpz Tetherin 63-RAVMECRNVTHLLQQELTEAQKGFQDVEAQAATCNHTVMALMASLDAEKAQGQKKVEELEEE-124
rhesus Tetherin 61-RAVMECRNVTYLLQQELAEAQRGFRDAEAQAVTCNQTVMALMASLDAEKAQGQRKVEELEGE-122
agm Tetherin 61-RAVMECHNVTYLLQQELAEAQRGFRDAEAQAVTCNQTVMALMASLDAEKAQGQRKVEELEGE-122
150
160
human Tetherin 120-ITTLNHKLQDASAEVERLRRENQVLSVRIADKKYYPSSQDSSSAAAPQLLIVLLGLSALLQ-180
cpz Tetherin 125-ITTLNHKLQDASAEVERLRRENQVLSVRIADKKYYSSSQDSSSAAAPQLLIVLLGLSALLQ-185
rhesus Tetherin 123-ITTLNHKLQDASAEVERLRRENHVLNARIADTDS-ASPQDSSCAAEPPLLILLLGLSALLL-182
agm Tetherin 123-ITTLNHKLQDASAEVERLRRENQVLNVRIADTNS-ASSQDSSCAAEPPLLILLLGLGALLL-182

Figure 4: Schematic representations of possible direct tethering modes

(A) Tethering by interaction via the ectodomains of Tetherin dimers. One Tetherin molecule is inserted into the virus while the other is anchored into the cellular membrane. (B) Tethering by incorporation of one of the molecule anchors in the virus and the other in the cellular membrane. Different options are shown, including GPI anchors or transmembrane domains of parallel Tetherin homodimers incorporated into a virion and (C) both type of anchors from an antiparallel tetherin homodimer incorporated into virion. The fact that deleting either the GPI anchor or the TM domain prevents the restriction suggests that either configuration A and C are not important contributors of the tethering process or that a single tethering domain is not sufficient to retain virions at the cell surface. Indeed, it is also conceivable that all these potential configurations may contribute to the restrictive activity albeit to different extent.

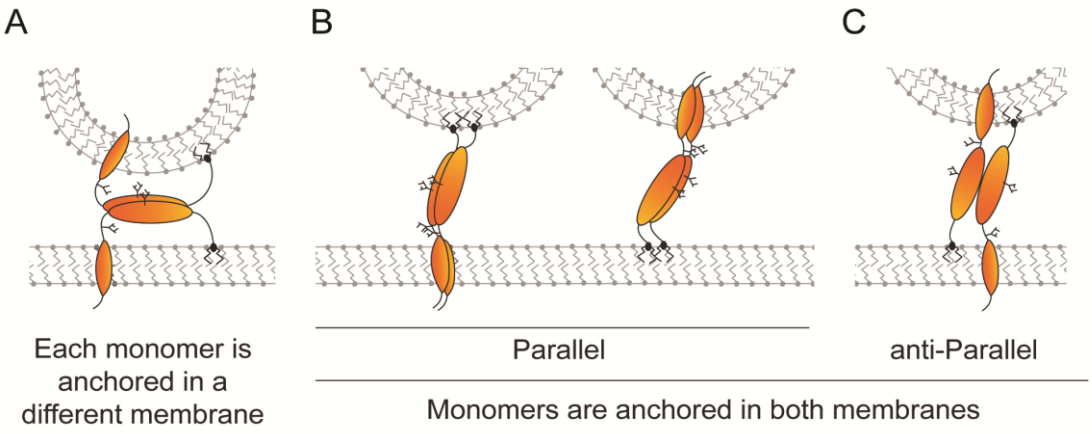
A
B
C
Each monomer is anchored in a different membrane
Parallel
anti-Parallel
Monomers are anchored in both membranes

Figure 5. Unified model of Vpu-mediated cell-surface Tetherin downregulation

Tetherin traffics along the anterograde trafficking pathway and reaches the plasma membrane. The protein is endocytosed in clathrin-coated pits, transported to the TGN and most probably recycles back to the cell surface. Upon expression of Vpu, Tetherin is forming complexes with the viral protein, thus trapping the restriction factor in the TGN, away from sites of viral assembly at the plasma membrane where Tetherin is cross-linking progeny virions. Vpu could intercept endocytosed Tetherin as well as Tetherin arriving from the ER although this remains to be determined. Subsequently, Vpu could induce Tetherin ubiquitination through recruitment of β-TrCP-2, leading to a stronger retention in the TGN. Sequestered ubiquitinated Tetherin conjugates could ultimately be targeted for proteosomal and/or lysosomal degradation. As such, Vpu-mediated Tetherin degradation may represent a complementary mechanism that Vpu could exploit to reach optimal Tetherin antagonism, perhaps, in specific cellular environments.

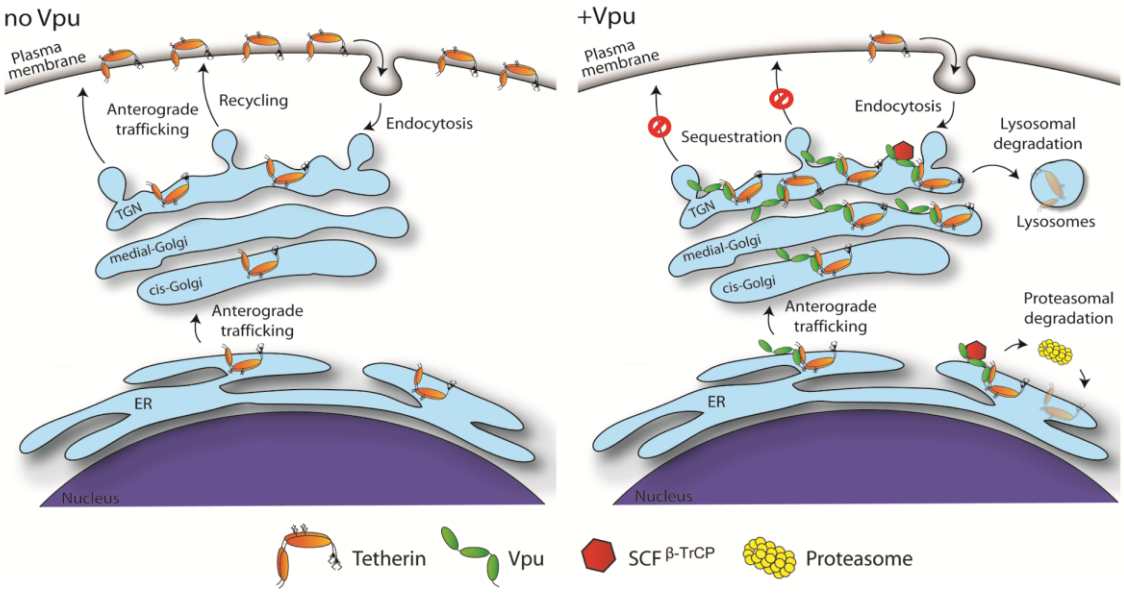
no Vpu
Plasma membrane
Anterograde trafficking
Recycling
Endocytosis
TGN
medial-Golgi
cis-Golgi
Anterograde trafficking
ER
Nucleus
+Vpu
Plasma membrane
Sequestration
Endocytosis
Lysosomal degradation
Lysosomes
TGN
medial-Golgi
cis-Golgi
Anterograde trafficking
Proteasomal degradation
ER
Nucleus
Tetherin
Vpu
SCF β-TrCP
Proteasome

Figure 6: Adaptations of primate lentiviruses during cross-species transmission and the emergence of pandemic HIV-1 strains.

The SIV from chimpanzee is believed to result from recombination events through successive cross-species transmission between the precursors of the SIVgsn/mon/mus and the SIVrcm lineages. The transmembrane domain of Tetherin evolved primarily during transition from the non hominoïd lineage to the hominoïd lineage, explaining why the Vpu protein inherited from the SIVgsn/mon/mus lineage does not exhibit any activity against chimpanzee Tetherin. After transmission from chimpanzees to humans, SIVcpz was unable anymore to use Nef to counteract Tetherin due to a deletion of five amino acids in the cytoplasmic domain of human Tetherin, which usually confers responsiveness to Nef. During evolution/adaptation from SIVcpz to HIV-1, modifications mapped to two regions of the Vpu transmembrane domain have conferred human Tetherin a susceptibility to Vpu, except in the case of the HIV-1 group O. Furthermore, the HIV-1 group N Vpu somehow has lost its ability to mediate CD4 degradation in the process. Only the pandemic HIV-1 group M harbors the two primary Vpu functions. Susceptibility of the transmembrane domain of Tetherin to Vpu is represented by similar colour pairing. The deletion of the five amino acids in human Tetherin cytoplamic tail is represented by the absence of the D/GDIWK sequence. The colour gradient indicates co-evolution between SIV/HIV and host.

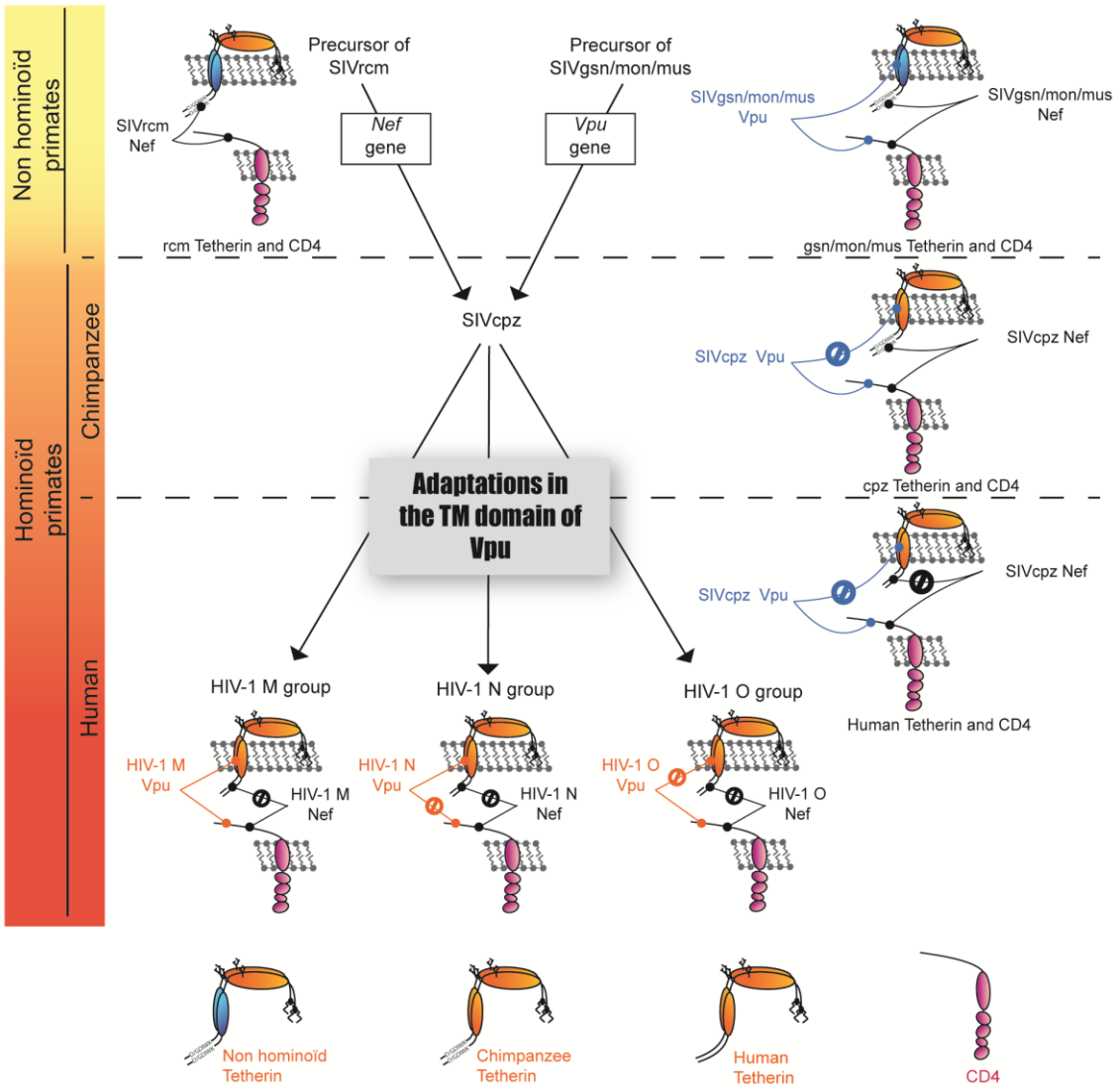
Non hominoid primates
Hominoïd primates
Chimpanzee
Human
Precursor of SIVrcm
Precursor of SIVgsn/mon/mus
SIVrcm Nef
Nef gene
Vpu gene
SIVgsn/mon/mus Vpu
SIVgsn/mon/mus Nef
rcm Tetherin and CD4
gsn/mon/mus Tetherin and CD4
SIVcpz
SIVcpz Vpu
SIVcpz Nef
cpz Tetherin and CD4
Adaptations in the TM domain of Vpu
SIVcpz Vpu
SIVcpz Nef
Human Tetherin and CD4
HIV-1 M group
HIV-1 N group
HIV-1 O group
HIV-1 M Vpu
HIV-1 M Nef
HIV-1 N Vpu
HIV-1 N Nef
HIV-1 O Vpu
HIV-1 O Nef
Non hominoïd Tetherin
Chimpanzee Tetherin
Human Tetherin
CD4

INTRODUCTION (suite)

Vpu et Tetherin : mise à jour des connaissances depuis la parution de la revue

Depuis la parution de notre revue dans *Retrovirology*, quelques études sont venues clarifier certaines questions importantes. D'une part, l'impact dela Tetherin sur la transmission de cellules à cellules a été nuancé. En effet, il était initialement hypothétisé que l'inefficacité de la relâche virale en absence de Vpu était compensée par une amélioration conséquente de la transmission de cellules à cellules puisque : 1) l'absence de la protéine virale ne semblait pas avoir d'impact sur la rapidité de la propagation virale *in vitro* (132, 216, 235, 242); 2) certains clones viraux sélectionnés pour leur propagation rapide *in vitro* se sont avérés défectifs pour l'expression de Vpu (92); 3) l'expression de Vpu n'a pas semblé influer sur l'efficacité de la transmission de cellules à cellules dans de précédentes études (228). La récente étude de Jolly et collègues abonde dans ce sens (120). Il y est en effet révélé que la Tetherin, en s'accumulant au niveau de la synapse virologique, y augmente le titre du virus mature et favorise ainsi la transmission virale. Bien que les études de Casertelli et al 2010 et de Kuhl et al 2011 s'accordent sur l'accumulation de la Tetherin au niveau des synapses virologiques (30, 138), elles se distinguent en suggérant que cette accumulation semble plutôt nuire à la transmission. En fait, ces deux études soutiennent plutôt un modèle où l'expression de la Tetherin à la synapse virologiqueentraîne l'agglutination du virus mature. Ces amas, une fois transférés à la cellule cible, ne fusionneraient avec elle que très innefficacement, ce qui n'est pas sans rappeller l'effet négatif de Tetherin sur l'infectivité virale lorsque fortement exprimée (272). Il semblerait que les contradictions entre les études de Jolly, Casertelli et Kuhl pourraient s'expliquer par un niveau différentiel d'expression de la Tetherin (119). Ainsi, une expression modérée de la Tetherin (telle que dans l'étude de Jolly) augmenterait localement la multiplicité d'infection au niveau de la synapse virologique alors qu'à plus forts niveaux d'expression (tels que dans certains systèmes de Casertelli et Kuhl), l'agglutination du virus diminuerait plutôt l'efficacité de la transmission. Il sera cependant nécessaire de vérifier la validité de ces modèles dans des systèmes plus physiologiques.

Outre la question de la transmission de cellules à cellules, un nouvel antagoniste de la Tetherin aurait été attribué chez influenza. En effet, la neuraminidase la surmonterait par un mécanisme encore inconnu (268). Nous avons aussi désormais une meilleure compréhension du mécanisme par lequel Vpu dégrade Tetherin. Des expériences de marquage métabolique suivi d'une chasse ont suggéré que Vpu cause la dégradation des formes matures de Tetherin néo-synthétisées, excluant par le fait même tout mécanisme de dégradation au niveau du RE, avant que ces dernières n'atteignent la surface (5). Notamment, cette augmentation de la dégradation de Tetherin par Vpu serait dépendante du recrutement de HRS, une composante importante d'ESCRT-0 (113). En effet, la déplétion de cette composante au moyen de petits ARN d'interférence a bloqué la dégradation de Tetherin par Vpu, confirmant du même coup la nature lysosomale de ce processus de dégradation. La déplétion de HRS a aussi mené à une stabilisation du facteur de restriction même en absence de Vpu, suggérant que cette dernière accélère une voie de dégradation préexistante (113). Néanmoins, l'importance de ce mécanisme demeure incertaine car une autre étude a confirmé que l'antagonisme de Tetherin par Vpu pouvait se produire en absence de β-TrCP, un cofacteur essentiel à la dégradation du facteur de restriction par la protéine virale (241).

5. Thérapie antivirale

La thérapie anti-VIH-1 actuelle, la thérapie antirétrovirale (HAART), implique l'usage d'au moins trois agents antiviraux. Trois principales classes sont actuellement employées à cet effet, soit les inhibiteurs de la transcriptase inverse analogues aux nucléosides (NRTI; zidovudine, didanosine, lamivudine, emtricitabine, abacavir et tenofovir), les inhibiteurs de la transcriptase inverse non-analogues aux nucléosides (NNRTI; nevirapine, delavirdine, efavirenz et etravidine) et les inhibiteurs de la protéase (PI; saquinavir, ritonavir, indinavir, nelfinavir, fosamprenavir, liponavir, atazanavir, tipranavir et darunavir) (résumé dans (81, 246)). La combinaison de ces différentes drogues permet de réduire la probabilité d'émergence de souches virales résistantes.

Les NRTIs sont des analogues de nucléosides : ils compétitionnent avec les nucléosides cellulaires lors de la transcription inverse. Plusieurs effets secondaires lui sont associés tels que l'acidose lactique, la lypodystrophie et des désordres hépatiques, musculaires, nerveux et peut-être rénaux (résumé dans (246)). Au contraire des NRTIs, les NNRTIS ne compétitionnent pas avec les nucléosides mais inhibent la RT en la liant hors de son site actif (246). Efficace, cette classe est cependant plus susceptible aux interactions médicamenteuses. Finalement, les PIs empêchent le clivage de Gag par la protéase virale en sous-produits polypeptides matures. Contrairement aux autres classes d'antiviraux, plusieurs mutations dans la protéase sont nécessaires à l'émergence de souches résistantes, réduisant de tels événements. Par contre, ces molécules peuvent causer de la dyslipidémie. Récemment, d'autres molécules anti-VIH-1 ont été homologuées telles que les inhibiteurs de l'intégrase (raltegravir) et de l'entrée virale (enfuvirtide et maraviroc), quoique leurs effets secondaires ne soient pas encore bien connus (81, 246). L'usage d'inhibiteurs de l'entrée est présentement limité par l'actuelle formulation (injection bi-hebdomadaire et effets secondaires associés), sans compter que les antagonistes de CCR5 (maraviroc) sont innefficaces contre les souches de virus CXCR4-tropique.

La trithérapie sous sa formule actuelle prévoit généralement l'usage de deux NRTIs (généralement tenofovir et emtricitabine en coformulation) avec soit un NNRTI (généralement efavirenz) ou un PI (généralement atazanavir ou darunavir). La formulation peut changer en fonction de l'apparition d'effets secondaires indésirables, de résistance virale ou d'autres spécificités du patient. Le souci d'augmenter la tolérance du traitement tout en réduisant sa toxicité, son coût et la probabilité d'émergence de souches virales résistantes évoquent l'importance du développement de nouvelles classes de médicaments. En ce sens, plusieurs nouvelles molécules sont présentement en essai clinique (38), dont plusieurs inhibiteurs d'entrée, d'intégration et de doigt de zinc, une classe expérimentale prévenant l'incorporation de l'ARN génomique dans la particule en formation (56).

Plusieurs essais cliniques sur des vaccins anti-VIH-1 ont aussi retenu l'attention ces dernières années (résumé dans (181). Deux modalités de réponse immunitaire ont jusqu'à maintenant été visés, soit une réponse humorale via des anticorps neutralisant

(73, 194) soit une exacerbation de la réponse à médiation cellulaire via les lymphocytes T CD8 cytotoxiques (26, 38)i l'une ni l'autre ne s'est avérée efficace. Bien que de nombreuses autres études soient encore en cours, les données actuelles suggèrent que l'élaboration d'un vaccin efficace nécessitera d'abord une meilleure compréhension des différents éléments contribuant à l'immunité contre le VIH-1 chez l'humain.

Aucune des approches thérapeutiques développées ou envisagées à ce jour n'a le potentiel de purger les réservoirs viraux, ces cellules à longue vie où le virus intégré peut demeurer sous-forme latente. Ces cellules sont innefficacement reconnues par le système immunitaire et persistent à long terme, empêchant ainsi la clairance complète du virus chez le patient, même sous trithérapie (225).

OBJECTIF GÉNÉRAL

Au début de mon doctorat, il était bien connu que Vpu stimule la relâche de différents types de virus dans certaines cellules dites « restrictives » (HeLa, Jurkat, CEM, lymphocyte T CD4 primaire, macrophage…) par opposition aux cellules « permissives » dans lesquelles l'effet de cette protéine accessoire n'est pas observé (COS, HEK 293T, HT1080, SupT1, Vero…) (80, 206, 216). L'existence du facteur de restriction fut mise à jour au moyen d'hétérokaryons nés d'une fusion entre une cellule restrictive et permissive. À l'époque, cette approche expérimentale avait prouvé le caractère dominant et restreignant du facteur cellulaire (249). Divers critères ont ensuite été employés afin d'identifier ce facteur de restriction. Il se devait d'être : 1) exprimé de façon endogène dans les cellules restrictives; 2) inductible par l'IFN dans les cellules permissives (185); 3) capable de restreindre la relâche de différents types de virus et 4) inhibé par Vpu. Tetherin s'est avéré répondre à tous ces critères (185, 248).

Bien que le facteur de restriction fût ainsi identifié, le mécanisme par lequel il était contré par Vpu demeurait largement inconnu. Une réduction du niveau de Tetherin à la surface des cellules infectées exprimant Vpu fut tout de même rapidement remarquée (248). Cependant, il n'était pas clair comment ce phénotype pouvait expliquer l'antagonisme d'autant plus qu'une autre étude questionnait sa pertinence fonctionnelle (174). Dans ce contexte, l'objectif général de ma thèse de doctorat était de comprendre la stratégie employée par Vpu afin de surmonter l'activité restrictive de Tetherin. Ce large objectif comprenait 1) l'identification du(des) compartiment(s) d'où Vpu contrecarre l'action antivirale de Tetherin; 2) l'investigation du mécanisme qui lui est sous-jacent; 3) l'identification du pool de Tetherin ciblé par Vpu.

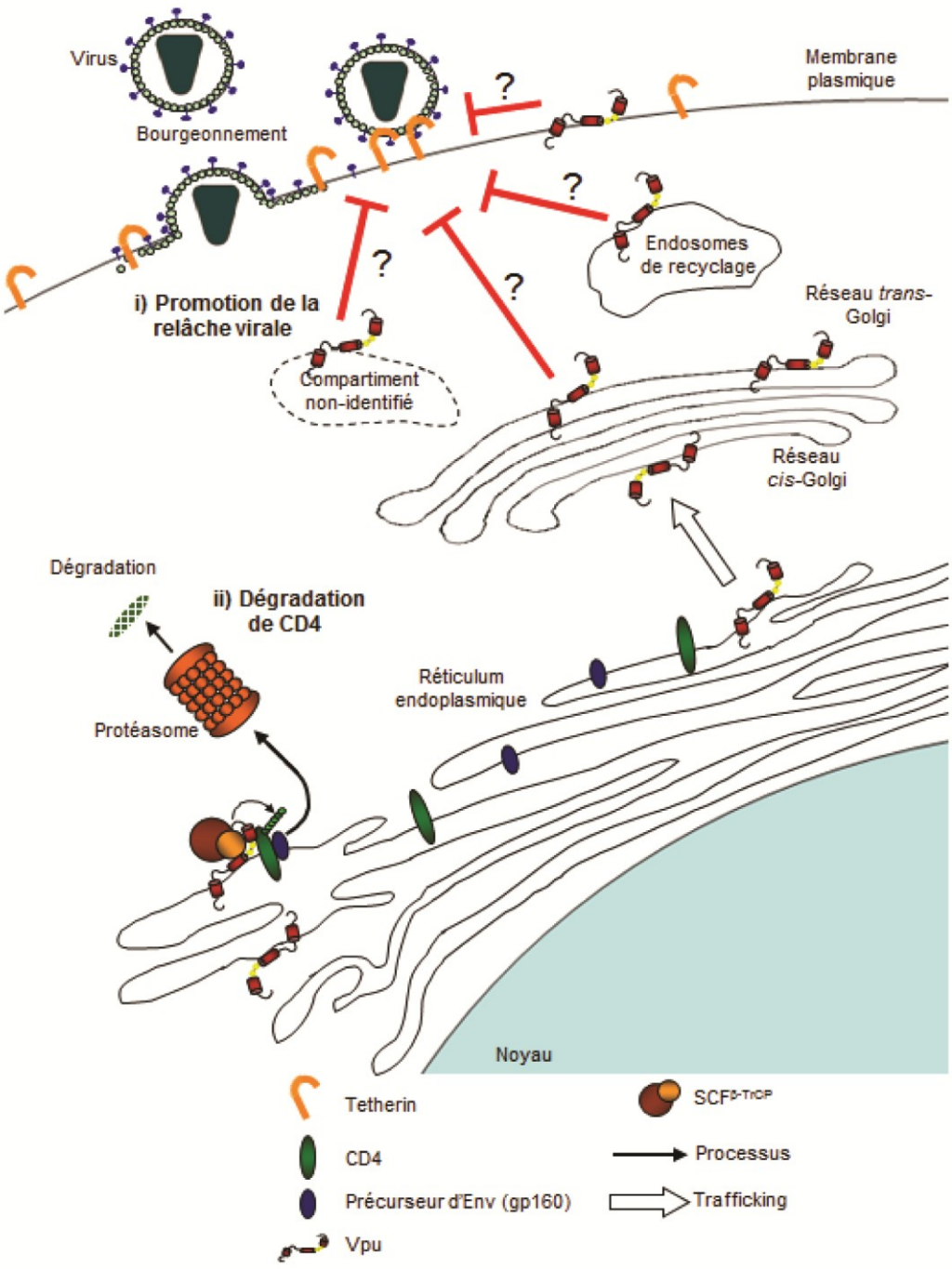

Figure 3: Modèle de l'effet de Vpu à l'origine de cette thèse
Représentation schématique du modèle tel qu'envisagé avant la contribution de la présente thèse. La promotion de la relâche virale par Vpu prend place dans un compartiment post-réticulum endoplasmique (RE) mal défini, soit à partir du réseau *trans*-Golgi, des endosomes de recyclage, de la surface, ou d'un compartiment non-identifié. Le mécanisme d'action est inconnu. Par opposition, le mécanisme de dégradation protéasomale de CD4 par Vpu se situe au niveau du RE et implique le recrutement de β-TrCP.

CHAPITRE 1

De quel(s) compartiment(s) intracellulaire(s) Vpu du VIH-1 surmonte-t-il la restriction de la relâche des particules virales?

Avant la découverte de l'activité antivirale de Tetherin, bien peu d'indices sur le mécanisme par lequel Vpu était en mesure de stimuler la relâche des particules virales étaient connus. Tout de même, il fut démontré par l'usage de la Brefeldin A, une drogue inhibant la sortie des protéines membranaires du RE, que Vpu agissait à partir d'un compartiment post-RE, peut-être dans les endosomes de recyclage (218, 250). Cette notion contrastait ainsi avec la fonction de dégradation de CD4, cantonnée à ce compartiment cellulaire (218). Ces études ont été les premières à soulever une possible relation entre la localisation de Vpu et ses fonctions. L'accumulation de Vpu du sous-type B dans le RTG, et dans une moindre mesure dans le RE ainsi que dans les endosomes de recyclage fut attestée par de précédentes études (188, 250). Par contre, malgré cette bonne connaissance de la localisation de Vpu, aucune donnée fonctionnelle satisfaisante n'avait permis de situer précisément l'antagonisme de Tetherin par Vpu. Inversement, aucune fonction n'était associée au pool majeur de Vpu situé dans le RTG. De plus, la neutralisation d'une restriction en surface par une protéine ne s'y trouvant pas représentait un paradoxe. Nous avons donc raisonné que l'identification de ce compartiment pourrait donner de précieuses informations quant à la nature du mécanisme régissant l'augmentation de la relâche virale.

L'objectif de ce premier chapitre était donc d'identifier le(s) compartiment(s) d'où Vpu exerce son action contre Tetherin afin de promouvoir la relâche de particules virales. Cet objectif comprend une analyse approfondie 1) de la localisation de Vpu de sous-type B; 2) des régions de Vpu responsables de cette localisation et 3) des conséquences fonctionnelles de la délocalisation de Vpu hors de ce compartiment.

Ce chapitre fut l'objet d'un article publié en 2009 dans *Journal of Virology*, un journal couvrant différents sujets de recherche en virologie (60). Bibhuti Bhusan Roy, Ph.D., a réalisé la caractérisation fonctionelle des mutants de délétion de Vpu (Figure 8) alors que Pierre Guiot-Guillain, Johanne Mercier, Julie Binette, Ph.D., Grace Leung et Éric Cohen, Ph.D., ont fourni une aide technique et/ou conceptuelle. Mathieu Dubé a exécuté les expériences des Figures 1-7, 9 et supplémentaires. Le manuscrit fut écrit par Mathieu Dubé et Éric Cohen, Ph.D.

RÉSUMÉ

Vpu augmente l'efficacité de la relâche du VIH-1 en surmontant l'activité de Tetherin, un facteur de l'hôte qui retient les virions à la surface de la cellule infectée. Dans cette étude, nous avons analysé la localisation intracellulaire de Vpu du sous-type B dans des cellules humaines produisant des virus du VIH-1. Nous avons découvert que la mutation des résidus conservés chargés positivement (R30 et K31), qui se trouvent au milieu de motifs putatifs de triage tyrosine et dileucine se chevauchant dans la région charnière de Vpu, affecte à la fois l'accumulation de la protéine dans le RTG et l'efficacité de son transport vers des compartiments endosomaux tardifs. La caractérisation fonctionnelle de ce mutant a révélé une corrélation entre la délocalisation de Vpu hors du RTG et l'atténuation de la relâche du VIH-1. De façon intéressante, l'abrogation du trafic de Vpu du RTG vers le système endosomal par l'usage d'ARN d'interférence dirigé contre les chaînes légères de la clathrine a légèrement stimulé la relâche en présence de Vpu mais complètement rétabli l'activité du mutant Vpu R30A,K31A. L'analyse de mutants de délétion de la région C-terminale de Vpu a permis d'identifier des déterminants additionnels dans la seconde hélice-α de la protéine qui réguleraient sa rétention/localisation dans le RTG ainsi que l'importance fonctionnelle de cette localisation. Finalement, nous avons montré qu'une large proportion de Vpu co-localise avec Tetherin dans le RTG et que ce haut degré de co-localisation est important pour la facilitation de la relâche du VIH-1. Pris ensemble, nos résultats démontrent un trafic de Vpu entre le RTG et le système endosomal et suggèrent que la distribution de Vpu dans le RTG est critique pour surmonter l'activité restrictive de Tetherin sur la relâche du VIH-1.

Suppression of Tetherin-Restricting Activity on HIV-1 Particle Release Correlates with Localization of Vpu in the *trans*-Golgi Network

Mathieu Dubé[1,2], Bibhuti Bhusan Roy[1], Pierre Guiot-Guillain[1,2], Johanne Mercier[1], Julie Binette[1,2], Grace Leung[1] and Éric A. Cohen[1,2] *

[1]Laboratory of Human Retrovirology, Institut de recherches cliniques de Montréal (IRCM),

[2]Department of Microbiology and Immunology, Université de Montréal, Montreal, Québec, Canada.

Running Title: Vpu enhances HIV-1 release from the TGN

*Corresponding author:

Manuscript information: 44 pages, 9 figures.

Word counts: abstract = 248 words; text word count = 6991 words.

ABSTRACT

Vpu promotes efficient release of HIV-1 by overcoming the activity of tetherin, a host cell restriction factor that retains assembled virions at the cell surface. In this study, we analyzed the intracellular localization and trafficking of subtype B Vpu in HIV-1-producing human cells. We found that mutations of conserved positively charged residues (R30 and K31) within the putative overlapping tyrosine and dileucine-based sorting motifs of the Vpu hinge region affected both the accumulation of the protein in the *trans*-Golgi network (TGN) and its efficient delivery to late endosomal degradative compartments. Functional characterization of this mutant revealed that mislocalization of Vpu from the TGN correlated with an attenuation of HIV-1 release. Interestingly, clathrin light chains siRNA-directed disruption of Vpu trafficking from the TGN to the endosomal system slightly stimulated Vpu-mediated HIV-1 release and completely restored the activity of the Vpu R30A,K31A mutant. Analysis of C-terminal deletion mutants of Vpu identified an additional determinant in the second helical structure of the protein, which regulated TGN retention/localization, and further revealed the functional importance of Vpu localization in the TGN. Finally, we show that a large fraction of Vpu co-localizes with tetherin in the TGN and provide evidence that the degree of Vpu co-localization with tetherin in the TGN is important for efficient HIV-1 release. Taken together, our results reveal that Vpu traffics between the TGN and the endosomal

system and suggest that proper distribution of Vpu in the TGN is critical to overcome the restricting activity of tetherin on HIV-1 release.

INTRODUCTION

Human immunodeficiency virus type-1 (HIV-1) viral protein U (Vpu) is an oligomeric type 1 integral membrane protein that is associated with two major functions during HIV-1 infection (1, 16). First, it contributes to CD4 receptor down-regulation by targeting newly synthesized CD4 molecules for degradation by the ubiquitin-proteasome system in the endoplasmic reticulum (ER) via a mechanism that most likely involves a dislocation step (2, 19). Second, Vpu expression enhances the release of HIV-1 particles and of widely divergent retroviruses, such as murine leukemia virus (MLV), in most human cells by a mechanism that does not rely on a specific interaction with Gag structural proteins (11, 13, 34, 35). Importantly, these Vpu biological activities play an active role in HIV-1 pathogenesis since Vpu-defective simian-HIV-1 strains were found to be less pathogenic *in vivo* (33).

Vpu enhances the release of retroviral particles by counteracting a human-specific host cell dominant restriction to particle release in some human cell types (41). This host cell restriction was shown to consist of protein-based factors that caused retention of fully formed virions on infected cells surface or in endosomes after endocytosis (21). Indeed, recent studies provided strong evidence that a membrane protein of unknown function called bone marrow stromal antigen-2 (BST-2; also known

as CD317 or HMI 1.24), and now designated tetherin, is the host factor that mediates this restriction on HIV-1 and MLV particles (22, 39). Accordingly, the effect of Vpu on HIV-1 release is prominent in many human cell types (termed restrictive or Vpu-responsive cells) constitutively expressing high or moderate levels of tetherin, including epithelial cell lines (HeLa), T cell lines (Jurkat, CEM) and primary T lymphocytes, but is not observed in some human cell lines such as HEK 293, HOS and HT1080 (termed permissive or Vpu-unresponsive cells) that do not express the restriction factor (22, 39). Indeed, these cells allow efficient viral particle release in absence of Vpu and enhancement of virus production by Vpu is not observed.

The mechanism and the intracellular sites through which Vpu overcomes the antiviral activity of tetherin and enhances release of HIV-1 particles are not currently precisely defined. Although Vpu appears to act on a host protein that exerts its restricting activity on HIV particle release at the cell surface, the most studied subtype B Vpu was found to localize predominantly in the *trans*-Golgi network (TGN) and to lower extent in the ER and the recycling endosomes (23, 42). However, in contrast to prototypical subtype B Vpu, the subtype C Vpu protein was found to localize both at the plasma membrane and in the Golgi (23). While ER localization is required for CD4 degradation, artificial retention of Vpu in the ER appear to interfere with enhancement of viral particle release, suggesting that Vpu needs to reach a post-ER compartment to mediate this function (32). In that regard, a previous study showed that expression of DN Rab11a or DN myosin Vb, which are known to disrupt protein trafficking through the recycling endosomes, can inhibit HIV-1 release in the presence of Vpu, suggesting that a functioning recycling endosome compartment is required (42). Moreover,

disruption of exit from recycling endosomes led to a marked trapping of Vpu in these structures, suggesting that Vpu normally traffics through recycling endosomes. Finally, recent studies that examined the subcellular distribution of Vpu relative to native tetherin have found that the two proteins co-localize within cytoplasmic structures that still remain to be characterized (22, 39). Furthermore, although Vpu had no overt effect on the overall levels of tetherin in condition of efficient viral particle release (22), its expression down-regulated tetherin from the cell surface (39).

In this study, we investigated the intracellular sites through which subtype B Vpu must traffic to counteract the activity of tetherin and perform its viral particle release enhancing function. Notably, we show that Vpu traffics between the TGN and the endosomal system. Furthermore, we provide evidence that the steady-state distribution of Vpu in the TGN is regulated by determinants within the hinge region of the protein as well as by sequences encompassing the second helical structure of the protein cytoplasmic domain. Additionally, we show that a large proportion of Vpu co-localizes with tetherin within the TGN. Importantly, we find that proper distribution of Vpu in the TGN might represent a critical requirement to overcome the restricting activity of tetherin on HIV-1 particle release.

MATERIAL AND METHODS

Antibodies and chemical compounds. BrefeldinA (BFA), Chloroquine (CQ) as well as rabbit polyclonal anti-actin antibodies were all obtained from Sigma. The anti-Vpu

rabbit polyclonal serum was described previously (6). The following antibodies were obtained from commercial sources: mouse anti-CD63 (Hybridoma Bank (NICHD, University of Iowa)), mouse anti-lysosome-associated membrane protein-1 (LAMP1), (Santa Cruz Biotechnology), mouse anti-Calreticulin (Santa Cruz Biotechnology), sheep anti-TGN46 (Serotec), mouse anti-Rab5 (BD Biosciences), mouse anti-BST-2 (Novus Biologicals), rabbit anti-clathrin light chains (CLCs) (Millipore) mouse anti-clathrin heavy chains (CHCs) (BD Biosciences) and mouse anti-cation-independent mannose-6-phosphate receptor (CI-MPR) (Abcam). The anti-CD4 (OKT4) and anti-p24 monoclonal antibodies were isolated from ascitic fluids of Balb/c mice that were injected with the OKT4 or p24 hybridoma (American Type Culture Collection (ATCC), catalog nos.CRL-8002 and HB9725, respectively). The human anti-HIV (#153) serum was obtained from an HIV-1 infected individual (15). Anti-GFP monoclonal antibody, Transferrin-Alexa 488 conjugates and all Alexa 488, 594 and 647-conjugated IgG antibodies were obtained from Molecular Probes. All reagents were stored according to the manufacturer's instructions.

Cells, transfection and siRNAs. HeLa TZM cells were obtained from the AIDS Research and Reference Program (NIH). HEK 293T and HeLa cells were obtained from ATCC. All cells were maintained as described previously (15). Unless specified, HEK 293T and HeLa cells were transfected by the calcium-phosphate method, and analyses were performed 48h post-transfection. All specific siRNAs were synthesized by Dharmacon as 21-mers with UU overhangs. SiRNAs were transfected using Oligofectamine (Invitrogen) according to the manufacturer instructions. Briefly, siRNA

were pre-incubated with 15 µl of Oligofectamine and overlayed on cells at 50% confluence. Both siRNA specific to CLCa (GGAAAGUAAUGGUCCAACA) and CLCb (GGAACCAGCGCCAGAGUGA) were used for CLCs depletion at a final concentration of 62.5 nM each. SiRNA specific to CHCs (GCAAUGAGCUGUUUGAAGA) or tetherin (Dharmacon Smartpool, catalogue number L-011817) and the non-targeting siRNA Scrambled #2 from Dharmacon were used at a final concentration of 125 nM. SiRNA-transfected cells were then transfected with the appropriate proviral construct 72h post-siRNA transfection using lipofectamine 2000 (Invitrogen) and processed 24h later. Empty plasmid DNA was added to each transfection to keep the amount of transfected DNA constant.

Plasmid constructs. The mammalian expression plasmids SVCMV-*vpu wt*, SVCMV-*vpu*- and SVCMV-*CD4* have been described previously (2). HxBH10-*vpu wt* and HxBH10-*vpu*- are two isogenic infectious HIV-1 molecular clones that only differ in the expression of Vpu (35). HxBH10-*vpu R30A,K31A,* HxBH10-*vpu Y29A,* HxBH10-*vpu I32A,L33A,* SVCMV-*vpu R30A,K31A,* SVCMV-*vpu I32A,L33A,* and SVCMV-*vpu Y29A* were generated by PCR-based site-directed mutagenesis as described previously (38). The plasmids pEGFP-Rab7 wt, pEGFP-Rab7 N125I and pEGFP-Rab7 Q67L were kindly provided by Dr. Robert Lodge (Université Laval, QC, Canada). To construct pEYFP-N1-Vpu wt, Vpu was amplified by PCR from the molecular clone HxBH10-*vpu wt* using the forward primer 5'-TCAAAGCAGTCTAGAGTACATGTA-3' and the fusion primer 5'-TCCGCCGCCCCCCAGATCATCAACATC-3'. EYFP was amplified by PCR from the mammalian expression plasmid pEYFP-N1 (Clontech) using the

fusion primer 5'-GGGGGCGGCGGAGTGAGCAAGGGCGAG-3' and reverse primer 5'-GATTATGATCTATAGTCGCGGCCGC-3'. Fusion of EYFP in C-terminal of Vpu was achieved by a second PCR on the two previously generated fragments using the forward and reverse primers. The resulting PCR product was inserted in pEYFP-N1 within the NheI/NotI restriction sites. The Vpu deletion mutants were generated using a similar strategy. The forward primer mentionned above was used to amplify Vpu Δ9, Δ13, Δ14, Δ18, Δ23 with the fusion primers 5'-CTCACTCCGCCGCCCCCGTGCCCCATCTCCACCCCCATC-3', 5'-CTCACTCCGCCGCCCCCCACCCCCATCTCCACAAGTGC-3', 5'-CTCACTCCGCCGCCCCCCCCCCATCTCCACAATGCTGA-3', 5'-CTCA CTCCGCCGCCCCCAAGTGCTGATATTTCTCCTTC-3', 5'-CTCACTCCGCCGCCC CCTCCTTCACTCTCATTGCCACTG-3', respectively. To amplify EYFP, the same reverse primer described above and the fusion primer 5'GGGGGCGGCGGAGTG AGCAAG-3' were used. The resulting PCR fragments were inserted in the pEYFP-N1 vector within the NheI/NotI restriction sites. All constructs were confirmed by automatic DNA sequencing.

*Pulse-chase and radio-immunoprecipitation experiments***.** Pulse-chase experiments were performed as described previously (2). Briefly, transfected HEK 293T cells were pulse-labeled for 30 min with 800 μCi/ml of [^{35}S]methionine and [^{35}S]cysteine (Perkin Elmer) and chased in DMEM containing 5% FBS. For some experiments, 10 μM BFA was added throughout the labeling and chase periods. At the indicated time periods, radio-labeled cells were lysed in radio-immunoprecipitation assay (RIPA-DOC) buffer

(10mM tris pH 7.2, 140 mM NaCl, 8 mM Na_2HPO_4, 2 mM NaH_2PO_4, 1% Nonidet-P40, 0.5% sodium dodecyl sulfate, 1.2 mM deoxycholate) supplemented with a cocktail of protease inhibitors (Protease Inhibitors Complete, Roche Diagnostics). Following lysis, labeled proteins were immunoprecipitated with the indicated antibodies and analyzed by SDS-PAGE and autoradiography (38).

*Steady-state detection of proteins by western blot***.** HeLa or HEK 293T cell transfectants were lysed in RIPA-DOC. Proteins from lysates were resolved on 10-12.5% SDS-PAGE tricine gels and electro-blotted as described elsewhere (2). Western blot was performed as described previously (10).

*Fluorescent and confocal microscopy***.** Immunofluorescence procedures were described previously (10). Briefly, immunostaining was performed on HeLa cells transfected with either the HxBH10 proviral DNA constructs or the Vpu-expressing plasmids. Cells were fixed with 4% paraformaldehyde and permeabilized with 0.2% Triton X-100. Next, cells were incubated with the first antibody and incubated with the appropriate secondary antibody, and for samples analyzed by fluorescence microscopy, nuclei were stained with DAPI for 5 min. To increase the EYFP signal, anti-GFP antibodies were used. Cells were examined by conventional epifluorescence micrographs on a Zeiss Cell Observer system (Zeiss) equipped with an Axiovert 200M microscope using the 100X oil lens. Where specified, analyses were also performed with a Axiovert 100M confocal microscope (Zeiss). Images were digitally deconvoluted with the AxioVision

3.1 software, using the nearest-neighbor deconvolution method. Quantitation of Vpu accumulation in the TGN was determined using the Zeiss LSM510 software. The percentage of Vpu accumulating in the TGN was calculated by evaluating the Vpu signal intensity in the TGN, as delimited by the TGN46 marker, relative to the total Vpu signal intensity in the cell. Statistical analysis was performed using an unpaired Student's *t* test, and statistical significance was considered at $p < 0.05$.

Transferrin uptake assay. For transferrin uptake experiments, siRNA-transfected HeLa cells were washed with PBS 96h post-siRNA transfection. Cells were incubated at 4°C in serum-free DMEM. After 15 min, Alexa-Fluor-488-conjugated transferrin (Molecular Probes) was added and the cells were incubated for 30 min at 4°C. Cells were then washed with PBS, and shifted to 37°C in serum-free DMEM for 10 min. The internalization process was blocked by shifting the cells at 4°C. Uninternalized transferrin on the cell membrane was washed away by washing the cells with 150 mM glycine (pH 2.5), and the uptake was determined by flow cytometry.

*Viral release assays***.** HeLa cells were seeded on 100-mm^2 dishes and transfected as described above. Transfectants were metabolically labeled with 200 μCi/ml [35S]methionine-cysteine for 5h. Virus particles from supernatants were clarified by centrifugation, filtered through a 45 μm filter, and then pelleted by ultracentrifugation onto a 20% sucrose cushion in PBS for 90 min at 130 000 g at 4°C. Cells and virions were subsequently lysed in RIPA-DOC. Gag-related products were immunoprecipitated

from cell and virus lysates using a mixture of human anti-HIV (#153) serum and mouse anti-p24 monoclonal antibody. Additionally, Vpu was immunoprecipitated from cell lysates using a polyclonal rabbit anti-Vpu serum. Radio-labeled proteins were resolved on 10% SDS-PAGE tricine gels and analyzed by autoradiography. For steady-state analysis, viral particles were pelleted from supernatant of transfected HeLa cells using the procedure described above. Proteins were analyzed by western blot using specific antibodies. To measure infectious virus released from transfected cells, HeLa-TZM indicator cells were innoculated with an aliquot of virus-containing supernatant. After 48h, HeLa-TZM cells were lysed and luciferase activity was determined using the Promega Luciferase Assay System. Statistical analysis was performed using a paired Student's *t* test, and statistical significance was considered at $p < 0.05$.

Scanning and quantitation Scannings of autoradiograms and western blots were performed on a Storm860 PhosphoImager (Molecular Dynamics) and Duoscan T1200 scanner (AGFA), respectively, followed by densitometric quantitation using the Image Quant 5.0 software (Molecular Dynamics). Viral release efficiency was evaluated by determining the ratio of viral particle-associated Gag signal over the total Gag signal (virion and cell-associated Gag signals). Statistical analysis was performed using a paired Student's *t* test, and statistical significance was considered at $p < 0.05$.

RESULTS

Vpu localizes to the TGN and is associated to late endosomes. Prototypical subtype B Vpu has been previously shown to reside predominantly in a perinuclear region corresponding to the TGN (23, 42). While a significant overlap of Vpu with TGN markers was observed in these studies, it was also apparent that not all of the population of Vpu localized within the TGN. Given that we obtained evidence indicating that Vpu turnover was increased upon exit from the ER (Fig. S1), we hypothesized that Vpu may also traffic through late endosomal compartments. To investigate this, we examined the subcellular localization of native Vpu in HIV-1-producing restrictive HeLa cells using immunostaining and fluorescence microscopy. As reported by others (23, 42), we found that Vpu co-localized predominantly with the TGN marker, TGN46. (Fig.1A). In addition to its TGN localization, Vpu was also detected in cytoplasmic punctuated structures in some Vpu-expressing HeLa cells. These cells displayed a close association of Vpu with the late endosomal marker CD63, but not with the ER marker calreticulin nor with LAMP1, a type I transmembrane glycoprotein that is associated primarily with lysosomes and late endosomes (Fig. 1 B). Taken together, these results indicate that native Vpu is localized primarily in the TGN but can also be found closely associated to CD63-positive late endosomal structures.

Mutations in the hinge region of Vpu affect the subcellular localization of the protein. The finding that Vpu is localized in the TGN and associated to some extent to late

endosomal compartments suggests that the protein is trafficking through the endosomal network and as such might contain motifs or/and domains governing trafficking or retention of the protein to specific subcellular compartments. Structurally, Vpu consists of two major domains: an N-terminal transmembrane (TM) domain that anchors Vpu in cellular membranes (29, 34, 37), and a cytoplasmic tail consisting of two putative alpha helices (alpha helix 1 (H1) : a.a. 37 to 51 and alpha helix 2 (H2): a.a. 57 to 72) separated by a conserved DSGϕXS β-TrCP recognition site phosphorylated by casein kinase II (Fig. 2A) (9, 30, 31). Upon analysis of our Vpu mutant collection, we identified a mutant of Vpu that was more stable than Vpu wt. This mutant, Vpu R30A,K31A, harbored two alanine substitutions at the well conserved arginine (Arg) and lysine (Lys) basic residues located at position 30 and 31 in the hinge region between the TM and the cytoplasmic domains of the protein (Fig. 2A). Interestingly, these two positively charged residues are part of a putative tyrosine-based, YXXϕ, sorting signal (Y corresponds to Tyr, XX are residues that are highly variable and ϕ corresponds to residues with bulky hydrophobic side chains) and an overlapping dileucine-based motif, [D/E]XXXL[L/I] (D/E corresponds to Asp or Glu, XXX are residues that are highly variable while L or I corresponds to Leu or Ile) (Fig.2A). In contrast to Vpu wt, Vpu R30A,K31A levels remained relatively similar throughout a 5h pulse-chase experiment and were not affected when the protein was prevented from trafficking out of the ER by treatment with BFA, a fungal metabolite that blocks protein sorting from the ER to the Golgi (8) (Fig. S1). These results suggested that these highly conserved positively charged a.a. residues (96% conservation throughout Vpu subtypes) located in the hinge

region of Vpu may affect Vpu trafficking and/or stability. In fact, single R30A or K31A mutations were also found to be sufficient to stabilize Vpu (data not shown).

To investigate the effect of mutations in the hinge region on Vpu trafficking, we compared the subcellular localization of native Vpu wt and Vpu R30A,K31A in HIV-1-producing HeLa cells. As shown in Figure 2, the R30A,K31A mutations decreased very significantly the accumulation of native Vpu in the TGN (~40% of total Vpu R30A,K31A is detected in the TGN compared to ~80% for Vpu wt, see Fig. 2B and C) while increasing the association of the protein with the late endosomal CD63 marker (Fig. 2B). Furthermore, in contrast to wt Vpu, we observed a strong co-localization of Vpu R30A,K31A with LAMP1 (compare Fig. 2B to Fig.1B). Importantly, no significant co-localization was observed between Vpu R30A,K31A and calreticulin, thus ruling-out the possibility that the decreased accumulation of the mutant protein in the TGN resulted from a sequestration in the ER.

Overall, these findings suggest that mutations at Arg30 and Lys31 within the hinge region of Vpu affect both the accumulation of the protein in the TGN as well as its efficient delivery to late endosomal degradative compartments, indicating that Vpu might traffic between the TGN and the endosomal sytem.

Vpu traffics through the late endosomal network and is degraded in lysosomes. To further examine whether Vpu is targeted for degradation in late endosomal structures, we treated Vpu-expressing HEK 293T and HeLa cells with chloroquine (CQ), a lysosomotropic agent that inhibits lysosomal protein degradation by neutralizing the

acidic environment of endocytic vesicles (7). As shown in Figure 3A, treatment of transfected cells with CQ led to a dose-dependent accumulation of Vpu. Similar results were obtained when Vpu-expressing HEK 293T cells were treated with ammonium chloride, another lysosomotropic weak base that acts as a lysosomal protein degradation inhibitor (data not shown). Furthermore, to provide direct evidence that Vpu is targeted for degradation in lysosomes, we analyzed Vpu degradation and subcellular localization in conditions where we interfered with the function of Rab7, a small GTPase that is found in late endosomes (26) and is implicated in the biogenesis and maintenance of the perinuclear lysosomal compartment (5). For that purpose, we took advantage of constructs encoding enhanced green fluorescent protein (EGFP)-Rab7 fusion proteins that do not perturb the delivery of cargo to lysosomes (Rab7 wt and the constitutively active Rab7 Q67L) or inversely, that interfere with lysosomal targeting and degradation (Rab7 N125I) (5, 26). While overexpression of EGFP-Rab7 wt or EGFP-Rab7 Q67L did not alter the level of Vpu at steady-state, the dominant negative (DN) EGFP-Rab7 N125I drastically increased the steady-state levels of Vpu (Fig. 3B, compare lanes 8-10 to lanes 2-7). Interestingly, expression of DN EGFP-Rab7 N125I in Vpu+ HIV-1-expressing HeLa cells led to an accumulation of Vpu in Rab7-positive vesicular structures while expression of EGFP-Rab7 wt (Fig. 3C) or EGFP-Rab7 Q67L did not (data not shown). Importantly, accumulation of Vpu in the TGN was not significantly affected by the overexpression of the DN Rab7 N125I mutant, suggesting that endosomes-to-TGN trafficking was not perturbed under these conditions (Fig. 3D). Altogether, these data indicate that native Vpu traffics through the late endosomal network and undergoes degradation in lysosomes.

Mutations in the hinge region of Vpu interfere with Vpu-mediated enhancement of HIV-1 particle release. Having shown that the Vpu R30A,K31A mutant displayed defects in lysosomal delivery and degradation as well as in accumulation in the TGN, we examined the implication of these defects on Vpu-mediated enhancement of viral particle release. Equal DNA amounts of Vpu-defective proviral construct (HxBH10-*vpu-)* or proviral constructs encoding Vpu wt (HxBH10-*vpu wt*) or Vpu R30A,K31A (HxBH10-*vpu R30A,K31A*) were transfected in restrictive HeLa cells. Forty-eight hours post-transfection, HIV-1-producing cell cultures were metabolically labeled for 5h and both cells and extracellular supernatants were harvested. Virus particles were further isolated from supernatants by clarification, filtration and ultracentrifugation as described in the material and methods. Gag protein levels were then analyzed in cell and viral particle lysates by immunoprecipitation using a serum from an HIV-1-positive individual combined with anti-24 polyclonal antibodies. Figures 4A and B reveal that while newly synthesized Vpu wt viral particles were released more efficiently that Vpu-defective particles, the Vpu R30A,K31A mutant virus exhibited a significant ($p<0.001$) ~40% attenuation of viral particle release efficiency compared to the Vpu wt virus control. Interestingly, this attenuation was accentuated to ~80% when viral particle release was evaluated in conditions where Vpu wt and Vpu R30A,K31A protein levels were comparable (Fig.4C and D, compare lane 5 to lane 4). In this context, the Vpu R30A,K31A mislocalization from the TGN was slightly enhanced (data not shown). Importantly, the Vpu R30A,K31A mutant was found to mediate CD4 degradation as efficiently as Vpu wt (Fig. S2), indicating that these mutations in the hinge region did

not affect the overall conformation of the protein but rather specifically interfered with the protein's ability to promote viral particle release. These results suggest that mislocalization of Vpu outside of the TGN and/or inefficient delivery of the protein to lysosomal compartments leads to impairment of Vpu-mediated enhancement of viral particle release. To discriminate between these two possibilities, we examined the effect of disrupting Rab7-mediated transport on the release of HIV-1 particles in HeLa cells. The Vpu-defective proviral construct was co-transfected with Vpu-expressing or control plasmids and the pEGFP-Rab7 wt or pEGFP-Rab7 N125I plasmids. As shown in Figures 4E and F, expression of the DN Rab7 N125I mutant stabilized Vpu, as expected, but had no significant effect on the enhancement of viral particle release. Similarly, abrogation of endocytic vesicle acidification and lysosomal degradation by CQ treatment did not affect the release of Vpu wt HIV-1 particles (data not shown). These findings indicate that delivery and degradation of Vpu in lysosomes do not represent essential steps in the process underlying Vpu-mediated enhancement of viral particle release and consequently, point toward accumulation of Vpu in the TGN as a possible important requirement for the protein's ability to promote HIV-1 particle release.

Disruption of Vpu trafficking from the TGN to the endosomal system stimulates HIV-1 particle release. Clathrin-coated vesicles are major carriers for endocytic cargo and mediate important intracellular trafficking events at the TGN and endosomes. Whereas clathrin heavy chains (CHCs) provides the structural backbone of the clathrin coat and is critical for all clathrin mediated trafficking process, recent evidence suggest that clathrin light chains (CLCs) are not required for clathrin-mediated endocytosis but are critical

for clathrin-mediated trafficking between the TGN and the endosomal system (25). For instance, CLCs depletion by siRNA did not have any influence on clathrin-mediated endocytosis of transferrin but caused the cation-independent mannose-6-phosphate receptor (CI-MPR) to cluster near the TGN (25). To obtain direct evidence that localization of Vpu in the TGN is important for Vpu function on HIV-1 particle release, we assessed the effect of disrupting clathrin-mediated trafficking from the TGN to the endosomal system on Vpu-mediated enhancement of HIV-1 particle release using siRNA specific for CLCs or CHCs. Equal DNA amounts of proviral constructs defective for Vpu or encoding wt Vpu, or the Vpu R30A,K31A mutant were transfected in HeLa cells that were depleted for CLCs beforehand. Viral particle release efficiency was then evaluated 96h post-siRNA transfection by measuring the levels of Gag associated with cell or viral particle lysates (Fig. 5A) as well as by evaluating the relative infectivity of released viral particles using the HeLa-TZM indicator cell line (Fig. 5B). Hela cells showed reduced levels of CLCs (approximately a 60% decrease) after transfection of siRNA specific for CLCs compared to control Hela cells transfected with a non-specific scrambled siRNA (Fig. 5A, compare lanes 4-6 to lanes 1-3). As previously reported (25), depletion of CLCs led to a clustering of CI-MPR near the TGN and did not affect clathrin-mediated endocytosis of transferrin from the cell surface (Fig. S3A and B). Although depletion of CLCs did not influence the release of Vpu-defective HIV-1 particle, it had a stimulatory effect on the release of Vpu+ HIV-1 particles. Indeed, a signifiant ~30% increase ($p = 0.035$) in viral particle release efficiency was observed in Vpu-expressing cells transfected with CLCs siRNA compared to control (Fig. 5A and B). This stimulation correlated with a stabilization of

Vpu wt (Fig.5A, compare lane 2 to lane 5), suggesting that depletion of CLC is indeed efficiently retaining Vpu within the TGN and as such preventing its trafficking to lysosomes. Interestingly, the defect in viral particle release observed with the Vpu R30A,K31A mutant was completely abrogated in condition where CLCs levels were reduced. Indeed, under these conditions the release efficiency of the Vpu R30A, K31A mutant was comparable to Vpu wt. Importantly, this abrogation of the viral particle release defect correlated with an increased accumulation of the Vpu R30A,K31A mutant in compartments that co-stained with the TGN marker TGN46 (Fig. 5C and D). As expected, Vpu R30A,K31A was not increasingly stabilized upon CLC siRNA treatment (Fig. 5A, compare lane 3 with lane 6) since this mutant is already impaired in its ability to be targeted for degradation in lysosomes. Overall, these findings suggest that this mutant is not impaired in its ability to overcome the restricting activity of tetherin but is rather inefficient at localizing at the TGN. As expected, similar results were obtained when viral particle release was analyzed in Hela cells that were transfected with CHCs siRNA. Under these conditions, the release efficiency of Vpu wt and Vpu R30A,K31A-encoding HIV-1 particles was equivalent (Fig. S4). Taken together, these results further suggest that native Vpu is trafficking between the TGN and the endosomal system. Additionnally, they provide strong evidence that proper distribution of Vpu in the TGN at steady-state is a key requirement to overcome the restricting activity of tetherin on HIV-1 particle release.

The membrane proximal tyrosine and dileucine-based sorting motifs of subtype B Vpu are not functionally active. Having obtained evidence that Vpu traffics between the

TGN and the endosomal system and that mutations at Arg30 and Lys31 in the Vpu hinge region affect this process, we next evaluated whether these residues are part of *bona fidae* tyrosine (YXXϕ or dileucine-based ([D/E]XXXL[L/I]) sorting signals, which might regulate Vpu trafficking between the TGN and late endosome/lysosome compartments. Toward this goal we generated expression plasmids encoding Vpu mutants that harbored substitution mutations at the Tyr residue located at position 29 (SVCMV-*vpu Y29A*) or at the Ile and Leu residues located at position 32 and 33 (SVCMV-*vpu I32A,L33A*) (Fig. 2A) since residues at these positions have been previously shown to be essential for the function of tyrosine and dileucine-based trafficking signals (3). Analysis of Vpu Y29A and Vpu I32A,L33A subcellular localization did not reveal any marked redistribution of the mutant proteins as compared to wt Vpu (Fig. 6A and B). Furthermore, mutations at Tyr29 or at Ile32 and Leu33 did not reveal any significant change in the ability of Vpu to enhance HIV-1 particle release (Fig. 6C and D). Moreover, in contrast to Vpu R30A,K31A, the Vpu Y29 and Vpu I32A,L33A mutants did not display any increase in their steady-state levels as compared to Vpu wt (Fig. 6C, compare lanes 4 and 5 with lanes 2 and 3). These findings indicate that the tyrosine and the dileucine-based trafficking motifs do not appear to actively regulate Vpu trafficking from the TGN to the endosomal system and, additionally, are not essential for the viral particle release enhancing function of the protein at least in the context of subtype B Vpu. Consequently, the phenotypes observed when the Arg30 and Lys31 residues are mutated might result from a limited activation of these putative trafficking motifs.

Deletion analysis of Vpu cytosolic tail identifies a determinant important for Vpu retention/localization in the TGN and efficient HIV-1 viral particle release. To further delineate region of the cytoplasmic tail that might be important for the subcellular localization of Vpu, we used a Vpu-EYFP reporter system to assess the intracellular localization of Vpu C-terminal deletion mutants by fluorescence microscopy. This approach was previously used by Pacyniak et al. (23) to identify a region within the cytoplasmic domain of subtype B Vpu that might be responsible for retention of the protein in the TGN. The Vpu-EYFP fusion protein expressed in restrictive HeLa cells demonstrated a subcellular distribution pattern similar to that observed with native Vpu expressed from an infectious molecular clone (compare Fig. 7B to Fig. 1A). Notably, ~87% of the Vpu fluorescence staining was found to localize in a perinuclear region that overlapped with the Golgi marker TGN46 (Fig. 7B and C). No accumulation of wt Vpu-EYFP was observed at the plasma membrane. We next examined the subcellular localization of various Vpu-EYFP deletion mutants (Fig. 7A). As reported by Pacyniak et al. (23), removal of 9 (VpuΔ9-EYFP) or 13 (VpuΔ13-EYFP) a.a. from the carboxyl-terminus of Vpu had, overall, marginal effects on the localization of the protein (Fig. 7B and C). In contrast, deletion of the C-terminal 14, 18 and 23 amino-acids, which encompass the second helical structure of the Vpu cytoplasmic tail, decreased significantly the accumulation of Vpu-EYFP in the TGN while increasing its detection within cytosolic vesicular structures, which co-stained in part with the early endosome marker, Rab5, and with CD63 (Fig. 7B-D). Interestingly, VpuΔ14, Δ18 and Δ23 could also be detected at the plasma membrane in some cells (data not shown).

We next assessed the effect of Vpu cytoplasmic tail deletion on the ability of the protein to promote the release of HIV-1 particle. Vpu-EYFP or Vpu-EYFP deletion mutants were co-transfected with the Vpu-defective proviral construct HxBH10-*vpu*- in HeLa cells and viral particle release was determined 48h post-transfection by measuring Gag proteins levels in cell and viral particle lysates by western blot (Fig. 8A). In addition, we also determined viral particle release efficiency by evaluating the relative infectivity of released viral particles (Fig. 8B). Results revealed that the VpuΔ9-EYFP and VpuΔ13-EYFP mutants, which were minimally affected in their localization to the TGN, promoted the release of HIV-1 viral particle almost as efficiently as wt Vpu-EYFP (Fig. 8B, compare lanes 3 and 4 to lane 8). In contrast, the VpuΔ14-EYFP, VpuΔ18-EYFP and VpuΔ23-EYFP deletion mutants, which displayed a significant decrease in the accumulation of the protein in the TGN, showed an attenuation of their viral particle release enhancing function (Fig. 8, compare lanes 5-7 to lane 8). Removal of the C-terminal 23 amino acids of Vpu abrogated the capacity of the protein to enhance particle release to a level comparable to the Vpu-defective HIV-1 virus control (Fig. 8, compare lane 7 to lane 2). Overall, these findings suggest that the C-terminal 23 amino acids of Vpu, which contains the second alpha-helical domain of the Vpu cytoplasmic domain, might be important for the localization/retention of the protein in the TGN. Furthermore, these results provide additional evidence that proper distribution of Vpu in the TGN is important for efficient release of viral particles from the cell surface.

Subtype B Vpu co-localizes with tetherin in the TGN. Vpu was recently shown to co-localize with tetherin within cytoplasmic structures (22, 40). However, the identity of the intracellular compartments where the two proteins co-localize remains undefined. To characterize the intracellular organelles where Vpu and tetherin reside, we transfected a proviral construct encoding Vpu in HeLa cells, which are known to express tetherin, and determined the subcellular localization of native Vpu and tetherin by immunostaining using specific antibodies. Tetherin localized predominantly within cytoplasmic structures that corresponded at least in part to the TGN (Fig. 9A). We observed a strong co-localization of Vpu and tetherin in the TGN as shown by the strong co-staining of Vpu, tetherin and TGN46, yet very low if any co-localization was observed in other tetherin-containing subcellular compartments (Fig. 9A). Similar results were obtained when VpuΔ23-EYFP fusion proteins were expressed in Hela cells (Fig. 9B). Quantitation of the proportion of total Vpu that co-localized with tetherin revealed that ~70% of Vpu (green pixels) overlapped with tetherin (blue pixels) (Fig. 9C). Having shown that a large proportion of Vpu wt co-localizes with tetherin in the TGN, we next assessed the localization of the Vpu R30A,K31A or the VpuΔ23-EYFP mutants relative to tetherin. Overall, the extent of co-localization between the Vpu mutants and tetherin was not as extensive as that of Vpu wt. Although a fraction of Vpu R30A,K31A and VpuΔ23-EYFP mutants still co-localized with tetherin in the TGN, a significant proportion of Vpu mutant proteins did not reveal any significant co-localization with tetherin (Fig. 9A panels a-d and Fig. 9B, panels e-h). In fact, whereas ~70% of total Vpu wt co-localized with tetherin, only ~40% of total Vpu R30A,K31A and VpuΔ23-EYFP mutants displayed such a co-localization (Fig. 9C) suggesting that

mislocalization of Vpu outside of the TGN decreased the overall degree of Vpu co-localization with tetherin. Importantly, the localization of Vpu did not appear to be influenced by the presence of tetherin since depletion of tetherin using specific siRNA did not alter the subcellular localization of wt or Vpu R30A,K31A mutant proteins (data not shown). Taken together, these results suggest a strong correlation between the degree of Vpu co-localization with tetherin in the TGN and efficient viral particle release.

DISCUSSION

In this study, we have analyzed the intracellular localization and trafficking of native subtype B Vpu in HIV-1-producing human cells. The data presented herein provide evidence that native Vpu traffics between the TGN and the endosomal system and that during this process some Vpu proteins are ultimately delivered to lysosomal compartments where they undergo degradation. Interestingly, mutations of highly conserved positively charged a.a. residues (Arg30 and Lys31) within the hinge region of Vpu were shown to decrease the steady-state localization of the protein in the TGN while increasing the localization of the protein in CD63/LAMP1-positive late endosomal compartments. Furthermore, disruption of clathrin-mediated trafficking between the TGN and the endosomal system using siRNA directed against CLCs had a stabilizing effect on wild-type Vpu and restored Vpu R30A,K31A distribution in the TGN to Vpu wt levels. Since the Vpu R30A,K31A mutant was found to be less

efficiently targeted for degradation in the lysosomes as compared to Vpu wt, it seems therefore likely that these positively charged a.a are affecting the efficiency or/and specificity of Vpu trafficking between the TGN and the endosomal system. Interestingly, Arg30 and Lys31 are part of sequences that were recently proposed to encode overlapping a tyrosine-based (YXXϕ) and dileucine-based [D/E]XXXL[L/I] sorting motifs in subtype C Vpu (27) (Fig. 2A). Tyrosine and dileucine-based sorting signals are found in the cytosolic domain of transmembrane proteins and are implicated in endocytosis as well as targeting of transmembrane proteins to lysosomes and lysosome-related organelles (12, 17). While the Y residue of YXXϕ sorting motifs is essential for function, the ϕ position can accommodate several residues with bulky hydrophobic side chains, which depending on their identity can specify the properties of the signal (3). With regard to [D/E]XXXL[L/I] dileucine-based sorting motifs, the acidic residue (D/E) has been previously shown to be important for targeting to late endosomes or lysosomes, whereas the first of the two leucines is generally invariant and its substitution with an isoleucine, as in subtype B Vpu (EYRK**I**L), reduces the potency of the signal (3). Interestingly, in both of these motifs, the X residues have been shown to contribute to the strength and fine specificity of the signal (14). Surprisingly, mutation of the key Tyr or Ile and Leu residues within these overlapping sorting motifs did not affect the subcellular distribution and stability of Vpu nor its enhancing function on HIV-1 particle release, suggesting that at least in the context of subtype B Vpu, these putative sorting motifs are not fully active and do not appear to regulate Vpu trafficking and function. These findings raise the possibility that subtype B Vpu TGN-to-endosome trafficking may not be actively regulated and may indeed occur by bulk flow. These

results are in sharp contrast with recent observations made by Ruiz et al., which found that mutation of the conserved Tyr residue in the hinge region of subtype C Vpu drastically decreased viral replication of SHIV virus encoding subtype C Vpu (27). This same group also showed that mutation of the second leucine (L39G) of the dileucine-based motif (EYRKLL) of subtype C Vpu leads to a protein that is transported to the cell suface less efficiently with the majority retained within the Golgi complex (27). It is therefore likely that the distinct requirement of subtype C and subtype B Vpu for tyrosine and dileucine-based sorting signals is related to the activity of their respective sorting motifs as well as their different patterns of localization. Importantly, the finding that the putative overlapping sorting motifs of subtype B Vpu are not fully active, suggests that mutations of the conserved positively charged a.a. residues may have restored to some extent their activities, thus resulting in a change of Vpu subcellular localization and stability. Although it is still conceivable at this point that these conserved positively charged a.a. residues may regulate Vpu trafficking by a mechanism that is independent from these putative sorting motifs, the fact that current evidence suggests that subtype C Vpu contains conserved functional trafficking signals makes this possibility less likely. Clearly, a more detailed analysis of the functional requirements of these canonical tyrosine and dileucine-based sorting motifs will be required to fully understand their respective roles in Vpu trafficking and function.

Even though our data suggest that subtype B Vpu traffics to some extent between the TGN and the endosomal system, at steady-state, the protein is predominantly localized in the TGN. In this regard, it has been shown that the steady-state distribution of the well-studied endoprotease furin in the TGN is achieved by a

mechanism involving two independent signals, which consist of a CK-II-phosphorylated acidic peptide (SDSEEDE, in which the serines can be phosphorylated) and the tetrapeptide YKGL (36). While the phosphorylated acidic domain is responsible for the retention of furin in the TGN, specifically by regulating the transport from late endosomes to the TGN through binding to the adaptor protein PACS1, the YKGL signal is involved in the endosomal retrieval of furin that have escaped to the cell surface (20, 28, 43). TGN38 is another protein that also uses two non-overlapping signals to mediate its steady state localization in the TGN (18). In the case of TGN38, the membrane spanning domain contains a retention signal that localizes the protein in the TGN, while a tyrosine-containing motif is responsible for retrieving escaped TGN38 from the plasma membrane via the recycling endosomes (4, 24). This type of retention/retrieval mechanism establishes an intracellular recycling loop, which allows a predominant Golgi distribution at steady state because the endocytic recycling is fast compared with the exit rate from the Golgi to the plasma membrane (18). Interestingly, our deletion analysis of the cytoplasmic tail of subtype B Vpu confirmed previous results from Pacyniak et al. (23), indicating that a domain encompassing the second helical structure of Vpu was important for the retention or localization of the protein in the TGN. However, in contrast to the data obtained by Pacyniak et al., deletion of these putative retention/localization sequences did not lead to a marked relocalization of the protein to the plasma membrane. In HeLa cells, we rather observed a predominant accumulation of mutant proteins in intracellular vesicles that co-stained in part with the Rab5 and CD63 endosomal markers, as exemplified by the VpuΔ23-EYFP mutant. This discrepancy is not currently understood but may be related to the distinct cell lines

(HeLa vs 293) that were used. While speculative at this juncture, our data raise the possibility that the steady-state TGN distribution of Vpu may be determined by two targeting signals in the cytoplasmic domain of the protein; a signal in the second alpha helical domain that ensures retention/localization of Vpu within the TGN by preventing its exit to more distal compartments and trafficking signals in the hinge region that regulates trafficking between the TGN and the endosomal system and that may also act as a retrieval motif for Vpu proteins that have escaped to other distal compartments. Given the functional importance of Vpu localization in the TGN (as discussed below), the sequence heterogeneity observed at the level of these YXXΦ□or [D/E]XXXL[L/I] motifs among different Vpu subtypes (**C**XXL for subtype D or EXXX**IL** for subtype B (Fig. 2A)) may indeed reflect the selective pressure for maintaining trafficking/retrieval signals of different type and strength in the context of Vpu proteins that are more or less retained in the TGN, as exemplified by subtype B and C Vpu proteins. Clearly more studies will be required to precisely define and dissect these targeting/retention signals and to analyze their individual and combined contributions to Vpu trafficking and steady-state distribution in the TGN.

Our finding that mutations that mislocalize Vpu outside the TGN impair Vpu-mediated enhancement of HIV-1 particle release suggests that proper distribution of Vpu in the TGN is critical to overcome the restricting activity of tetherin. This notion is indeed consistent with results from our experiments showing that retention of Vpu wt or the Vpu R30A,K31A mutant in TGN-related structures following disruption of clathrin-mediated TGN to endosome trafficking, stimulates Vpu-mediated enhancement of viral particle release. Interestingly, mutation of the dileucine motif of subtype C Vpu, which

resulted in an increased accumulation of the protein in the TGN, led to a similar stimulation of Vpu-mediated enhancement of viral particle release (27). Thus, the TGN could conceivably represent one key intracellular site from where Vpu overcomes the restricting activity of tetherin on HIV-1 particle release. In support of this model, we have also shown that Vpu co-localizes with tetherin specifically in the TGN: no significant co-localization of subtype B Vpu and tetherin was observed outside the TGN. Furthermore, mutants of Vpu, which were mislocalized from the TGN and impaired in their ability to enhance HIV-1 particle release, displayed a marked decrease in their degree of co-localization with tetherin in the TGN. These findings suggest that a threshold level of the total pool of Vpu needs to be present in the TGN at steady-state to encounter tetherin and efficiently overcome its antiviral activity. Since Vpu was recently shown to downregulate tetherin from the cell surface (44), it is therefore conceivable that Vpu overcomes the restricting activity of tetherin at the cell surface by trapping the protein in the TGN.

In conclusion the results presented herein suggest that native Vpu traffics between the TGN and the endosomal system in HIV-1 producing cells. Importantly, we provide evidence suggesting that proper distribution of Vpu in the TGN is critical to overcome the restricting activity of tetherin on HIV-1 particle release.

ACKNOWLEDGMENTS

We thank Dr. Robert Lodge for the kind gift of, the pEGFP-Rab7 plasmids used in this study as well as René-Pierre Lorgeoux and Alexandre Orthwein for experimental help and for sharing reagents and unpublished data. We also thank present and former members of the Cohen group for helpful discussion. HeLa-TZM cells were obtained from the AIDS Research and Reference Program (NIH). This work was performed by MD in partial fulfillment of his doctoral thesis and was supported by grants from the Canadian Institutes of Health Research (CIHR) (MOP-14228) and from the Fonds de la Recherche en Santé du Québec (FRSQ) to EAC. MD and PGG are the recipients of studentships from the CIHR strategic training program in Cancer research while JB is recipient of a studenstship from the FRSQ. EAC holds the Canada Research Chair in Human Retrovirology.

REFERENCES

1. **Binette, J., and E. A. Cohen.** 2004. Recent advances in the understanding of HIV-1 Vpu accessory protein functions. Curr Drug Targets Immune Endocr Metabol Disord **4:**297-307.

2. **Binette, J., M. Dube, J. Mercier, and E. A. Cohen.** 2007. Requirements for the selective degradation of CD4 receptor molecules by the human immunodeficiency virus type 1 Vpu protein in the endoplasmic reticulum. Retrovirology **4:**75.

3. **Bonifacino, J. S., and L. M. Traub.** 2003. Signals for sorting of transmembrane proteins to endosomes and lysosomes. Annu Rev Biochem **72:**395-447.

4. **Bos, K., C. Wraight, and K. K. Stanley.** 1993. TGN38 is maintained in the trans-Golgi network by a tyrosine-containing motif in the cytoplasmic domain. Embo J **12:**2219-28.

5. **Bucci, C., P. Thomsen, P. Nicoziani, J. McCarthy, and B. van Deurs.** 2000. Rab7: a key to lysosome biogenesis. Mol Biol Cell **11:**467-80.

6. **Cohen, E. A., E. F. Terwilliger, J. G. Sodroski, and W. A. Haseltine.** 1988. Identification of a protein encoded by the vpu gene of HIV-1. Nature **334:**532-4.

7. **de Duve, C., T. de Barsy, B. Poole, A. Trouet, P. Tulkens, and F. Van Hoof.** 1974. Commentary. Lysosomotropic agents. Biochem Pharmacol **23:**2495-531.

8. **Doms, R. W., G. Russ, and J. W. Yewdell.** 1989. Brefeldin A redistributes resident and itinerant Golgi proteins to the endoplasmic reticulum. J Cell Biol **109:**61-72.

9. **Federau, T., U. Schubert, J. Flossdorf, P. Henklein, D. Schomburg, and V. Wray.** 1996. Solution structure of the cytoplasmic domain of the human immunodeficiency virus type 1 encoded virus protein U (Vpu). Int J Pept Protein Res **47:**297-310.

10. **Finzi, A., A. Brunet, Y. Xiao, J. Thibodeau, and E. A. Cohen.** 2006. Major histocompatibility complex class II molecules promote human immunodeficiency virus

type 1 assembly and budding to late endosomal/multivesicular body compartments. J Virol **80:**9789-97.

11. **Gottlinger, H. G., T. Dorfman, E. A. Cohen, and W. A. Haseltine.** 1993. Vpu protein of human immunodeficiency virus type 1 enhances the release of capsids produced by gag gene constructs of widely divergent retroviruses. Proc Natl Acad Sci U S A **90:**7381-5.

12. **Gough, N. R., M. E. Zweifel, O. Martinez-Augustin, R. C. Aguilar, J. S. Bonifacino, and D. M. Fambrough.** 1999. Utilization of the indirect lysosome targeting pathway by lysosome-associated membrane proteins (LAMPs) is influenced largely by the C-terminal residue of their GYXXphi targeting signals. J Cell Sci **112 (Pt 23):**4257-69.

13. **Klimkait, T., K. Strebel, M. D. Hoggan, M. A. Martin, and J. M. Orenstein.** 1990. The human immunodeficiency virus type 1-specific protein vpu is required for efficient virus maturation and release. J Virol **64:**621-9.

14. **Kongsvik, T. L., S. Honing, O. Bakke, and D. G. Rodionov.** 2002. Mechanism of interaction between leucine-based sorting signals from the invariant chain and clathrin-associated adaptor protein complexes AP1 and AP2. J Biol Chem **277:**16484-8.

15. **Levesque, K., Y. S. Zhao, and E. A. Cohen.** 2003. Vpu exerts a positive effect on HIV-1 infectivity by down-modulating CD4 receptor molecules at the surface of HIV-1-producing cells. J Biol Chem **278:**28346-53.

16. **Malim, M. H., and M. Emerman.** 2008. HIV-1 accessory proteins--ensuring viral survival in a hostile environment. Cell Host Microbe **3:**388-98.

17. **Marks, M. S., P. A. Roche, E. van Donselaar, L. Woodruff, P. J. Peters, and J. S. Bonifacino.** 1995. A lysosomal targeting signal in the cytoplasmic tail of the beta chain directs HLA-DM to MHC class II compartments. J Cell Biol **131:**351-69.

18. **Maxfield, F. R., and T. E. McGraw.** 2004. Endocytic recycling. Nat Rev Mol Cell Biol **5:**121-32.

19. **Meusser, B., and T. Sommer.** 2004. Vpu-mediated degradation of CD4 reconstituted in yeast reveals mechanistic differences to cellular ER-associated protein degradation. Mol Cell **14:**247-58.

20. **Molloy, S. S., L. Thomas, J. K. VanSlyke, P. E. Stenberg, and G. Thomas.** 1994. Intracellular trafficking and activation of the furin proprotein convertase: localization to the TGN and recycling from the cell surface. Embo J **13:**18-33.

21. **Neil, S. J., S. W. Eastman, N. Jouvenet, and P. D. Bieniasz.** 2006. HIV-1 Vpu promotes release and prevents endocytosis of nascent retrovirus particles from the plasma membrane. PLoS Pathog **2:**e39.

22. **Neil, S. J., T. Zang, and P. D. Bieniasz.** 2008. Tetherin inhibits retrovirus release and is antagonized by HIV-1 Vpu. Nature **451:**425-30.

23. **Pacyniak, E., M. L. Gomez, L. M. Gomez, E. R. Mulcahy, M. Jackson, D. R. Hout, B. J. Wisdom, and E. B. Stephens.** 2005. Identification of a region within the cytoplasmic domain of the subtype B Vpu protein of human immunodeficiency virus type 1 (HIV-1) that is responsible for retention in the golgi complex and its absence in the Vpu protein from a subtype C HIV-1. AIDS Res Hum Retroviruses **21:**379-94.

24. **Ponnambalam, S., C. Rabouille, J. P. Luzio, T. Nilsson, and G. Warren.** 1994. The TGN38 glycoprotein contains two non-overlapping signals that mediate localization to the trans-Golgi network. J Cell Biol **125:**253-68.

25. **Poupon, V., M. Girard, V. Legendre-Guillemin, S. Thomas, L. Bourbonniere, J. Philie, N. A. Bright, and P. S. McPherson.** 2008. Clathrin light chains function in mannose phosphate receptor trafficking via regulation of actin assembly. Proc Natl Acad Sci U S A **105:**168-73.

26. **Press, B., Y. Feng, B. Hoflack, and A. Wandinger-Ness.** 1998. Mutant Rab7 causes the accumulation of cathepsin D and cation-independent mannose 6-phosphate receptor in an early endocytic compartment. J Cell Biol **140:**1075-89.

27. **Ruiz, A., M. S. Hill, K. Schmitt, J. Guatelli, and E. B. Stephens.** 2008. Requirements of the membrane proximal tyrosine and dileucine-based sorting signals for efficient

transport of the subtype C Vpu protein to the plasma membrane and in virus release. Virology **378:**58-68.

28. **Schafer, W., A. Stroh, S. Berghofer, J. Seiler, M. Vey, M. L. Kruse, H. F. Kern, H. D. Klenk, and W. Garten.** 1995. Two independent targeting signals in the cytoplasmic domain determine trans-Golgi network localization and endosomal trafficking of the proprotein convertase furin. Embo J **14:**2424-35.

29. **Schubert, U., S. Bour, A. V. Ferrer-Montiel, M. Montal, F. Maldarell, and K. Strebel.** 1996. The two biological activities of human immunodeficiency virus type 1 Vpu protein involve two separable structural domains. J Virol **70:**809-19.

30. **Schubert, U., P. Henklein, B. Boldyreff, E. Wingender, K. Strebel, and T. Porstmann.** 1994. The human immunodeficiency virus type 1 encoded Vpu protein is phosphorylated by casein kinase-2 (CK-2) at positions Ser52 and Ser56 within a predicted alpha-helix-turn-alpha-helix-motif. J Mol Biol **236:**16-25.

31. **Schubert, U., T. Schneider, P. Henklein, K. Hoffmann, E. Berthold, H. Hauser, G. Pauli, and T. Porstmann.** 1992. Human-immunodeficiency-virus-type-1-encoded Vpu protein is phosphorylated by casein kinase II. Eur J Biochem **204:**875-83.

32. **Schubert, U., and K. Strebel.** 1994. Differential activities of the human immunodeficiency virus type 1-encoded Vpu protein are regulated by phosphorylation and occur in different cellular compartments. J Virol **68:**2260-71.

33. **Stephens, E. B., C. McCormick, E. Pacyniak, D. Griffin, D. M. Pinson, F. Sun, W. Nothnick, S. W. Wong, R. Gunderson, N. E. Berman, and D. K. Singh.** 2002. Deletion of the vpu sequences prior to the env in a simian-human immunodeficiency virus results in enhanced Env precursor synthesis but is less pathogenic for pig-tailed macaques. Virology **293:**252-61.

34. **Strebel, K., T. Klimkait, F. Maldarelli, and M. A. Martin.** 1989. Molecular and biochemical analyses of human immunodeficiency virus type 1 vpu protein. J Virol **63:**3784-91.

35. **Terwilliger, E. F., E. A. Cohen, Y. C. Lu, J. G. Sodroski, and W. A. Haseltine.** 1989. Functional role of human immunodeficiency virus type 1 vpu. Proc Natl Acad Sci U S A **86:**5163-7.

36. **Thomas, G.** 2002. Furin at the cutting edge: from protein traffic to embryogenesis and disease. Nat Rev Mol Cell Biol **3:**753-66.

37. **Tiganos, E., J. Friborg, B. Allain, N. G. Daniel, X. J. Yao, and E. A. Cohen.** 1998. Structural and functional analysis of the membrane-spanning domain of the human immunodeficiency virus type 1 Vpu protein. Virology **251:**96-107.

38. **Tiganos, E., X. J. Yao, J. Friborg, N. Daniel, and E. A. Cohen.** 1997. Putative alpha-helical structures in the human immunodeficiency virus type 1 Vpu protein and CD4 are involved in binding and degradation of the CD4 molecule. J Virol **71:**4452-60.

39. **Van Damme, N., D. Goff, C. Katsura, R. L. Jorgenson, R. Mitchell, M. C. Johnson, E. B. Stephens, and J. Guatelli.** 2008. The interferon-induced protein BST-2 restricts HIV-1 release and is downregulated from the cell surface by the viral Vpu protein. Cell Host Microbe **3:**245-52.

40. **Van Damme, N., and J. Guatelli.** 2008. HIV-1 Vpu inhibits accumulation of the envelope glycoprotein within clathrin-coated, Gag-containing endosomes. Cell Microbiol **10:**1040-57.

41. **Varthakavi, V., R. M. Smith, S. P. Bour, K. Strebel, and P. Spearman.** 2003. Viral protein U counteracts a human host cell restriction that inhibits HIV-1 particle production. Proc Natl Acad Sci U S A **100:**15154-9.

42. **Varthakavi, V., R. M. Smith, K. L. Martin, A. Derdowski, L. A. Lapierre, J. R. Goldenring, and P. Spearman.** 2006. The pericentriolar recycling endosome plays a key role in Vpu-mediated enhancement of HIV-1 particle release. Traffic **7:**298-307.

43. **Wan, L., S. S. Molloy, L. Thomas, G. Liu, Y. Xiang, S. L. Rybak, and G. Thomas.** 1998. PACS-1 defines a novel gene family of cytosolic sorting proteins required for trans-Golgi network localization. Cell **94:**205-16.

Fig. 1. Analysis of Vpu subcellular localization.

HeLa cells expressing HxBH10-*vpu wt* were co-stained with the anti-Vpu serum (red) and anti-TGN46, anti-CD63, anti-LAMP1 or anti-calreticulin antibodies (green). Nuclei were counter-stained with DAPI (blue). Cells were observed by deconvolution fluorescence microscopy. Pictures show representative examples of Vpu association with TGN46 (A and B) and with CD63 (B). Enlarged pictures are shown beside panel (B). White arrows show noticeable examples of punctuate co-localization. White bars represent a distance of 10 μm.

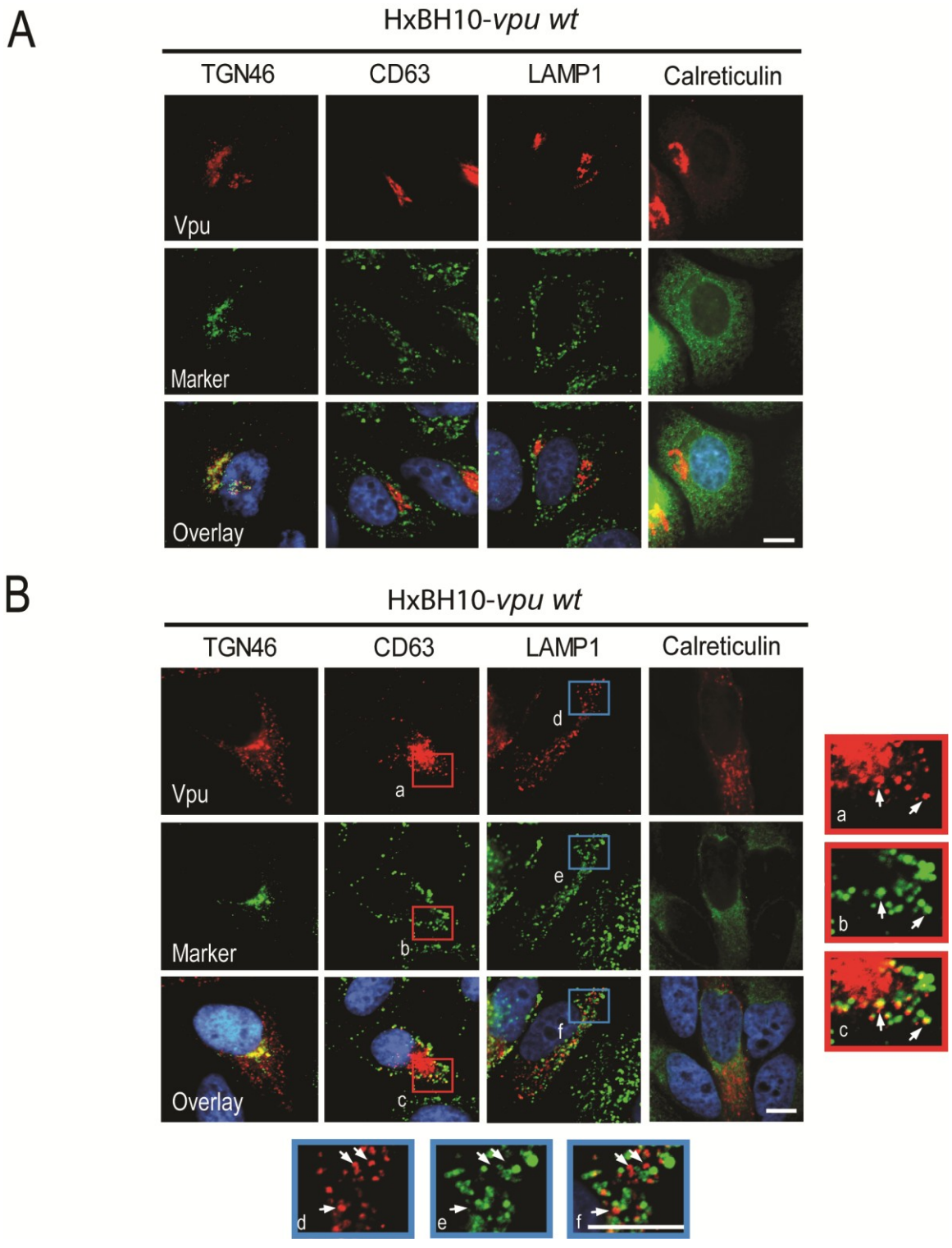
A
HxBH10-vpu wt
TGN46
CD63
LAMP1
Calreticulin
Vpu
Marker
Overlay
B
HxBH10-vpu wt
TGN46
CD63
LAMP1
Calreticulin
Vpu
Marker
Overlay
a
b
c
d
e
f

Fig. 2. Mutations in the hinge region between the TM and cytoplasmic domains of Vpu affect its subcellular localization.

(A) Schematic representation of the Vpu structural domains with the a.a. sequence of the hinge region derived from several strains of HIV-1 group M. Representative consensus a.a. sequences of the Vpu hinge region for each HIV-1 subtype are indicated. The red rectangle highlights the overlapping tyrosine-based (YXXϕ and dileucine-based ([D/E]XXXL[L/I]) sorting motifs. Among sequences of all HIV-1 strains from the HIV databases of the National Institute of Allergy and Infectious diseases (NIAID) of the National Institute of Health (NIH; www.hiv.lanl.gov/content/index), 65% of the sequences show RK residues at positions 30 and 31 (red letters) while 96 % of the sequence show a conservation of positively charged residues (RR, KR or KK) at those positions within the hinge region. Yellow circled a.a. indicate phosphoacceptor sites at serines 52 and 56 (bold); (–): a.a. identical to Vpu from HxBH10; (αH): alpha-helix. (B) HeLa cells expressing HxBH10-*vpu R30A,K31A* were co-stained with the anti-Vpu serum (red) and anti-TGN46, anti-CD63, anti-LAMP1 or anti-calreticulin antibodies (green). Nuclei were counter-stained with DAPI (blue). Pictures show representative examples of Vpu R30A,K31A-expressing cells. Enlarged pictures are shown beside the panels. White arrows show noticeable examples of punctuate co-localization. White bars represent a distance of 10 μm. (C) Quantitation of Vpu wt and Vpu R30A,K31A accumulation in the TGN as determined by the Vpu signal measured in the TGN (region 1) relative to the total Vpu signal (region 2) in the cell. Error bars indicate the standard deviation of the mean from the quantitative analysis of at least 25 distinct Vpu-expressing cells.

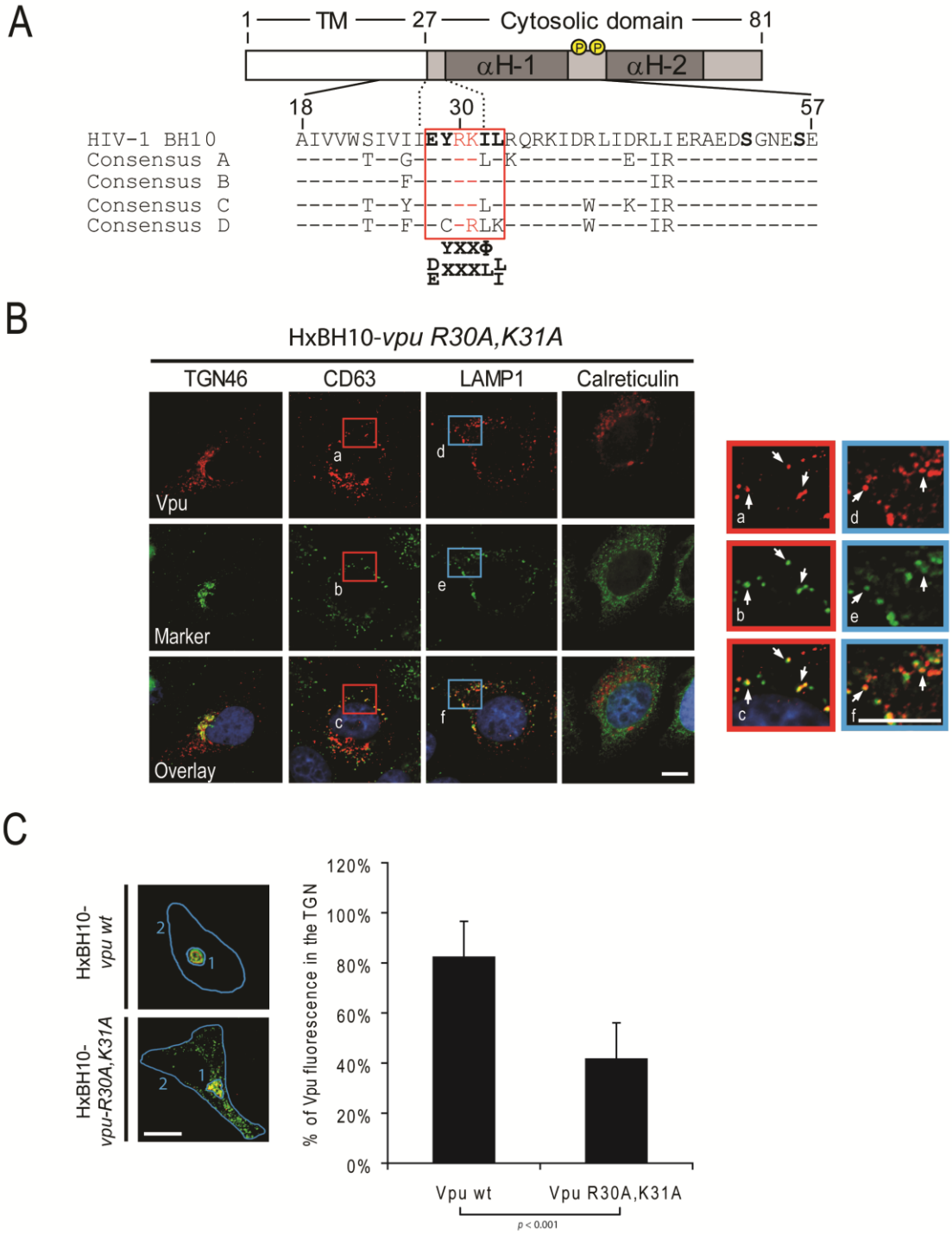
A
1
TM
27
Cytosolic domain
81
αH-1
αH-2
18
30
57
HIV-1 BH10 AIVVWSIVIIEYRKILRQRKIDRLIDRLIERAEDSGNESE
Consensus A -----T--G-----L-K--------E-IR----------
Consensus B --------F-----------------IR----------
Consensus C -----T--Y-----L-------W--K-IR----------
Consensus D -----T--F--C-RLK------W----IR----------
YXXΦ
DXXXLL
E I
B
HxBH10-vpu R30A,K31A
TGN46
CD63
LAMP1
Calreticulin
Vpu
Marker
Overlay
a
b
c
d
e
f
C
HxBH10-vpu wt
HxBH10-vpu-R30A,K31A
% of Vpu fluorescence in the TGN
120%
100%
80%
60%
40%
20%
0%
Vpu wt
Vpu R30A,K31A
p < 0.001

Fig. 3. Abrogation of lysosomal function or targeting increases Vpu stability.

(A) Vpu wt-expressing HEK 293T (upper panel; SVCMV-*vpu*+) or HeLa cells (lower panel; HxBH10-*vpu wt*) were treated for 20h with the indicated increasing concentrations of CQ prior to lysis. Vpu was subsequently resolved on SDS-PAGE and detected by western blot using anti-Vpu antibodies. Actin served as a loading control. (B) HEK 293T cells were co-transfected with SVCMV-*vpu wt* and the pEGFP-Rab7 plasmids as indicated. Proteins were resolved on SDS-PAGE and detected by western blot using anti-Vpu, anti-actin and anti-GFP antibodies. Note that the blots in A and B (lanes 2) are underexposed to clearly show Vpu stabilization upon CQ treatment or pEGFP-Rab7 N125I co-expression. (C) HeLa cells were co-transfected with the HxBH10-*vpu wt* proviral construct and either the pEGFP-Rab7 wt or pEGFP-Rab7 N125I plasmids. Transfected cells were stained with the anti-Vpu rabbit serum (red). Nuclei were counter-stained with DAPI (blue). White arrows show noticeable co-localization of Vpu with EGFP-Rab7 N125I in vesicular structures. The white bar represents a distance of 20 μm. (D) Quantitation of Vpu accumulation in the TGN was performed as described in Figure 2.

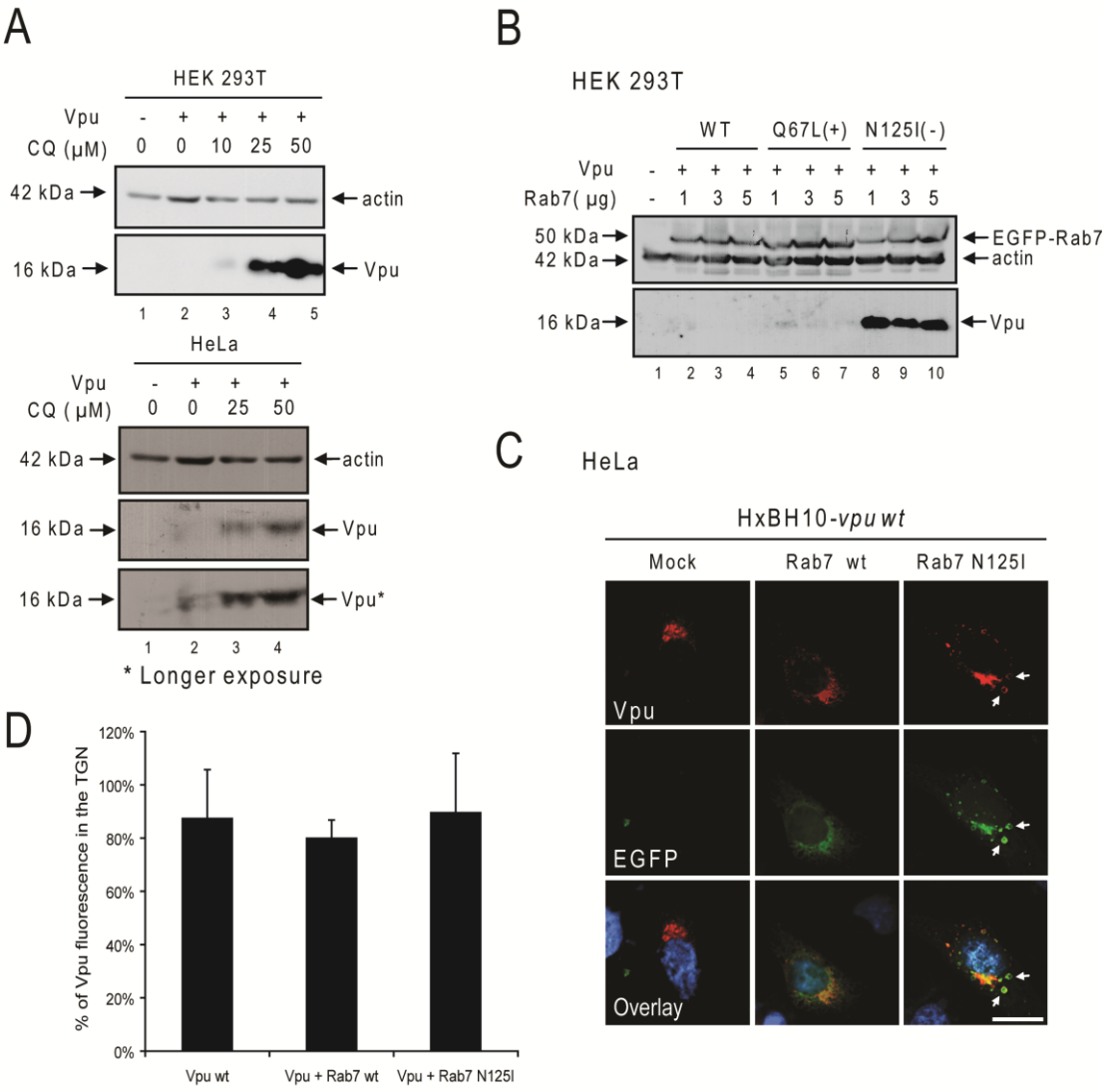
A
HEK 293T
Vpu - + + + +
CQ (μM) 0 0 10 25 50
42 kDa
actin
16 kDa
Vpu
1 2 3 4 5
HeLa
Vpu - + + +
CQ (μM) 0 0 25 50
42 kDa
actin
16 kDa
Vpu
16 kDa
Vpu*
1 2 3 4
* Longer exposure
B
HEK 293T
WT
Q67L(+)
N125I(-)
Vpu - + + + + + + + + +
Rab7(μg) - 1 3 5 1 3 5 1 3 5
50 kDa
42 kDa
EGFP-Rab7
actin
16 kDa
Vpu
1 2 3 4 5 6 7 8 9 10
C
HeLa
HxBH10-vpu wt
Mock
Rab7 wt
Rab7 N125I
Vpu
EGFP
Overlay
D
% of Vpu fluorescence in the TGN
120%
100%
80%
60%
40%
20%
0%
Vpu wt
Vpu + Rab7 wt
Vpu + Rab7 N125I

Fig. 4. Mutations in the hinge region of Vpu interfere with Vpu-mediated enhancement of HIV-1 particle release.

(A) HeLa cells were mock-transfected (lane 1) or transfected with either the HxBH10-*vpu*- (lane 2), HxBH10-*vpu wt* (lane 3) or HxBH10-*vpu R30A,K31A* (lane 4) proviral plasmids as indicated. Radio-labeled cells and supernatant-containing viral particles were harvested 48h post-transfection and analyzed for the presence of Vpu and Gag proteins by immunoprecipitation as described in material and methods. (B) Densitometric quantitation of viral release efficiency. Bands corresponding to Gag products in cells and viral particles were scanned by laser densitometry. The release efficiency of HxBH10-*vpu wt* was arbitrarily set at 100%. Error bars indicate the standard deviation of the mean from 4 separate experiments. (C) HeLa cells were transfected with HxBH10-*vpu*- alone (lane 1) or with increasing quantities of HxBH10-*vpu wt* (lanes 2-4) or HxBH10-*vpu R30A,K31A* (lanes 5-7). The total amount of proviral DNA transfected in each condition was identical. Cells and supernatant-containing viral particles were harvested 48h post-transfection and Gag proteins in cell and virus lysates were analyzed by western blot using anti-p24 antibodies. Vpu was detected by western blot using anti-Vpu antibodies. The asterisk shows a non-specific band. (D) Same as (C) except that infectious virions in culture supernatants were measured using HeLa-TZM indicator cells and a chemiluminescence assay in relative light units (RLU) as described in material and methods. The maximal RLU value obtained with HxBH10-*vpu wt*-expressing cells (lane 4) was arbitrarily set at 100%. Note that the levels of Vpu wt and Vpu R30A,K31A were comparable in lanes 4 and 5. (E) HeLa cells were co-transfected with the HxBH10-*vpu*- proviral construct, the indicated pEGFP-Rab7

plasmids, and the SVCMV-*vpu wt* or control constructs. Cells and virus particles were processed and analysed as described in (C). (F) Densitometric quantitation of (E). Viral particle release efficiency obtained in cells co-expressing HxBH10-*vpu*- and SVCMV-*vpu wt* was arbitrarily set at 100%. Error bars indicate the standard deviations of the mean from 3 separate experiments.

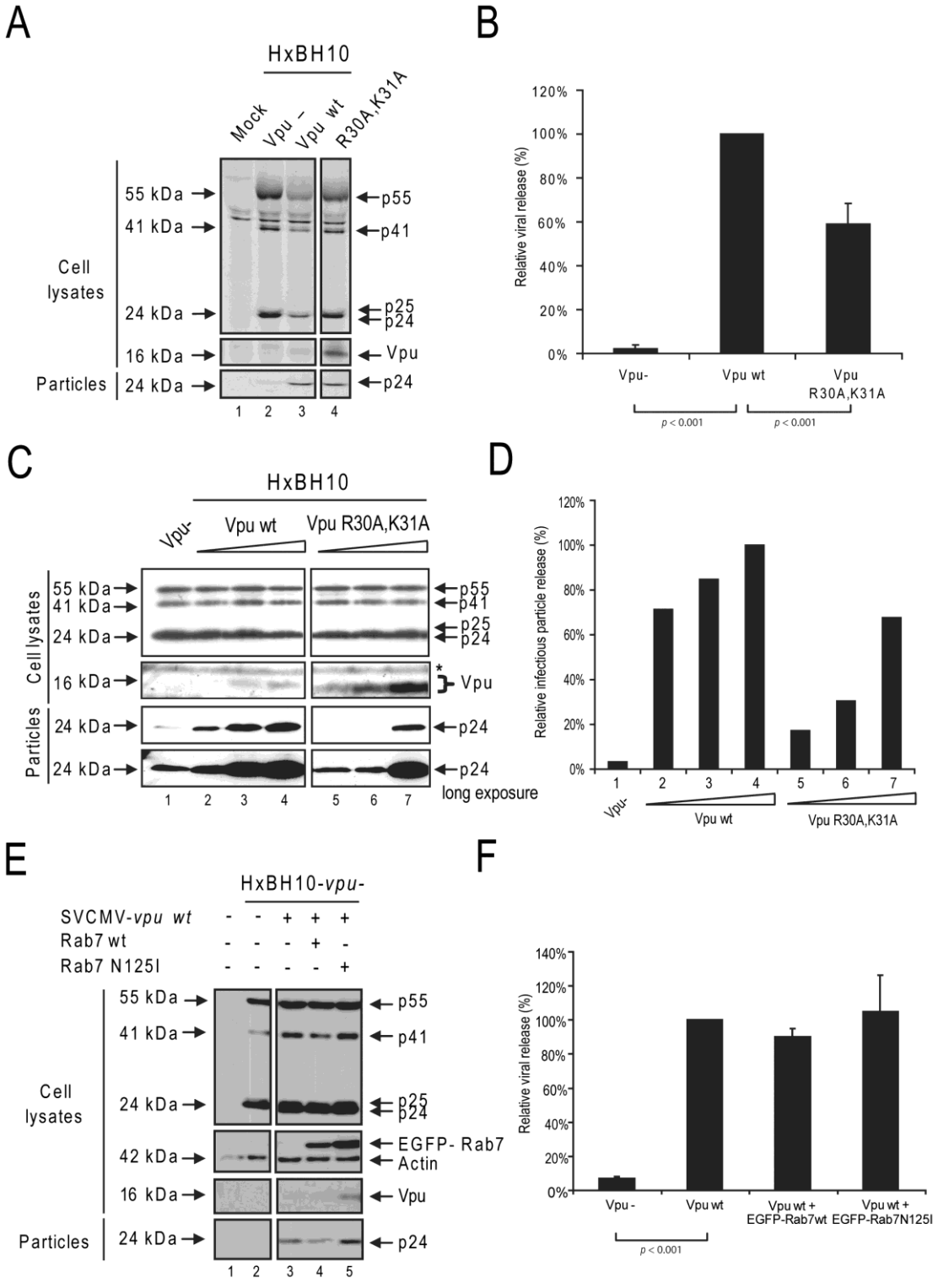
A
HxBH10
Mock
Vpu -
Vpu wt
R30A,K31A
55 kDa
41 kDa
24 kDa
16 kDa
Cell lysates
Particles
24 kDa
p55
p41
p25
p24
Vpu
p24
1 2 3 4
B
Relative viral release (%)
120%
100%
80%
60%
40%
20%
0%
Vpu-
Vpu wt
Vpu R30A,K31A
p < 0.001
p < 0.001
C
HxBH10
Vpu-
Vpu wt
Vpu R30A,K31A
Cell lysates
Particles
55 kDa
41 kDa
24 kDa
16 kDa
24 kDa
24 kDa
p55
p41
p25
p24
Vpu
p24
p24
long exposure
1 2 3 4 5 6 7
D
Relative infectious particle release (%)
120%
100%
80%
60%
40%
20%
0%
1 2 3 4 5 6 7
Vpu-
Vpu wt
Vpu R30A,K31A
E
HxBH10-vpu-
SVCMV-vpu wt - - + + +
Rab7 wt - - - + -
Rab7 N125I - - - - +
Cell lysates
Particles
55 kDa
41 kDa
24 kDa
42 kDa
16 kDa
24 kDa
p55
p41
p25
p24
EGFP- Rab7
Actin
Vpu
p24
1 2 3 4 5
F
Relative viral release (%)
140%
120%
100%
80%
60%
40%
20%
0%
Vpu -
Vpu wt
Vpu wt + EGFP-Rab7wt
Vpu wt + EGFP-Rab7N125I
p < 0.001

Fig. 5. Effect of depletion of CLCs on the subcellular localization of Vpu and its viral particle release enhancing function.

(A) HeLa cells were transfected either with control siRNA (scrambled siRNA) (lanes 1-3) or specific siRNA against CLCa and CLCb (CLCs siRNA) (lanes 4-6). Seventy-two hours post-siRNA transfection, cells were transfected with similar amounts of the HxBH10-*vpu*- (lanes 1 and 4), HxBH10-*vpu wt* (lanes 2 and 5) or HxBH10-*vpu R30A,K31A* (lanes 3 and 6) proviral constructs as indicated. Cells and supernatant-containing viral particles were harvested 96h post-siRNA transfection. Gag proteins in cell and virus lysates were analyzed by western blot using anti-p24 antibodies. Vpu and CLCs levels were determined using specific antibodies. Actin served as a loading control. (B) Same as (A) except that infectious virions in culture supernatants were measured using HeLa-TZM indicator cells and a chemiluminescence assay in relative light units (RLU) as described in material and methods. The RLU value obtained in HxBH10-*vpu wt*-expressing cells transfected with the non-targeting control siRNA was arbitrarily set at 100%. Error bars indicate the standard deviation of the mean from 4 independent experiments. (C) HeLa cells were transfected with either the scrambled siRNA or with CLCs siRNA. Cells were transfected with HxBH10-*vpu wt* or HxBH10-*vpu R30A,K31A* proviral plasmids 72 h later. Twenty-four hours later, cells were co-stained for Vpu (red) and TGN46 (green). Nuclei were counter-stained with DAPI (blue). The white bar represents a distance of 10 μm. (D) Quantitation of Vpu accumulation in the TGN was performed as described in Figure 2.

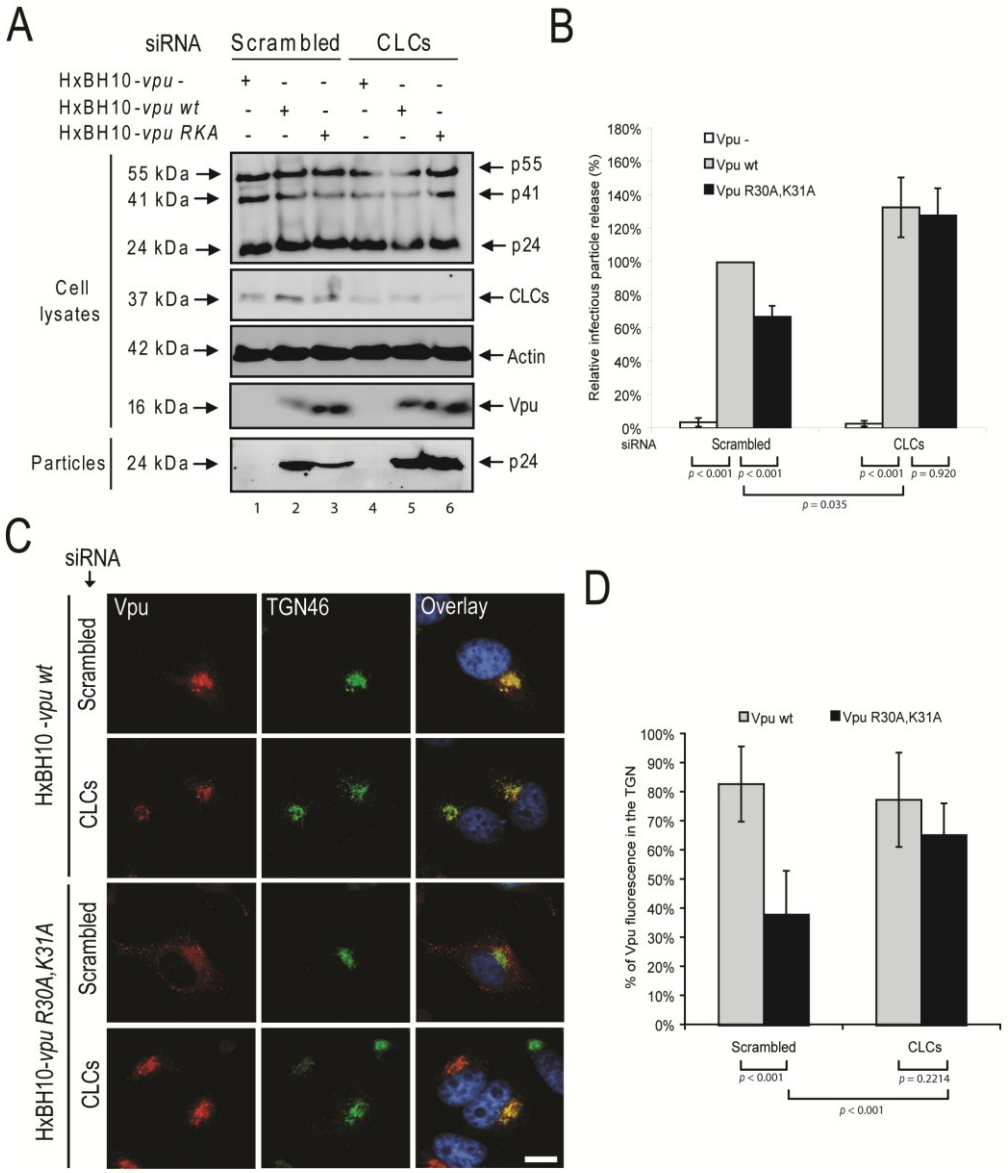
A
siRNA
Scrambled
CLCs
HxBH10-vpu-
HxBH10-vpu wt
HxBH10-vpu RKA
55 kDa
41 kDa
24 kDa
37 kDa
42 kDa
16 kDa
24 kDa
Cell lysates
Particles
p55
p41
p24
CLCs
Actin
Vpu
p24
1 2 3 4 5 6
B
Relative infectious particle release (%)
Vpu -
Vpu wt
Vpu R30A,K31A
siRNA
Scrambled
CLCs
p < 0.001
p < 0.001
p < 0.001
p = 0.920
p = 0.035
C
siRNA
Vpu
TGN46
Overlay
HxBH10 -vpu wt
HxBH10-vpu R30A,K31A
Scrambled
CLCs
D
Vpu wt
Vpu R30A,K31A
% of Vpu fluorescence in the TGN
Scrambled
CLCs
p < 0.001
p = 0.2214
p < 0.001

Fig. 6. Mutations in the putative overlapping tyrosine- and dileucine-based trafficking signals do not interfere with Vpu subcellular localization or Vpu-mediated enhancement of HIV-1 particle release.

(A) HeLa cells transfected with the SVCMV-*vpu wt*, SVCMV-*vpu Y29A* or SVCMV-*vpu I32A,L33A* plasmids were co-stained with the anti-Vpu serum (red) and anti-TGN46 antibodies (green) 48h post-transfection and observed by confocal microscopy. Pictures show representative examples of Vpu localization patterns. The white bar represents a distance of 10 μm. (B) Quantitation of Vpu accumulation in the TGN as determined by the Vpu signal measured in the TGN relative to the total Vpu signal in the cell. Error bars indicate the standard deviation of the mean from the quantitative analysis of at least 25 distinct Vpu-expressing cells. (C) HeLa cells were co-transfected with the specified HxBH10 proviral constructs. Cells and supernatant-containing viral particles were analyzed as described in Figure 4C. (D) Same as C) except infectious virions in culture supernatants were measured using HeLa-TZM indicator cells and a chemiluminescence assay. The RLU value obtained in Vpu wt-expressing cells (lane 2) was arbitrarily set at 100%. Error bars indicate the standard deviation of the mean from 4 independent experiments.

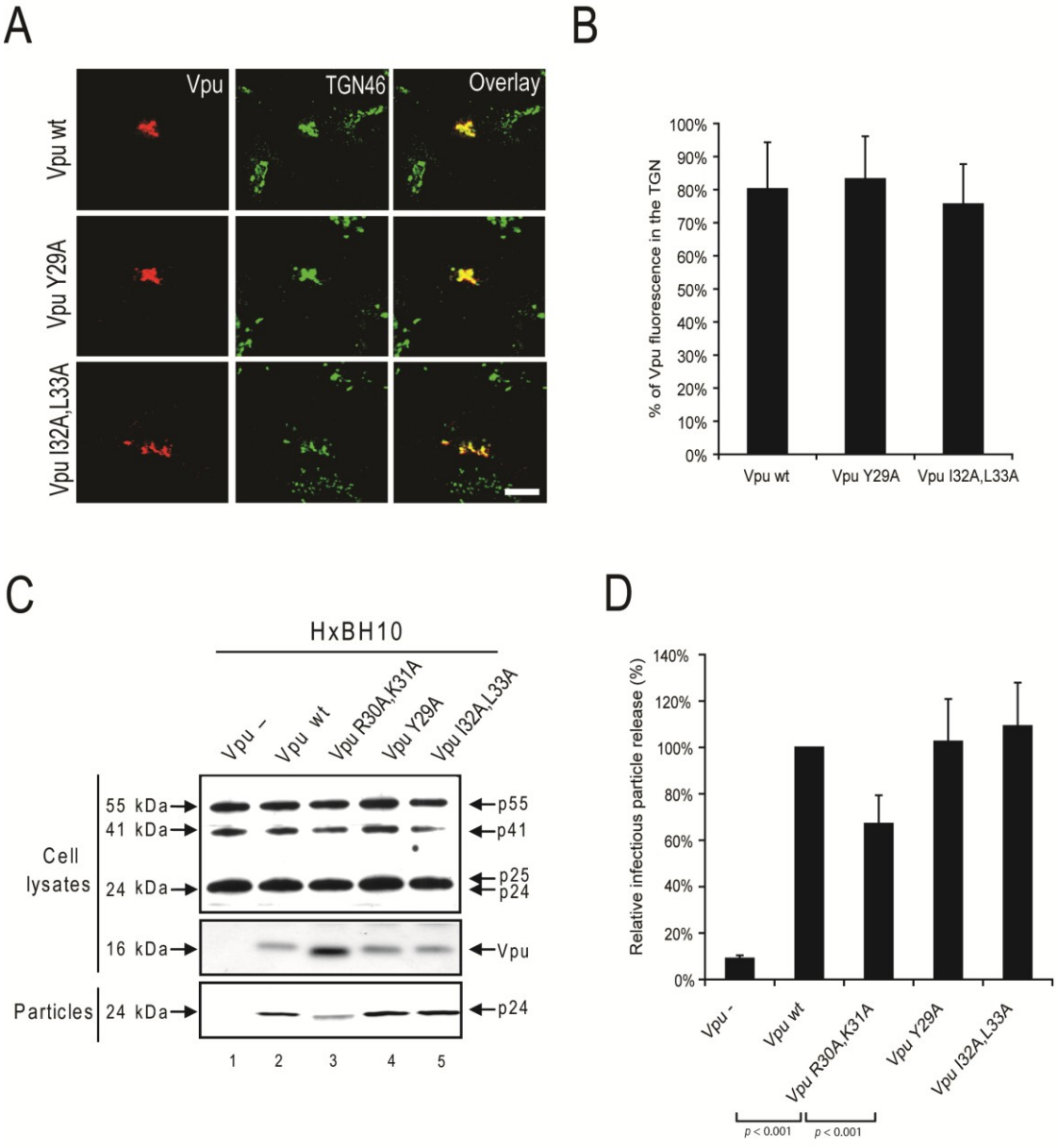
A
Vpu
TGN46
Overlay
Vpu wt
Vpu Y29A
Vpu I32A,L33A
B
% of Vpu fluorescence in the TGN
100%
90%
80%
70%
60%
50%
40%
30%
20%
10%
0%
Vpu wt
Vpu Y29A
Vpu I32A,L33A
C
HxBH10
Vpu –
Vpu wt
Vpu R30A,K31A
Vpu Y29A
Vpu I32A,L33A
55 kDa
41 kDa
Cell lysates
24 kDa
16 kDa
Particles
24 kDa
p55
p41
p25
p24
Vpu
p24
1
2
3
4
5
D
Relative infectious particle release (%)
140%
120%
100%
80%
60%
40%
20%
0%
Vpu -
Vpu wt
Vpu R30A,K31A
Vpu Y29A
Vpu I32A,L33A
p < 0.001
p < 0.001

Fig. 7. Effect of deletions of the Vpu cytosolic tail on Vpu subcellular localization

(A) Schematic representation of the Vpu-EYFP deletion constructs. (B) HeLa cells transfected with plasmids encoding the indicated Vpu-EYFP deletion mutant were co-stained with the anti-GFP (green) and anti-TGN46 (red) antibodies. Cells were observed by confocal microscopy. Pictures show representative examples of the localization pattern observed for each deletion mutants. (C) Quantitation of Vpu accumulation in the TGN was performed as described in Figure 2. (D) HeLa cells expressing Vpu-EYFP or VpuΔ23-EYFP were co-stained with anti-GFP (green) and anti-CD63 or anti-Rab5 (red) antibodies. Cells were observed by confocal microscopy. Enlarged pictures are shown beside panels. White arrows show noticeable examples of punctuate co-localization. All the white bars represent a distance of 10 μm.

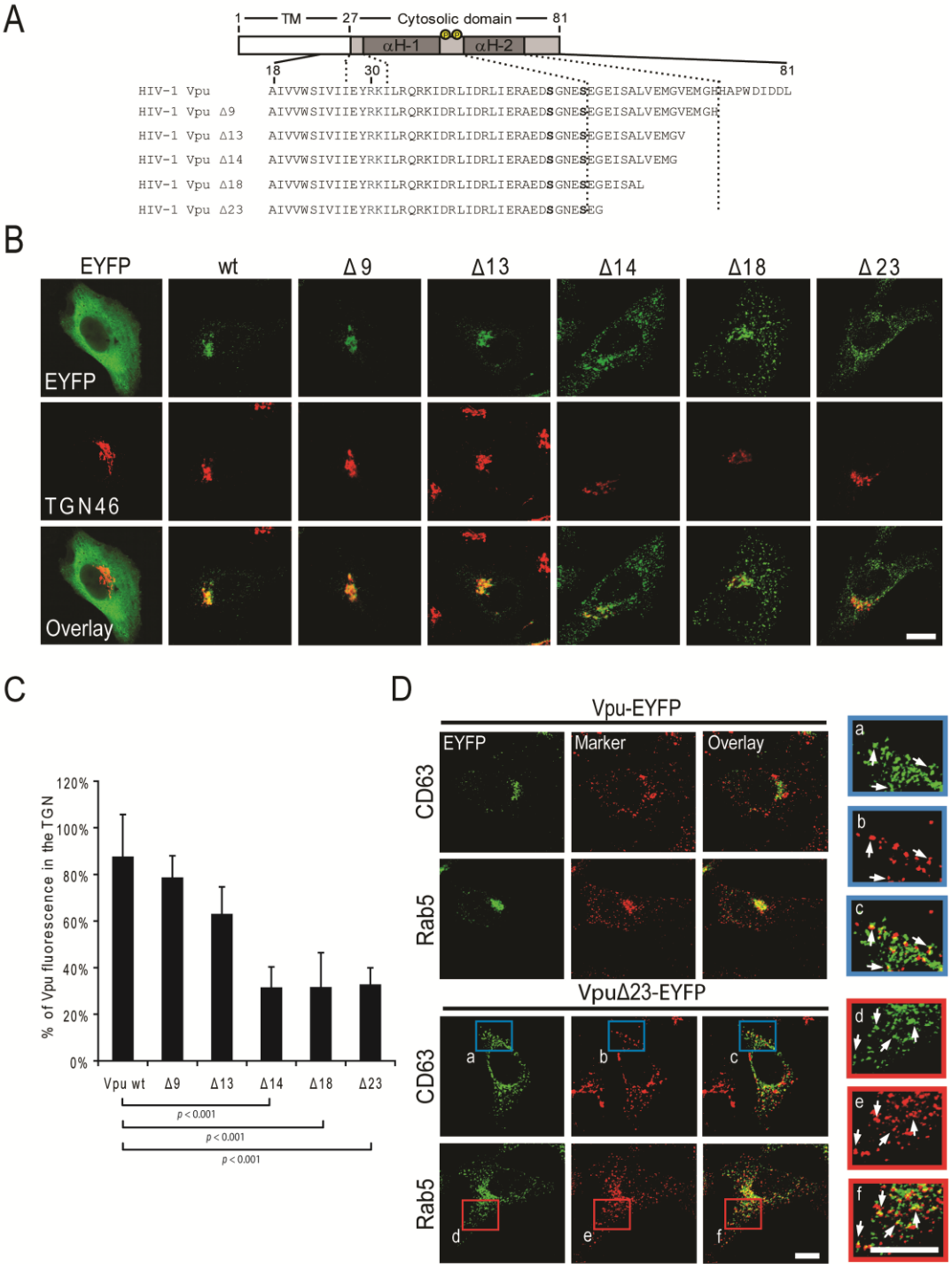
A
1
TM
27
Cytosolic domain
81
αH-1
αH-2
18
30
81
HIV-1 Vpu AIVVWSIVIIEYRKILRQRKIDRLIDRLIERAEDSGNESSEGEISALVEMGVEMGHHAPWDIDDL
HIV-1 Vpu Δ9 AIVVWSIVIIEYRKILRQRKIDRLIDRLIERAEDSGNESSEGEISALVEMGVEMGH
HIV-1 Vpu Δ13 AIVVWSIVIIEYRKILRQRKIDRLIDRLIERAEDSGNESSEGEISALVEMGV
HIV-1 Vpu Δ14 AIVVWSIVIIEYRKILRQRKIDRLIDRLIERAEDSGNESSEGEISALVEMG
HIV-1 Vpu Δ18 AIVVWSIVIIEYRKILRQRKIDRLIDRLIERAEDSGNESSEGEISAL
HIV-1 Vpu Δ23 AIVVWSIVIIEYRKILRQRKIDRLIDRLIERAEDSGNESSEG
B
EYFP
wt
Δ9
Δ13
Δ14
Δ18
Δ23
EYFP
TGN46
Overlay
C
% of Vpu fluorescence in the TGN
120%
100%
80%
60%
40%
20%
0%
Vpu wt
Δ9
Δ13
Δ14
Δ18
Δ23
p < 0.001
p < 0.001
p < 0.001
D
Vpu-EYFP
EYFP
Marker
Overlay
CD63
Rab5
VpuΔ23-EYFP
CD63
Rab5
a
b
c
d
e
f

Fig. 8. Effect of deletions of the Vpu cytosolic tail on Vpu-mediated enhancement of viral HIV-1 release.

(A) HeLa cells were mock-transfected (lane 1) or transfected with HxBH10-*vpu*- and plasmids encoding EYFP (lane 2) or Vpu-EYFP (lane 8) or the specified Vpu-EYFP deletion mutants (lanes 3-7). Cells and supernatants were analyzed as described in Figure 4C. EYFP or Vpu-EYFP derivatives were detected using anti-GFP antibodies. (B) Same as (A) except that infectious virions in culture supernantants were measured using HeLa-TZM indicator cells and a chemiluminescence assay as described in material and methods. The RLU measured with Vpu-EYFP wt was arbitrarily set at 100%. Error bars indicate the standard deviation of the mean from 4 independent experiments.

A

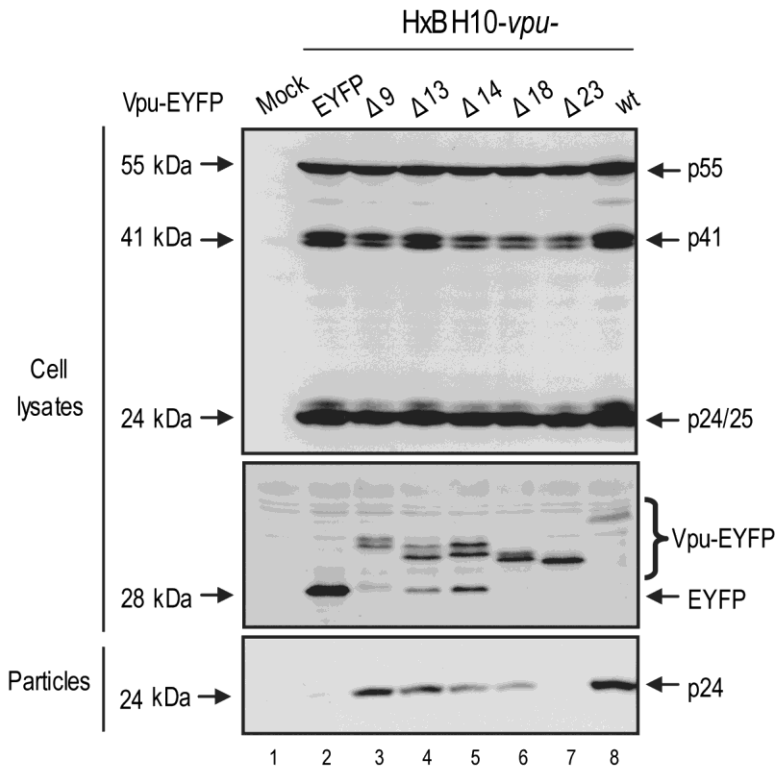
HxBH10-vpu-
Vpu-EYFP
Mock
EYFP
Δ9
Δ13
Δ14
Δ18
Δ23
wt
55 kDa
41 kDa
24 kDa
p55
p41
p24/25
Cell lysates
Vpu-EYFP
28 kDa
EYFP
Particles
24 kDa
p24
1 2 3 4 5 6 7 8

B

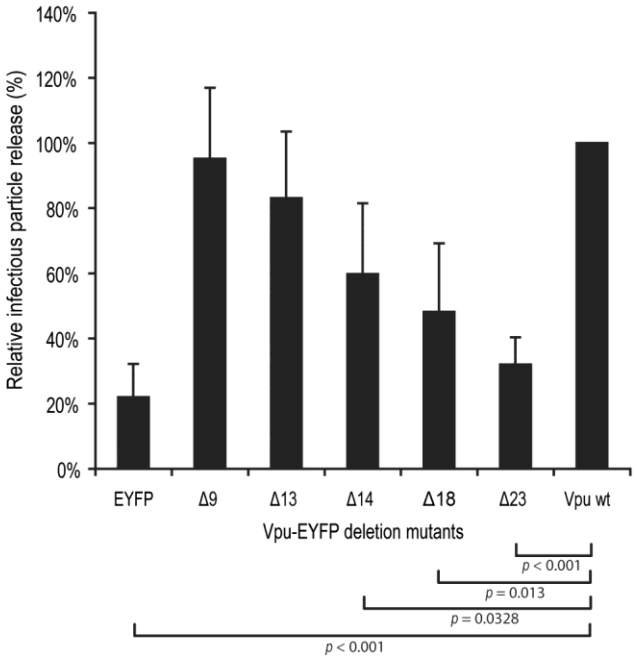
Relative infectious particle release (%)
140%
120%
100%
80%
60%
40%
20%
0%
EYFP
Δ9
Δ13
Δ14
Δ18
Δ23
Vpu wt
Vpu-EYFP deletion mutants
p < 0.001
p = 0.013
p = 0.0328
p < 0.001

Fig. 9. Analysis of the subcellular localization of native Vpu and tetherin

HeLa cells expressing HxBH10-*vpu-,* HxBH10-*vpu wt*, HxBH10-*vpu R30A,K31A* (A) or Vpu-EYFP or VpuΔ23-EYFP (B) were co-stained for Vpu (A) or GFP (B) (green) as well as for tetherin (blue) and TGN46 (red). Cells were observed by confocal microscopy. Enlarged pictures are shown beside panels A and B. White arrows show noticeable examples of punctuate Vpu localization. White bars represent a distance of 10 μm. (C) Quantitation of the extent of Vpu co-localization with tetherin using the Zeiss LSM-510 software. The values (%) represent the fraction of Vpu (green pixels) that overlapped with tetherin (blue pixels) relative to total Vpu in the cell. Error bars indicate the standard deviation of the mean from the quantitative analysis of at least 25 distinct Vpu-expressing cells.

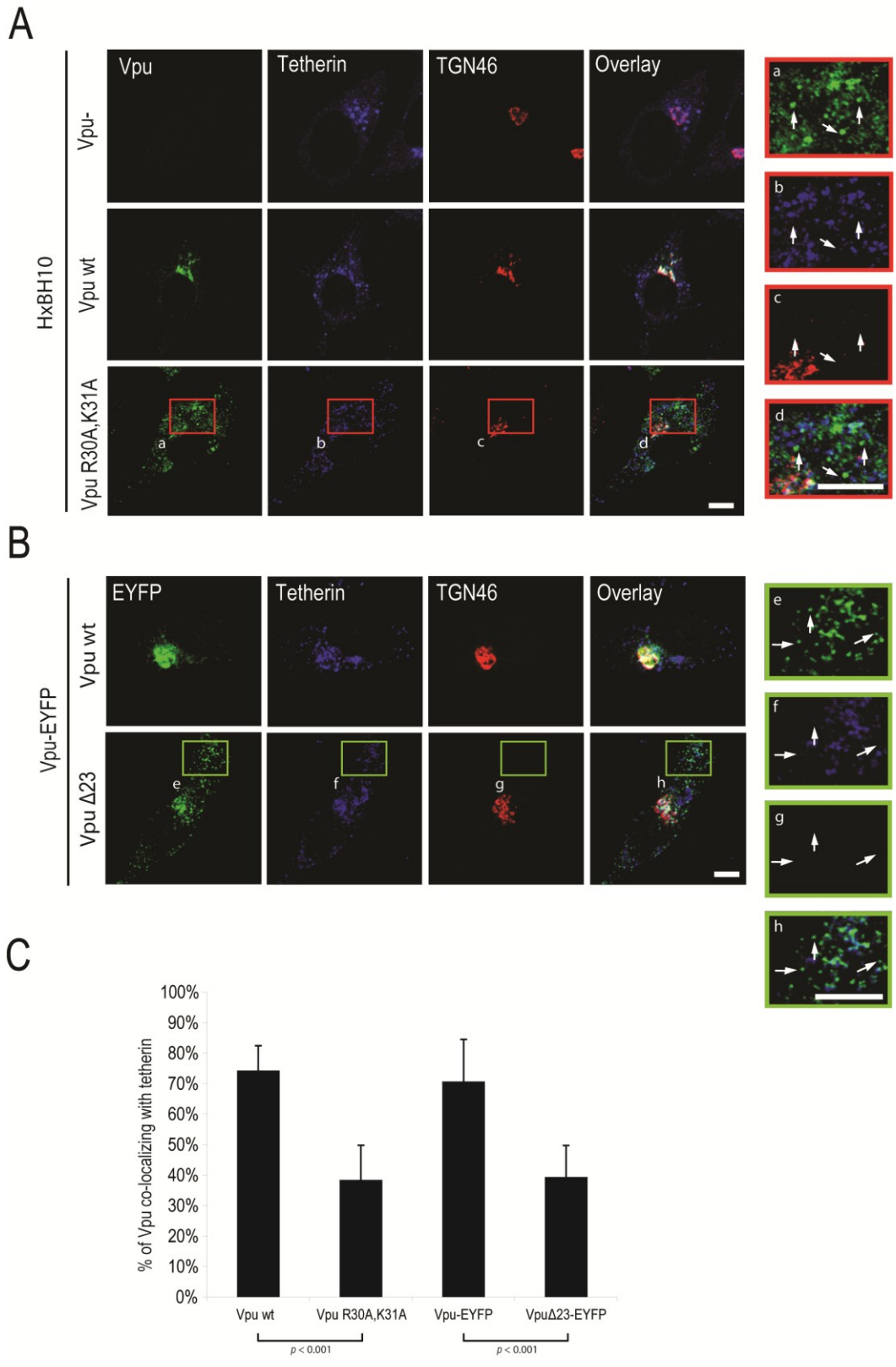
A
HxBH10
Vpu-
Vpu wt
Vpu R30A,K31A
Vpu
Tetherin
TGN46
Overlay
a
b
c
d
B
Vpu-EYFP
Vpu wt
Vpu Δ23
EYFP
Tetherin
TGN46
Overlay
e
f
g
h
C
% of Vpu co-localizing with tetherin
100%
90%
80%
70%
60%
50%
40%
30%
20%
10%
0%
Vpu wt
Vpu R30A,K31A
Vpu-EYFP
VpuΔ23-EYFP
p < 0.001
p < 0.001

Supplementary Fig. S1. Mutations in the hinge region between the TM and cytoplasmic domains of Vpu affect the protein turnover.

(A) HEK 293T cells were transfected with SVCMV-*vpu*- (lanes 1-2), *vpu wt* (lanes 3-10), or *vpu R30A,K31A* (lanes 11-18). Forty-eight hours post-transfection, cells were pulse-labeled and chased for the indicated time intervals in presence or absence of 10 μM BFA. Vpu was immunoprecipitated with an anti-Vpu serum and analyzed by SDS-PAGE and autoradiography. The graph represents the relative levels of Vpu, as determined by densitometric scanning of Vpu bands, at the indicated time points as compared to time 0 (set at 100%). Solid line: untreated cells. Dotted line: BFA-treated cells. Black lines and squares: Vpu wt. Blue lines and triangles: Vpu R30A,K31A. Error bars indicate the standard deviation of the mean of 2 independent experiments. (B) HeLa cells were transfected with SVCMV-*vpu*- or SVCMV-*vpu wt*. Transfected cells were treated or not with 10 μM BFA for 5h prior to lysis 48h post-transfection. Vpu was detected by western blot using an anti-Vpu serum. Actin was used as a loading control.

A HEK 293T

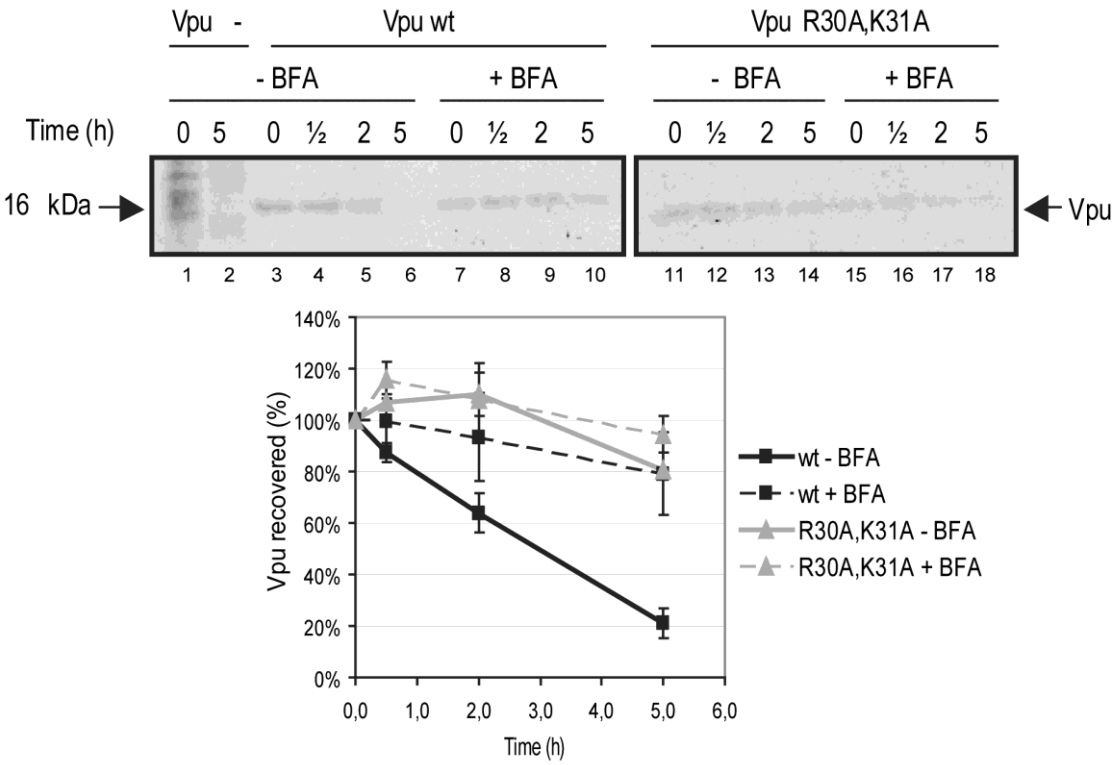

B HeLa

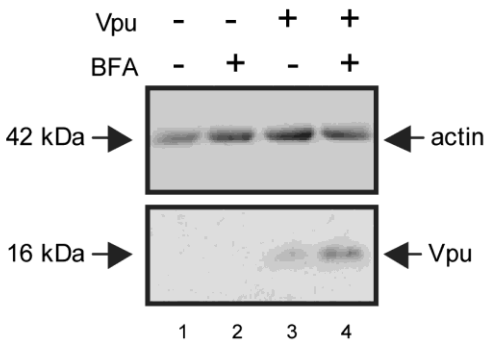

Supplementary Fig. S2. R30A,K31A mutations does not affect Vpu-mediated CD4 degradation

(A) HEK 293T cells were mock-transfected (lanes 1-4) or co-transfected with SVCMV-*CD4* and SVCMV-*vpu*- (lanes 5-8), SVCMV-*vpu*+ (lanes 9-12) or SVCMV-vpu *R30A,K31A* (lanes 13-16). Forty-eight hours post-transfection, cells were pulse-labeled and chased for the indicated time intervals in presence of 10 μM BFA as indicated. Proteins were immunoprecipitated and analyzed by SDS-PAGE and autoradiography. (B) Vpu expression was detected by immunoprecipitation at the initial time point. (C) Quantification of (A). CD4 levels were determined by densitometric scanning of CD4 bands at the indicated time points as compared to time 0 (set at 100%). Solid line: Vpu wt. Dotted line: Vpu-. Dashed line: Vpu R30A,K31A. Error bars indicate the standard deviation of the mean of 2 independent experiments.

A

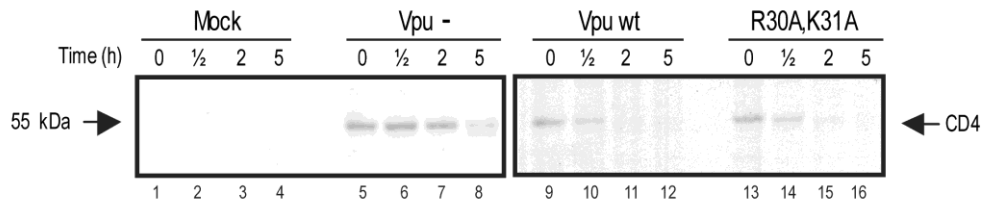
Mock
Vpu -
Vpu wt
R30A,K31A
Time (h)
0 ½ 2 5 0 ½ 2 5 0 ½ 2 5 0 ½ 2 5
55 kDa
CD4
1 2 3 4 5 6 7 8 9 10 11 12 13 14 15 16

B

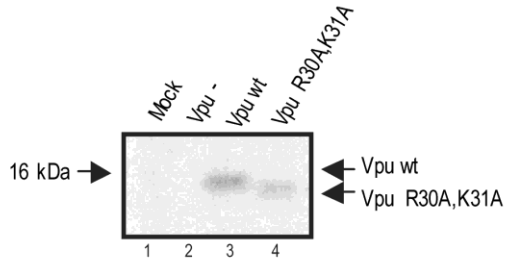
Mock
Vpu -
Vpu wt
Vpu R30A,K31A
16 kDa
Vpu wt
Vpu R30A,K31A
1 2 3 4

C

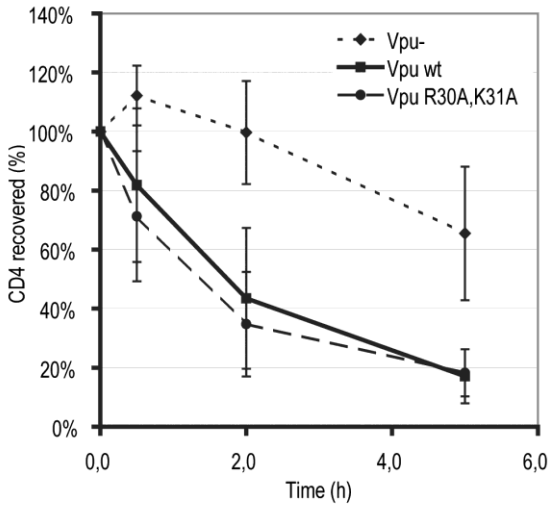
140%
120%
100%
80%
60%
40%
20%
0%
CD4 recovered (%)
0,0
2,0
4,0
6,0
Time (h)
Vpu-
Vpu wt
Vpu R30A,K31A

Supplementary Fig. S3. Effect of CLCs depletion on the localization of CI-MPR and the uptake of transferrin

(A) HeLa cells were transfected either with the scrambled siRNA or with specific CLCs siRNAs. Transfected cells were fixed, permeabilized and co-stained for CI-MPR (red) and TGN46 (green) with specific antibodies, 96h post-transfection. Nuclei were counter-stained with DAPI (blue). The white bar represents a distance of 10 μm. (B) In parallel, siRNA-transfected cells were harvested and labeled with transferrin-Alexa 488 conjugates 96h post-transfection. Cells were then processed for transferrin uptake as described in material and methods and analyzed by flow cytometry. Filled histogram: unlabeled cells; blue line: cells at 4°C; red line: cells shifted at 37°C.

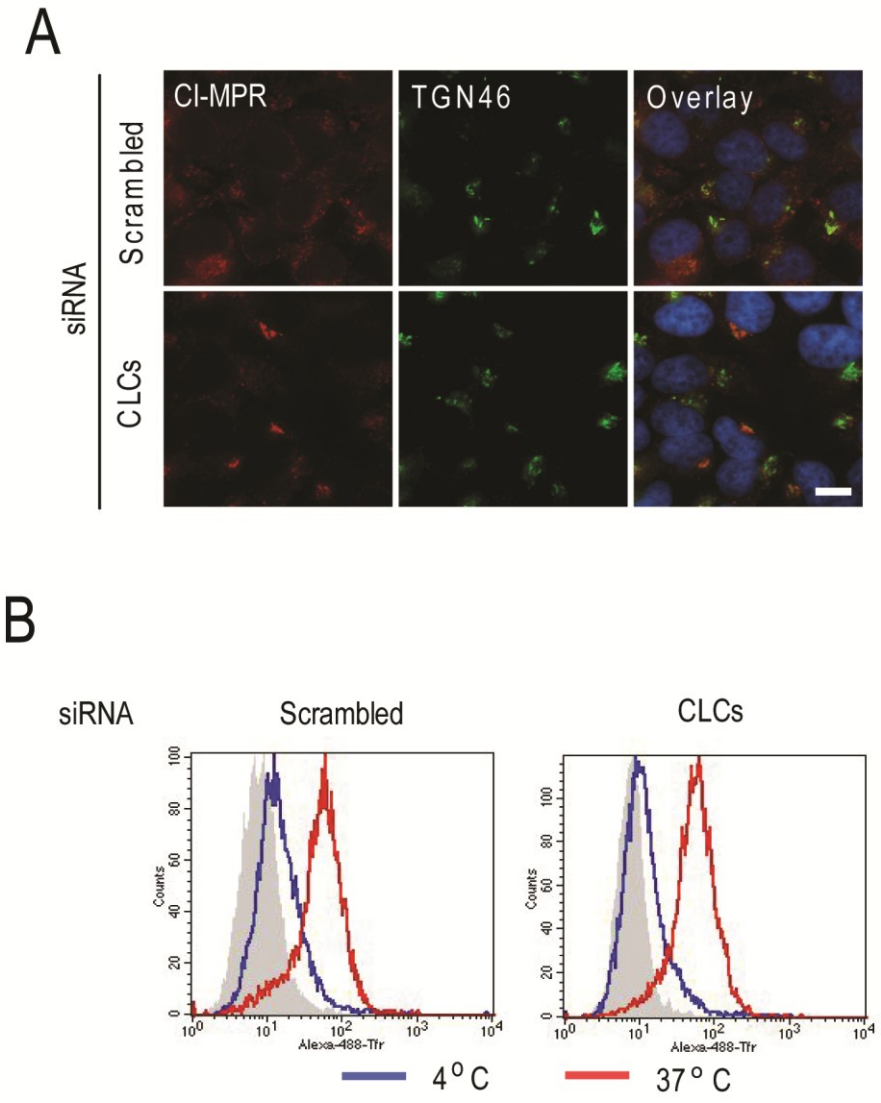
A
siRNA
Scrambled
CLCs
CI-MPR
TGN46
Overlay
B
siRNA
Scrambled
CLCs
Counts
Alexa-488-Tfr
4° C
37° C

Supplementary Fig. S4. Effect of CHCs depletion on Vpu-mediated enhancement of HIV particle release

(A) HeLa cells were transfected either with scrambled siRNA (lanes 1-3) or specific siRNAs directed against CHCs (lanes 4-6). Seventy-two hours later, cells were transfected with similar amounts of HxBH10-*vpu*- (lanes 1 and 4), HxBH10-*vpu wt* (lanes 2 and 5) or HxBH10-*vpu R30A,K31A* (lanes 3 and 6) proviral constructs. Cells and supernatant-containing viral particles were harvested 96h post-siRNA transfection. Gag proteins in cell and virus lysates were analyzed by western blot using anti-p24 antibodies. CHCs levels were determined using specific antibodies. Actin served as a loading control. (B) Same as (A) except infectious virions in culture supernatants were measured using HeLa-TZM indicator cells and a chemiluminescence assay. The RLU value obtained in HxBH10-*vpu wt*-expressing cells transfected with the non-targeting control siRNA was arbitrarily set at 100%. Error bars indicate the standard deviation of the mean from 3 independent experiments. (C) HeLa cells were transfected with either scrambled siRNAs or with specific CHCs siRNA. Transfected cells were fixed, permeabilized and co-stained for CI-MPR (red), TGN46 (green) using specific antibodies 96h post-transfection. Nuclei were counter-stained with DAPI (blue). The white bar represents a distance of 10 μm. (D) In parallel, siRNA-transfected cells were harvested and labeled with transferrin-Alexa 488 conjugates 96h post-transfection. Cells were processed for transferrin uptake as described in material and methods and analyzed by flow cytometry. Filled histogram: unlabeled cells; blue line: cells at 4°C; red line: cells shifted at 37°C.

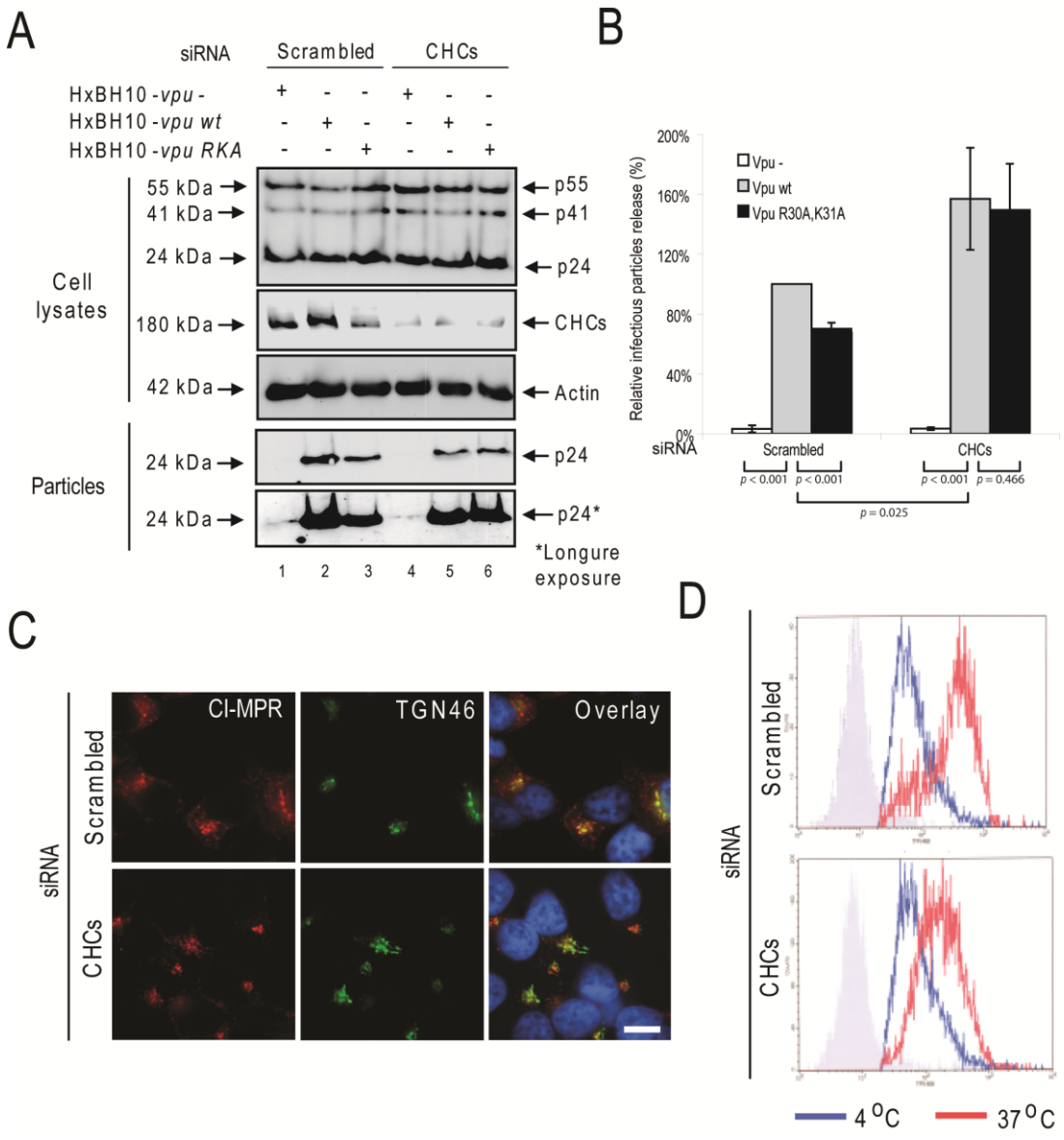
A
siRNA
Scrambled
CHCs
HxBH10 -vpu -
HxBH10 -vpu wt
HxBH10 -vpu RKA
55 kDa
41 kDa
24 kDa
180 kDa
42 kDa
Cell lysates
Particles
24 kDa
24 kDa
p55
p41
p24
CHCs
Actin
p24
p24*
*Longure exposure
1 2 3 4 5 6
B
Relative infectious particles release (%)
200%
160%
120%
80%
40%
0%
Vpu -
Vpu wt
Vpu R30A,K31A
siRNA
Scrambled
CHCs
p < 0.001
p < 0.001
p < 0.001
p = 0.466
p = 0.025
C
siRNA
Scrambled
CHCs
CI-MPR
TGN46
Overlay
D
siRNA
Scrambled
CHCs
4 °C
37 °C

CHAPITRE 2

Comment Vpu du VIH-1 prévient-elle l'expression de Tetherin au niveau de la membrane plasmique?

Bien qu'une seule fois mise en doute (174), la réduction des niveaux de surface de Tetherin qui évite sa nuisible incorporation à la membrane des particules virales en bourgeonnement fait désormais consensus (71, 97, 99, 193, 248). Or, nos données présentées dans le précédent chapitre ont démontré la co-localisation de Vpu et de Tetherin dans le RTG, compartiment à partir duquel Vpu semble contrecarrer l'activité antivirale de ce facteur de restriction. Par contre, il demeurait obscur comment Vpu pourrait réduire les niveaux de surface de Tetherin à partir de ce compartiment intracellulaire.

Très tôt, l'hypothèse selon laquelle le recrutement de β-TrCP par Vpu provoque la dégradation protéasomale ou lysosomale de Tetherin fut avancée (54, 85, 93, 155). Une autre idée fut aussi suggérée selon laquelle Vpu influerait plutôt sur l'internalisation et/ou le trafic post-endocytique du facteur de restriction (110, 173). Finalement, la séquestration intracellulaire, mécanisme antagoniste prédominant dans le cas des protéines d'enveloppe du virus VIS du singe tantalus (tan) et du VIH-2, fut aussi considérée (54, 60, 96, 143). L'objectif de ce deuxième chapitre était donc de discriminer entre ces différents potentiels mécanismes.

Ce chapitre fut l'objet d'un article publié en 2010 dans *PLoS Pathogens*, un journal couvrant une vaste gamme de sujets sur les pathogènes humains (59). Bibhuti Bhusan Roy a généré la version de type sauvage du provirus HIV-1-rtTA-MA-EGFP-*vpu*+; Catherine Paquay, M.D., a généré les lignées HeLa contrôle et HeLa-shRNA β-TrCP en plus de fournir la caractérisation en Figure S1, Mariana Bego, Ph.D., a contribué à mettre au point le système de B18R décrit à la Figure S4. Mathieu Dubé a exécuté les expériences des Figures 1-8 et supplémentaires S1B-S4. Tous les auteurs ont

fourni une aide technique et/ou conceptuelle. Mathieu Dubé a écrit le manuscrit en collaboration avec Éric Cohen, Ph.D.

RÉSUMÉ

La protéine accessoire Vpu facilite la relâche du VIH-1 en contrant Tetherin/BST-2, un facteur de restriction régulé par l'IFN retenant les virus à la surface cellulaire. De récentes études ont évoqué la possibilité que l'antagonisme de Tetherin par la diminution de son niveau de surface soit la conséquence d'une dégradation protéasomale et/ou endo-lysosomale impliquant β-TrCP. Dans toutes ces études, la dégradation de Tetherin ne peut cependant pas expliquer complètement l'activité anti-Tetherin de Vpu. Ici, nous montrons que Vpu peut faciliter la relâche du VIH-1 sans effet détectable sur le niveau cellulaire de Tetherin à l'équilibre ou sur son taux de dégradation, suggérant que la dégradation de Tetherin pourrait ne pas être nécessaire et/ou suffisante à son antagonisme. Sans influencer l'internalisation de Tetherin à partir de la membrane plasmique, l'expression de Vpu a ralenti tout de même fortement son transport général vers la surface. Conséquemment, l'expression de cette protéine virale a causé une déplétion spécifique de Tetherin en surface et sa relocalisation dans un compartiment périnucléaire positif pour Vpu et le marqueur du RTG, TGN46. Cette relocalisation a été observée avec un mutant de Vpu incapable de recruter β-TrCP, suggérant que cette activité se produit indépendamment d'un trafic ou d'un processus de dégradation requérant ce cofacteur. Nous avons aussi démontré que Vpu coimmunoprécipite avec Tetherin et que cette interaction implique le domaine transmembranaire de chacune des deux protéines. Cette association s'est avérée critique à la réduction du niveau d'expression de Tetherin en surface, à sa relocalisation dans le RTG ainsi qu'à la promotion de la relâche virale. Globalement, nos résultats suggèrent que l'association de Vpu à Tetherin affecte le transport antérograde et/ou le recyclage du facteur de restriction à partir du RTG et résulte en sa séquestration loin de la membrane plasmique d'où les particules du VIH-1 sont assemblées et relâchées. Ce mécanisme d'antagonisme est probablement complémenté par la dégradation de Tetherin dépendante de β-TrCP, soulignant l'éventuelle nécessité de stratégies complémentaires et peut-être synergiques afin de contrer efficacement la puissante activité restrictive de Tetherin.

Antagonism of Tetherin Restriction of HIV-1 Release by Vpu Involves Binding and Sequestration of the Restriction Factor in a Perinuclear Compartment

Mathieu Dubé[1], Bibhuti Bhusan Roy[1], Pierre Guiot-Guillain[1], Julie Binette[1], Johanne Mercier[1], Antoine Chiasson[1], and Éric A. Cohen[1,2 *]

[1]Laboratory of Human Retrovirology, Institut de recherches cliniques de Montréal (IRCM), 110 avenue des Pins ouest, Montreal, Quebec, Canada, H2W 1R7;

[2]Department of Microbiology and Immunology, Université de Montréal, Montreal, Quebec, Canada, H3C 3J7

[*]Corresponding author:

Running Title: Antagonism of Tetherin by HIV-1 Vpu

Manuscript information: 58 pages, 10 figures + 3 supplemental figures.

Word and character counts: abstract = 300/300 words; text word count = 8898 words

ABSTRACT

The Vpu accessory protein promotes HIV-1 release by counteracting Tetherin/BST-2, an interferon-regulated restriction factor, which retains virions at the cell-surface. Recent reports proposed β-TrCP-dependent proteasomal and/or endo-lysosomal degradation of Tetherin as potential mechanisms by which Vpu could down-regulate Tetherin cell-surface expression and antagonize this restriction. In all of these studies, Tetherin degradation did not however entirely account for Vpu anti-Tetherin activity. Here, we show that Vpu can promote HIV-1 release without detectably affecting Tetherin steady-state levels or turnover, suggesting that Tetherin degradation may not be necessary and/or sufficient for Vpu anti-Tetherin activity. Even though Vpu did not enhance Tetherin internalization from the plasma membrane (PM), it did significantly slow-down the overall transport of the protein towards the cell-surface. Accordingly, Vpu expression caused a specific removal of cell-surface Tetherin and a re-localization of the residual pool of Tetherin in a perinuclear compartment that co-stained with the TGN marker TGN46 and Vpu itself. This re-localization of Tetherin was also observed with a Vpu mutant unable to recruit β-TrCP, suggesting that this activity is taking place independently from β-TrCP-mediated trafficking and/or degradation processes. We also show that Vpu co-immunoprecipitates with Tetherin and that this interaction involves the transmembrane domains of the two proteins. Importantly, this association was found to be critical for reducing cell-surface Tetherin expression, re-localizing the restriction factor in the TGN and promoting HIV-1 release. Overall, our results suggest that association of Vpu to Tetherin affects the outward trafficking and/or recycling of the

restriction factor from the TGN and as a result promotes its sequestration away from the PM where productive HIV-1 assembly takes place. This mechanism of antagonism that results in TGN trapping is likely to be augmented by β-TrCP-dependent degradation, underlining the need for complementary and perhaps synergistic strategies to effectively counteract the powerful restrictive effects of human Tetherin.

AUTHOR SUMMARY

Restriction factors are cellular proteins that interfere with the multiplication and transmission of viruses and are therefore important components of natural immunity. Tetherin (also known as BST-2) is a recently identified restriction factor that traps viruses at the cell-surface, preventing their release and thus infection of other cells. Viruses have however developed means to counteract this restriction factor. Viral protein U (Vpu) is an accessory protein encoded by HIV-1, the causative agent of AIDS. Vpu antagonizes Tetherin and consequently promotes the release of HIV-1 particles. A series of recent reports proposed that Vpu would induce the degradation of this restriction factor in order to overcome its anti-viral activity. Here, we report that Vpu is able to enhance HIV-1 release in absence of Tetherin degradation. Instead, we found that Vpu interacts with Tetherin and interferes with the transport of the restriction factor towards the cell-surface. This would lead to re-localization of Tetherin in an intracellular organelle called the *trans*-Golgi network, resulting in insufficient levels of Tetherin at the cell-surface to trap progeny viruses. This mechanism of antagonism that results in TGN trapping could be augmented by the induction of degradation to effectively counteract the powerful restrictive effects of human Tetherin. Further characterization of this mechanism will improve our understanding of host antiviral defenses as well as provide new targets for the development of novel anti-HIV drugs.

INTRODUCTION

Recent advances in retrovirology have revealed that mammalian cells do not always provide a hospitable environment for the replication of viruses that parasitize them. It is indeed becoming increasingly clear that mammalian cells express a variety of molecules and activities that interfere with specific steps of the replication cycle of retroviruses and other viruses [1]. Among these so-called restriction factors, the cellular protein CD317/BST-2/HM1.24, also designated as Tetherin in reference to its ability to tether HIV-1 virions to infected cells, was recently identified as a potent inhibitor of the release step of retroviruses [2,3]. Tetherin is a heavily glycosylated type II integral membrane protein with an unusual topology in that it harbors two completely different types of membrane anchor at the N- and C-terminus; it is composed of a short N-terminal cytoplasmic tail linked to a transmembrane anchor (TM), an extracellular domain that include three cysteine residues important for dimerization, a predicted coiled-coil and a putative C-terminal glycophosphatidyl-inositol (GPI)-linked lipid anchor that is believed to ensure incorporation of Tetherin into cholesterol-rich lipid rafts [4,5]. Tetherin inhibits the release of widely divergent enveloped viruses, including members of the lentivirus (primate immunodeficiency viruses), gammaretroviruses (murine leukemia virus), spumaretrovirus (foamy virus), arenavirus (Lassa virus), Filovirus (Ebola and Marburg virus) families as well as Kaposi's sarcoma herpesvirus (KSHV) [2,3,6,7,8,9,10]. This broad-spectrum inhibition of enveloped virus particle release by Tetherin indicates that this restriction is unlikely to require specific interactions with viral proteins. In that regard, recent evidence indicates that Tetherin

configuration rather than primary sequences is critical for antiviral activity since an entirely artificial Tetherin-like protein consisting solely of domains from three proteins that were analogous to Tetherin in terms of size and topology but lacking sequence homology with native Tetherin, inhibited particle release in a manner strikingly similar to Tetherin [11]. Tetherin-mediated restriction of virus particle release is believed to occur at sites of virus particle assembly at the plasma membrane since a strong co-localization between Tetherin and nascent particles generated from retroviral or filoviral structural proteins was observed at the cell-surface [7,12]. In fact, recent findings using the artificial Tetherin-like protein support a model of restriction in which Tetherin directly cross-links virions to the plasma membrane [11]. Under basal conditions, Tetherin is expressed in B and T cells, plasmacytoid dendritic cells and myeloid cells and many transformed cell lines [2,13,14,15,16]. In addition, Tetherin expression is induced in many cell-types by type I and type II interferon (IFN), which suggests that it might be an important component of a broader antiviral innate immune defense [2,13,17]. In response to this restriction, many viruses express Tetherin antagonists such as KSHV K5, Ebola virus envelope glycoprotein (GP), simian immunodeficiency virus (SIVmac/smm) Nef, HIV-2 Env, SIVtan Env and HIV-1 viral protein U (Vpu), which was the first anti-Tetherin factor identified [2,3,9,10,18,19,20,21,22].

Vpu is an oligomeric type 1 integral membrane protein with two major activities during HIV-1 infection [23]. It contributes to the down-regulation of the CD4 receptor by targeting newly synthesized CD4 molecules that are bound to envelope glycoproteins (Env) in the endoplasmic reticulum (ER) for degradation by the ubiquitin-proteasome system [24,25]. This degradation process relies on Vpu ability to associate with CD4

and to recruit β-TrCP, a component of the $SCF^{\beta\text{-}TrCP}$ E3 ubiquitin (Ub) ligase, via phosphorylation of serines 52 and 56 within its DSGΦXS β-TrCP recognition motif [26,27]. In addition, Vpu promotes HIV-1 particle release by suppressing human Tetherin activity in restrictive Tetherin-expressing cells such as epithelial cell lines (HeLa), T cell lines (Jurkat, CEM) and primary T lymphocytes and macrophages [2,3,17]. In contrast, no effect of Vpu is observed in permissive human cell lines devoid of Tetherin expression such as HEK 293T and HT1080. Interestingly, Vpu does not exert its anti-Tetherin activity in non-human cell lines regardless of their Tetherin expression levels [6,28]. Indeed, although Tetherin variants found in rhesus macaques, African green monkeys (agm) and mouse cells were able to inhibit HIV-1 particle release, they were resistant to antagonism by HIV-1 Vpu [29,30]. Analysis of Tetherin variants encoded by different species highlighted positively selected determinants in the Tetherin TM domain responsible for conferring sensitivity to Vpu antagonism [29,30,31,32]. The mechanism by which Vpu counteracts Tetherin antiviral activity on HIV-1 particle release is still a matter of debate. Vpu was found to decrease the expression of Tetherin at the cell-surface [3] and to prevent Tetherin and Gag co-localization at sites of particle assembly [7,12], suggesting that removal of Tetherin from its site of tethering action could underlie the mechanism by which Vpu counteracts this cellular restriction, although this model has lately been challenged [33]. Recently, a series of reports proposed proteasomal and/or endo-lysosomal degradation of Tetherin through a β-TrCP-dependent process as potential mechanisms by which Vpu antagonizes Tetherin antiviral activity [12,20,30,31,34,35]. However, in all of these studies, Vpu-induced Tetherin degradation did not entirely account for the anti-Tetherin

activity of Vpu. Thus, the precise mechanism(s) through which Vpu antagonizes Tetherin is yet to be elucidated.

In this study, we investigated the effect of Vpu on Tetherin expression and trafficking to obtain a better insight into the mechanism through which Vpu antagonizes Tetherin-mediated restriction of HIV-1 particle release. Here, we provide evidence that Vpu can promote HIV-1 particle release without affecting the total steady-state levels or the turnover rate of Tetherin. We further show that even though Vpu did not enhance Tetherin internalization from the plasma membrane, it did significantly slow-down the transport of the restriction factor towards the cell-surface. Notably, expression of Vpu led to a specific removal of cell-surface Tetherin and a re-localization of the residual pool of Tetherin to a perinuclear compartment that extensively overlapped with the TGN. Finally, we show that Vpu and Tetherin associate most probably via their TM domains and provide evidence that this association is necessary to relocate Tetherin from the cell-surface to the TGN and to counteract its restrictive activity on HIV-1 release. Overall, our results are consistent with a model whereby antagonism of Tetherin by Vpu involves sequestration of the restriction factor in a perinuclear compartment, away from virus assembly sites on the plasma membrane, a process that could be augmented by the induction of degradation.

RESULTS

Vpu can promote HIV-1 particle release without altering the steady-state levels or turnover of Tetherin

To assess whether the reduction of Tetherin levels by Vpu was necessary and sufficient to promote efficient HIV-1 particle release, we analyzed the steady-state levels of fixed amounts of exogenously-expressed HA-Tetherin in permissive HEK 293T cells in conditions where varying levels of virally-encoded Vpu was co-expressed (Fig. 1A). This cellular system was previously used to evaluate the effect of Vpu on Tetherin steady-state levels [30,31,34]. At low Vpu expression levels (1 μg of Vpu+ proviral construct), the levels of Tetherin were essentially similar to those detected in absence of Vpu (1 μg of Vpu-defective proviral construct) (compare lane 5 with lane 6), while at higher levels of Vpu expression (2 μg of Vpu+ proviral construct), they were significantly reduced (compare lane 3 with lane 4). As expected, ectopic expression of HA-Tetherin strongly inhibited the release of Vpu-defective HIV-1 particle relative to the Tetherin-negative control as demonstrated by the drastic reduction of virion-associated p24 levels in the supernatants (Fig. 1A, compare lanes 3 and 5 with lane 1; quantified in Fig. 1B). Interestingly, although Vpu did not affect the total levels of exogenous HA-Tetherin at low concentration, it still promoted efficient release of HIV-1 particle (Fig. 1A, compare lane 5 with lane 6; quantified in Fig. 1B). These results suggest that Vpu can reduce the total levels of Tetherin, yet this process does not appear to be absolutely necessary to promote HIV-1 particle release.

To further confirm these observations, we analyzed the turnover of exogenously-expressed native Tetherin in condition of efficient Vpu-mediated virus particle release by pulse-chase labeling analysis (Fig. 2A-C). HEK 293T cells were co-transfected with the proviral constructs HxBH10-*vpu*- or HxBH10-*vpu*+ and with a plasmid encoding native Tetherin. Forty-eight hours post-transfection, cells were pulse-labeled, chased for different intervals of time and analyzed for Tetherin and Vpu expression levels by sequential immunoprecipitation using specific antibodies (Abs). In parallel, transfected cells as well as virus-containing supernatants were collected prior to radio-labeling to monitor HIV-1 particle release by western blot. Tetherin-specific bands ranging from ~20 kDa to ~29 kDa and likely representing putative glycosylated forms of monomeric Tetherin were immunoprecipitated (Fig. 2A). Ectopic Tetherin turnover was not altered by Vpu since none of the Tetherin-specific bands showed any significant accelerated reduction over time in the presence of the viral protein (Fig. 2A; compare lanes 7-10 with lanes 3-6). Quantitative analysis of Tetherin turnover revealed that exogenous Tetherin has a half-life of approximately 3.5h regardless of the presence of Vpu (Fig. 2B). Importantly, this lack of effect of Vpu on Tetherin turnover was observed in conditions of efficient Vpu-mediated HIV-1 particle release (Fig. 2C).

We further evaluated the half-life of endogenous Tetherin in infected HeLa cells in the presence or absence of Vpu. Vesicular stomatitis virus glycoprotein G (VSV-G)-pseudotyped HxBH10-*vpu*- or HxBH10-*vpu*+ virus-infected HeLa cells were pulse-labeled, chased for different intervals of time and analyzed for Tetherin expression levels as described above. In this system, endogenous mature Tetherin was detected as a ~30-37 kDa smear (Fig. 2D). A lower ~ 27 kDa band, distinct from the predicted *M*r of

20 kDa for unglycosylated Tetherin, was also detected at time 0 and most probably corresponds to immature glycosylated forms of newly synthesized Tetherin still residing in the ER. Exogenously- and endogenously-expressed Tetherin were recently reported to display distinct mobilities (~20-29 kDa (Fig.2A) vs ~27 and 30-37 kDa (Fig.2D)) because they undergo different types of carbohydrate modifications [36]. Indeed, as demonstrated by Andrew and colleagues, we found that treatment of exogenous and endogenous Tetherin with Peptide: N-Glycosidase F (PNGase), an enzyme that cleaves all N-linked oligosaccharides, resulted in both cases in deglycosylated Tetherin proteins with a *M*r of 19-20 kDa that were recognized by our anti-Tetherin serum (data not shown).

Figure 2D reveals that mature endogenous Tetherin has a half-life ($t_{½}$) of approximatively 8h (Fig. 2D, lanes 1-5; quantified in Fig.2E), which is indeed longer than exogenously-expressed Tetherin ($t_{½}$: 3.5h). Tetherin turnover was accelerated in presence of Vpu ($t_{½}$: 3.5h) (compare lanes 6-10 to lanes 1-5; quantified in Fig. 2E), consistent with recent results reported by Douglas and colleagues using HeLa cells transduced with Vpu-expressing adenoviral vectors [20]. Since Vpu-mediated Tetherin degradation was reported to rely on its capacity to recruit β-TrCP [12,20,34,35], we evaluated the turnover of the restriction factor in presence of the β-TrCP-binding defective Vpu S52D,S56D mutant. This mutant harbors mutations at the key amino-acids required for interaction with β-TrCP (Ser52, and Ser56 for Asp) and displays a phenotype very similar to the well-characterized Vpu S52N,S56N mutant [3,12,20,27,33,35,37,38]. Notably, Vpu S52D,S56D is unable to mediate CD4 degradation [25] and to recruit β-TrCP (Fig. S1A), but is however able to partially

down-regulate Tetherin from the cell-surface (Fig. S1B) and to promote HIV-1 particle release, albeit to a different extent than WT Vpu (Fig. S1C-D). Interestingly, even though Vpu S52D,S56D was still capable of promoting HIV-1 particle release, its expression did not affect Tetherin turnover (Fig.2D, compare lanes 11-15 and lanes 1-5; quantified in Fig. 2E), consistent with the reported role of β-TrCP in Vpu-mediated Tetherin degradation [12,20,34,35]. Taken together, these results provide evidence that Vpu can promote HIV-1 particle release without a detectable reduction of Tetherin intracellular levels or a notable modification of its turnover, suggesting that reduction of total levels of Tetherin by a degradative process may not be necessary and/or sufficient to fully explain the anti-Tetherin activity of Vpu.

Vpu does not promote Tetherin endocytosis.

Rodent Tetherin is internalized from the plasma membrane and delivered back to the TGN through a clathrin-dependent pathway that requires the sequential action of AP2 and AP1 adaptor complexes [5]. Importantly, internalization was found to be dependent upon a dual tyrosine (Tyr)-based motif (YXXΦ, where Y corresponds to Tyr, the Xs are residues that are highly variable, and Φ corresponds to residues with bulky side chains) in the N-terminal cytoplasmic tail (amino acids at position 6 and 8) of the protein (Fig. 3A). One alternative mechanism to explain how Vpu down-regulates Tetherin cell-surface expression and counteracts its antiviral activity is by enhancing the rate of Tetherin endocytosis. To evaluate whether the natural pathway of Tetherin endocytosis was necessary for the anti-Tetherin activity of Vpu, we generated a mutant of Tetherin that harbored alanine substitutions at the two key Tyr residues within the

dual Tyr-based internalization motif of the protein (HA-Tetherin Y6Y8) (Fig. 3A). Consistent with the previously reported role of this Tyr-based motif in rodent Tetherin endocytosis, substitution mutation of Tyr6 and Tyr8 prevented HA-Tetherin from being efficiently internalized from the cell-surface (Fig. 3B). To assess whether mutation of the Tyr-based motif affected Tetherin sensitivity to Vpu, HEK 293T cells were co-transfected with HxBH10-*vpu*- or HxBH10-*vpu*+ proviral constructs and plasmids encoding for HA-Tetherin or HA-Tetherin Y6Y8. Even though HA-Tetherin Y6Y8 was expressed at higher levels at the cell-surface (mean fluorescence intensity (MFI) =240) as compared to HA-Tetherin wt (MFI=90), both proteins were down-regulated from the cell-surface by Vpu and indeed appeared to reach similar cell-surface steady state levels (MFI of 51 and 41, respectively) (Fig. 3C). HIV-1 particle release was also monitored by western blot, 48h post-transfection. Consistent with its higher cell-surface expression levels, the restriction of virus particle release was more pronounced in presence of HA-Tetherin Y6Y8 than with HA-Tetherin wt (Fig. 3D; compare lanes 5 and 3 with lane 1; quantified in Fig. 3D). It is interesting to note that the mutant protein was overall expressed at higher levels than the WT protein (Fig. 3D, compare lanes 5 and 3). This is likely the result of the inefficient clearance of HA-Tetherin Y6Y8, which is not efficiently internalized from the cell-surface. Nevertheless, Vpu was still proficient at overcoming the restricting activity of HA-Tetherin Y6Y8 on HIV-1 particle release as demonstrated by the increased levels of virion-associated p24 released in the supernatant (Fig. 3D, compare lane 6 with lane 5; quantified in Fig. 3E). Similarly, a 2h treatment with 10 μM chlorpromazine, a drug that blocks clathrin-coated pit assembly at the plasma membrane [39], did not affect the ability of Vpu to overcome Tetherin-mediated

restriction of HIV-1 particle release in HeLa cells (data not shown). Altogether, these results suggest that Vpu does not manipulate clathrin-mediated endocytosis, the natural pathway of Tetherin endocytosis, as a mean to deplete the restriction factor from the cell-surface or to antagonize its antiviral activity.

Since Vpu could accelerate Tetherin endocytosis by a clathrin-independent process, we next asked whether Vpu affected Tetherin internalization kinetics from the cell-surface using an assay that measures the contribution of all endocytosis pathways. To this end, we compared the rate of endocytosis of endogenous Tetherin in HeLa cells that were producing Vpu-positive HIV-1 (HxBH10-*vpu*+) with those producing a Vpu-defective virus (HxBH10-*vpu*-) (Fig. 4). Consistent with previous studies of rodent Tetherin [5], human Tetherin was internalized constitutively. Interestingly, even though Vpu down-regulated Tetherin expression on the cell-surface (data not shown), the internalization kinetics of cell-surface Tetherin was unaffected (Fig. 4). These results indicate that Vpu does not counteract Tetherin restriction by promoting Tetherin endocytosis.

Vpu interferes with Tetherin trafficking to the cell-surface.

We have recently reported that regulation of HIV-1 release correlates with co-localization of Vpu and Tetherin in the TGN, thus raising the possibility that Vpu could act intracellularly by affecting Tetherin trafficking [40]. A cell-surface Tetherin re-expression assay was developed to determine whether Vpu affects Tetherin trafficking to the cell-surface. Conceptually, this assay implies the loss of Tetherin epitopes at the cell-surface and their subsequent recovery over time as demonstrated previously for

analysis of the *Mtv-1* Superantigen protein trafficking [41]. HeLa cells were co-transfected with the HxBH10-*vpu*- or HxBH10-*vpu*+ proviral constructs as well as with a GFP-encoding plasmid to allow gating of transfected cells. Forty-eight hours post-transfection, cells were harvested and treated with pronase (0.05%) to proteolytically remove cell-surface protein epitopes. After quenching the proteolytic reaction, stripped cells were incubated at 37°C for different time intervals to allow protein intracellular trafficking and re-expression at the cell-surface and then stained at 4°C with anti-Tetherin Abs. Expression of Tetherin in transfected (GFP-positive) or untransfected (GFP-negative) subpopulations was analyzed by flow cytometry (Fig. 5). As expected, dot plots revealed that Tetherin levels were down-regulated by Vpu in the untreated cells (compare the GFP-positive/HxBH10-*vpu*+ subpopulation MFI (MFI=36.8) with those of the GFP-negative/HxBH10-*vpu*+ (MFI=56.7) or GFP-positive/HxBH10-*vpu*- (MFI=61.0) subpopulations) (Fig. 5A, untreated). Pronase treatment markedly reduced the levels of Tetherin at the cell-surface, indicating that Tetherin epitopes were efficiently removed from the cell-surface. Interestingly, the levels of Tetherin detected at time 0 in the GFP-positive/HxBH10-*vpu*+ subpopulation was still lower (MFI=6.7) than those detected in the GFP-negative/HxBH10-*vpu*+ (MFI=9.7) or GFP-positive/HxBH10-*vpu*- (MFI=12.7) subpopulations (Fig. 5A, time 0 min). Similar levels of Tetherin re-expression was detected at the cell-surface of GFP-positive/HxBH10-*vpu*- cells and GFP-negative cells after 180 min of incubation as demonstrated by the comparable MFI detected in the two subpopulations. In contrast, Vpu caused a substantial reduction in Tetherin re-expression after 180 min, as shown by the lower MFI value in the GFP-positive/HxBH10-*vpu*+ population (MFI=19) compared to GFP-

negative/HxBH10-*vpu*+ cells (MFI=38.1) (Fig. 5A; 180 min). Treatment of cells with 10 μM Brefeldin A (BFA), a fungal metabolite that blocks protein sorting from the ER to the Golgi, prevented efficient Tetherin re-expression at the cell-surface both in transfected (GFP-positive) and untransfected (GFP-negative) cells, demonstrating the specificity of the re-expression assay (Fig. 5A, BFA). It is interesting to note that the absolute difference (Δ) in MFI detected between the Vpu-expressing cells and control cells (GFP-positive or negative/HxBH10-*vpu*- and GFP-negative/HxBH10-*vpu*+) was amplified after 180 min (Δ = ~19) as compared to time 0 (Δ = ~3-6), suggesting an effect of Vpu on cell-surface Tetherin re-expression kinetics. Indeed, the kinetics of Tetherin re-expression at the cell-surface, as measured by evaluating Tetherin levels (MFI) at the surface of pronase-treated cells relative to the corresponding untreated GFP-negative control over 180 min, increased linearly in the GFP-positive/HxBH10-*vpu*- and was indistinguishable from that of the GFP-negative/HxBH10-*vpu*+ control (slope of 0.27-0.29; Fig. 5B). After 180 min, approximately 75% of cell-surface Tetherin was recovered in both cases. In contrast, in presence of Vpu only ~35% of Tetherin expression was recovered at the cell-surface. Indeed, the kinetics of Tetherin re-expression in these Vpu-expressing cells was much slower than the controls (slope of ~0.14; Fig. 5B). Interestingly, the kinetics of Tetherin re-expression was similarly delayed in presence of the Vpu S52D,S56D mutant (slope of ~0.11), indicating that the observed effect of Vpu on Tetherin re-expression at the cell-surface is not the consequence of Tetherin degradation. Similar analysis based on the proportion of Tetherin-positive cells as a read-out (cut-off was arbitrarily set on the pronase-treated HxBH10-*vpu*+/GFP+ time 0 sample) revealed analogous results (data not shown). Thus,

our results suggest that Vpu expression interferes with Tetherin trafficking along the secretory and/or recycling pathways.

Vpu expression causes a re-localization of the cellular pool of Tetherin in a perinuclear compartment

To further support these observations and identify the intracellular compartment where Tetherin might accumulate in presence of Vpu, we analyzed the intracellular distribution of endogenous Tetherin in VSV-G-pseudotyped HxBH10-*vpu*- and HxBH10-*vpu*+ virus-infected HeLa cells by immunostaining and confocal microscopy. To this end, we developed a staining protocol, which allowed simultaneous detection of Tetherin at the cell-surface and in intracellular compartments as described in the Materials and Methods. In the absence of Vpu, Tetherin was detected primarily at the plasma membrane but also to a lower extent on internal membranes that overlapped partially with TGN46, a cellular marker of the TGN (Fig. 6, Vpu- panels), consistent with previous intracellular localization studies of rodent Tetherin [4,13]. This localization pattern was drastically altered by the presence of Vpu, which caused an effective removal of Tetherin from the cell-surface without, however, significantly affecting the pool of proteins localized in the perinuclear compartment that co-stained with TGN46 (Fig. 6A, Vpu+ panels and Fig. 6B). Notably, as reported previously by our laboratory [40], Vpu and Tetherin co-localized extensively in the TGN. This altered localization pattern of Tetherin was not observed in neighbouring untransfected cells, which indeed displayed a strong Tetherin staining at the plasma membrane. Since we found that Vpu was accelerating Tetherin turnover in HeLa cells in a β-TrCP-dependent

manner (Fig. 2D), we next analyzed the distribution of Tetherin in presence of the Vpu S52D,S56D mutant. In contrast to infected HeLa cells expressing WT Vpu, residual Tetherin was still readily detected at the plasma membrane of infected cells expressing the Vpu S52D,S56D mutant (Fig. 6A, Vpu S52D,S56D panels), a finding that most probably reflects the fact that this mutant is less efficient at down-regulating Tetherin from the cell-surface than WT Vpu (Fig. S1B). Interestingly, expression of this mutant resulted in a re-localization of the cellular pool of Tetherin in the TGN (Fig.6A). Importantly, Vpu S52D,S56D caused an ~4-fold increase of the absolute staining signal of Tetherin in the TGN relative to WT Vpu or the Vpu- control (Fig. 6B), suggesting that in absence of degradation, Vpu traps Tetherin in the TGN. Taken together, these microscopy studies suggest that HIV-1 Vpu promotes the sequestration of endogenous Tetherin in the TGN, most probably before triggering β-TrCP-dependent Tetherin degradation, thus preventing Tetherin's trafficking to the plasma membrane. Since these localization studies were performed in HIV-1-infected cells, these results further indicate that Tetherin sequestration occurs at physiological levels of Vpu expression.

Association of Vpu and Tetherin involves their transmembrane anchor domains

Having shown that Vpu expression affects the intracellular trafficking of Tetherin to the cell-surface and promotes a sequestration of Tetherin in the TGN, we next assessed whether Vpu can associate with Tetherin. HEK 293T cells were co-transfected with the HxBH10-*vpu*- or HxBH10-*vpu*+ proviral constructs as well as with a plasmid encoding HA-tagged Tetherin. Forty-eight hours post-transfection, cells were lysed in stringent detergent conditions with RIPA-DOC lysis buffer to avoid unspecific

association resulting from membrane bridging. Tetherin was then immunoprecipitated from cell lysates with anti-Tetherin antibodies and the immunocomplexes were analyzed for the presence of Vpu by western blot. Immunoprecipitation of HA-Tetherin led to a selective pull-down of the Vpu protein, suggesting that Vpu can directly or indirectly interact with Tetherin in cells where it can antagonize Tetherin antiviral activity (Fig. 7B, lane 8). Early studies aimed at mapping the regions of Vpu necessary for enhancing HIV-1 release identified the TM domain of the protein as an important functional determinant since Vpu mutants that contained a randomized TM region (Vpu RD) or harbored point mutations within the TM spanning domain, such as Vpu KSL, failed to enhance virus particle release, yet were still stable, properly localized in a perinuclear compartment and able to induce efficient CD4 degradation [42,43]. Vpu KSL contains a three amino-acid substitution in which Ile6, Ile8, and Val9 were replaced by Lys, Ser, and Leu, respectively, and contains a positively charged amino-acid in an area that is devoid of charge. To evaluate whether Vpu interacted with Tetherin through the TM anchor domain, we performed similar co-immunoprecipitations in HEK293T cells co-transfected with a plasmid encoding HA-tagged Tetherin and proviral constructs encoding Vpu RD (HxBH10-*vpu RD*) or Vpu KSL (HxBH10-*vpu KSL)* (Fig. 7A). In contrast to WT Vpu, both the Vpu RD and Vpu KSL mutants failed to co-immunoprecipitate efficiently with HA-Tetherin (Fig. 7B, compare lanes 9 and 10 with lane 8), suggesting that the association between the two proteins involves the TM domain of Vpu.

Since the TM of Vpu represents an important determinant for the association with Tetherin, we next determined whether the TM domain of Tetherin was also

involved. Tetherin TM was recently proposed to contain the determinants responsible for the species-specific sensitivity to Vpu [29,31,32]. Notably, reciprocal exchange of TM domains between human (h) and rhesus monkey Tetherin (THN) proteins conferred sensitivity and resistance to Vpu and alterations in the human Tetherin TM domain that correspond to differences found in rhesus and agm Tetherin proteins were sufficient to render human Tetherin completely resistant to HIV-1 Vpu [29,31,32]. We constructed a set of expression plasmids encoding HA-tagged Tetherin chimeras with reciprocal exchanges of the TM between the human and agm proteins (Fig. S2A). In addition, we generated an expression plasmid encoding a HA-tagged human Tetherin that harbors double mutations in the TM domain (HA-human Tetherin ΔGI,T45I) comprising a deletion of Gly25 and Ile26 residues and substitution of Thr45 for an Ile (Fig. S2A). This mutant was previously reported to strongly inhibit HIV-1 particle release but was completely resistant to antagonism by Vpu [29]. HEK 293T cells were co-transfected with the HxBH10-*vpu*- or HxBH10-*vpu*+ proviral constructs as well as with the indicated HA-Tetherin-encoding plasmids (Fig. 7C-E). Forty-eight hours post-transfection, Tetherin was immunoprecipitated from cell lysates and immunocomplexes were further analyzed for the presence of Vpu by western blot. Since HA-agm Tetherin and the HA-agmTHN(hTM) chimeras were less expressed and/or detected using our anti-human Tetherin Abs (these chimeras were not efficiently precipitated with anti-HA Abs), Vpu association was compared between Tetherin variants displaying similar expression profile. As shown in Figure 7C, immunoprecipitation of HA-human Tetherin co-precipitated Vpu (Fig. 7C, lane 12). As expected, HA-agm Tetherin, which was reported to be resistant to Vpu antagonism [29,32], did not show a strong and specific

association with Vpu. In contrast, replacement of the agm Tetherin TM domain with that of human Tetherin (HA-agmTHN(hTM)) restored the association with Vpu (Fig. 7C, compare lane 14 with lanes 16 and 12). Exchange of the human Tetherin TM with that of agm Tetherin (HA-hTHN(agmTM)) led to a marked reduction of Vpu association despite comparable levels of Tetherin expression (Fig. 7D, compare lane 12 with lane 10). Finally, introduction of the ΔGI,T45I mutations in the TM domain of HA-human Tetherin drastically reduced the association with Vpu (Fig. 7E, compare lane 12 with lane 10). These results suggest that the integrity of the TM domain of human Tetherin is necessary for the association with Vpu. Taken together, our data suggests that association of Vpu and human Tetherin involves their TM anchor domains.

Association of Vpu to Tetherin is required to down-regulate the expression of the restriction factor at the cell-surface and to promote HIV-1 particle release.

We next assessed whether association of Vpu to Tetherin was required to counteract Tetherin antiviral activity (Fig. 8). To do so, we transfected a proviral construct encoding WT Vpu or the Vpu KSL mutant in HeLa cells and first assessed their ability to associate with endogenous Tetherin. Wild type Vpu co-precipitated with endogenous Tetherin while Vpu KSL did not, confirming the results obtained when exogenous HA-tagged Tetherin was overexpressed in HEK293T cells expressing HxBH10-*vpu*+ or HxBH10-*vpu KSL* proviruses (Fig. 8A, compare lane 6 with lane 5). Association of Vpu with endogenous Tetherin was specific since HIV-1 envelope glycoprotein precursor gp160, another type 1 integral protein, did not co-precipitate with Tetherin (Fig. 8A). Interestingly, the Vpu KSL mutant was strongly attenuated in its

ability to down-regulate efficiently the steady-state levels of Tetherin at the cell-surface relative to WT Vpu since Tetherin cell-surface expression in presence of Vpu KSL was significantly higher than in presence of WT Vpu (MFI of 191 vs 138), yet still slightly lower than in the Vpu-negative control (MFI= 235) (Fig. 8B). Importantly, as previously reported [43], this mutant was drastically attenuated in its ability to promote efficient HIV-1 particle release (Fig 8C, compare lanes 3 and 2 with lane 1; quantified in Fig. 8D). Similarly to Vpu KSL, the Vpu RD mutant, which is also defective for Tetherin binding, was also markedly attenuated in its ability to down-regulate Tetherin cell-surface expression and to promote efficient HIV-1 release in HEK 293T cells ectopically-expressing Tetherin (Fig. S3A and B), consistent with results reported by previous studies [3,42]. Human Tetherin containing the agm TM domain (HA-hTHN(agmTM)) or the ΔGI,T45I mutations (HA-human Tetherin ΔGI,T45I) lost the ability to bind Vpu (Fig 7D and E) and as expected still restricted HIV-1 particle release even in the presence of Vpu (Fig. S2B and C for HA-hTHN(agmTM) and Fig. S2D and E for HA-human Tetherin ΔGI,T45I). Unexpectedly, introduction of the human Tetherin TM domain in agm Tetherin (HA-agmTHN(hTM), did not reinstate a significant sensitivity to Vpu (Fig. S2 B and C), despite a detectable restoration of the Vpu binding (Fig. 7C). This functional phenotype (absence of Vpu sensitivity) is different from that obtained by McNatt and colleagues [29] using agm or rhesus Tetherins containing the human Tetherin TM domain but is similar to that reported by Goffinet and colleagues [30] using rodent Tetherin proteins containing the human Tetherin TM domain. Difference in the configuration of the TM domain in these Tetherin chimeric constructs may explain this discrepancy. The result obtained with the HA-agmTHN(hTM)

chimeric construct suggests that association of Tetherin with Vpu is necessary but not sufficient to overcome Tetherin-mediated restriction of HIV-1 particle release. However, we cannot rule-out the possibility that the binding of Vpu to the HA-agmTHN(hTM) chimeric protein may indeed be less efficient than with HA-human Tetherin since our antibody may underestimate the levels of expressed HA-agmTHN(hTM) proteins (Fig. 7C, compare lane 14 and lane 12). Thus, alternatively, a threshold level of Vpu association to Tetherin may be necessary to antagonize the antiviral activity of the restriction factor. Nonetheless, overall, these results suggest that association of Vpu to Tetherin is required to antagonize the antiviral function of the restriction factor.

Association of Vpu to Tetherin is critical for the re-localization of the restriction factor in the TGN

Since we showed that expression of Vpu could cause a re-localization of Tetherin from the plasma membrane to the TGN, we next tested whether the Vpu TM domain mutants, Vpu RD and Vpu KSL, which are unable to associate with Tetherin, could still sequester endogenous Tetherin in the TGN. Hela cells were infected with VSV-G-pseudotyped viruses expressing WT Vpu or Vpu RD or Vpu KSL and infected cells were immunostained and analyzed by confocal microscopy. Figure 9 reveals that both the Vpu RD and Vpu KSL lost the ability to efficiently remove Tetherin from the cell-surface and to relocate the restriction factor to the TGN. Indeed, quantitative analysis of the Tetherin signal localized in the TGN relative to the total cellular Tetherin signal showed that cells expressing the Tetherin degradation-defective Vpu S52D,S56D

mutant displayed an increased proportion of Tetherin signal in the TGN compared to the Vpu- control. (~57% relative to ~18%; $p<0.001$) (Fig.6). In contrast, cells expressing the Vpu RD or Vpu KSL mutants showed ~25% of the Tetherin signal in the TGN, a proportion that was in fact just slightly higher than that found in cells infected with a Vpu-defective virus (Fig. 9). Accordingly, in contrast to Vpu S52D,S56D, these mutants did not show any increase in the absolute levels of Tetherin signal in the TGN (Fig. 9). These results indicate that Vpu promotes the sequestration of Tetherin in the TGN by a process that is dependent on the association of the two proteins. Taken together with the functional analysis and the co-precipitation experiments, these results further suggest that the antagonism of Tetherin function by Vpu involves binding and sequestration of the restriction factor in the TGN.

DISCUSSION

The Vpu accessory protein stimulates the release of HIV-1 virions by antagonizing a restriction on virus particle release mediated by Tetherin at the cell-surface [2,3]. This antagonism appears to closely correlate with the ability of Vpu to mediate down-regulation of Tetherin expression from the cell-surface [3,12,20]. While this down-regulation is accompanied by enhanced degradation of Tetherin in several infected cell types, such as Jurkat [20] and CEM-G37 T cells [21] or macrophages [33], several lines of evidence also suggest that degradation of Tetherin *per se* cannot entirely account for Vpu-mediated counteraction against the restriction factor since: 1) Vpu decreased total cellular Tetherin to a lesser extent than cell-surface Tetherin in HeLa cells [12]; 2) Vpu expression did not result in a reduction of intracellular Tetherin in infected CEMx174 and H9 cells, yet virus replication in these cells was Vpu-responsive [33]; 3) Vpu mutants that contained substitution mutation in the DSGΦXS β-TrCP recognition motif that rendered them deficient for directing β-TrCP-dependent degradation of Tetherin were still able to partially [3,12,20,34,37] (Fig. S1C and D) or in some instances totally [33,44] overcome the particle release restriction; 4) Binding of Vpu to Tetherin was recently shown to be sufficient for a partial relief of the restriction [20,34].

We show here that Vpu can promote efficient HIV-1 particle release without a detectable reduction of the total steady-state levels of Tetherin (Fig.1) nor a notable modification of the restriction factor turnover rate in transfected HEK 293T cells

(Fig.2A -C), suggesting that degradation of the antiviral factor *per se* is not necessary and/or sufficient to account for Tetherin antagonism at least in this experimental system. Interestingly, Vpu expression in HeLa cells increased endogenous Tetherin turnover (Fig. 2D and E), as reported previously by Douglas and colleagues [20]. This Vpu-mediated degradation process was however still relatively slow (half-life of Tetherin decreases from ~8h to 3.5h in presence of Vpu) as compared to the very efficient CD4 receptor degradation induced by Vpu (half-life of CD4 decreases from ~6h to ~12 min in presence of Vpu) [45], and as such is unlikely to explain the powerful antagonism of Tetherin by Vpu. Thus, Vpu-mediated counteraction of Tetherin restriction must involve other mechanisms. Our results further indicate that Vpu does not promote endocytosis of Tetherin as a mechanism to antagonize the restriction factor. Indeed, mutation of the two critical tyrosine residues located within a dual tyrosine-based sorting motif in the cytoplasmic domain of the protein, did not abolish the sensitivity of Tetherin to Vpu, as was indeed recently reported by Iwabu and colleagues [35], yet led to an increased accumulation of the restriction factor at the cell-surface and to a more potent restriction of HIV-1 particle release (Fig. 3). Moreover, although analysis of Tetherin endocytosis kinetics showed that the protein is constitutively internalized, it did not reveal any increase in the rate of Tetherin endocytosis in presence of Vpu (Fig.4), and as such confirmed the results recently reported by Mitchell and colleagues [12]. These results are consistent with previous findings showing that Vpu-mediated enhancement of virus particle release is not significantly affected by expression of dominant negative (DN) mutants of Dynamin or Rab5 nor by depletion of clathrin heavy chain or by treatment with inhibitors of endocytosis such as chlorpromazine (data not shown) [6,40,46].

Collectively, they indicate that Vpu does not antagonize Tetherin by enhancing its endocytosis from the cell-surface. Instead, these findings suggest that Vpu affects Tetherin anterograde trafficking events whose net effect is depletion of the restriction factor from the cell-surface. In support of this hypothesis, a previous report suggested that Vpu may acts as a regulator of protein transport along the secretory pathway [47]. In fact, upon analyzing the kinetics of Tetherin expression at the cell-surface of protease-treated HeLa cells, we noticed that Tetherin re-expression was significantly reduced in presence of Vpu (Fig. 5). It is important to note, here, that this effect is occurring regardless of whether Vpu is inducing Tetherin degradation in these experimental conditions since: 1) it is the rate of re-expression, as defined by the slope of the graph of figure 5B that is affected in presence of Vpu; 2) re-expression of cell-surface Tetherin was also delayed in presence of the Tetherin degradation-defective Vpu S52D,S56D mutant (Fig. 5B). Consistent with this observation, examination of infected HeLa cells expressing Vpu revealed that the cellular pool of Tetherin was re-localized from the cell-surface to a perinuclear compartment that stained positive with the TGN marker TGN46 and Vpu itself (Fig.6). Although some of the loss of cell-surface Tetherin in Vpu-expressing HeLa cells could be attributed to Vpu-mediated degradation of the restriction factor, similar experiments performed with the Vpu S52D,S56D mutant demonstrated that Vpu can cause a redistribution of Tetherin from the plasma membrane to the TGN. These results suggest that reduction of Tetherin levels at the plasma membrane involves a step whereby Vpu sequesters Tetherin in the TGN. They also provide a possible mechanism to explain the partial relief of Tetherin restriction observed by several groups upon expression of β-TrCP-binding defective Vpu mutants

[12,20,34]. However, since residual Tetherin was still readily detected at the plasma membrane of HeLa cells expressing the Vpu S52D,S56D mutant (Fig.6A and Fig.S1B), this sequestration may not be sufficient to effectively prevent Tetherin to reach the cell-surface at least in this model. These observations underline, perhaps, the need for β-TrCP-mediated trafficking and degradation processes as a complementary mechanism to efficiently remove Tetherin from the cell-surface, particularly in certain cell types or under specific conditions, such as IFN exposure, where cellular Tetherin expression levels are high. Thus, the different particle release phenotypes observed with Vpu mutants that are unable to recruit β-TrCP, such as Vpu S52D,S56D, (these range from as efficient than WT Vpu to a ~50% attenuation) [3,12,20,33,34,37,44] may in fact relate to differing levels of Tetherin expression in the target cells. Although, it is conceivable that Vpu-mediated sequestration of Tetherin in the TGN may explain how Vpu antagonizes Tetherin in the absence of a decrease in total Tetherin expression, it still remains unclear how Vpu could antagonize Tetherin in the absence of down-regulation from the cell-surface and a decrease in total cellular expression in certain cell types [33].

We also confirmed by co-immunoprecipitation studies that Vpu interacts with Tetherin [20,32,34,35] and demonstrated using well-characterized Vpu and Tetherin mutants as well as chimeric proteins between human and African green monkey Tetherin molecules that this physical interaction involves the transmembrane domains of the two proteins (Fig. 7 and Fig. 8). These findings are consistent with previous results showing that the transmembrane domain of Vpu is required for both the down-regulation of surface Tetherin and the enhancement of HIV-1 particle release [3,42,43]. They are also supported by recent data indicating that the inability of Vpu to antagonize

the restrictive effect of African green monkey and rhesus Tetherin proteins is a consequence of amino-acid changes in the transmembrane domain of the rhesus and African green monkey protein relative to the human form [29,32]. Importantly, our data establish a direct functional link between association of Vpu to Tetherin and Tetherin antagonism since we showed that Vpu's ability to interact with Tetherin was necessary: 1) to counteract the restriction on HIV-1 particle release and down-regulate Tetherin from the cell-surface (Fig. 8, Fig. S2 and S3); and, 2) to induce a re-localization of the cellular pool of Tetherin from the plasma membrane to the TGN (Fig. 9). Unexpectedly, our observation showing that introduction of the human Tetherin TM domain in African green monkey Tetherin did not reinstate a significant sensitivity to Vpu (Fig, S2B and C) despite a detectable restoration of the Vpu binding raises the possibility that this interaction may not be sufficient to explain Tetherin antagonism. The requirement for additional cellular factor(s) in the Vpu-mediated Tetherin antagonism is therefore a possibility that warrants further investigations.

Since our co-immunoprecipitation and functional data indicate that a physical interaction between Vpu and Tetherin is required for Tetherin antagonism and sequestration, this raise the possibility that Vpu may simply interact with Tetherin and inhibit its outward trafficking from the TGN since all membrane proteins are transported to the plasma membrane through the TGN (Fig. 10). Since mutation of the dual Tyr signal in the Tetherin cytoplasmic tail does not abolish the sensitivity to Vpu, it appears that Tetherin sequestration in the TGN may occur before its endocytosis from the cell-surface and as such may involve newly synthesized Tetherin en route to the plasma membrane. However, we cannot completely rule-out that Vpu could interact with

endocytosed Tetherin in the TGN and prevent its recycling back to the cell-surface, given that previous data from the Spearman group demonstrated a requirement for the recycling endosomes in Vpu function [48]. Furthermore, recent studies reported that AP-2 depletion [12] or over-expression of DN mutant of Dynamin (Dyn2-K44A) [35] could partially interfere with Vpu-mediated down-regulation of Tetherin expression from the cell-surface. Indeed, since Vpu is expressed from a Rev-dependent bicistronic mRNA encoding Env and consequently is made late during the virus life cycle [49], the direct removal of Tetherin from the plasma membrane via endosomal trafficking may be critical to ensure a rapid and efficient neutralization of the restriction on HIV-1 release. It is nevertheless surprising that mutation of the Tetherin dual Tyrosine-based endocytosis motif did not affect the ability of Vpu to counteract Tetherin-mediated restriction of HIV-1 particle release. Perhaps co-expressing transiently the two proteins simultaneously may not adequately reflect physiological conditions given that Tetherin is normally already present at the plasma membrane when Vpu is expressed. Alternatively, it is also possible that sequestration of newly synthesized Tetherin in the TGN may rapidly clear the restriction factor from its site of virion-tethering action at the plasma membrane depending on the physiologic rate of Tetherin turnover at the plasma membrane. More studies will be required to assess whether Vpu affects Tetherin trafficking at a pre- or/and post-endocytic step.

Vpu-mediated sequestration of Tetherin in the TGN could be complemented by β-TrCP-dependent degradation processes, thus enhancing Tetherin antagonism. It is conceivable that Vpu by forming a complex with β-TrCP and Tetherin in the membrane of the TGN could potentially induce ubiquitination via interaction with the $SCF^{\beta\text{-}TrCP}$ E3

ubiquitin ligase. This ubiquitination event could either enhance the sequestration by preventing Tetherin recycling to the cell-surface or/and targets it to lysosomes for degradation (Fig.10). Our data indicating that Vpu causes a re-localization of the cellular pool of Tetherin in the TGN, where indeed the two proteins strongly co-localize, suggests that Vpu affects Tetherin trafficking and potentially its degradation from a post-ER compartment(s), and as such is difficult to reconcile with a mechanism of proteasomal degradation of the antiviral factor through the cellular ER-associated degradation (ERAD) pathway [30,31,34]. However, given the fact that Vpu induces degradation of the CD4 receptor in the ER by an ERAD-like mechanism [25], it is still possible that some proteasomal degradation in the ER may contribute to Tetherin depletion. Whether Vpu and Tetherin trafficking cross each other in the TGN, thus permitting a physical interaction between the two proteins, remains to be determined. In this regard, it is interesting to note that recent data from our laboratory have shown that the ability of Vpu to suppress Tetherin-mediated restriction of HIV-1 particle release was linked to its localization in the TGN [40]. Further studies aimed at identifying the determinants regulating Vpu trafficking and localization in the TGN will likely shed light on this mechanism.

HIV-1 Vpu appears to share the ability to sequester Tetherin in the TGN with other Tetherin antagonists, namely HIV-2 Rod and SIVtan Env. Like HIV-1 Vpu, HIV-2 Rod Env was recently shown to interact with Tetherin and to cause a redistribution of Tetherin in the TGN, although in the case of HIV-2 Env, no evidence of Tetherin degradation was observed [21]. Similarly, SIVtan Env was also shown to downregulate cell-surface Tetherin by sequestering the restriction factor in intracellular

compartment(s) [22]. Collectively, these findings suggest a common mechanism of antagonism that results in TGN trapping, which can be augmented by the induction of degradation in the case of Vpu. Given the powerful restrictive effects of human Tetherin on HIV production, this dual mechanism of antagonism mediated by Vpu may have provided HIV-1 with stronger countermeasures to antagonize Tetherin. This genetic and functional divergence between HIV-1 and HIV-2 may perhaps account for the different virulence properties displayed by these two closely related viruses [21,50]. Future studies on the role of Tetherin antagonism in the pathogenesis of primate immunodeficiency virus will likely shed light on the contribution of this innate antiviral factor in the control of viral infection and spread in *vivo* and will reveal whether enhancing the antiviral activity of Tetherin is a valid option to thwart HIV-1 replication.

MATERIALS AND METHODS

Antibodies and chemical compounds. Anti-Vpu rabbit polyclonal serum was described previously [40]. Anti-Tetherin rabbit polyclonal serum was generated by immunization of rabbits with a bacterially-produced Glutathione-S-transferase (GST) fusion protein containing a polypeptide corresponding to amino-acids 40 to 180 of human Tetherin. Rabbit pre-immune serum was collected prior to rabbit immunization. Monoclonal anti-HA (clone 12CA5), anti-p24 (catalog no. HB9725) and anti-myc (clone 9E10) Abs were isolated from the supernatants of cultured hybridoma cells obtained from the American Type Culture Collection (ATCC). The monoclonal anti-gp120 antibody [51,52] was obtained from NIH AIDS research and Reference Reagent Program. All secondary Alexa-conjugated IgG Abs were obtained from Invitrogen. Sheep anti-TGN46 (Serotec), mouse anti-BST2 (Abnova), anti-actin Abs (Sigma), pronase (Calbiochem), PNGase (New England Biolabs), BFA, paraformaldehyde (PFA) and chlorpromazine (Sigma) were all obtained from commercial sources. All reagents were stored according to the manufacturer's instructions.

Cells and transfection. HEK 293T, HeLa and Cos-7 cells were obtained from ATCC. All cells were maintained as described previously [40]. HEK 293T and HeLa cells were transfected using the calcium-phosphate method and lipofectamine 2000 (Invitrogen), respectively. Functional and biochemical analyses were performed 48h post-

transfection. Empty plasmid DNA was added to each transfection to keep the amount of transfected DNA constant.

Plasmid constructs. HxBH10-*vpu*+ and HxBH10-*vpu*- are two infectious molecular clones of HIV-1 that are isogenic except for the expression of Vpu [53]. HxBH10-*vpu S52D,S56D,* SVCMV-*vpu*- and SVCMV-*vpu*+ were previously described, [25]. HxBH10-*vpu KSL*, HxB10-*vpu RD* and SVCMV-*vpu S52D,S56D* were generated by PCR-based site-directed mutagenesis [40]. The pcDNA/Myc-His-β-TrCP plasmid was kindly provided by Dr. Richard Benarous [27]. To generate pcDNA-Tetherin and pCMV-HA-Tetherin, the human Tetherin open reading frame was amplified by PCR from pCMV-SPORT6-hBST2 plasmid (Open Biosystems) and cloned into pcDNA3.1/Hygro (+) (Invitrogen) and pCMV-HA (Clontech). The agmTetherin open reading frame was amplified from Cos-7 cells mRNA using RT-PCR as described [29]. Tetherin chimeras were designed according to the structure prediction from Kupzig and Banting [4]. All Tetherin genes were inserted into pcDNA3.1/Hygro (+) using NheI and Asp718 restriction sites or into the pCMV-HA plasmid using BglII and Asp718 restriction sites to generate pcDNA-Tetherin and pCMV-HA-Tetherin constructs, respectively. pCMV-HA-Tetherin Y6Y8 and pCMV-HA-Tetherin ΔGI,T45I were generated by PCR-based site-directed mutagenesis. The vesicular stomatitis virus (VSV) glycoprotein G-expressing plasmid, pSVCMVin-VSV-G, was previously described [54]. The pQBI25 GFP-expressing plasmid was obtained from Qbiogene.

Steady-state detection of proteins by western blot. Transfected HeLa or HEK 293T cells were lysed in CHAPS lysis buffer (50 mM Tris, 5 mM EDTA, 100 mM NaCl, 0.5% CHAPS, pH 7.2) or in radio-immunoprecipitation assay (RIPA-DOC) buffer (10 mM Tris pH 7.2, 140 mM NaCl, 8 mM Na_2HPO_4, 2 mM NaH_2PO_4, 1% Nonidet-P40, 0.5% sodium dodecyl sulfate, 1.2 mM deoxycholate), respectively. Proteins from lysates were resolved on 12.5% SDS-PAGE, electro-blotted and analyzed by western blot as described previously [40].

Pulse-chase and radio-immunoprecipitation experiments. Pulse-chase experiments were perfomed as described previously [40]. Briefly, transfected HEK 293T or HeLa cells infected with VSV-G-pseudotyped HxBH10-derived virus at a MOI of 1 were pulse-labeled for 30 min and 2h respectively, with 800 μCi/ml of [^{35}S]methionine and [^{35}S]cysteine (Perkin Elmer) and chased for different interval of times. Following lysis of radio-labeled cells in RIPA-DOC, lysates were first pre-cleared with protein A sepharose beads coated with pre-immune rabbit serum for 1h. Pre-cleared cell lysates were then incubated with anti-Tetherin Abs for 2h at 4°C prior to immunoprecipitation using protein A sepharose beads. In HEK 293T cells, Vpu proteins were sequentially immunoprecipitated using the same method. Labeled proteins were analyzed by SDS-PAGE and autoradiography.

PNGase treatment. Cells were lysed in RIPA-DOC. Tetherin-containing lysates were incubated with anti-Tetherin Abs for 2h at 4°C prior to addition of protein A sepharose

beads. Following an incubation of 2h at 4°C, beads were isolated by centrifugation, washed with denaturing buffer (New England Biolabs), resuspended in denaturing buffer and then boiled at 95°C for 10 min. The supplied reaction buffer was added along with NP-40 (0.1%) according to the manufacturer's suggestion. Samples were then digested with 1500 units of PNGase (New England Biolabs) at 37°C for 3h. Control samples were incubated without the enzyme. Proteins were eluted from beads by boiling in an equal volume of sample buffer for 10 min and analyzed by immunoblotting.

Virus release assay. The virus release assay was described previously [40]. Briefly, supernatants of transfected cells were clarified by centrifugation and filtered through a 45μm filter. Viral particles were pelleted by ultracentrifugation onto a 20% sucrose cushion in PBS for 2h at 130000 g at 4°C and lysed in RIPA-DOC. Gag products were analyzed by western blot. Viral release efficiency was evaluated by determining the ratio between the virion-associated Gag (p24) band signal and all intracellular Gag-related band signal using laser scanning densitometry.

Production of VSVg-pseudotyped HIV-1 virus. HEK 293T cells were transfected with HxBH10 proviral constructs and pSVCMVin-VSV-G as described previously [54]. Supernatants of transfected cells were clarified, filtered and pelleted by ultracentrifugation as described above and resuspended in DMEM supplemented with 10% bovine serum (FBS). Viruses were titrated using a standard MAGI assay [54].

Flow cytometry. Cells were washed in PBS, resuspended at a concentration of $1x10^6$cells/ml and stained with the specific anti-Tetherin serum for 45 min at 4°C. After incubation, cells were washed and stained using appropriate fluorochrome-coupled secondary Abs for 30 min at 4°C. Cells were then washed, fixed with 2% PFA. Transfected GFP-expressing cells were analyzed for cell-surface Tetherin expression by flow cytometry. Rabbit pre-immune serum served as a staining control. Fluorescence intensities were acquired using a FACScalibur flow cytometer (BD Biosciences) and data was analyzed using FlowJo software v. 7.25 (Treestar). MFI values presented in the histograms correspond to the specific signal obtained after substraction of the MFI value from the pre-immune control.

Internalization assay. Cells were washed in PBS, re-suspended in PBS containing the anti-Tetherin serum at a concentration of $1x10^6$cells/ml and incubated for 45 minutes at 4°C. Following washes in cold PBS, cells were incubated at 37°C in DMEM medium supplemented with 5% FBS for different time intervals. At each time point, cells were harvested, washed in cold PBS and stained with the appropriate fluorochrome-coupled secondary Abs for 30 min at 4°C. Transfected GFP-expressing cells were analyzed for cell-surface Tetherin expression by flow cytometry.

Cell-surface Tetherin re-expression assay. Cells were harvested, washed in PBS, re-suspended at a concentration of $1x10^6$ cells/ml in PBS-pronase 0.05% and incubated for

30 minutes at 37°C. Cold DMEM containing 10% FBS was added to block surface protein proteolysis. Cells were then washed, incubated at 37°C for different time intervals and stained for cell-surface Tetherin as described above. Expression of Tetherin at the cell-surface of transfected GFP-positive and untransfected GFP-negative cells was analyzed by flow cytometry.

Confocal microscopy. HeLa cells were infected with VSV-G-pseudotyped HxBH10-derived viruses at a MOI of 0.125. Forty-eight hours post-infection, cells were immunostained with anti-Tetherin Abs (Abnova) for 30 min at 4°C, washed in cold PBS, fixed with 4% PFA and permeabilized with 0.2% Triton X-100. Next, cells were incubated with anti-Tetherin (Abnova), anti-Vpu and anti-TGN46 Abs for 2h at 37°C, washed and incubated with the appropriate secondary Abs for 30 min at room temperature. Analyses were performed with a LSM710 laser scanning confocal microscope (Zeiss). Quantitation of Tetherin signal was performed using the Zeiss LSM510 software. The absolute Tetherin signal in the TGN was determined by measuring the specific Tetherin signal in the region delineated by the TGN46 marker on digital pictures produced using similar acquisition time. Percentage of Tetherin accumulating in the TGN was calculated by evaluating Tetherin signal intensity in the TGN relative to the total Tetherin signal intensity detected in the cell as described previously [40]. Analysis was performed on at least 25 distinct cells.

Co-precipitation assay. For co-immnuoprecipitation of Vpu and Tetherin, transfected HEK 293T and HeLa cells were harvested 48h post-transfection and lysed in RIPA-DOC or CHAPS buffer, respectively. Five percent of the lysate was preserved to control for protein expression. Cell lysates were first pre-cleared with protein A sepharose beads coated with pre-immune rabbit serum for 1h at 4°C and then, incubated with anti-Tetherin Abs for 2h at 4°C, prior to precipitation with protein A sepharose beads. Immunoprecipitates were analyzed for the presence of Vpu and Tetherin by western blot.

For co-immunoprecipitation of Vpu and β-TrCP, HEK 293T cells were transfected with SVCMV-*vpu*- or SVCMV-*vpu*+ *or* SVCMV-*vpu S52D,S56D and* pcDNA/Myc-His-β-TrCP. Transfected cells were then radiolabelled with 800 μCi/ml of [^{35}S]methionine and [^{35}S]cysteine (Perkin Elmer) and lysed in CHAPS buffer. Lysates were first pre-cleared with protein A sepharose beads coated with pre-immune rabbit serum for 1h. Pre-cleared cell lysates were then incubated with anti-myc Abs for 2h at 4°C prior precipitation using protein A sepharose beads. Vpu was then sequentially immunoprecipitated using anti-Vpu Abs using the same method. Labeled proteins were analyzed by SDS-PAGE and autoradiography.

Scanning and quantitation. Scans were performed on a Duoscan T1200 scanner (AGFA) followed by densitometric quantitation using the Image Quant 5.0 software (Molecular Dynamics). Statistical analysis was performed using a paired Student's *t* test, and statistical significance was considered at $p < 0.001$.

Accession numbers: NCBI reference number for HxBH10 Vpu and human Tetherin proteins are P69699 and AAH33873, respectively. Genebank accession number for agm Tetherin is FJ943430.

ACKNOWLEDGMENTS

We thank Dr. Richard Benarous for the kind gift of the pcDNA/Myc-His-β-TrCP. We also want to thank present and former members of the Cohen group for helpful discussion, Mariana Bego for revision of the manuscript, Dominic Filion for technical help on the confocal microscope and Angelo Tiganos for the HxBH10-*vpu RD* construct. The following reagent was obtained through the AIDS Research and Reference Reagent Program, Division of AIDS, NIAID, NIH: Hybridoma 902 (anti-gp120) from Dr. Bruce Chesebro [51,52]. This work was performed by MD in partial fulfillment of his doctoral thesis.

REFERENCES

1. Wolf D, Goff SP (2008) Host restriction factors blocking retroviral replication. Annu Rev Genet 42: 143-163.

2. Neil SJ, Zang T, Bieniasz PD (2008) Tetherin inhibits retrovirus release and is antagonized by HIV-1 Vpu. Nature 451: 425-430.

3. Van Damme N, Goff D, Katsura C, Jorgenson RL, Mitchell R, et al. (2008) The interferon-induced protein BST-2 restricts HIV-1 release and is downregulated from the cell surface by the viral Vpu protein. Cell Host Microbe 3: 245-252.

4. Kupzig S, Korolchuk V, Rollason R, Sugden A, Wilde A, et al. (2003) Bst-2/HM1.24 is a raft-associated apical membrane protein with an unusual topology. Traffic 4: 694-709.

5. Rollason R, Korolchuk V, Hamilton C, Schu P, Banting G (2007) Clathrin-mediated endocytosis of a lipid-raft-associated protein is mediated through a dual tyrosine motif. J Cell Sci 120: 3850-3858.

6. Neil SJ, Eastman SW, Jouvenet N, Bieniasz PD (2006) HIV-1 Vpu promotes release and prevents endocytosis of nascent retrovirus particles from the plasma membrane. PLoS Pathog 2: e39.

7. Jouvenet N, Neil SJ, Zhadina M, Zang T, Kratovac Z, et al. (2009) Broad-spectrum inhibition of retroviral and filoviral particle release by tetherin. J Virol 83: 1837-1844.

8. Sakuma T, Noda T, Urata S, Kawaoka Y, Yasuda J (2009) Inhibition of Lassa and Marburg virus production by tetherin. J Virol 83: 2382-2385.

9. Kaletsky RL, Francica JR, Agrawal-Gamse C, Bates P (2009) Tetherin-mediated restriction of filovirus budding is antagonized by the Ebola glycoprotein. Proc Natl Acad Sci U S A 106: 2886-2891.

10. Mansouri M, Viswanathan K, Douglas JL, Hines J, Gustin J, et al. (2009) Molecular mechanism of BST2/tetherin downregulation by K5/MIR2 of Kaposi's sarcoma-associated herpesvirus. J Virol 83: 9672-9681.

11. Perez-Caballero D, Zang T, Ebrahimi A, McNatt MW, Gregory DA, et al. (2009) Tetherin inhibits HIV-1 release by directly tethering virions to cells. Cell 139: 499-511.

12. Mitchell RS, Katsura C, Skasko MA, Fitzpatrick K, Lau D, et al. (2009) Vpu antagonizes BST-2-mediated restriction of HIV-1 release via beta-TrCP and endo-lysosomal trafficking. PLoS Pathog 5: e1000450.

13. Blasius AL, Giurisato E, Cella M, Schreiber RD, Shaw AS, et al. (2006) Bone marrow stromal cell antigen 2 is a specific marker of type I IFN-producing cells in the naive mouse, but a promiscuous cell surface antigen following IFN stimulation. J Immunol 177: 3260-3265.

14. Ishikawa J, Kaisho T, Tomizawa H, Lee BO, Kobune Y, et al. (1995) Molecular cloning and chromosomal mapping of a bone marrow stromal cell surface gene, BST2, that may be involved in pre-B-cell growth. Genomics 26: 527-534.

15. Vidal-Laliena M, Romero X, March S, Requena V, Petriz J, et al. (2005) Characterization of antibodies submitted to the B cell section of the 8th Human Leukocyte Differentiation Antigens Workshop by flow cytometry and immunohistochemistry. Cell Immunol 236: 6-16.

16. Cao W, Bover L, Cho M, Wen X, Hanabuchi S, et al. (2009) Regulation of TLR7/9 responses in plasmacytoid dendritic cells by BST2 and ILT7 receptor interaction. J Exp Med 206: 1603-1614.

17. Neil SJ, Sandrin V, Sundquist WI, Bieniasz PD (2007) An interferon-alpha-induced tethering mechanism inhibits HIV-1 and Ebola virus particle release but is counteracted by the HIV-1 Vpu protein. Cell Host Microbe 2: 193-203.

18. Jia B, Serra-Moreno R, Neidermyer W, Rahmberg A, Mackey J, et al. (2009) Species-specific activity of SIV Nef and HIV-1 Vpu in overcoming restriction by tetherin/BST2. PLoS Pathog 5: e1000429.

19. Zhang F, Wilson SJ, Landford WC, Virgen B, Gregory D, et al. (2009) Nef proteins from simian immunodeficiency viruses are tetherin antagonists. Cell Host Microbe 6: 54-67.

20. Douglas JL, Viswanathan K, McCarroll MN, Gustin JK, Fruh K, et al. (2009) Vpu directs the degradation of the human immunodeficiency virus restriction factor BST-2/Tetherin via a {beta}TrCP-dependent mechanism. J Virol 83: 7931-7947.

21. Le Tortorec A, Neil SJ (2009) Antagonism to and intracellular sequestration of human tetherin by the human immunodeficiency virus type 2 envelope glycoprotein. J Virol 83: 11966-11978.

22. Gupta RK, Mlcochova P, Pelchen-Matthews A, Petit SJ, Mattiuzzo G, et al. (2009) Simian immunodeficiency virus envelope glycoprotein counteracts tetherin/BST-2/CD317 by intracellular sequestration. Proc Natl Acad Sci U S A. 106: 20889-20894

23. Malim MH, Emerman M (2008) HIV-1 accessory proteins--ensuring viral survival in a hostile environment. Cell Host Microbe 3: 388-398.

24. Schubert U, Anton LC, Bacik I, Cox JH, Bour S, et al. (1998) CD4 glycoprotein degradation induced by human immunodeficiency virus type 1 Vpu protein requires the function of proteasomes and the ubiquitin-conjugating pathway. J Virol 72: 2280-2288.

25. Binette J, Dube M, Mercier J, Cohen EA (2007) Requirements for the selective degradation of CD4 receptor molecules by the human immunodeficiency virus type 1 Vpu protein in the endoplasmic reticulum. Retrovirology 4: 75.

26. Bour S, Schubert U, Strebel K (1995) The human immunodeficiency virus type 1 Vpu protein specifically binds to the cytoplasmic domain of CD4: implications for the mechanism of degradation. J Virol 69: 1510-1520.

27. Margottin F, Bour SP, Durand H, Selig L, Benichou S, et al. (1998) A novel human WD protein, h-beta TrCp, that interacts with HIV-1 Vpu connects CD4 to the ER degradation pathway through an F-box motif. Mol Cell 1: 565-574.

28. Varthakavi V, Smith RM, Bour SP, Strebel K, Spearman P (2003) Viral protein U counteracts a human host cell restriction that inhibits HIV-1 particle production. Proc Natl Acad Sci U S A 100: 15154-15159.

29. McNatt MW, Zang T, Hatziioannou T, Bartlett M, Fofana IB, et al. (2009) Species-specific activity of HIV-1 Vpu and positive selection of tetherin transmembrane domain variants. PLoS Pathog 5: e1000300.

30. Goffinet C, Allespach I, Homann S, Tervo HM, Habermann A, et al. (2009) HIV-1 antagonism of CD317 is species specific and involves Vpu-mediated proteasomal degradation of the restriction factor. Cell Host Microbe 5: 285-297.

31. Gupta RK, Hue S, Schaller T, Verschoor E, Pillay D, et al. (2009) Mutation of a single residue renders human tetherin resistant to HIV-1 Vpu-mediated depletion. PLoS Pathog 5: e1000443.

32. Rong L, Zhang J, Lu J, Pan Q, Lorgeoux RP, et al. (2009) The transmembrane domain of BST-2 determines its sensitivity to down-modulation by human immunodeficiency virus type 1 Vpu. J Virol 83: 7536-7546.

33. Miyagi E, Andrew AJ, Kao S, Strebel K (2009) Vpu enhances HIV-1 virus release in the absence of Bst-2 cell surface down-modulation and intracellular depletion. Proc Natl Acad Sci U S A 106: 2868-2873.

34. Mangeat B, Gers-Huber G, Lehmann M, Zufferey M, Luban J, et al. (2009) HIV-1 Vpu neutralizes the antiviral factor Tetherin/BST-2 by binding it and directing its beta-TrCP2-dependent degradation. PLoS Pathog 5: e1000574.

35. Iwabu Y, Fujita H, Kinomoto M, Kaneko K, Ishizaka Y, et al. (2009) HIV-1 accessory protein Vpu internalizes cell-surface BST-2/tetherin through transmembrane interactions leading to lysosomes. J Biol Chem 284: 35060-35072.

36. Andrew AJ, Miyagi E, Kao S, Strebel K (2009) The formation of cysteine-linked dimers of BST-2/tetherin is important for inhibition of HIV-1 virus release but not for sensitivity to Vpu. Retrovirology 6: 80.

37. Schubert U, Clouse KA, Strebel K (1995) Augmentation of virus secretion by the human immunodeficiency virus type 1 Vpu protein is cell type independent and occurs in cultured human primary macrophages and lymphocytes. J Virol 69: 7699-7711.

38. Schubert U, Strebel K (1994) Differential activities of the human immunodeficiency virus type 1-encoded Vpu protein are regulated by phosphorylation and occur in different cellular compartments. J Virol 68: 2260-2271.

39. Wang LH, Rothberg KG, Anderson RG (1993) Mis-assembly of clathrin lattices on endosomes reveals a regulatory switch for coated pit formation. J Cell Biol 123: 1107-1117.

40. Dube M, Roy BB, Guiot-Guillain P, Mercier J, Binette J, et al. (2009) Suppression of Tetherin-restricting activity upon human immunodeficiency virus type 1 particle release correlates with localization of Vpu in the trans-Golgi network. J Virol 83: 4574-4590.

41. Grigg ME, McMahon CW, Morkowski S, Rudensky AY, Pullen AM (1998) Mtv-1 superantigen trafficks independently of major histocompatibility complex class II directly to the B-cell surface by the exocytic pathway. J Virol 72: 2577-2588.

42. Schubert U, Bour S, Ferrer-Montiel AV, Montal M, Maldarell F, et al. (1996) The two biological activities of human immunodeficiency virus type 1 Vpu protein involve two separable structural domains. J Virol 70: 809-819.

43. Tiganos E, Friborg J, Allain B, Daniel NG, Yao XJ, et al. (1998) Structural and functional analysis of the membrane-spanning domain of the human immunodeficiency virus type 1 Vpu protein. Virology 251: 96-107.

44. Friborg J, Ladha A, Gottlinger H, Haseltine WA, Cohen EA (1995) Functional analysis of the phosphorylation sites on the human immunodeficiency virus type 1 Vpu protein. J Acquir Immune Defic Syndr Hum Retrovirol 8: 10-22.

45. Willey RL, Maldarelli F, Martin MA, Strebel K (1992) Human immunodeficiency virus type 1 Vpu protein induces rapid degradation of CD4. J Virol 66: 7193-7200.

46. Harila K, Salminen A, Prior I, Hinkula J, Suomalainen M (2007) The Vpu-regulated endocytosis of HIV-1 Gag is clathrin-independent. Virology 369: 299-308.

47. Vincent MJ, Abdul Jabbar M (1995) The human immunodeficiency virus type 1 Vpu protein: a potential regulator of proteolysis and protein transport in the mammalian secretory pathway. Virology 213: 639-649.

48. Varthakavi V, Smith RM, Martin KL, Derdowski A, Lapierre LA, et al. (2006) The pericentriolar recycling endosome plays a key role in Vpu-mediated enhancement of HIV-1 particle release. Traffic 7: 298-307.

49. Schwartz S, Felber BK, Fenyo EM, Pavlakis GN (1990) Env and Vpu proteins of human immunodeficiency virus type 1 are produced from multiple bicistronic mRNAs. J Virol 64: 5448-5456.

50. de Silva TI, Cotten M, Rowland-Jones SL (2008) HIV-2: the forgotten AIDS virus. Trends Microbiol 16: 588-595.

51. Chesebro B, Wehrly K (1988) Development of a sensitive quantitative focal assay for human immunodeficiency virus infectivity. J Virol 62: 3779-3788.

52. Pincus SH, Wehrly K, Chesebro B (1989) Treatment of HIV tissue culture infection with monoclonal antibody-ricin A chain conjugates. J Immunol 142: 3070-3075.

53. Terwilliger EF, Cohen EA, Lu YC, Sodroski JG, Haseltine WA (1989) Functional role of human immunodeficiency virus type 1 vpu. Proc Natl Acad Sci U S A 86: 5163-5167.

54. Yao XJ, Mouland AJ, Subbramanian RA, Forget J, Rougeau N, et al. (1998) Vpr stimulates viral expression and induces cell killing in human immunodeficiency virus type 1-infected dividing Jurkat T cells. J Virol 72: 4686-4693.

Figure 1: Enhancement of viral particle release in absence of Vpu-dependent reduction of Tetherin steady-state levels.

HEK 293T cells were co-transfected with a fixed amount of the HA-Tetherin-expressing plasmid (235 ng) and the indicated amounts of HxBH10 proviral constructs. Forty-eight hours post-transfection, cells and virus-containing supernatants were harvested and processed for western blot analysis. (A) Proteins in the viral and cell lysates were detected using specific Abs. (B) Quantification of HIV-1 release efficiency. Bands corresponding to Gag products in cells and viral particles in panel (A), as detected using anti-p24 Abs, were scanned by laser densitometry. The virus particle release efficiency was determined as described in the Materials and Methods and calculated as a percentage of the release of HxBH10-*vpu*+ (100%) in absence of HA-Tetherin. The values within the graph represent the fold increase of virus particle release upon Vpu expression.

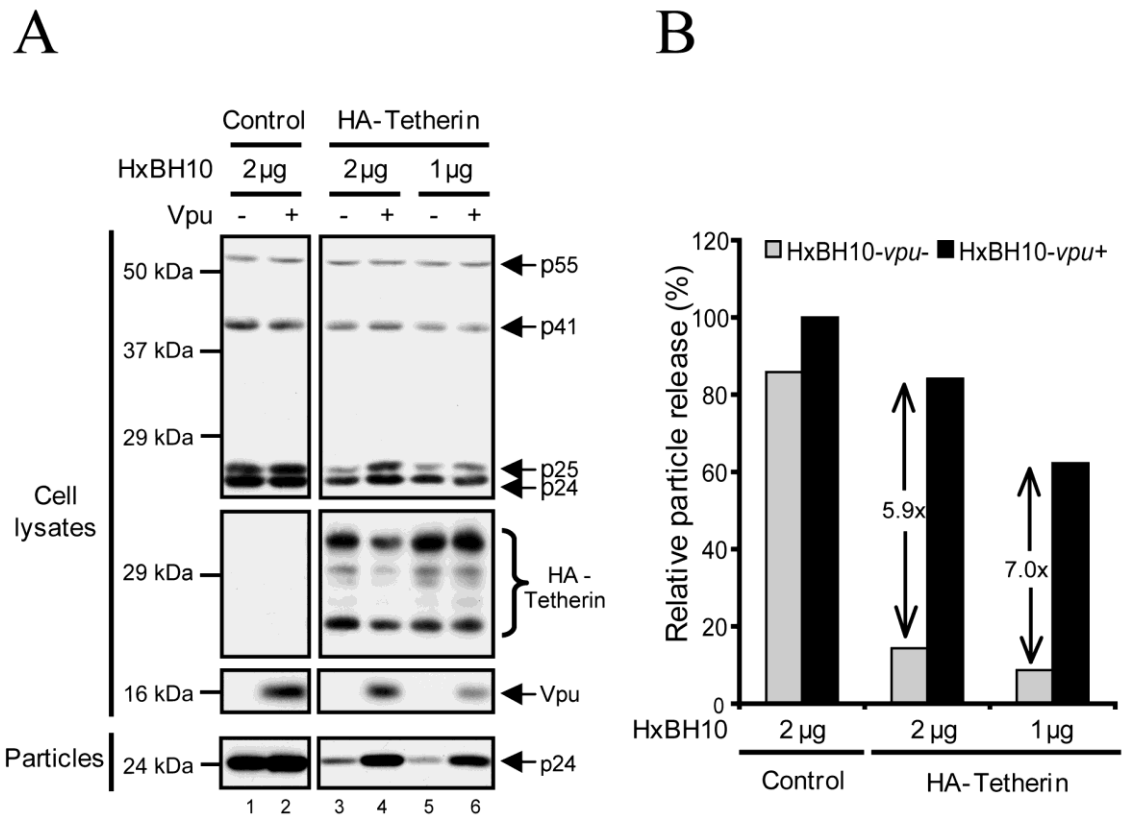
A
Control
HA-Tetherin
HxBH10
2 µg
2 µg
1 µg
Vpu
- + - + - +
50 kDa
37 kDa
29 kDa
p55
p41
p25
p24
Cell lysates
29 kDa
HA - Tetherin
16 kDa
Vpu
Particles
24 kDa
p24
1 2 3 4 5 6
B
HxBH10-vpu-
HxBH10-vpu+
Relative particle release (%)
120
100
80
60
40
20
0
5.9x
7.0x
HxBH10
2 µg
2 µg
1 µg
Control
HA-Tetherin

Figure 2: Analysis of the turnover of endogenous and exogenously-expressed Tetherin in the presence of Vpu.

(A-C) Turnover of exogenously-expressed Tetherin. (A) HEK 293T cells were co-transfected with the indicated HxBH10 proviral constructs and the pcDNA-Tetherin plasmid. Forty-eight hours post-transfection, cells were pulse-labeled and chased for the indicated time intervals. Tetherin and Vpu were immunoprecipitated with specific Abs, and analyzed by autoradiography. The asterisk indicates the presence of a non-specific signal. (B) Quantitation of (A). The graph represents the percentage of Tetherin recovered relative to time 0. The signal intensity of all Tetherin-specific bands was determined for each time point by densitometric scanning. The percentage of Tetherin recovered was calculated as the ratio of the Tetherin bands signal at a given time relative to the signal at time 0. Error bars indicate the standard deviation of the mean from 2 independent experiments. (C) Virus-containing supernatant and a fraction of the cells from (A) were collected prior to labeling. Gag proteins from the cell and viral lysates were analyzed by western blot using anti-p24 Abs. (D-E) Turnover of endogenous Tetherin. (D) HeLa cells were infected with the indicated VSV-G-pseudotyped HxBH10 virus. Forty-eight hours post-infection, cells were pulse-labeled and chased for the indicated time intervals. Tetherin was immunoprecipitated with specific Abs, and analyzed by autoradiography. Vpu and actin were detected by western blot from cell lysates harvested prior to labeling. (E) Quantitation of (D) as described in (B). Full black line: HxBH10-*vpu+;* Dashed line: HxBH10-*vpu-;* Full grey line: HxBH10-*vpu S52D,S56D*.

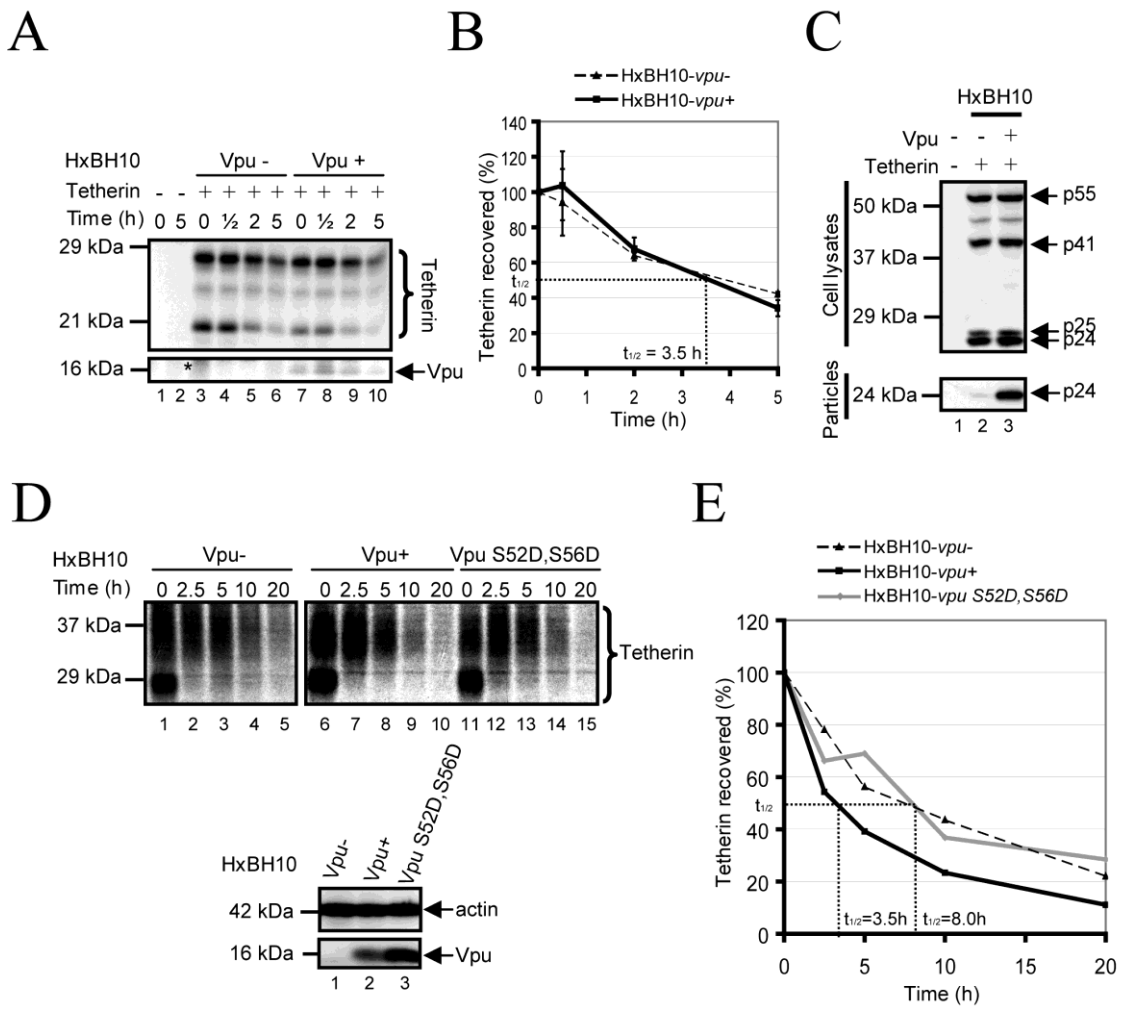
A
HxBH10
Vpu -
Vpu +
Tetherin
Time (h)
0 5 0 ½ 2 5 0 ½ 2 5
29 kDa
21 kDa
16 kDa
Tetherin
Vpu
1 2 3 4 5 6 7 8 9 10
B
HxBH10-vpu-
HxBH10-vpu+
Tetherin recovered (%)
t1/2
t1/2 = 3.5 h
Time (h)
C
HxBH10
Vpu - - +
Tetherin - + +
Cell lysates
50 kDa
37 kDa
29 kDa
p55
p41
p25
p24
Particles
24 kDa
p24
1 2 3
D
HxBH10
Vpu-
Vpu+
Vpu S52D,S56D
Time (h)
0 2.5 5 10 20 0 2.5 5 10 20 0 2.5 5 10 20
37 kDa
29 kDa
Tetherin
1 2 3 4 5 6 7 8 9 10 11 12 13 14 15
HxBH10
Vpu-
Vpu+
Vpu S52D,S56D
42 kDa
actin
16 kDa
Vpu
1 2 3
E
HxBH10-vpu-
HxBH10-vpu+
HxBH10-vpu S52D,S56D
Tetherin recovered (%)
t1/2
t1/2=3.5h
t1/2=8.0h
Time (h)

Figure 3: Mutation of Tetherin dual Tyrosine-based sorting motif does not affect sensitivity to Vpu

(A) Schematic representation of HA-Tetherin wt and HA-Tetherin Y6Y8. The overlapping Tyr-based motifs are presented in the grey box. X and Φ correspond to variable and hydrophobic amino-acid residues, respectively. Hyphens represent unchanged amino-acids. The site that is cleaved prior to addition of the GPI lipid anchor is represented by the dashed line. Glycosylation sites are represented at position 65 and 92. (B) Kinetics of HA-Tetherin Y6Y8 internalization. HEK 293T cells were co-transfected with the indicated HxBH10 constructs and a GFP-expressing plasmid. Forty-eight hours post-transfection, cell-surface Tetherin was labeled with Tetherin specific Abs at 4°C before incubating cells at 37°C for the indicated time intervals to allow endocytosis. Cells were then incubated at 4°C in presence of appropriate secondary Abs. The graph depicts the relative levels of Tetherin at the surface of GFP-expressing cells (time 0 = 100%) and represents the loss of Tetherin-specific signal following endocytosis. (C) Cell-surface expression of HA-Tetherin Y6Y8. HEK 293T cells were co-transfected with the indicated HA-Tetherin plasmid and HxBH10 proviral constructs in presence of a GFP-expressing plasmid. Cell-surface Tetherin expression was analyzed on GFP-positive cells by flow cytometry 48h post-transfection. Geo mean values (depicted as MFI) are shown. Full lines: HxBH10-*vpu*+; dashed lines: HxBH10-*vpu*-; filled histogram: pre-immune control. The results are representative of two independent experiments. (D) Effect of HA-Tetherin Y6Y8 on HIV-1 particle release. HEK 293T cells were co-transfected with the indicated HxBH10 proviral constructs and HA-Tetherin-expressing plasmids. Forty-eight hours post-transfection, transfected cells

and virus-containing supernatants were harvested. Proteins from cell and viral lysates were analyzed by western blot using specific Abs. (E) Quantitation of HIV-1 particle release. Bands corresponding to Gag products in cells and viral particles were scanned by laser densitometry. The virus particle release efficiency was determined as described in the Materials and Methods and calculated as a percentage of the release of HxBH10-*vpu*+ (100%) in absence of HA-Tetherin. Error bars indicate the standard deviation of the mean from two independent experiments

.

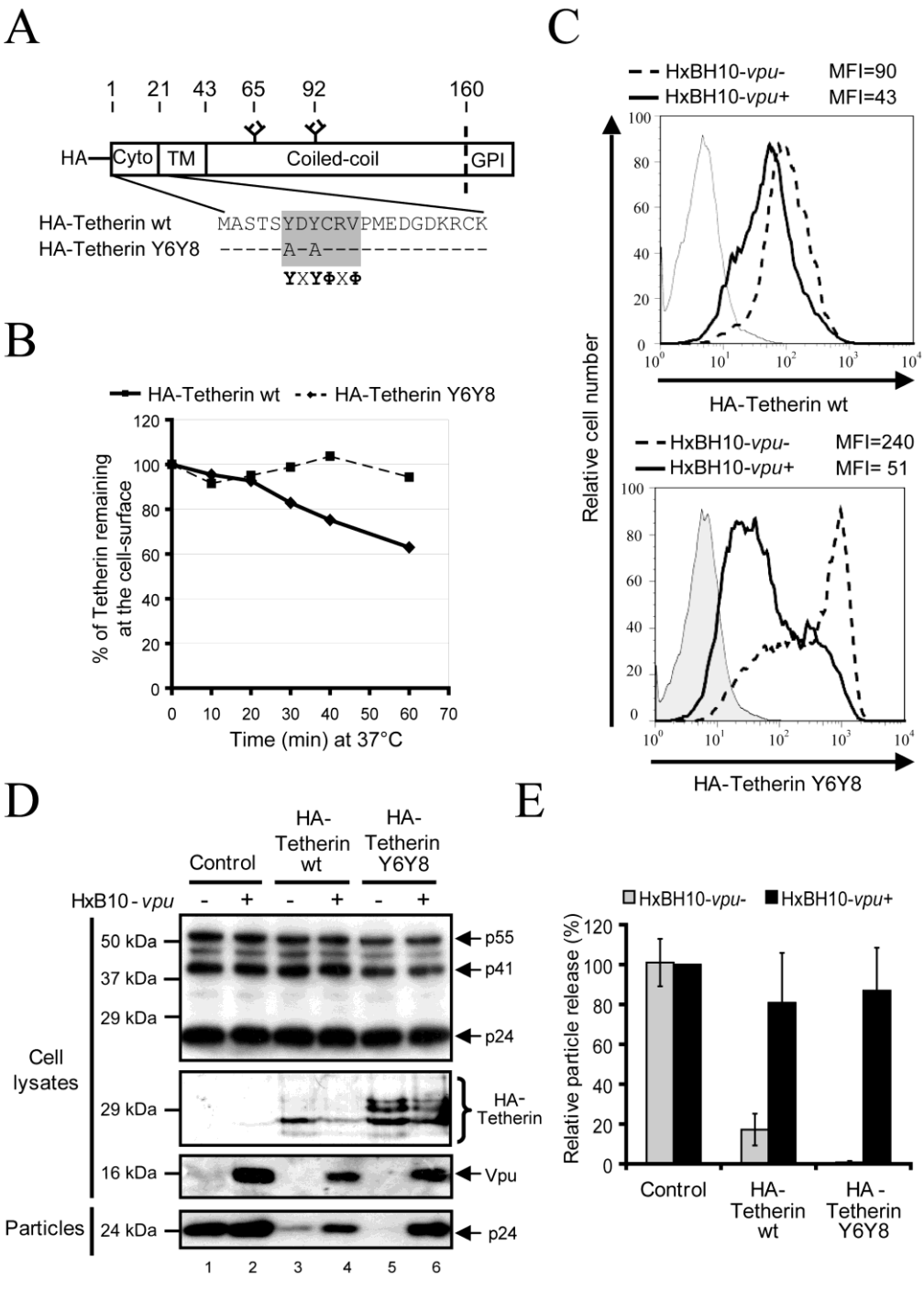
A
1 21 43 65 92 160
HA
Cyto
TM
Coiled-coil
GPI
HA-Tetherin wt MASTSYDYCRVPMEDGDKRCK
HA-Tetherin Y6Y8 -----A-A----------
YXYΦXΦ
B
HA-Tetherin wt
HA-Tetherin Y6Y8
% of Tetherin remaining at the cell-surface
Time (min) at 37°C
C
HxBH10-vpu- MFI=90
HxBH10-vpu+ MFI=43
HA-Tetherin wt
HxBH10-vpu- MFI=240
HxBH10-vpu+ MFI= 51
HA-Tetherin Y6Y8
Relative cell number
D
Control
HA-Tetherin wt
HA-Tetherin Y6Y8
HxB10 - vpu
Cell lysates
Particles
50 kDa
37 kDa
29 kDa
16 kDa
24 kDa
p55
p41
p24
HA-Tetherin
Vpu
1 2 3 4 5 6
E
HxBH10-vpu-
HxBH10-vpu+
Relative particle release (%)
Control
HA-Tetherin wt
HA - Tetherin Y6Y8

Figure 4: Vpu antagonizes Tetherin without promoting its endocytosis.

HeLa cells were co-transfected with the indicated HxBH10 constructs and a GFP-expressing plasmid. Forty-eight hours post-transfection, cell-surface Tetherin was labeled with Tetherin specific Abs at 4°C before incubating cells at 37°C for the indicated time intervals to allow endocytosis. Cells were then incubated at 4°C in presence of the appropriate secondary Abs. The graph depicts the relative levels of Tetherin at the surface of GFP-expressing cells (time 0 = 100%) and represents the loss of Tetherin-specific signal resulting from endocytosis. Error bars indicate the standard deviation of the mean from two independent experiments.

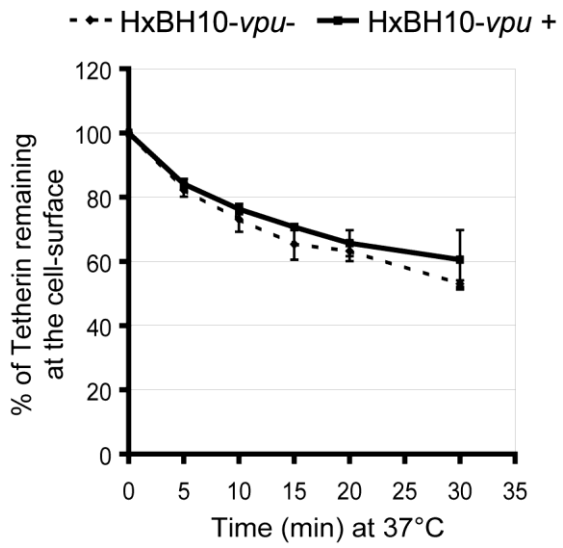
HxBH10-vpu-
HxBH10-vpu +
% of Tetherin remaining at the cell-surface
120
100
80
60
40
20
0
0
5
10
15
20
25
30
35
Time (min) at 37°C

Figure 5: Vpu affects Tetherin trafficking to the cell surface.

(A-B) HeLa cells were transfected with the indicated HxBH10 proviral constructs and a GFP-expressing plasmid. Forty-eight hours post-transfection, cells were harvested and treated with pronase (0.05%). After quenching of the proteolytic reaction, cells were cultured at 37ºC for different time intervals and then immunostained for cell-surface Tetherin. (A) Dot plots representing cell-surface Tetherin levels relative to GFP expression. MFI values are presented for each gate. Treatment with BFA (10 μM) served as a positive control for intracellular retention. BFA was added to the media immediately after treatment with pronase and kept throughout the chase period. (B) Quantitative representation of panel (A). Kinetics of Tetherin re-expression were determined by calculating the percentage of Tetherin expression (MFI) at the surface of pronase-treated cells relative to the corresponding untreated GFP-negative control at different time intervals. Equations pertaining to each linear equation are shown above the graph. Error bars represent the standard deviation of at least two separate experiments. Black dashed line: HxBH10-*vpu*+/GFP-; Black full line: HxBH10-*vpu*-/GFP+; Red full line: HxBH10-*vpu*+/GFP+; Blue full line: HxBH10-*vpu S52D,S56D/*GFP+. Similar results were obtained when the proportion of cells expressing Tetherin at the cell-surface was used as a read-out instead of Tetherin MFI. For these latter analyses, the cut-off was arbitrarily set on the pronase-treated HxBH10-*vpu*+/GFP+ time 0 sample (illustrated by the dotted line in Figure 5A) so that the background level of Tetherin-positive cells corresponded to 1%.

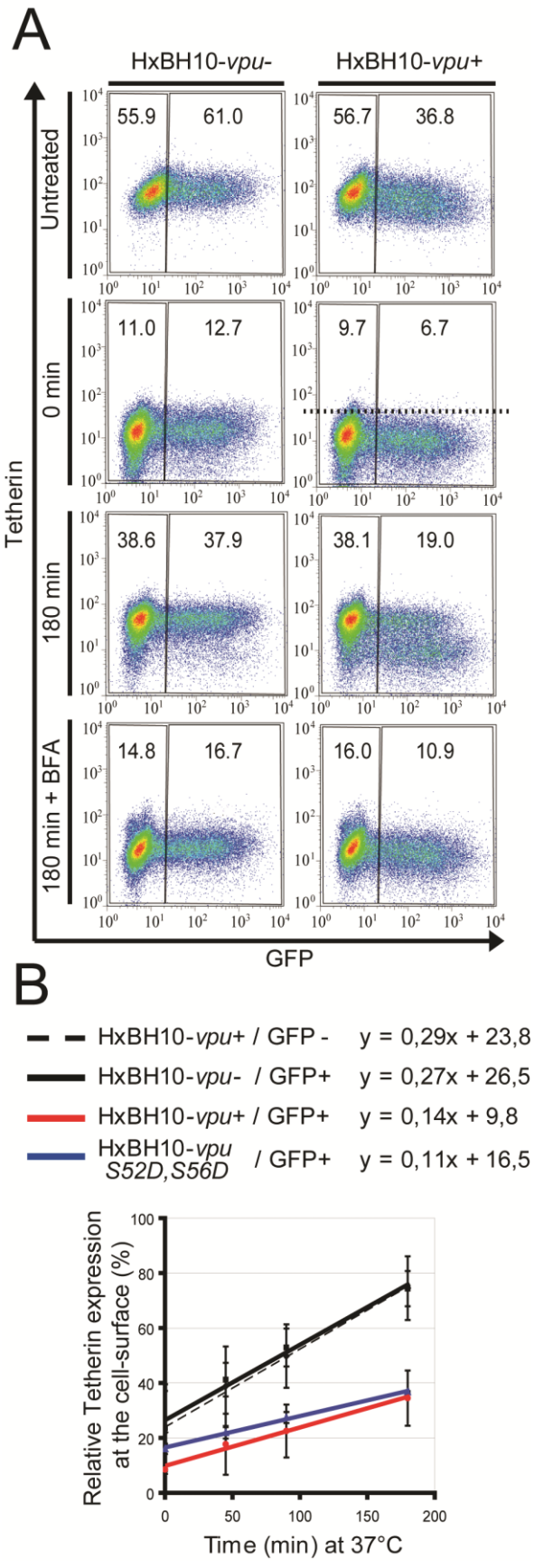
A
HxBH10-vpu-
HxBH10-vpu+
Untreated
0 min
180 min
180 min + BFA
Tetherin
GFP
55.9
61.0
56.7
36.8
11.0
12.7
9.7
6.7
38.6
37.9
38.1
19.0
14.8
16.7
16.0
10.9
B
HxBH10-vpu+ / GFP - y = 0,29x + 23,8
HxBH10-vpu- / GFP+ y = 0,27x + 26,5
HxBH10-vpu+ / GFP+ y = 0,14x + 9,8
HxBH10-vpu S52D,S56D / GFP+ y = 0,11x + 16,5
Relative Tetherin expression at the cell-surface (%)
Time (min) at 37°C

Figure 6: Vpu expression causes a re-localization of the cellular pool of Tetherin in a perinuclear compartment.

HeLa cells were infected with VSV-G pseudotyped HxBH10-*vpu*-, HxBH10-*vpu*+ or HxBH10-*vpu S52D,S56D* virus. Forty-eight hours post-infection, cells were immunostained for cell-surface Tetherin, fixed, permeabilized and co-stained with anti-Tetherin (red), anti-Vpu (green) and anti-TGN46 (blue) specific Abs. Nuclei were counterstained with DAPI (cyan). Cells were observed by confocal microscopy. The white scale bar represents a distance of 10 μm. (B) Quantitation of the absolute Tetherin signal in the TGN was determined by measuring the specific Tetherin signal in the region delineated by the TGN46 marker on digital picture produced using similar acquisition time. Error bars indicate the standard deviation of the mean from the quantitative analysis of at least 25 distinct cells per conditions.

A

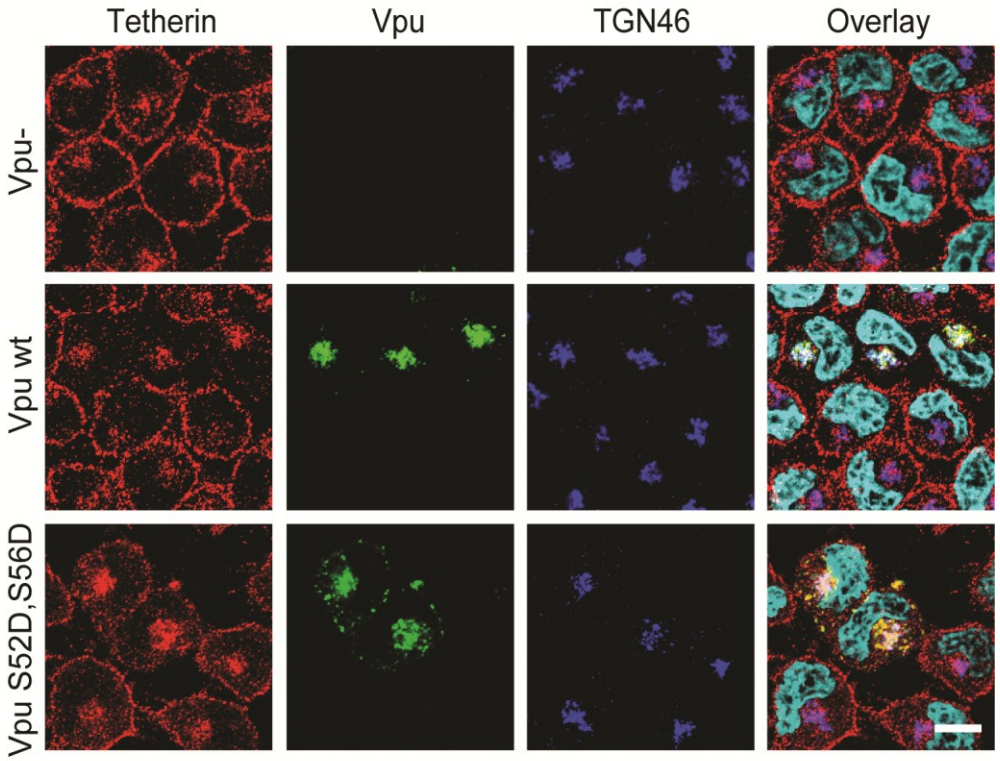
Tetherin
Vpu
TGN46
Overlay
Vpu-
Vpu wt
Vpu S52D,S56D

B

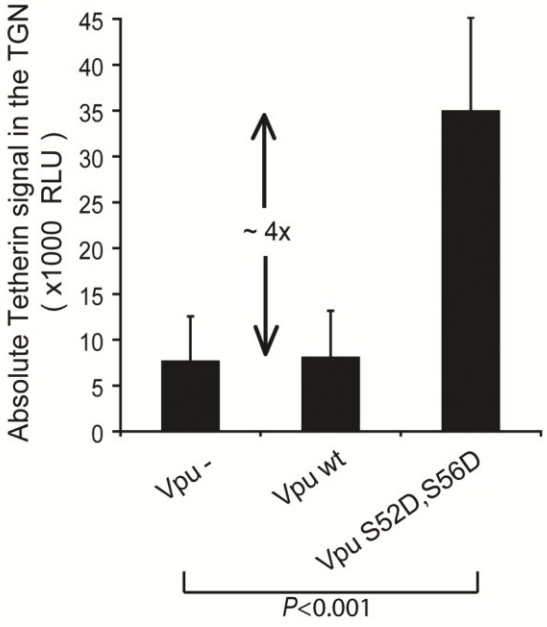
Absolute Tetherin signal in the TGN
(x1000 RLU)
45
40
35
30
25
20
15
10
5
0
~ 4x
Vpu -
Vpu wt
Vpu S52D,S56D
P<0.001

Figure 7: Association of Vpu and Tetherin involves their transmembrane anchor domains.

(A) Schematic representation of WT Vpu, Vpu KSL and Vpu RD. The TM domain is represented by the unfilled box while the cytosolic domain with the two predicted □□helices (H-1 and H-2) is indicated by the filled box. Phosphorylation sites are represented by the small circles. The amino-acid sequence of the TM anchor region is represented below. Hyphens represent identical amino-acids. (B-E) Co-immunoprecipitation experiments of Tetherin and Vpu. (B) HEK 293T cells were transfected with a HA-human Tetherin-expressing plasmid and the indicated HxBH10-derived proviral constructs. Forty-eight hours post-transfection, cells were lysed and proteins were co-immunoprecipitated using anti-Tetherin Abs. Co-immunoprecipitated proteins were analyzed by western blot using anti-Tetherin and anti-Vpu Abs. (C-E) HEK 293T cells were transfected with the indicated HA-Tetherin-expressing plasmids and the specified HxBH10 proviral constructs. Forty-eight hours post-transfection, cells were lysed and proteins were co-immunoprecipitated and analyzed as described above. In (D), HA-Tetherin proteins were revealed by western blot using anti-HA Abs. Amounts of protein in the lysate prior to immunoprecipitation (input) is shown in the left panels. Non-specific bands, depicted by the asterisks, were used as loading controls.

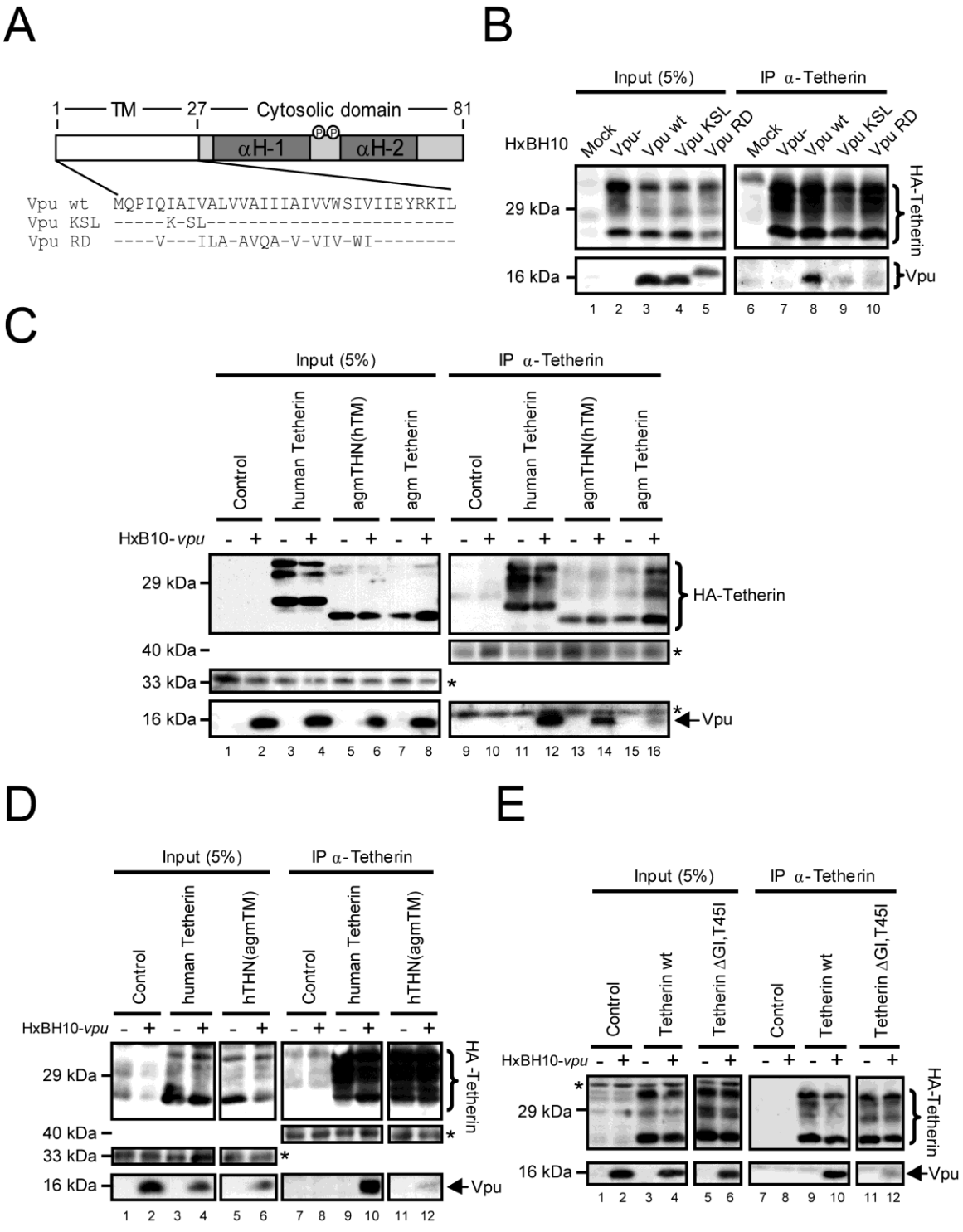
A
1
TM
27
Cytosolic domain
81
αH-1
αH-2
Vpu wt MQPIQIAIVALVVAIIIAIVVWSIVIIEYRKIL
Vpu KSL -----K-SL-------------------------
Vpu RD ----V---ILA-AVQA-V-VIV-WI--------
B
Input (5%)
IP α-Tetherin
HxBH10
Mock
Vpu-
Vpu wt
Vpu KSL
Vpu RD
29 kDa
16 kDa
HA-Tetherin
Vpu
1 2 3 4 5 6 7 8 9 10
C
Input (5%)
IP α-Tetherin
Control
human Tetherin
agmTHN(hTM)
agm Tetherin
HxB10-vpu
29 kDa
40 kDa
33 kDa
16 kDa
HA-Tetherin
Vpu
1 2 3 4 5 6 7 8 9 10 11 12 13 14 15 16
D
Input (5%)
IP α-Tetherin
Control
human Tetherin
hTHN(agmTM)
HxBH10-vpu
29 kDa
40 kDa
33 kDa
16 kDa
HA-Tetherin
Vpu
1 2 3 4 5 6 7 8 9 10 11 12
E
Input (5%)
IP α-Tetherin
Control
Tetherin wt
Tetherin ΔGI,T45I
HxBH10-vpu
29 kDa
16 kDa
HA-Tetherin
Vpu
1 2 3 4 5 6 7 8 9 10 11 12

Figure 8: Association of Vpu to Tetherin is required to antagonize the antiviral activity of the restriction factor.

(A) Association of Vpu with endogenous Tetherin. HeLa cells were transfected with the indicated HxBH10 proviral constructs. Forty-eight hours post-transfection, cells were lysed and proteins were co-immunoprecipitated using anti-Tetherin Abs. Co-immunoprecipitated proteins were analyzed by western blot using anti-Tetherin, anti-Vpu and anti-Env Abs. The amount of proteins in the lysate prior to immunoprecipitation (input) is shown in the left panel. Non-specific bands, depicted by the asterisks, were used as loading controls. (B) Cell-surface expression of Tetherin. HeLa cells were transfected with the indicated HxBH10 proviral constructs and a GFP-expressing plasmid. Cell-surface Tetherin expression was analyzed on GFP-positive cells by flow cytometry, 48h post-transfection. MFI values are shown beside the histogram. Filled histogram: pre-immune control; dashed line: HxBH10-*vpu*-; full line: HxBH10-*vpu*+; dotted line: HxBH10-*vpu KSL*. (C) Effect of Vpu on HIV-1 particle release. Cells and virus-containing supernatants were collected from the experiment described in (A), lysed and analyzed for the detection of Gag-related products by western blot using specific Abs. (D) Quantitation of virus particle release. Bands corresponding to Gag products in cells and virus particles were scanned by laser densitometry. The virus particle release efficiency was determined as described in the Materials and Methods and calculated as a percentage of the HxBH10-*vpu*+ virus release (100%). The error bars represent the standard deviation from the mean of three independent experiments.

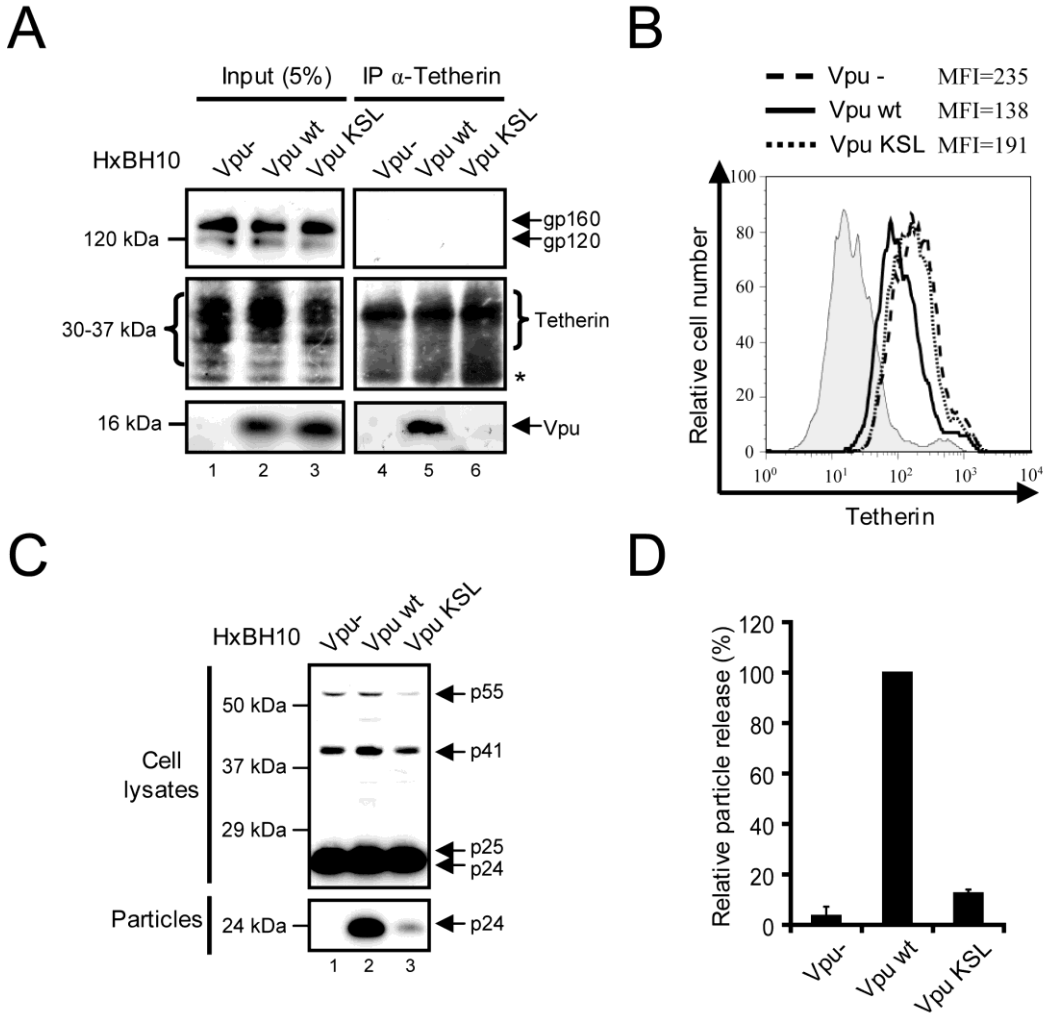
A
Input (5%)
IP α-Tetherin
HxBH10
Vpu-
Vpu wt
Vpu KSL
120 kDa
gp160
gp120
30-37 kDa
Tetherin
*
16 kDa
Vpu
1 2 3 4 5 6
B
Vpu - MFI=235
Vpu wt MFI=138
Vpu KSL MFI=191
Relative cell number
Tetherin
C
HxBH10
Cell lysates
50 kDa
37 kDa
29 kDa
p55
p41
p25
p24
Particles
24 kDa
p24
1 2 3
D
Relative particle release (%)
Vpu-
Vpu wt
Vpu KSL

Figure 9: Re-localization of Tetherin in the TGN requires the association of Vpu to the restriction factor.

HeLa cells were infected with the indicated VSV-G pseudotyped HxBH10-derived virus. Forty-eight hours post-infection, cells were immunostained for cell-surface Tetherin, fixed, permeabilized and co-stained with anti-Tetherin (red), anti-Vpu (green) and anti-TGN46 (blue) specific Abs. Nuclei were counterstained with DAPI (cyan). Cells were observed by confocal microscopy. The white bar represents a distance of 10 μm.

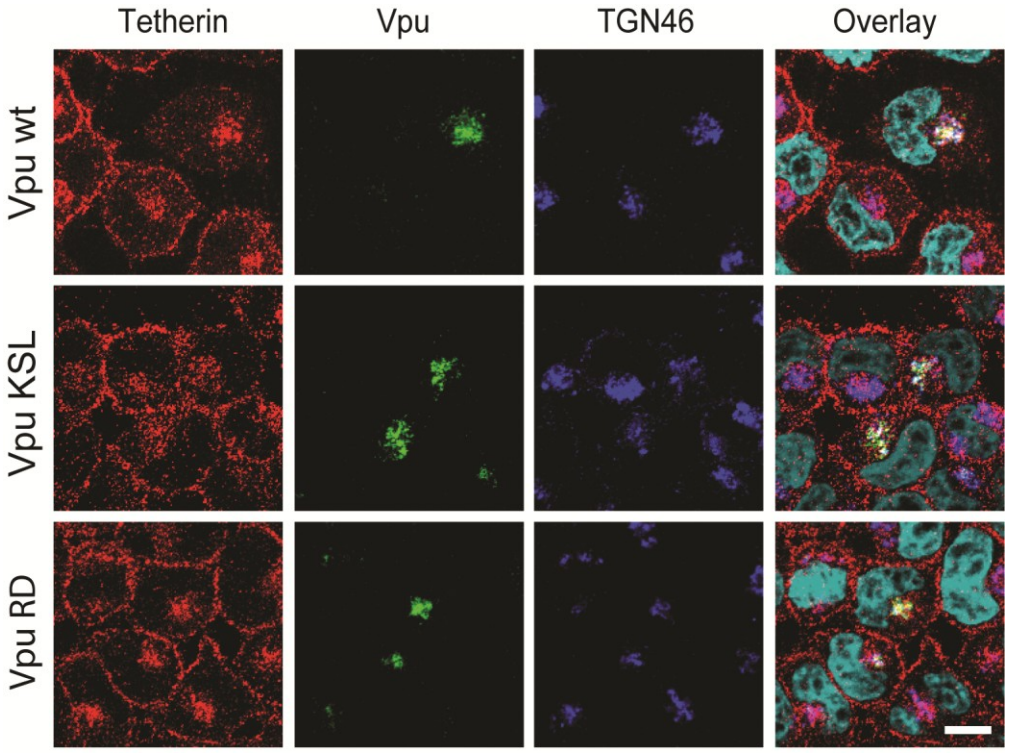
Tetherin
Vpu
TGN46
Overlay
Vpu wt
Vpu KSL
Vpu RD

Figure 10. Model of Vpu-mediated down-regulation of Tetherin from the cell-surface.

In absence of Vpu, Tetherin traffics along the secretory pathway and reaches the plasma membrane. The protein is endocytosed, transported to the TGN and is then recycled back to the cell-surface. In presence of Vpu, Tetherin is forming complexes with the viral protein in the membrane of the ER. Recruitment of $SCF^{\beta\text{-}TrCP}$ by Vpu leads to ubiquitination and proteosomal degradation of a fraction of Tetherin. Tetherin escaping degradation exits the ER. In the membrane of the TGN, Vpu binds endocytosed Tetherin and/or Tetherin arriving from the ER and causes the sequestration of the restriction factor. Subsequently, Vpu induces Tetherin ubiquitination through the recruitment of $SCF^{\beta\text{-}TrCP}$, targeting the ubiquitinated protein to lysosomal degradation.

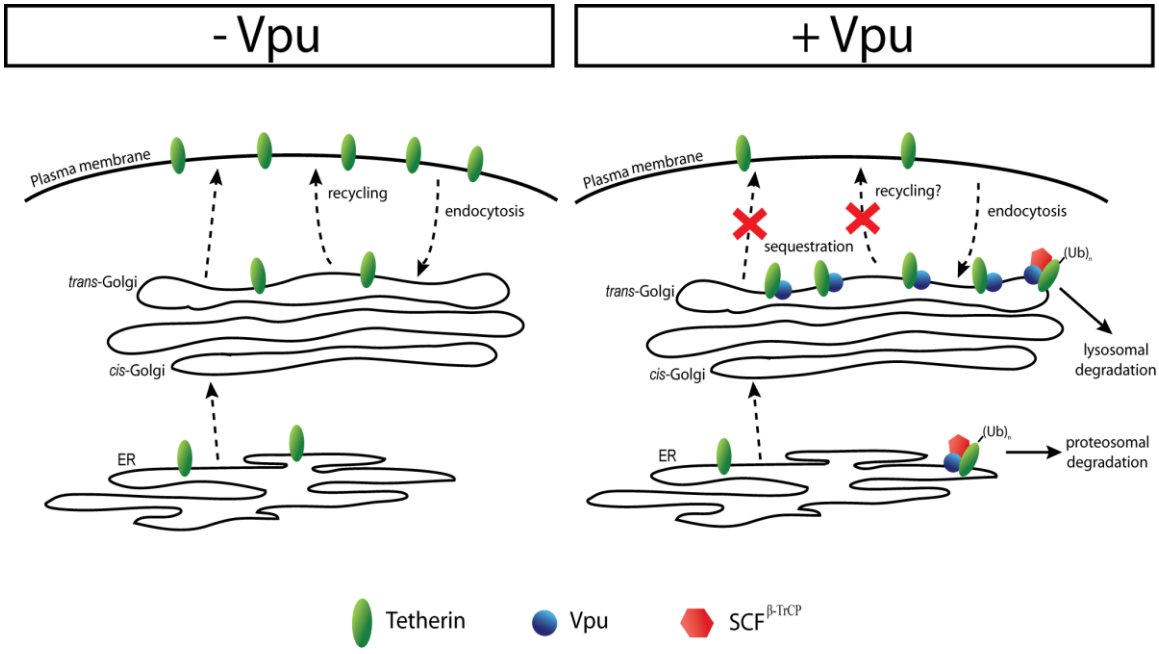
- Vpu
+ Vpu
Plasma membrane
recycling
endocytosis
trans-Golgi
cis-Golgi
ER
Plasma membrane
recycling?
endocytosis
sequestration
(Ub)n
trans-Golgi
lysosomal degradation
cis-Golgi
(Ub)n
ER
proteosomal degradation
Tetherin
Vpu
SCFβ-TrCP

Figure S1 : Characterization of the Vpu S52D,S56D mutant.

(A) Association of Vpu with β-TrCP. HEK 293T cells were transfected with the indicated Vpu-expressing constructs and the myc-β-TrCP-encoding plasmid pcDNA/Myc-His-β-TrCP. Forty-eight hours post-transfection, cells were radio-labeled for 2h and lysed prior to sequential immunoprecipitation using anti-myc and, subsequently, anti-Vpu Abs. Co-immunoprecipitated proteins were separated by SDS-PAGE and analyzed by autoradiography. (B) Effect of Vpu S52D,S56D on Tetherin cell-surface expression. HeLa cells were transfected with the indicated HxBH10 proviral constructs and a GFP-expressing plasmid. Cell-surface Tetherin expression was analyzed on GFP-positive cells by flow cytometry, 48h post-transfection. MFI values are shown beside the histogram. Filled histogram: pre-immune control; dashed line: HxBH10-*vpu*-; full black line: HxBH10-*vpu*+; full grey line: HxBH10-*vpu S52D,S56D.* (C) Effect of Vpu S52D,S56D on HIV-1 particle release. HeLa cells were transfected with the indicated HxBH10 proviral constructs. Cells and virus-containing supernatants were collected 48h post-transfection, lysed and analyzed for the detection of Gag-related products and Vpu by western blot using specific Abs. (D) Quantitation of virus particle release. Bands corresponding to Gag products in cells and virus particles were scanned by laser densitometry. The relative virus particle release efficiency was determined as described in the Materials and Methods and calculated as a percentage of the HxBH10-*vpu*+ virus release (100%). The error bars represent the standard deviation from the mean of three independent experiments.

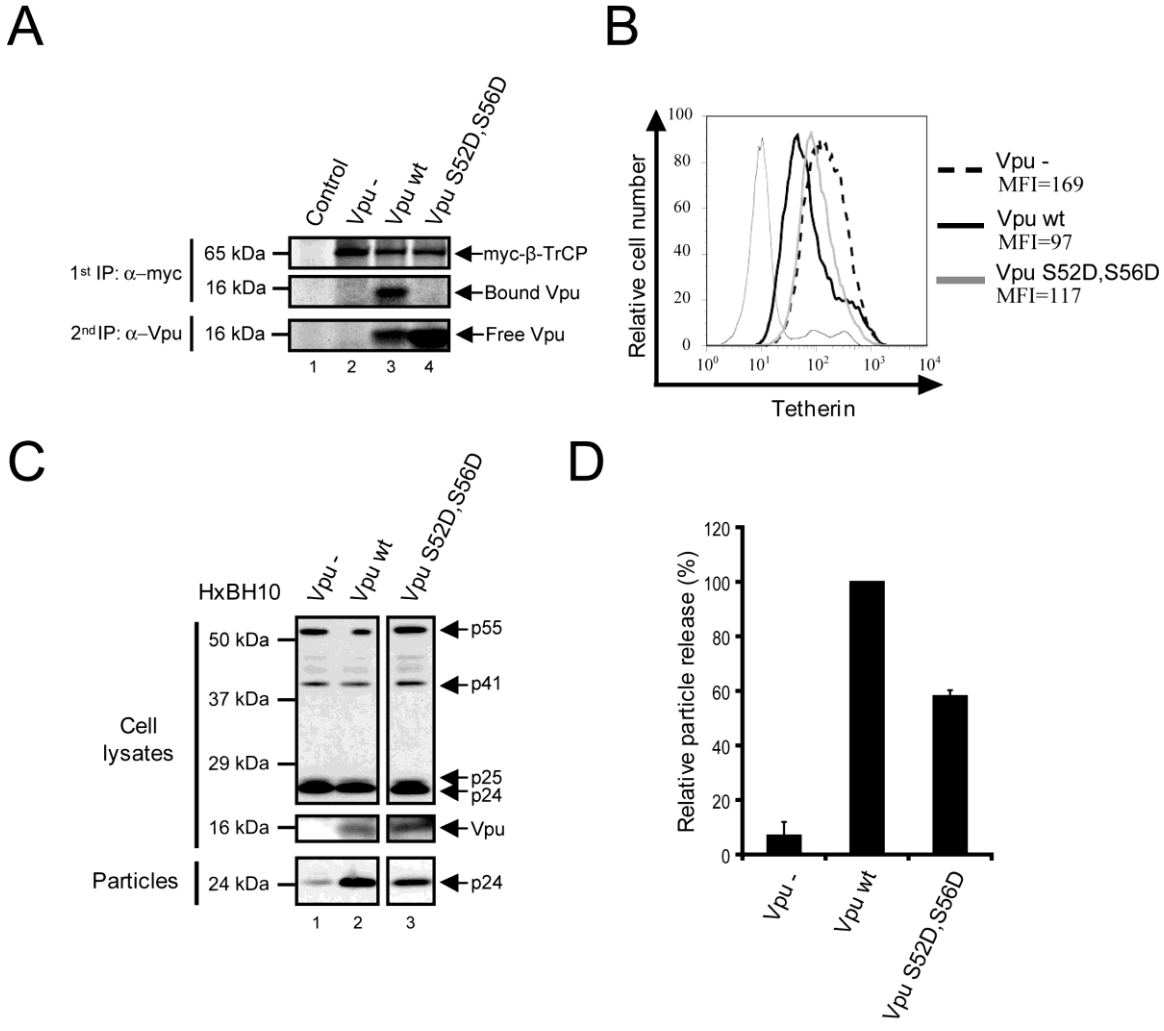
A
Control
Vpu -
Vpu wt
Vpu S52D,S56D
1st IP: α–myc
65 kDa
myc-β-TrCP
16 kDa
Bound Vpu
2nd IP: α–Vpu
16 kDa
Free Vpu
1 2 3 4
B
Relative cell number
Tetherin
Vpu -
MFI=169
Vpu wt
MFI=97
Vpu S52D,S56D
MFI=117
C
HxBH10
Vpu -
Vpu wt
Vpu S52D,S56D
Cell lysates
50 kDa
p55
37 kDa
p41
29 kDa
p25
p24
16 kDa
Vpu
Particles
24 kDa
p24
1 2 3
D
Relative particle release (%)
Vpu -
Vpu wt
Vpu S52D,S56D

Figure S2: Functional analysis of Tetherin chimeric proteins and the ΔGI,T45I mutant.

(A) Design of Tetherin chimeric proteins and the human Tetherin ΔGI-T45I mutant. Cytoplasmic (Cyto), TM, coiled-coil and GPI domain as well as glycosylation and cleavage sites (dashed line) are represented. White: human Tetherin; grey: agm Tetherin. The amino-acid sequence of the mutant Tetherin ΔGI,T45I within the TM domain is shown below. Dots indicate deleted residues while hyphens indicate similar residues. (B-E) HEK 293T cells were transfected with the specified HxBH10 proviral constructs and the indicated plasmids expressing (B) native or (D) HA-tagged Tetherin proteins. Forty-eight hours post-transfection, cells and virus-containing supernatants were harvested, lysed and proteins were analyzed by western blot using specific Abs. (C and E) Quantitation of B and D, respectively. Bands corresponding to Gag products in cells and viral particles of panels B or D were scanned by laser densitometry. The virus particle release efficiency was determined as described in the Materials and Methods and calculated as a percentage of the HxBH10-*vpu*+ release (100%) in absence of ectopically-expressed Tetherin. Error bars represent the standard deviation from the mean of two independent experiments.

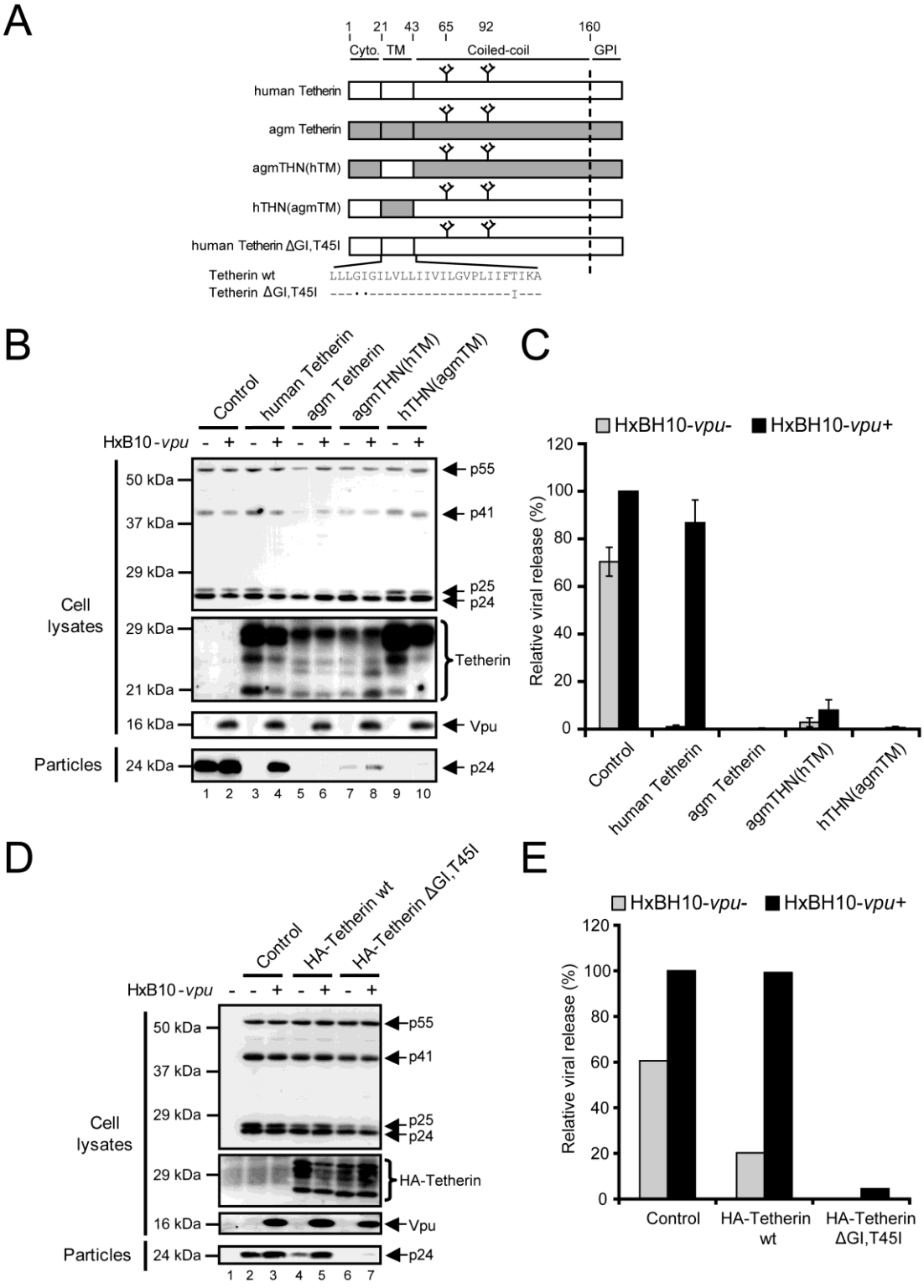
A
1 21 43 65 92 160
Cyto. TM Coiled-coil GPI
human Tetherin
agm Tetherin
agmTHN(hTM)
hTHN(agmTM)
human Tetherin ΔGI,T45I
Tetherin wt LLLGIGILVLLIIVILGVPLIIFTIKA
Tetherin ΔGI,T45I ---••----------I---
B
Control
human Tetherin
agm Tetherin
agmTHN(hTM)
hTHN(agmTM)
HxB10-vpu - + - + - + - + - +
50 kDa
37 kDa
29 kDa
p55
p41
p25
p24
Cell lysates
29 kDa
21 kDa
Tetherin
16 kDa
Vpu
Particles
24 kDa
p24
1 2 3 4 5 6 7 8 9 10
C
HxBH10-vpu- HxBH10-vpu+
Relative viral release (%)
120
100
80
60
40
20
0
Control
human Tetherin
agm Tetherin
agmTHN(hTM)
hTHN(agmTM)
D
Control
HA-Tetherin wt
HA-Tetherin ΔGI,T45I
HxB10-vpu - - + - + - +
50 kDa
37 kDa
29 kDa
p55
p41
p25
p24
Cell lysates
29 kDa
HA-Tetherin
16 kDa
Vpu
Particles
24 kDa
p24
1 2 3 4 5 6 7
E
HxBH10-vpu- HxBH10-vpu+
Relative viral release (%)
120
100
80
60
40
20
0
Control
HA-Tetherin wt
HA-Tetherin ΔGI,T45I

Figure S3: Functional analysis of Vpu mutants in HEK 293T cells.

HEK 293T cells were transfected with plasmids encoding native Tetherin, the indicated HxBH10 proviral constructs and a GFP-expressing plasmid. (A) Forty-eight hours post-transfection, cells and virus-containing supernatant were harvested, lysed and proteins were analyzed by western blot using specific Abs. (B) In parallel, cell-surface Tetherin expression was analyzed on GFP-positive cells by flow cytometry. Geo mean values (depicted as MFI) are presented in the histograms. Filled histogram: pre-immune control; dashed line: HxBH10-*vpu*-; full black line: HxBH10-*vpu*+; dotted line: HxBH10-*vpu KSL;* full grey line: HxBH10-*vpu RD.*

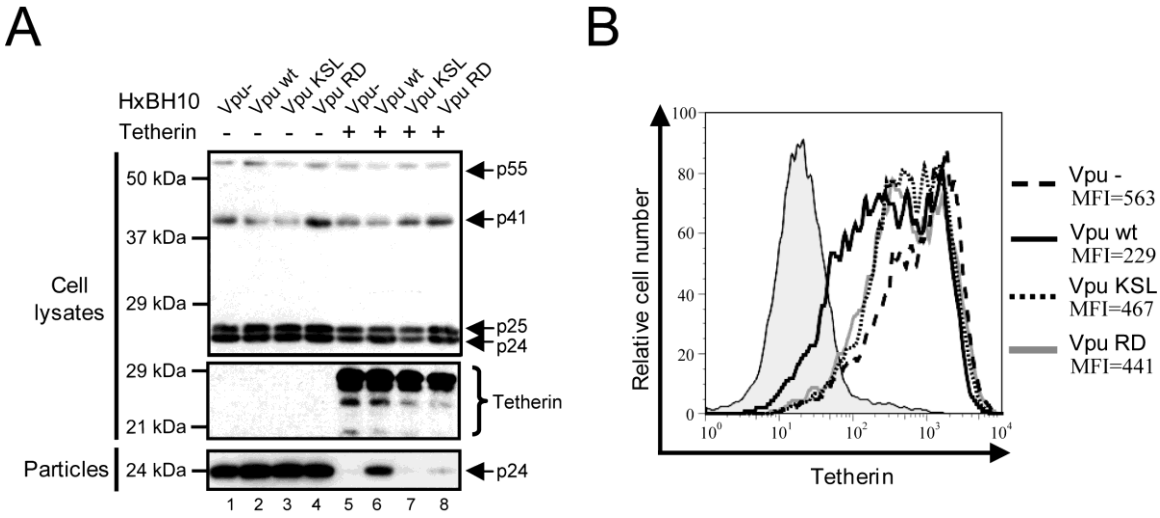
A
HxBH10
Vpu-
Vpu wt
Vpu KSL
Vpu RD
Tetherin
- - - - + + + +
50 kDa
37 kDa
29 kDa
Cell lysates
29 kDa
21 kDa
Particles
24 kDa
p55
p41
p25
p24
Tetherin
p24
1 2 3 4 5 6 7 8
B
Relative cell number
100
80
60
40
20
0
10^0 10^1 10^2 10^3 10^4
Tetherin
Vpu -
MFI=563
Vpu wt
MFI=229
Vpu KSL
MFI=467
Vpu RD
MFI=441

CHAPITRE 3

Quel est le pool de Tetherin affecté par Vpu?

Le chapitre 2 démontre clairement l'existence et la prédominance du mécanisme de séquestration dans les cellules HeLa. Sans nier la possibilité d'une contribution modérée, il exclut un rôle critique des mécanismes de dégradation ou d'internalisation. Or, un paradoxe d'ordre chronologique s'est imposé. Le souci d'efficacité au moindre coût énergétique et génétique est un critère constant façonnant l'évolution des virus. Il est intuitif d'imaginer que l'antagonisme de Tetherin devrait être complété avant l'initiation de l'assemblage et de la relâche virale afin de maximiser le rendement du cycle viral. Or, Vpu n'est exprimé que très peu de temps avant l'initiation de ces processus et il est conceptuellement difficile d'imaginer que la séquestration de la Tetherin néo-synthétisée puisse suffire à la tâche et ce, sans que Vpu n'agisse directement sur la population du facteur de restriction déjà exprimée en surface. L'un de nos objectifs dans ce troisième chapitre était d'abord de comparer la rapidité relative du processus de neutralisation de la Tetherin par Vpu avec celle de l'initiation de la relâche virale. Nous visions aussi à résoudre le dilemme chronologique mentionné ci-haut en évaluant l'effet de Vpu sur les pools de Tetherin néo-synthétisée et de surface. Cette approche devait nous renseigner indirectement sur la voie de trafic de Tetherin bloquée par la protéine virale et valider notre modèle de séquestration de la Tetherin nouvellement synthétisée.

Ce chapitre est actuellement en révision au journal *Traffic*, un journal couvrant la biologie cellulaire et la biochimie du transport cellulaire. Pierre Guiot-Guillain a fourni la Figure 4 du manuscrit alors que Johanne Mercier et Bibhuti Bhusan Roy, Ph.D., ont respectivement contribué aux Figures 2 et 7. Mathieu Dubé a exécuté les expériences des Figures 1-3, 5-9 et supplémentaires. Julie Binette, Ph.D., a construit le provirus HxBh10-*vpu* R30A,K31A. Piette Guiot Guillain, Johanne Mercier, Antoine Chiasson et Éric Cohen, Ph.D., ont tous fourni une aide technique et/ou conceptuelle. Mathieu Dubé a écrit le manuscrit en collaboration avec Éric Cohen, Ph.D.

RÉSUMÉ

BST-2 inhibe la relâche du VIH-1 en liant les virions en cours de bourgeonnement à la membrane plasmique des cellules infectées. La protéine Vpu du VIH-1 neutraliserait BST-2 en réduisant ses niveaux en surface par un mécanisme qui impliquerait une séquestration intracellulaire et une dégradation lysosomale. Dans cette étude, nous avons étudié l'importance fonctionnelle de la déplétion de BST-2 en surface et les pools du facteur de restriction affectés par Vpu en utilisant un système d'expression proviral inductible. Vpu a imposé un nouvel équilibre de BST-2 en surface à ~60% de son niveau initial après 6h d'expression, phénomène qui a coïncidé avec la détection de la relâche virale. L'analyse du trafic post-endocytic de BST-2 a révélé que son engagement dans la voie des endosomes tardifs indépendamment de Vpu. Alors que Vpu a augmenté modérément la clairance de BST-2 en surface surface, elle a fortement affecté son réapprovisionnement par des protéines nouvellement synthétisées. Collectivement, nos données révèlent que Vpu impose un nouvel équilibre de BST-2 en surface incompatible avec la restriction efficace de la relâche du VIH-1 en combinant une modeste accélération de la clairance de surface normale du facteur de restriction et un sévère défaut sévère au niveau de son réapprovisionnement.

HIV-1 Vpu antagonizes BST-2 by interfering mainly with the trafficking of newly synthesized BST-2 to the cell surface

Mathieu Dubé[1], Catherine Paquay[1], Bibhuti Bhusan Roy[1], Mariana Bego[1], Johanne Mercier[1], and Éric A. Cohen[1,2 *]

[1]Laboratory of Human Retrovirology, Institut de recherches cliniques de Montréal (IRCM), 110 avenue des Pins ouest, Montreal, Quebec, Canada, H2W 1R7;

[2]Department of Microbiology and Immunology, Université de Montréal, Montreal, Quebec, Canada, H3C 3J7

[*]Corresponding author:

Abstract

BST-2 inhibits HIV-1 release by cross-linking nascent virions on infected cell surface. HIV-1 Vpu is thought to antagonize BST-2 by downregulating its surface levels via a mechanism that involves intracellular sequestration and lysosomal degradation. Here, we investigated the functional importance of cell-surface BST-2 downregulation and the BST-2 pools targeted by Vpu using an inducible proviral expression system. Vpu established a surface BST-2 equilibrium at ~60% of its initial levels within 6h, a condition that coincided with detection of viral release. Analysis of BST-2 post-endocytic trafficking revealed that the protein is engaged in a late endosomal pathway independently of Vpu. While Vpu moderately

enhanced cell-surface BST-2 clearance, it strongly affected the protein re-supply to the plasma membrane via newly synthesized proteins. Noticeably, Vpu affected clearance of surface BST-2 more substantially in Jurkat T cells than in HeLa cells, suggesting a cell-dependent impact of Vpu on the pool of surface BST-2. Collectively, our data reveal that Vpu imposes a new BST-2 equilibrium, incompatible with efficient restriction of HIV-1 release, by combining an acceleration of surface BST-2 natural clearance, whose degree might be cell-type dependent, to a severe impairment of the protein re-supply to the plasma membrane.

Keywords: HIV-1, viral particle release, Vpu, BST-2 downregulation, BST-2 antagonism, BST-2 trafficking

Introduction

Although the accessory proteins (Vif, Vpr, Vpu and Nef) encoded by human immunodeficiency virus type 1 (HIV-1) were originally considered dispensable for virus replication *in vitro,* they are now thought to play a critical role in viral pathogenesis given their functions in subduing a hostile target cell environment (1). Among these accessory proteins, Vpu is a small oligomeric type 1 transmembrane protein that is unique to HIV-1 and primate lentiviruses related to simian immunodeficiency virus found in chimpanzee. This protein, which resides primarily in the *trans*-Golgi Network (TGN) and the endosomal system, exerts several biological activities during HIV-1 infection (reviewed in (2)). First, Vpu was found to target newly synthesized CD4 molecules for proteasomal degradation through an endoplasmic reticulum (ER)-associated protein

degradation (ERAD)-like process (3, 4). The cytoplasmic domain of Vpu contains a $DS_{52}GxxS_{56}$ phosphoserine motif that recruits β-TrCP and the $SCF^{\beta\text{-}TrCP}$ E3 ligase complex to ubiquitin-mark CD4 for degradation (5). The resulting depletion of CD4 receptor molecules is believed to promote the transport of Env glycoproteins to the plasma membrane and to minimize superinfection of infected cells (6, 7). However, the Vpu biological activity that has attracted considerable attention in recent years is the antagonism of bone marrow stromal cell antigen-2 (BST-2, also designated Tetherin/CD317/HM1.24), an interferon-inducible host restriction factor that strongly inhibits the release of HIV-1 from infected cells (8, 9).

BST-2 is a type II membrane protein of 181 amino-acids with a molecular weight of 29 and 33 kDa depending on its glycosylation state. The protein has an atypical topology with both extremities embedded in the cellular membranes through two different types of membrane anchors: a transmembrane domain proximal to an intracellular N-terminus cytosolic region and a C-terminal glycosyl-phosphatidylinositol (GPI) anchor (10). The two membrane anchors are connected by an extracellular domain that contains an extended coiled-coil structure that mediates BST-2 homodimerization (11, 12). The protein is localized not only at the plasma membrane but also within several endosomal membrane compartments, including the TGN as well as early and recycling endosomes (10, 13-16). Trafficking of BST-2 between the plasma membrane and the TGN was shown to require a tyrosine-based sorting signal in the BST-2 cytoplasmic domain. This YxYxxΦ motif was shown to interact with both clathrin adaptors AP1 and AP2, suggesting the involvement of the sequential action of AP-2 and AP-1 complexes in BST-2 internalization and delivery back to the TGN (15, 17).

As a GPI-anchored protein, BST-2 is found within cholesterol-enriched lipid domains from which HIV-1 and other enveloped viruses preferentially assemble

and bud (10, 15, 18). Up to now, BST-2 has been shown to restrict the release of a broad variety of enveloped viruses, including all classes of retroviruses (reviewed in (19)). This broad spectrum antiviral activity appears to reside in the ability of the protein to target a virion component common to this diverse group of viruses, the host cell-derived lipid bilayer. Indeed, biochemical, structural and electron microscopic evidence, mostly from studies of HIV-1, currently favors a direct tethering mechanism of virus restriction whereby parallel BST-2 dimers physically crosslink not only virion and cellular membranes but also virion membranes together (11, 16, 20-25).

The mechanism underlying BST-2 antagonism by HIV-1 Vpu is still a matter of debate. It is generally agreed that Vpu expression causes a downregulation of surface BST-2 levels (8) and a reduction of the total levels of the protein in most cellular systems (26-29). This Vpu-mediated depletion of BST-2, which indeed requires a physical interaction between the transmembrane domains of the two proteins (30-34), is thought to remove the restriction factor from the plasma membrane, the site of its tethering action, although this model has previously been challenged (35). Several studies reported the involvement of proteasomal (26-28) or endo-lysosomal pathways (29, 36) in Vpu-mediated downregulation of BST-2 and suggested a dependence on β-TrCP2 engagement by Vpu. Consistent with the involvement of a lysosomal pathway, a recent study reported that Vpu accelerates BST-2 degradation by connecting the restriction factor to HRS, a component of the ESCRT-0 machinery that sorts ubiquitinated proteins to multivesicular bodies (MVB) and lysosomes for degradation (37). Additionally, other studies reported that Vpu could also sequester BST-2 away from the plasma membrane, most probably in the TGN (32, 38). Since this sequestration was sufficient to inhibit the restricting activity of BST-2, several recent reports suggested that β-TrCP2-dependent targeting of the restriction factor to lysosomal compartments for degradation could represent a subsequent step required to achieve optimal depletion of BST-2 at the cell surface (32, 37, 39). In that regard,

recent studies reported efficient enhancement of HIV-1 release by Vpu in absence of BST-2 degradation (32, 40, 41).

Since Vpu is expressed from a Rev-dependent bicistronic mRNA and consequently, is made late during HIV-1 infection (42), it is unclear how fast and to what extent surface BST-2 levels need to be reduced before efficient HIV-1 particle release is initiated. Furthermore, it is unknown whether Vpu acts at pre- and/or post-endocytic steps to induce BST-2 sequestration and degradation. Using an inducible HIV-1 proviral expression system, we evaluated the kinetics of cell-surface BST-2 downregulation and HIV-1 release. We show that optimal cell-surface BST-2 downregulation is achieved within 6h of Vpu expression. Importantly, the rapid emergence of this new BST-2 equilibrium coincided with detection of HIV-1 particle release. Analysis of BST-2 post-endocytic trafficking revealed that the protein is not sensitive to monensin, a drug interfering with fast recycling, but is rather engaged in a late endosomal pathway independently of the presence of Vpu. Lastly, our results show that, while Vpu accelerated surface BST-2 clearance and decay to varying degree in HeLa and Jurkat T cells, it severely affected the restriction factor re-supply to the plasma membrane via newly synthesized proteins independently of the cell type. Therefore. by combining a severe impairment of the restriction factor re-supply to the plasma membrane to an acceleration of the surface BST-2 natural clearance process, whose degree might be cell-type dependent, Vpu imposes a new BST-2 equilibrium, which is incompatible with efficient restriction of HIV-1 particle release.

Results

Characterization of an inducible HIV-1 proviral expression system.

To study the early effect of Vpu on the surface levels of BST-2, we used an inducible system in which expression of HIV-1 genes is driven by *tetO* responsive elements in presence of doxycycline (Dox). The wild type (WT) and Vpu-defective proviral constructs were derived from the previously described HIV-1 rtTA provirus in which the Tat-TAR regulatory axis of transcription was inactivated. Viral transcription and replication were made Dox-dependent by introducing eight *tetO* elements in the LTR promoter region between NF-κB and Sp1 sites and by replacing the *nef* gene by a genetically selected Dox-regulated rtTA transactivator gene (43). Additionally, we inserted EGFP in frame with the matrix protein (MA) as a marker of viral protein expression, thus generating inducible EGFP-encoding proviruses (HIV-1.rtTA.MA-EGFP) that are isogenic except for *vpu* expression (Figure 1A). Indeed, while transfection of HIV-1.rtTA.MA-EGFP in HeLa cells, a cell line that constitutively expresses BST-2 (8, 9), revealed only background levels of p55-EGFP and no virus particle production 48h post-transfection (Figure 1B lanes 1, 5 and 9), cells treated with a low dose of Dox (250 ng/ml) displayed a very strong upregulation of all viral proteins, including Vpu in the case of Vpu-proficient constructs (Figure 1B; lanes 2, 6, 10). Importantly, induction of HIV-1.rtTA.MA-EGFP.*vpu*+-expression led to downregulation of surface BST-2 on EGFP-positive cells and efficient virus particle release whereas induction of HIV-1.rtTA.MA-EGFP.*vpu*- expression did not (Figure 1B, compare lanes 6-8 to lanes 2-4 and Figure 1C). Importantly, the reduction of cell-surface BST-2 levels observed with this inducible system was comparable to that detected with replication-competent HIV-1 (32) and data not shown), indicating that the levels of Vpu expression reached with this system are physiological. Consistent with our previous observation (32), induction of a similar proviral construct encoding Vpu S52D,S56D, a mutant of Vpu that does not bind β-TrCP (32), resulted in an intermediate phenotype for both enhancement of virus particle release (Figure 1B; compare lanes 10-12 to lanes 6-8) and downregulation of cell-surface BST-2 (Figure 1C). Residual downregulation of surface BST-2 by Vpu S52D,S56D is likely to result from BST-2 intracellular sequestration since this mutant has the ability to bind and

redistribute BST-2 to the TGN but is unable to induce its degradation (32). Therefore, this inducible proviral expression system recapitulates BST-2 antagonism by Vpu.

A new BST-2 equilibrium is rapidly reached following Vpu induction.

We next evaluated the kinetics of BST-2 downregulation at the cell surface upon induction of Vpu expression. HeLa cells were transfected with the inducible isogenic HIV-1.rtTA.MA-EGFP constructs and further treated with 1 µg/ml of Dox for different intervals of time (0-24h) to induce viral protein expression. Cell-surface BST-2 levels were then analyzed 48h post-transfection by flow cytometry. Vpu-mediated BST-2 downregulation was detectable as rapidly as 3h after Dox induction, indicating expression of the viral protein, and reached its maximal effect of ~40% after 6h of treatment (Figure 2A). Longer Dox treatments did not result in any further downregulation, indicating that surface BST-2 reached a new equilibrium. Interestingly, optimal cell-surface BST-2 downregulation at 6h coincided with a detectable release of virus particle from Vpu-expressing cells (Figure 2B; compare lanes 8 to lane 3). Noticeably, virus particle release was significantly delayed and inefficient in absence of Vpu (compare lanes 2-5 to lanes 7-10). As expected, the new BST-2 equilibrium established by Vpu was reversible since extensive washing of the media to remove Dox and repress proviral expression restored initial surface BST-2 levels within 24h (Figure 2C). Interestingly, the kinetics of BST-2 downregulation measured in Vpu S52D,S56D-expressing cells was delayed relative to that of WT Vpu-expressing cells. It peaked at ~32% of downregulation after 12h of Dox treatment but failed to maintain this new equilibrium afterwards (Figure 2A). Similarly, the kinetics of WT Vpu-mediated cell-surface BST-2 downregulation was found to be delayed in β-TrCP2-depleted HeLa cells and indeed recapitulated the kinetics observed with the Vpu S52D,S56D mutant (Figure S1), confirming that recruitment of β-TrCP2 is required for optimal surface BST-2 downregulation. Overall, these results indicate that Vpu imposes a reduction in

the levels of BST-2 at the cell surface as rapidly as 6h following its expression and this coincides with detection of virus particle release.

Vpu reduces cell-surface BST-2 levels without altering the restriction factor distribution at the cell surface.

To rapidly overcome BST-2 restriction on HIV-1 release, Vpu could exclude BST-2 from viral assembly sites. In this regard, Vpu was previously shown to decrease the co-localization between Gag and BST-2 at the surface of infected cells (8, 36, 44). To address this possibility, we characterized the distribution of the restriction factor at the surface of Jurkat cells infected with GFP-marked HxBH10.GFP.IRES.*nef*- -derived viruses. In absence of Vpu, surface BST-2 accumulated in patches that co-stained with p17, a marker of mature viruses and viral assembly sites (Figure 3A). As expected, in similar conditions of image capture, surface levels of BST-2 were drastically decreased in presence of Vpu while levels of p17 were barely detectable presumably as a result of efficient virus particle release (Figure 3A and flow cytometry analysis in panel B). Interestingly, when the staining signal was increased to an intensity comparable to that detected in Vpu-deficient HIV-1 infected cells (Figure 3A, upper panels), residual surface BST-2 still strongly co-localized with p17 (Figure 3A, bottom panel, long exposure, and quantification in Figure 3D), suggesting that Vpu is not displacing surface BST-2 outside membrane microdomains where viral assembly is taking place. Consistent with these observations, surface BST-2 co-localized with CD59, a lipid raft marker, as well as with CD81 and CD63, two markers of the tetraspanin-enriched microdomains, both in absence or presence of Vpu (Figure 3C and D; the signal intensity in the Vpu+ images was increased). Overall, these results reveal that BST-2 co-localizes with markers associated with membrane microdomains that HIV-1 uses as assembly and budding platforms (45, 46). They further show that Vpu downregulates cell surface BST-2 levels without qualitatively affecting the distribution of the restriction factor at the plasma membrane.

The pool of BST2 at the cell surface is modestly downregulated by Vpu

Previous studies, including ours, showed that Vpu does not increase the rate of BST-2 internalization (32, 36, 39). However, since these experiments were performed at steady-state, once a new equilibrium was established at the plasma membrane, potential early effects of Vpu on the clearance of the pool of BST-2 at the surface may have been overlooked. To overcome this limitation, we took advantage of our inducible system. HeLa cells were transfected with HIV-1.rtTA.MA-EGFP constructs and analyzed 48h post-transfection for surface BST-2 expression by flow cytometry. Prior to analysis, cells were incubated at 37°C for 1.5h in presence of a polyclonal anti-BST-2 rabbit serum to specifically label surface BST-2, washed and incubated for 0-24h in presence of 1 µg/ml of Dox to induce viral protein expression (Figure 4A). The fluorescent signal detected with the secondary antibody (Ab) at each time interval was indicative of the BST-2 levels that remained at the cell surface. The endogenous half-life of cell-surface BST-2 was ~8h in absence of Vpu (Figure 4B). The rate of surface BST-2 clearance measured with this Ab-based assay was found similar to that reported using a different assay system in which BST-2 re-supply was blocked by the post-ER trafficking inhibitor Brefeldin A (47), indicating that the sum of processes governing the clearance of cell surface BST-2 were not altered by the anti-BST-2 Ab labelling (data not shown). Upon induction of WT Vpu or Vpu S52D,S56D, the half-life of cell-surface BST-2 slightly decreased to ~6.5h and ~7h, respectively. In fact at 6h, the levels of BST-2 at the surface of Vpu-expressing cells were decreased by ~11% relative to control cells (Figure 4B). Although reproducible, this modest difference in the rate of BST-2 clearance from the surface cannot explain the ~40% decrease observed in figure 2A at 6h post-Dox induction. Therefore, Vpu must affect another pool of BST-2 to achieve optimal downregulation from the cell surface.

We next analyzed the rate of decay of the BST-2 pool originating from the cell surface. To do so, half of the transfected cells processed in figure 4B were permeabilized prior to staining with an appropriate secondary Ab. In this experiment, cell permeabilization allowed the detection of surface-derived BST-2 molecules engaged in endocytic compartments as well as remaining cell surface-associated BST-2 (Figure 4A). In absence of Vpu, the turnover of cell-surface BST-2 was slow, with ~70% of the initial levels remaining after 24h. Thus, the rate of cell-surface BST-2 decay appears much slower than its rate of clearance (compare Figure 4C to 4B). Induction of Vpu slightly accelerated this process since ~80% of the initial surface BST-2 levels were detected at 6h post-induction while ~50% remained after 24h. Interestingly, induction of Vpu S52D,S56D led to a degradation kinetics that appeared similar to that of WT Vpu within the first 6h, but which then progressively slowed-down between 6h and 24h post-induction to reach levels comparable to the Vpu-negative control (~70% at 24h). These results suggest that a fraction of internalized BST-2 is slowly sorted towards degradative compartments and that Vpu modestly accelerates this process over time in a β-TrCP-dependent manner.

Internalized BST-2 accumulates in late endosomes.

Having shown that BST-2 was endocytosed, we next evaluated the localization of internalized BST-2 by confocal microscopy. Given that degradation of internalized BST-2 appeared very slow, we reasoned that long incubation with Abs would be necessary to fully detect the association of BST-2-Ab complexes with degradative compartments. Therefore, untransfected HeLa cells were incubated with a polyclonal anti-BST-2 rabbit serum for 12h at 37°C. Cells were then fixed, permeabilized and sequentially stained with Abs directed against specific cellular markers and secondary Abs that could recognize BST-2 and cellular markers specific Abs. Localization of internalized BST-2 was compared to Rab5 (early endosomes) (48), Rab11 (recycling endosomes) (49), TGN46 (TGN) (50), Rab9 (51) and CD63 (52) (late endosomes) (Figure 5A).

Surprisingly, only ~17-23% of internalized BST-2 signal overlapped with Rab5, Rab11 and TGN46 markers in these conditions, suggesting that internalized BST-2 is transiently trafficking through early and recycling endosomes and the TGN. In contrast, ~66-74% of the internalized BST-2 signal readily overlapped with CD63 and Rab9, two markers of late endosomes (Figure 5B). Importantly, internalized BST-2 similarly overlapped with late endosomal markers upon induction of Vpu expression in HIV-1.rtTA.MA-EGFP-transfected HeLa cells (Figure 5C and D). Co-localization of BST-2 with these late endosomal markers was also observed in fixed cells, thus excluding an aberrant intracellular distribution triggered by anti-BST-2 Abs (Fig. S2). Trafficking of internalized BST-2 was also characterized at shorter time intervals to obtain additional information about the pathway followed by BST-2 to ultimately reach lysosomal compartments. As expected, internalized BST-2 was found at the plasma membrane and in vesicles beneath the plasma membrane after 10_min of incubation. Strong accumulation in a TGN46-positive compartment could be observed at 30-60 min, whereas association to CD63-positive vesicles became predominant after 6h of incubation (Figure S3), suggesting a transient accumulation of internalized BST-2 within the TGN prior to its lysosomal sorting.

Overall, these results indicate that a large fraction of endogenous surface BST-2 is ultimately targeted to late endosomal compartments following its endocytosis. Although Vpu modestly accelerates the clearance of cell-surface BST-2, the intracellular distribution of internalized restriction factor molecules does not appear strongly affected by the viral protein.

Endogenous BST-2 is not sensitive to monensin, an inhibitor of fast recycling.

BST-2 was previously reported to co-localize on endosomal membranes with the Transferrin receptor (TfR) (15, 31), a protein that undergoes fast recycling back to the plasma membrane. To examine whether endogenous BST-2 is indeed

recycling through a similar pathway, we assessed the effect of monensin, an inhibitor of the fast recycling pathway that was previously shown to block the recycling of the Transferrin and the low-density lipoprotein receptors (LDLR) (53, 54). As expected, a 2h treatment of HeLa or Jurkat cells with 100 µM monensin, resulted in downregulation of LDLR at the surface as measured by flow cytometry (Figure 6A and C). Similar results were also obtained with the TfR (data not shown). In contrast, a 2h (Figure 6B and D) or 5h (data not shown) treatment of cells with similar concentrations of monensin did not have any effect on endogenous surface BST-2 levels, suggesting that BST-2 is not engaged in a recycling pathway similar to that used by LDLR or TfR.

Cell-surface downregulation of BST-2 by Vpu is primarily dependent upon BST-2 de novo-synthesis.

Since the effect of Vpu on the pool of BST-2 derived from the cell surface appeared modest at best, we next examined the effect of the viral protein on the pool of newly synthesized BST-2. To do so, we took advantage of BST-2 inducibility by type 1 interferon (IFN). Upregulation of IFN-inducible genes by exogenous IFN involves endogenous expression of IFN and the establishment of a durable positive feedback loop (55) whereby newly produced IFN continues to act on its targets. This IFN-mediated positive feedback loop can be neutralized by B18R, a vaccinia-encoded secreted protein with a higher affinity than the cellular IFN receptor for type I IFN (56). The capacity of B18R to inhibit IFN-driven BST-2 expression was evaluated in HEK293T cells, which are devoid of BST-2 expression. Consistent with the establishment of a durable positive feedback loop (55), a strong upregulation of surface BST-2 was still detected 24h after a 1h pulse of exogenous IFN-α. (Figure S4A). In contrast, addition of 10-100 ng/ml of B18R immediately after the IFN-α pulse completely prevented this upregulation. Indeed, using a type 1 IFN reporter system (HEK-blue IFN-α/β^{TM}) (57), we confirmed that at concentration of 50 or 100 ng/ml, B18R completely prevented the initiation of an IFN positive feedback loop since no active IFN

could be detected in the supernatant of IFN pulse-treated cells after 24h (Figure S4B).

Having shown that we could interfere with induction of BST-2 neo-synthesis by type 1 IFN using B18R, we next examined whether blocking BST-2 synthesis could affect Vpu-mediated downregulation of surface BST-2. HEK293T cells were transfected with Dox-inducible HIV-1.rtTA.MA-EGFP proviral constructs and immediately treated with IFN-α for 42h to ensure that steady-state levels of surface BST-2 were reached. Following extensive washes, Dox and recombinant B18R were added to cells to respectively induce expression of viral proteins and block IFN-α-induced BST-2 neo-synthesis. Six hours later, at the peak of Vpu-mediated downregulation of BST-2 (Figure 2), surface BST-2 levels were monitored by flow cytometry on EGFP-positive cells (Figure 7A). Consistent with an interruption of the IFN-mediated positive feedback loop and a block of IFN-induced BST-2 synthesis, B18R treatment resulted in a ~38% downregulation of cell-surface BST-2 (Figure 7B-C; compare MFI of the Vpu- condition in absence (26) and presence (16) of B18R). This downregulation was indeed very similar to that achieved upon Vpu induction in absence of B18R treatment (Figure 7B and D). We hypothesized that if Vpu acted primarily on the pool of newly synthesized BST-2, Vpu-mediated downregulation of BST-2 would be affected in presence of B18R. Indeed, as shown in figure 7C-D, the effect of Vpu on surface BST-2 levels was strongly attenuated in presence of B18R (downregulation of ~38% in absence of B18R and ~11% in presence of B18R). Taken together, these results suggest that downregulation of BST-2 by Vpu depends on a large part on BST-2 *de novo* synthesis. Furthermore, since inhibition of BST-2 neo-synthesis recapitulates to a large extent the effect of Vpu on BST-2 surface levels, it is therefore likely that Vpu targets primarily the pool of newly synthesized BST-2 en route to the plasma membrane.

Vpu reduces the expression of newly synthesized BST-2 at the cell surface

To examine directly whether Vpu targets preferentially the pool of newly synthesized BST-2 en route to the cell surface, we developed a second system in which the effect of Vpu on the pools of cell-surface and newly synthesized BST-2 could be distinguished and simultaneously compared. HeLa cells were transfected with HIV-1.rtTA.MA-EGFP-*vpu-/vpu+*/*vpu S52D,S56D* constructs. Forty-one hours post-transfection, cells were incubated for 1h at 37°C with a saturating concentration of the polyclonal anti-BST-2 rabbit serum to label all surface BST-2 molecules. Cells were then extensively washed and re-incubated for 6h at 37°C in presence of 1 µg/ml Dox. Subsequently, half of the cells were harvested and sequentially stained for 45 min at 4°C with the polyclonal anti-BST-2 mouse serum and an anti-mouse secondary Ab to specifically label newly synthesized proteins reaching the surface. In parallel, the other half of the cells was similarly incubated for 45 min at 4°C and then directly stained with the anti-rabbit secondary Ab to specifically label surface BST-2 (Figure 8A). Conceptually, the mouse serum will only recognize unlabeled BST-2 molecules that were not present at the surface during the initial staining with the rabbit anti-BST-2 Abs. Consistent with previous results, Vpu had only a marginal effect (~19%) on the levels of surface BST-2, as monitored by the signal issued from the anti-rabbit staining (Figure 8B and D). In contrast, analysis of the signal derived from the mouse Abs revealed a severe downregulation of the restriction factor (~76%), suggesting that Vpu strongly affected the re-supply of BST-2 to the surface through newly synthesized proteins (Figure 8C and D). To assess how efficiently the rabbit anti-BST-2 Abs blocked subsequent binding by mouse anti-BST-2 Abs, transfected cells were cultured for 7.5h in presence of rabbit anti-BST-2 Abs. Cells were then immediately washed at 4°C to prevent intracellular transport of unlabeled molecules towards the plasma membrane, sequentially stained at 4°C with mouse anti-BST-2 Abs and anti-mouse secondary Abs and then analyzed by flow cytometry. As shown in figure 8C, no BST-2 signal derived from the mouse Abs could be detected, indicating that rabbit anti-BST-2 Abs efficiently blocked the binding of mouse anti-BST-2 Abs

(Figure 8C; dashed line) and confirming that the signal detected with mouse anti-BST-2 (Figure 8C; full lines) indeed represented newly synthesized BST-2 molecules transported to the plasma membrane during the 6h of Dox treatment. Interestingly, expression of Vpu S52D,S56D, which lacks BST-2 degradation activity, still affected BST-2 re-supply to the surface although not as efficiently as WT Vpu (decrease of ~55% for Vpu S52D,S56D versus ~76% for WT Vpu, Figure 8C and D). This indicates that both BST-2 sequestration and degradation are likely contributing to the inhibition of BST-2 re-supply at the plasma membrane.

To assess whether these findings could be extended to HIV-1 target cells, we performed similar experiments in transfected CD4+ Jurkat T cells. As shown in figure 8F and G, newly synthesized BST-2 was similarly downregulated by Vpu in Jurkat cells (decrease of ~87% for WT Vpu and ~58% for Vpu S52D,S56D). Interestingly, in contrast to HeLa cells, the pool of cell-surface BST-2 appeared more significantly downregulated by Vpu and Vpu S52D,S56D (Figure 8E and G; decrease of ~42%, for WT Vpu versus ~17% for Vpu S52D,S56D). Overall, these results suggest that Vpu affects the global expression of cell-surface BST-2 primarily by interfering with the restriction factor re-supply to the plasma membrane via newly synthesized proteins but also by increasing BST-2 clearance from the surface, the extent of which might be cell-type dependent.

Discussion

In this study, we investigated the mechanisms through which Vpu antagonizes the restriction imposed by the IFN-inducible host factor, BST-2, on HIV-1 release. Several previous studies reported that Vpu downregulates BST-2 from the surface, the site of its tethering action, and proposed that this process could indeed underlie BST-2 antagonism by Vpu (8, 11, 29, 32, 36, 39). However,

since the surface downregulation of BST-2 is never complete and efficient virus release was not found to correlate with a cell-surface reduction of BST-2 levels in the course of productive infection of CEMx174 and H9 T-cell lines (35), it remains to be determined whether depletion of surface BST-2 levels is a prerequisite for enhanced particle release or a downstream consequence of Vpu function. Using a proviral expression system that allows inducible HIV-1 expression and production, we chronologically monitored the surface downregulation of BST-2 and the enhancement of viral release induced by Vpu. Our data show that surface BST-2 levels decrease to ~60% of their initial levels by 6h after initiation of Vpu expression and remain stable afterwards, indicating that a new BST-2 equilibrium was established at the cell surface (Figure 2). This rapid downregulation of BST-2 by HIV-1-encoded Vpu is consistent with the results of a recent study, which reported that transfection of plasmids encoding codon-optimized Vpu led to a detectable downregulation of BST-2 6h after initiation of the transfection (47). Importantly, the emergence of this new surface BST-2 equilibrium coincided with detection of viral particle release in Vpu-expressing cells, suggesting that all processes involved in both Vpu-mediated BST-2 downregulation and antagonism were resolved within the same time-frame. Although we cannot completely rule-out that this synchronism is coincidental, it is more likely to represent a causal relationship. Indeed, we were unable to find any evidence that Vpu would exclude BST-2 molecules from HIV-1 budding sites, as an alternative mechanism of antagonism. In fact, even though as previously reported (8, 36, 44), we observed a reduced co-localization between Gag and BST-2 in Vpu-expressing cells (8, 36, 44), residual surface BST-2 still co-localized with CD63- and CD81-positive viral budding sites (Figure 3). Thus, by establishing a new BST-2 equilibrium at the cell surface, Vpu appears to decrease the density of BST-2 molecules associated with HIV-1 budding platforms. The rather fast emergence of this new equilibrium is most probably necessary, so that Vpu, which is expressed relatively late during the HIV-1 life cycle, can reduce BST-2 levels before the onset of viral budding. Despite the fact that this reduction of surface BST-2 is incomplete, it seems that the residual

levels are incompatible with efficient restriction of HIV-1 release. Whether or not these residual molecules underwent additional qualitative changes that prevent them to restrict the release of nascent virus particle remains to be determined.

Previous studies have shown that BST-2 downregulation does not result from an acceleration of the rate of BST-2 internalization from the surface (32, 36, 39). One caveat about these analyses is that they were all conducted at steady state, once a new equilibrium was achieved, a condition that could potentially mask effects of Vpu on surface BST-2 before the onset of this new equilibrium. Indeed, our inducible proviral expression system revealed that Vpu slightly accelerated the clearance of BST-2 from the surface (Figure 4). This rather small effect might have been overlooked in previous reports studying the rate of BST-2 internalization, especially since ~40% of surface BST-2 clearance appears to occur within 20-30 min (32, 36, 39). Interestingly, the rate of decay of cell-surface BST-2, which reflects its post-endocytic transport towards degradative compartments, also appeared slightly increased within the first 6h of Vpu induction. This could represent an indirect consequence of accelerated BST-2 internalization or, alternatively, could indicate that Vpu enhances the targeting of internalized BST-2 molecules for lysosomal degradation. The accumulation of internalized BST-2 in Rab9- and CD63-positive late endosomes even in absence of Vpu (Figure 5) suggests that Vpu modulates the natural endocytic and/or post-endocytic BST-2 trafficking, a notion indeed consistent with the role of the ESCRT-0 complex in the lysosomal sorting of the restriction factor both in presence or absence of Vpu (37). Given that Vpu S52D,S56D did not display a similar acceleration of cell-surface BST-2 clearance and decay at least after 6h suggests that the recruitment of β-TrCP by Vpu and the recently demonstrated Vpu-mediated ubiquitination of BST-2 (58, 59) are likely involved in this process. Ubiquitination of internalized BST-2 could indeed interfere with its recycling back to the plasma membrane, thus forcing its trafficking towards lysosomes for degradation, as reported for the epidermal growth factor receptor (EGFR) (60).

However, the poor association of internalized BST-2 to Rab11-positive compartments (Figure 5) and its insensitivity to monensin (Figure 6) do not support such hypothesis, although it is still conceivable that internalized BST-2 could rather engage in a different and/or slower recycling pathway. Alternatively, β-TrCP-mediated ubiquitination of BST-2 could represent a signal triggering its endocytosis and sorting towards lysosomes, a process reminiscent of the SCF-$^{\beta\text{-TrCP}}$-mediated degradation of type I IFN receptor (61). These models would perhaps explain the partial inhibition of Vpu-mediated BST-2 downregulation observed upon abrogation of endocytosis either through AP-2 depletion or overexpression of a dominant negative mutant of Dynamin (31, 36). However, no matter how Vpu accelerates the clearance of BST-2 from the surface, this process cannot account for the overall 40-50% decrease of surface BST-2 observed 6h post-Vpu induction. This conclusion contrasts with the study of Skasko et al. (47), which conferred to Vpu a more important role in the removal of surface BST-2. Indeed, their data revealed a greater downregulation of the restriction factor (5-fold in 6h) than could be accounted for by spontaneous surface clearance (2-fold in 8h). These opposite interpretations rest on the magnitude of the Vpu-mediated-downregulation of surface BST-2 reported by the two studies, which indeed might be attributed to the use of different expression system, mainly virus-encoded Vpu construct in our study versus codon-optimized Vpu-expressing construct in the case of Skasko et al. (47). It is interesting to note that the effect of Vpu on the pool of cell-surface BST-2 appeared more pronounced in Jurkat CD4+ T cells (Figure 8). Similarly, Vpu appeared to remove quite efficiently BST-2 from the surface of COS cells exogenously-expressing the restriction factor (62). Therefore, the efficiency with which Vpu affects the pool of cell-surface BST-2 may be cell-type specific and as such may depend on the presence of cellular determinant(s) that remain to be identified.

Since the steady-state level of a cell-surface protein reflects a balance between its clearance from the plasma membrane (ie: a balance between endocytosis,

recycling and degradation) and its re-supply through the biosynthetic route, we hypothesized that Vpu could affect the pool of newly synthesized BST-2. In support of this possibility, blocking BST-2 *de novo* synthesis in IFN-treated HEK293T cells by adding recombinant B18R decreased surface BST-2 by ~38% within 6 h (Figure 7), indicating that surface BST-2 could be efficiently downregulated by reducing its re-supply. These results are indeed consistent with recent data showing that treatment with Brefeldin A or cycloheximide, which prevents re-supply of surface proteins, decreased by ~50% the levels of BST-2 at the plasma membrane within 8h (47). In contrast, Vpu had only a marginal effect on residual BST-2 expressed at the surface of IFN-treated HEK-293T in presence of B18R, suggesting that a large part of the viral protein antagonist activity depends on the pool of newly synthesized molecules. This notion is indeed further supported by the fact that surface expression of newly synthesized BST-2 is strongly reduced when Vpu expression is induced, while the pool of BST-2 molecules that reached the surface prior to induction of the viral protein is only slightly-to-moderately affected (Figure 8). These data provide direct evidence that Vpu blocks the re-supply of BST-2 from the pool of newly synthesized proteins. In contrast to its differential effect on the pool of cell-surface BST-2 in HeLa and Jurkat cells, Vpu blocked the re-supply of the restriction factor to the plasma membrane in these cells with a comparable efficiency, suggesting that this strategy is employed by the viral protein independently of the cell type. Interestingly, Vpu S52D,S56D, which is unable to mediate BST-2 degradation but is still able to redistribute the restriction factor particularly in the TGN (32), also blocked BST-2 re-supply. Therefore, the inefficient re-supply of surface BST-2 in presence of Vpu appears mainly caused by a slower transport of newly synthesized BST-2 en route to the plasma membrane. Nonetheless, the role of β-TrCP in this process is clearly important since the WT Vpu protein was more efficient than Vpu S52D,S56D at downregulating *de novo*-synthesized BST-2 molecules (Figure 8). These results suggest that Vpu would optimally block the re-supply of BST2 by using a β-TrCP-independent sequestration mechanism, as reported previously (32, 38), together

with a β-TrCP-dependent process that targets the restriction factor for degradation in the lysosomes (29, 37, 39).

While this manuscript was in preparation, Schmidt et al. (63) reported that Vpu blocked the recycling and biosynthetic transport of BST-2 to overcome the restriction to virion release. While, overall, our results agree with the conclusion of this study (ie: effect of Vpu on both the surface and newly synthesized pools of BST-2), they are inconsistent with their conclusion that interference of Vpu with BST-2 biosynthetic and post-endocytic transport pathways does not require recruitment of β-TrCP. Schmidt et al. reported that whereas a phosphoserine-defective mutant of Vpu failed to interfere with both BST-2 transport pathways, siRNA-directed depletion of β-TrCP did not affect significantly the Vpu-mediated block of BST-2 recycling. While the phenotype of Vpu S52A,56A suggests a defect unrelated to β-TrCP, the concurring phenotypes of the Vpu S52D,56D mutant and WT Vpu in β-TrCP2 depleted cells confirm the importance of this cellular factor for optimal Vpu-mediated downregulation of BST-2 at the cell surface (Figure 2 and Figure S1). This discrepancy could be attributed to the different Vpu mutants (S52A,56A vs S52D,56D) used in these studies.

Beside its broad anti-viral activity, BST-2 was identified as the ligand of the immunoglobulin-like transcript 7 (ILT7) receptor expressed at the surface of plasmacytoid dendritic cells (pDC's) and as such, was proposed to play a critical role in regulating the human pDC's IFN responses through ILT7 in a negative feedback manner (64). Such a role would imply that a tight and highly dynamic control of cell-surface BST-2 expression must exist. Based on our results, it is tempting to speculate that a reduced BST-2 re-supply in response to a decreased IFN concentration in the extracellular milieu coupled to a two-step clearance process from the plasma membrane- that includes a rapid internalization step that allows ~40% of molecules to be internalized in 20-30

minutes (32, 36, 39) and a slower step that clears remaining molecules within ~24hr (Figure 4) would allow cells to rapidly re-establish surface BST-2 levels present prior to IFN exposure. The results of our current study reveal that Vpu would use a similar strategy to rapidly downregulates BST-2 prior to the onset of viral budding. This strategy, which leads to a net but incomplete depletion of BST-2 from the surface, would involve two processes: 1) a β-TrCP-dependent acceleration of the natural clearance of BST-2 from the plasma membrane, with a variable efficiency depending of the cell type and importantly, 2) a block of BST-2 re-supply via the biosynthetic route through sequestration of molecules in a post-ER compartment, likely the TGN, and their β-TrCP-mediated sorting towards lysosomes for degradation.

Materials and methods

***Plasmid constructs*.** HxBH10-*vpu*+, HxBH10-*vpu*- and HxBH10-*vpu S52D,S56D* are isogenic infectious molecular clones of HIV-1 that differ only for *vpu* expression (32). HxBH10.GFP.IRES.*nef*- variants were constructed by introducing the BamHI-GFP.IRES.*nef*-XhoI fragment from HxBru.ADA.GFP.IRES.*nef*- (65) into the HxBH10 molecular clones. To construct HIV-1.rtTA.MA-EGFP-*vpu-/vpu*+/*vpu S52D,S56D,* the BssHII-SphI fragment from HIV.rtTA (43) was first replaced by the corresponding fragment from pNL4.3.MA-EGFP (66) to generate HIV-1.rtTA.MA-EGFP. Then, the SalI-BamHI fragments from HxBH10-*vpu-,* HxBH10-*vpu*+ or HxBH10-*vpu S52D,S56D* were introduced into HIV-1.rtTA.MA-EGFP to generate the isogenic HIV-1.rtTA.MA-EGFP.*vpu-,* HIV-1.rtTA.MA-EGFP.*vpu*+ and HIV-1.rtTA.MA-EGFP.*vpu S52D,S56D* proviral constructs. All constructs were validated by automatic DNA sequencing. The vesicular stomatitis virus (VSV) glycoprotein G-expressing plasmid, pSVCMVin-VSV-G, was previously described (32).

Antibodies and chemical compounds. The anti-Vpu and anti-BST-2 rabbit sera were described previously (32). Monoclonal anti-p17 Abs (catalog no. HB-8975), which recognize p17 but not the $p55^{Gag}$ precursor, and monoclonal anti-p24 Abs (catalog no. HB9725) were isolated from the supernatant of cultured hybridoma cells obtained from the American Type Culture Collection (ATCC). Polyclonal sheep anti-TGN46 (Serotec), mouse anti-BST-2 (Abnova), monoclonal mouse anti-CD81 (BD Pharmingen), mouse anti-CD63 (Hybridoma Bank [NICHD, University of Iowa]), mouse anti-LDLR (Santa Cruz Biotechnology), rabbit anti-Rab11a (Abcam) and mouse anti-Rab5 (BD transduction laboratories), mouse anti-Rab9 (Calbiochem, mouse anti-CD59 (BD Pharmingen) Abs, PE-coupled anti-p24 (Beckman Coulter) and transferrin conjugates-594 (Molecular Probe) were all obtained, as indicated, from commercial sources. All secondary Alexa-conjugated IgG Abs were obtained from Invitrogen. Human interferon-α and recombinant B18R were purchased from PBL Interferon Source and eBioscience, respectively, concanamycin A was obtained from MP Biochemicals, whereas Dox and monensin were purchased from Sigma. All reagents were stored according to the manufacturer's instructions.

Cells and transfection. HEK 293T, HeLa and Jurkat cells were obtained from ATCC. HEK-blue IFN-α/β^{TM} cells were obtained from InvivoGen. All cells were maintained as described previously (14).

The β-TrCP2–depleted cell line was generated by transducing HeLa cells with a pGIPZ lentiviral vecteur expressing a shRNAmir targeting specifically β-TrCP2 (shRNAmir #187 provided by Open Biosystems). The sequence of β-TrCP2 targeted by the shRNAmir is TGCCAATTATCTGTTTGAAATA, located in the 3' UTR of the complete β -TrCP2 cDNA. Lentiviral vectors were produced in 293T cells according to the manufacturer instructions. Transduced cells were selected using 1 µg/ml puromycin (Sigma-Aldrich). The control HeLa cell line was

generated by the same procedure using a non-silencing pGIPZ lentiviral shRNAmir control obtained from Open Biosystem .

HEK 293T, HeLa and Jurkat cells were transfected using the calcium-phosphate method, lipofectamine 2000™ and lipofectamine LTX™ (Invitrogen), respectively. Transfected cells were analyzed 48h post-transfection.

***Virus particle release assay*.** The viral particle release assay was described previously (14). Briefly, supernatants of transfected cells were clarified by centrifugation and filtered through a 45µm filter. Virus particles were pelleted by ultracentrifugation onto a 20% sucrose cushion in PBS for 2h at 130000 g at 4°C. Viruses and cells were lysed in radio-immunoprecipitation assay (RIPA-DOC) buffer (10 mM Tris pH 7.2, 140 mM NaCl, 8 mM Na_2HPO_4, 2 mM NaH_2PO_4, 1% Nonidet-P40, 0.5% sodium dodecyl sulfate, 1.2 mM deoxycholate). Proteins from lysates were resolved on 12.5% SDS-PAGE, electro-blotted and analyzed by western blot as described previously (14).

***Flow cytometry*.** Cells were washed in PBS, resuspended at a concentration of $5x10^5$cells/ml and stained with the specific rabbit (or mouse, where indicated) polyclonal anti-BST-2 rabbit serum for 45 min at 4°C. Cells were then washed and stained using appropriate Alexa Fluor-647-coupled secondary Abs for 30 min at 4°C, washed and fixed in 2% PFA. Jurkat cells were also stained with a LIVE⁄DEAD Fixable Aqua Dead Cell Stain Kit (Invitrogen) to exclude dead cells. EGFP-expressing cells or p24-positive cells (as determined by an intracellular staining following Beckman and Coulter's procedures) were then analyzed for surface BST-2 expression by flow cytometry. Normal rabbit serum served as a staining control (grey shades in histograms). Fluorescence intensities were acquired using a FACScalibur flow cytometer (BD Biosciences) and data was analyzed using the FlowJo software v. 7.25 (Treestar). MFI values presented in

histograms correspond to the specific signal obtained after subtraction of the MFI value from the staining control.

***Semi-quantitative RT PCR*.** The depletion of β-TrCP2 was controlled by RT PCR. Total cellular RNA was extracted using the QIAGEN® RNA extraction kit. After DNase (Invitrogen) treatment, total RNA was converted to cDNA using the Superscript II reverse transcriptase kit (Invitrogen). cDNAs were engaged in the PCR reaction using cloned Pfu (Agilent). The sequence of the primers used for β-TrCP2 cDNA amplification were: 5'-ACGAATGGTACGCACTGATCC-3' (sense) and 5'-ACTTCACCCGTGTTCACATCC-3' (antisense). GADPH was also amplified as control using primer sequences 5'-GCCATCAATGACCCCTTCATT-3' (sense); and 5'-TTGACGGTGCCATGGAATTT-3' (antisense). The products of the PCR reactions were analyzed using a conventional semi-quantitative approach on 1,5% agarose gel.

Cell-surface BST-2 clearance assay. Transfected cells were pre-incubated in DMEM + 5% FBS supplemented with the rabbit polyclonal anti-BST-2 serum for 1.5h at 37°C. Cells were then washed and incubated at 37°C in DMEM + 5% FBS with 1 µg/ml Dox for 0h, 3h, 6h, 12h or 24h to initiate internalization of Abs-BST-2 complexes. To measure the BST-2 levels remaining at the surface, cells from each sample were washed and harvested 48h post-transfection in cold PBS-EDTA, stained with an anti-rabbit Alexafluor-647 secondary Ab for 30 min at 4°C, washed, fixed in 2% PFA and analyzed by flow cytometry.

To detect intracellular BST-2, harvested cells were fixed, permeabilized using Cytofix/Cytoperm™ and intracellularly stained with the appropriate secondary Abs following the manufacturer protocol (BD Biosciences) and analyzed by flow cytometry.

Production of VSV-G-pseudotyped HIV-1 virus. HEK 293T cells were transfected with HxBH10 proviral constructs and pSVCMVin-VSV-G as described previously (32). Supernatants of transfected cells were clarified, filtered and pelleted by ultracentrifugation as described above and resuspended in DMEM supplemented with 10% bovine serum (FBS). Viruses were titrated using a standard MAGI assay as previously described (32).

Confocal microscopy. Jurkat were infected with VSV-G-pseudotyped HxBH10-derived viruses at a MOI of 0.125 with polybrene. Forty-eight hours post-infection, cells were immunostained with the indicated Abs (BST-2, CD81, CD59 and/or CD63) for 45 min at 4°C prior to extensive washes. Cells were then centrifuged at 4°C for 20 min on poly-D-lysine-treated coverslips and fixed for 30 min in 4% PFA. To detect p17, fixed cells were permeabilized in Triton 0.2% for 5 min, incubated for 2h at 37°C in 5% milk-PBS containing anti-p17 Abs, washed and incubated with the appropriate secondary Ab for 30 min at room temperature. Steady-state intracellular localization of BST-2 was performed as described previously (14). To study intracellular localization of internalized BST-2, coverslips-seeded HeLa cells were transfected with HIV-1.rtTA.MA-GFP proviral constructs. Thirty-six hours later, cells were incubated at 37°C for 0-12h in media containing rabbit anti-BST-2 serum as well as 1 µg/ml Dox to trigger viral protein expression. Twelve hours later, transfected cells were fixed, permeabilized with 0.2% Triton and stained for the indicated cellular markers for 2h at 37°C. Following extensive washes, cells were stained at room temperature for 30 min with Alexa Fluor 594 or 647-coupled secondary Abs to detect internalized BST-2 and the cellular markers. All analyses were acquired using a 63x Plan Apochromat oil immersion objective with an aperture of 1.4 on a LSM710 Observer Z1 laser scanning confocal microscope coupled with a Kr/Ar laser (488-, 594- and 633-nm lines) (Zeiss).

Type I IFN detection. 20 µl of the supernatant of HEK293T was added to a suspension of 50 000 HEK-blue IFN-α/β^{TM} cells in 180 µl DMEM containing 10% heat-inactivated FBS and incubated for 24h at 37°C. To quantitate secreted placental alkaline phosphatase (SEAP) in culture supernatants, 40 µl of HEK-blue cell supernatant were added to 160 µl of QUANTI-Blue reagent (InvivoGen) and incubated for 20 min at 37°C. SEAP levels were evaluated using a spectrophotometer at 620 nm.

Supporting information. Figure S1 depicts the effect of Vpu on the kinetics of cell-surface BST-2 downregulation in β-TrCP2-depleted cells. Figure S2 shows the steady-state localization of intracellular BST-2 in fixed cells. Figure S3 illustrates the pathway followed by internalized BST-2 to ultimately reach lysosomal compartments. Figure S4 shows the inhibitory effect of recombinant B18R on the IFN-induced upregulation of BST-2 at the cell surface and the production of active endogenous IFN in the extracellular media.

Acknowledgments

We thank Dr. Ben Berkhout (University of Amsterdam) and Dr. Hans-Georg Kräusslich (University of Heidelberg) for their kind gifts of the HIV-1.rtTA and pNL4.3-EGFP proviral constructs. We also want to thank present and former members of the Cohen laboratory for helpful discussion. Finally, the authors would like to thanks members of the Canadian Institutes of Health Research (CIHR) Team in HIV pathogenesis for helpful discussions. This work was performed by MD in partial fulfillment of his doctoral thesis. This work was supported by grants from CIHR (HET 85519 and MOP111226) and from the Fonds de la Recherche en Santé du Québec (FRSQ) to E.A.C. M.D. is recipient

of a Banting and Best studentship from the CIHR. E.A.C. holds the Canada research chair in human retrovirology.

References

1. Malim MH, Emerman M. HIV-1 accessory proteins--ensuring viral survival in a hostile environment. Cell Host Microbe 2008;3(6):388-398.

2. Dube M, Bego MG, Paquay C, Cohen EA. Modulation of HIV-1-host interaction: role of the Vpu accessory protein. Retrovirology 2010;7:114.

3. Binette J, Dube M, Mercier J, Cohen EA. Requirements for the selective degradation of CD4 receptor molecules by the human immunodeficiency virus type 1 Vpu protein in the endoplasmic reticulum. Retrovirology 2007;4(1):75.

4. Magadan JG, Perez-Victoria FJ, Sougrat R, Ye Y, Strebel K, Bonifacino JS. Multilayered mechanism of CD4 downregulation by HIV-1 Vpu involving distinct ER retention and ERAD targeting steps. PLoS Pathog 2010;6(4):e1000869.

5. Margottin F, Bour SP, Durand H, Selig L, Benichou S, Richard V, Thomas D, Strebel K, Benarous R. A novel human WD protein, h-beta TrCp, that interacts with HIV-1 Vpu connects CD4 to the ER degradation pathway through an F-box motif. Mol Cell 1998;1(4):565-574.

6. Wildum S, Schindler M, Munch J, Kirchhoff F. Contribution of Vpu, Env, and Nef to CD4 down-modulation and resistance of human immunodeficiency virus type 1-infected T cells to superinfection. J Virol 2006;80(16):8047-8059.

7. Cortes MJ, Wong-Staal F, Lama J. Cell surface CD4 interferes with the infectivity of HIV-1 particles released from T cells. J Biol Chem 2002;277(3):1770-1779.

8. Van Damme N, Goff D, Katsura C, Jorgenson RL, Mitchell R, Johnson MC, Stephens EB, Guatelli J. The interferon-induced protein BST-2 restricts HIV-1

release and is downregulated from the cell surface by the viral Vpu protein. Cell Host Microbe 2008;3(4):245-252.

9. Neil SJ, Zang T, Bieniasz PD. Tetherin inhibits retrovirus release and is antagonized by HIV-1 Vpu. Nature 2008;451(7177):425-430.

10. Kupzig S, Korolchuk V, Rollason R, Sugden A, Wilde A, Banting G. Bst-2/HM1.24 is a raft-associated apical membrane protein with an unusual topology. Traffic 2003;4(10):694-709.

11. Perez-Caballero D, Zang T, Ebrahimi A, McNatt MW, Gregory DA, Johnson MC, Bieniasz PD. Tetherin inhibits HIV-1 release by directly tethering virions to cells. Cell 2009;139(3):499-511.

12. Andrew AJ, Miyagi E, Kao S, Strebel K. The formation of cysteine-linked dimers of BST-2/tetherin is important for inhibition of HIV-1 virus release but not for sensitivity to Vpu. Retrovirology 2009;6:80.

13. Blasius AL, Giurisato E, Cella M, Schreiber RD, Shaw AS, Colonna M. Bone marrow stromal cell antigen 2 is a specific marker of type I IFN-producing cells in the naive mouse, but a promiscuous cell surface antigen following IFN stimulation. J Immunol 2006;177(5):3260-3265.

14. Dube M, Roy BB, Guiot-Guillain P, Mercier J, Binette J, Leung G, Cohen EA. Suppression of Tetherin-restricting activity upon human immunodeficiency virus type 1 particle release correlates with localization of Vpu in the trans-Golgi network. J Virol 2009;83(9):4574-4590.

15. Masuyama N, Kuronita T, Tanaka R, Muto T, Hirota Y, Takigawa A, Fujita H, Aso Y, Amano J, Tanaka Y. HM1.24 is internalized from lipid rafts by clathrin-mediated endocytosis through interaction with alpha-adaptin. J Biol Chem 2009;284(23):15927-15941.

16. Habermann A, Krijnse-Locker J, Oberwinkler H, Eckhardt M, Homann S, Andrew A, Strebel K, Krausslich HG. CD317/tetherin is enriched in the HIV-1

envelope and downregulated from the plasma membrane upon virus infection. J Virol 2010;84(9):4646-4658.

17. Rollason R, Korolchuk V, Hamilton C, Jepson M, Banting G. A CD317/tetherin-RICH2 complex plays a critical role in the organization of the subapical actin cytoskeleton in polarized epithelial cells. J Cell Biol 2009;184(5):721-736.

18. Waheed AA, Ablan SD, Soheilian F, Nagashima K, Ono A, Schaffner CP, Freed EO. Inhibition of human immunodeficiency virus type 1 assembly and release by the cholesterol-binding compound amphotericin B methyl ester: evidence for Vpu dependence. Journal of Virology 2008;82(19):9776-9781.

19. Evans DT, Serra-Moreno R, Singh RK, Guatelli JC. BST-2/tetherin: a new component of the innate immune response to enveloped viruses. Trends Microbiol 2010;18(9):388-396.

20. Hammonds J, Wang JJ, Yi H, Spearman P. Immunoelectron microscopic evidence for Tetherin/BST2 as the physical bridge between HIV-1 virions and the plasma membrane. PLoS Pathog 2010;6(2):e1000749.

21. Fitzpatrick K, Skasko M, Deerinck TJ, Crum J, Ellisman MH, Guatelli J. Direct restriction of virus release and incorporation of the interferon-induced protein BST-2 into HIV-1 particles. PLoS Pathog 2010;6(3):e1000701.

22. Hinz A, Miguet N, Natrajan G, Usami Y, Yamanaka H, Renesto P, Hartlieb B, McCarthy AA, Simorre JP, Gottlinger H, Weissenhorn W. Structural basis of HIV-1 tethering to membranes by the BST-2/tetherin ectodomain. Cell Host Microbe 2010;7(4):314-323.

23. Schubert HL, Zhai Q, Sandrin V, Eckert DM, Garcia-Maya M, Saul L, Sundquist WI, Steiner RA, Hill CP. Structural and functional studies on the extracellular domain of BST2/tetherin in reduced and oxidized conformations. Proc Natl Acad Sci U S A 2010;107(42):17951-17956.

24. Yang H, Wang J, Jia X, McNatt MW, Zang T, Pan B, Meng W, Wang HW, Bieniasz PD, Xiong Y. Structural insight into the mechanisms of enveloped virus tethering by tetherin. Proc Natl Acad Sci U S A 2010;107(43):18428-18432.

25. Swiecki M, Scheaffer SM, Allaire M, Fremont DH, Colonna M, Brett TJ. Structural and biophysical analysis of BST-2/tetherin ectodomains reveals an evolutionary conserved design to inhibit virus release. The Journal of biological chemistry 2011;286(4):2987-2997.

26. Gupta RK, Hue S, Schaller T, Verschoor E, Pillay D, Towers GJ. Mutation of a single residue renders human tetherin resistant to HIV-1 Vpu-mediated depletion. PLoS Pathog 2009;5(5):e1000443.

27. Mangeat B, Gers-Huber G, Lehmann M, Zufferey M, Luban J, Piguet V. HIV-1 Vpu neutralizes the antiviral factor Tetherin/BST-2 by binding it and directing its beta-TrCP2-dependent degradation. PLoS Pathog 2009;5(9):e1000574.

28. Goffinet C, Allespach I, Homann S, Tervo HM, Habermann A, Rupp D, Oberbremer L, Kern C, Tibroni N, Welsch S, Krijnse-Locker J, Banting G, Krausslich HG, Fackler OT, Keppler OT. HIV-1 antagonism of CD317 is species specific and involves Vpu-mediated proteasomal degradation of the restriction factor. Cell Host Microbe 2009;5(3):285-297.

29. Douglas JL, Viswanathan K, McCarroll MN, Gustin JK, Fruh K, Moses AV. Vpu directs the degradation of the human immunodeficiency virus restriction factor BST-2/Tetherin via a {beta}TrCP-dependent mechanism. J Virol 2009;83(16):7931-7947.

30. Rong L, Zhang J, Lu J, Pan Q, Lorgeoux RP, Aloysius C, Guo F, Liu SL, Wainberg MA, Liang C. The transmembrane domain of BST-2 determines its sensitivity to down-modulation by human immunodeficiency virus type 1 Vpu. J Virol 2009;83(15):7536-7546.

31. Iwabu Y, Fujita H, Kinomoto M, Kaneko K, Ishizaka Y, Tanaka Y, Sata T, Tokunaga K. HIV-1 accessory protein Vpu internalizes cell-surface BST-2/tetherin through transmembrane interactions leading to lysosomes. J Biol Chem 2009;284(50):35060-35072.

32. Dube M, Roy BB, Guiot-Guillain P, Binette J, Mercier J, Chiasson A, Cohen EA. Antagonism of tetherin restriction of HIV-1 release by Vpu involves binding and sequestration of the restriction factor in a perinuclear compartment. PLoS Pathog 2010;6(4):e1000856.

33. Kobayashi T, Ode H, Yoshida T, Sato K, Gee P, Yanamato S, Ebina H, Strebel K, Sato H, Koyanagi Y. Identification of amino acids in the human tetherin transmembrane domain responsible for HIV-1 Vpu interaction and susceptibility. J Virol 2011;85(2):932-945.

34. Vigan R, Neil SJ. Determinants of tetherin antagonism in the transmembrane domain of the human immunodeficiency virus type 1 vpu protein. J Virol 2010;84(24):12958-12970.

35. Miyagi E, Andrew AJ, Kao S, Strebel K. Vpu enhances HIV-1 virus release in the absence of Bst-2 cell surface down-modulation and intracellular depletion. Proc Natl Acad Sci U S A 2009;106(8):2868-2873.

36. Mitchell RS, Katsura C, Skasko MA, Fitzpatrick K, Lau D, Ruiz A, Stephens EB, Margottin-Goguet F, Benarous R, Guatelli JC. Vpu antagonizes BST-2-mediated restriction of HIV-1 release via beta-TrCP and endo-lysosomal trafficking. PLoS Pathog 2009;5(5):e1000450.

37. Janvier K, Pelchen-Matthews A, Renaud JB, Caillet M, Marsh M, Berlioz-Torrent C. The ESCRT-0 Component HRS is Required for HIV-1 Vpu-Mediated BST-2/Tetherin Down-Regulation. PLoS pathogens 2011;7(2):e1001265.

38. Hauser H, Lopez LA, Yang SJ, Oldenburg JE, Exline CM, Guatelli JC, Cannon PM. HIV-1 Vpu and HIV-2 Env counteract BST-2/tetherin by sequestration in a perinuclear compartment. Retrovirology 2010;7:51.

39. Andrew AJ, Miyagi E, Strebel K. Differential Effects of Human Immunodeficiency Virus Type 1 Vpu on the Stability of BST-2/Tetherin. Journal of Virology 2011;85(6):2611-2619.

40. Tervo HM, Homann S, Ambiel I, Fritz JV, Fackler OT, Keppler OT. beta-TrCP is dispensable for Vpu's ability to overcome the CD317/Tetherin-imposed restriction to HIV-1 release. Retrovirology 2011;8(1):9.

41. Goffinet C, Homann S, Ambiel I, Tibroni N, Rupp D, Keppler OT, Fackler OT. Antagonism of CD317 restriction of HIV-1 particle release and depletion of CD317 are separable activities of HIV-1 Vpu. J Virol 2010;84(8):4089-4094.

42. Schwartz S, Felber BK, Fenyo EM, Pavlakis GN. Env and Vpu proteins of human immunodeficiency virus type 1 are produced from multiple bicistronic mRNAs. J Virol 1990;64(11):5448-5456.

43. Das AT, Zhou X, Vink M, Klaver B, Verhoef K, Marzio G, Berkhout B. Viral evolution as a tool to improve the tetracycline-regulated gene expression system. J Biol Chem 2004;279(18):18776-18782.

44. Jouvenet N, Neil SJ, Zhadina M, Zang T, Kratovac Z, Lee Y, McNatt M, Hatziioannou T, Bieniasz PD. Broad-spectrum inhibition of retroviral and filoviral particle release by tetherin. J Virol 2009;83(4):1837-1844.

45. Nydegger S, Khurana S, Krementsov DN, Foti M, Thali M. Mapping of tetraspanin-enriched microdomains that can function as gateways for HIV-1. J Cell Biol 2006;173(5):795-807.

46. Waheed AA, Freed EO. Lipids and membrane microdomains in HIV-1 replication. Virus Res 2009;143(2):162-176.

47. Skasko M, Tokarev A, Chen CC, Fischer WB, Pillai SK, Guatelli J. BST-2 is rapidly down-regulated from the cell surface by the HIV-1 protein Vpu: Evidence for a post-ER mechanism of Vpu-action. Virology 2011;411(1):65-77.

48. Bucci C, Parton RG, Mather IH, Stunnenberg H, Simons K, Hoflack B, Zerial M. The small GTPase rab5 functions as a regulatory factor in the early endocytic pathway. Cell 1992;70(5):715-728.

49. Ullrich O, Reinsch S, Urbe S, Zerial M, Parton RG. Rab11 regulates recycling through the pericentriolar recycling endosome. The Journal of cell biology 1996;135(4):913-924.

50. Wan L, Molloy SS, Thomas L, Liu G, Xiang Y, Rybak SL, Thomas G. PACS-1 defines a novel gene family of cytosolic sorting proteins required for trans-Golgi network localization. Cell 1998;94(2):205-216.

51. Ganley IG, Carroll K, Bittova L, Pfeffer S. Rab9 GTPase regulates late endosome size and requires effector interaction for its stability. Molecular biology of the cell 2004;15(12):5420-5430.

52. Kobayashi T, Vischer UM, Rosnoblet C, Lebrand C, Lindsay M, Parton RG, Kruithof EK, Gruenberg J. The tetraspanin CD63/lamp3 cycles between endocytic and secretory compartments in human endothelial cells. Molecular biology of the cell 2000;11(5):1829-1843.

53. Basu SK, Goldstein JL, Anderson RG, Brown MS. Monensin interrupts the recycling of low density lipoprotein receptors in human fibroblasts. Cell 1981;24(2):493-502.

54. Stein BS, Bensch KG, Sussman HH. Complete inhibition of transferrin recycling by monensin in K562 cells. The Journal of biological chemistry 1984;259(23):14762-14772.

55. Fujita T, Kimura Y, Miyamoto M, Barsoumian EL, Taniguchi T. Induction of endogenous IFN-alpha and IFN-beta genes by a regulatory transcription factor, IRF-1. Nature 1989;337(6204):270-272.

56. Symons JA, Alcami A, Smith GL. Vaccinia virus encodes a soluble type I interferon receptor of novel structure and broad species specificity. Cell 1995;81(4):551-560.

57. Alain T, Lun X, Martineau Y, Sean P, Pulendran B, Petroulakis E, Zemp FJ, Lemay CG, Roy D, Bell JC, Thomas G, Kozma SC, Forsyth PA, Costa-Mattioli M, Sonenberg N. Vesicular stomatitis virus oncolysis is potentiated by impairing mTORC1-dependent type I IFN production. Proceedings of the National Academy of Sciences of the United States of America 2010;107(4):1576-1581.

58. Pardieu C, Vigan R, Wilson SJ, Calvi A, Zang T, Bieniasz P, Kellam P, Towers GJ, Neil SJ. The RING-CH ligase K5 antagonizes restriction of KSHV and HIV-1 particle release by mediating ubiquitin-dependent endosomal degradation of tetherin. PLoS Pathog 2010;6(4):e1000843.

59. Tokarev AA, Munguia J, Guatelli JC. Serine-threonine ubiquitination mediates downregulation of BST-2/tetherin and relief of restricted virion release by HIV-1 Vpu. J Virol 2011;85(1):51-63.

60. Waterman H, Katz M, Rubin C, Shtiegman K, Lavi S, Elson A, Jovin T, Yarden Y. A mutant EGF-receptor defective in ubiquitylation and endocytosis unveils a role for Grb2 in negative signaling. Embo J 2002;21(3):303-313.

61. Kumar KG, Krolewski JJ, Fuchs SY. Phosphorylation and specific ubiquitin acceptor sites are required for ubiquitination and degradation of the IFNAR1 subunit of type I interferon receptor. The Journal of biological chemistry 2004;279(45):46614-46620.

62. Iwabu Y, Fujita H, Tanaka Y, Sata T, Tokunaga K. Direct internalization of cell-surface BST-2/tetherin by the HIV-1 accessory protein Vpu. Commun Integr Biol 2010;3(4):366-369.

63. Schmidt S, Fritz JV, Bitzegeio J, Fackler OT, Keppler OT. HIV-1 Vpu Blocks Recycling and Biosynthetic Transport of the Intrinsic Immunity Factor CD317/Tetherin To Overcome the Virion Release Restriction. MBio 2011;2(3).

64. Cao W, Bover L, Cho M, Wen X, Hanabuchi S, Bao M, Rosen DB, Wang YH, Shaw JL, Du Q, Li C, Arai N, Yao Z, Lanier LL, Liu YJ. Regulation of TLR7/9 responses in plasmacytoid dendritic cells by BST2 and ILT7 receptor interaction. J Exp Med 2009;206(7):1603-1614.

65. Richard J, Sindhu S, Pham TN, Belzile JP, Cohen EA. HIV-1 Vpr up-regulates expression of ligands for the activating NKG2D receptor and promotes NK cell-mediated killing. Blood 2010;115(7):1354-1363.

66. Muller B, Daecke J, Fackler OT, Dittmar MT, Zentgraf H, Krausslich HG. Construction and characterization of a fluorescently labeled infectious human immunodeficiency virus type 1 derivative. J Virol 2004;78(19):10803-10813.

Figure 1: Characterization of inducible HIV-1 proviral constructs.

(A) Schematic representation of the HIV-1.rtTA.MA-EGFP genomic organization. rtTA consists of the DNA binding domain (BD) of the tetracycline repressor fused to herpes simplex virus VP16 activation domains (AD) (B-C) Characterization of HIV-1.rtTA.MA-EGFP proviral constructs. HeLa cells were transfected with the indicated constructs and treated or not with 0.25-1 µg/ml of Dox for 48h. (B) Virus and cell lysates were analyzed by western blot using anti-p24 or anti-Vpu Abs. (C) Transfected cells from (B) were stained for surface BST-2. The graph depicts levels of surface BST-2 on EGFP-positive cells except for the EGFP-negative control (EGFP-).

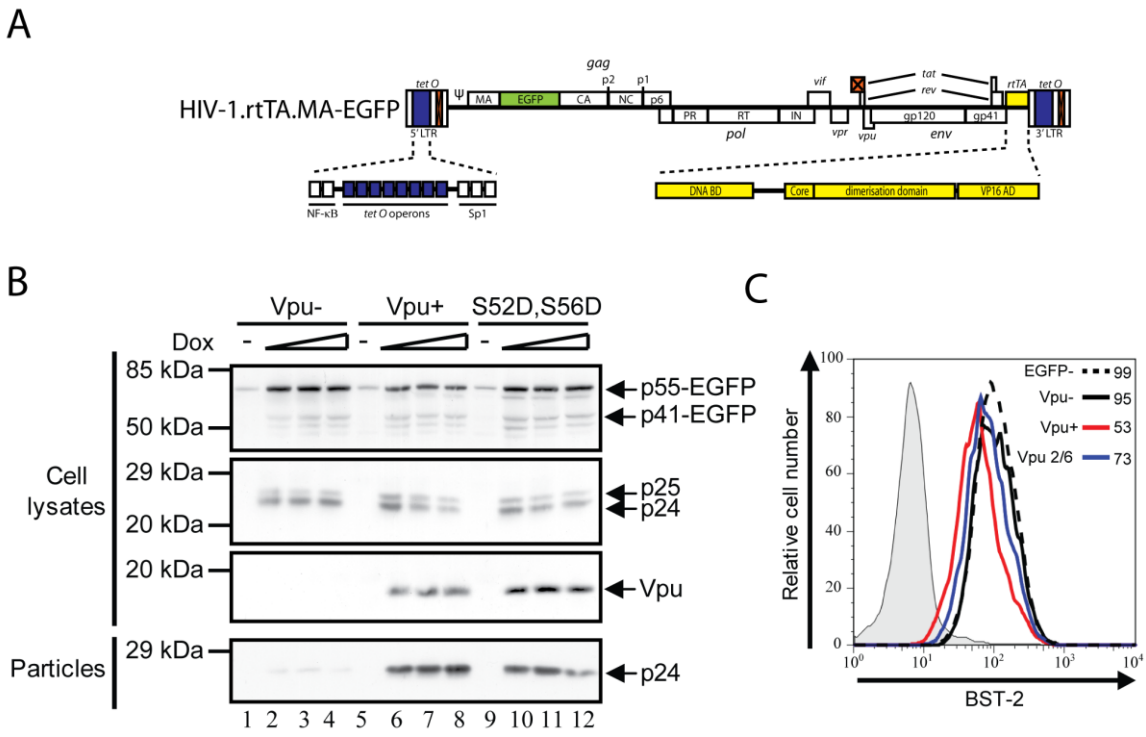
A
HIV-1.rtTA.MA-EGFP
tet O
Ψ
gag
p2
p1
MA
EGFP
CA
NC
p6
vif
tat
rev
rtTA
tet O
PR
RT
IN
pol
vpr
vpu
gp120
gp41
env
5' LTR
3' LTR
NF-κB
tet O operons
Sp1
DNA BD
Core
dimerisation domain
VP16 AD
B
Vpu-
Vpu+
S52D,S56D
Dox
85 kDa
50 kDa
29 kDa
20 kDa
20 kDa
29 kDa
Cell lysates
Particles
p55-EGFP
p41-EGFP
p25
p24
Vpu
p24
1 2 3 4 5 6 7 8 9 10 11 12
C
Relative cell number
BST-2
EGFP- 99
Vpu- 95
Vpu+ 53
Vpu 2/6 73

Figure 1

Figure 2: Vpu achieves optimal cell-surface BST-2 downregulation within 6h.

(A) HeLa cells were transfected with the indicated HIV-1.rtTA.MA-EGFP constructs and analyzed 48h post-transfection for surface BST-2 levels by flow cytometry. Prior to analysis, cells were treated for the indicated period of time with 1 µg/ml of Dox. Error bars represent the standard deviation calculated from three independent experiments. (B) Virus-containing supernatants and transfected cells from (A) were processed as described in material and methods to detect Gag proteins by western blot using anti-p24 Abs. The blot for analysis of virus particles was overexposed to detect p24 at early time points. (C) HeLa cells were transfected with the indicated HIV-1.rtTA.MA-EGFP constructs, treated with Dox for 24h and analyzed 48h post-transfection for surface BST-2 expression by flow cytometry. At the indicated time intervals, cells were washed to remove Dox.

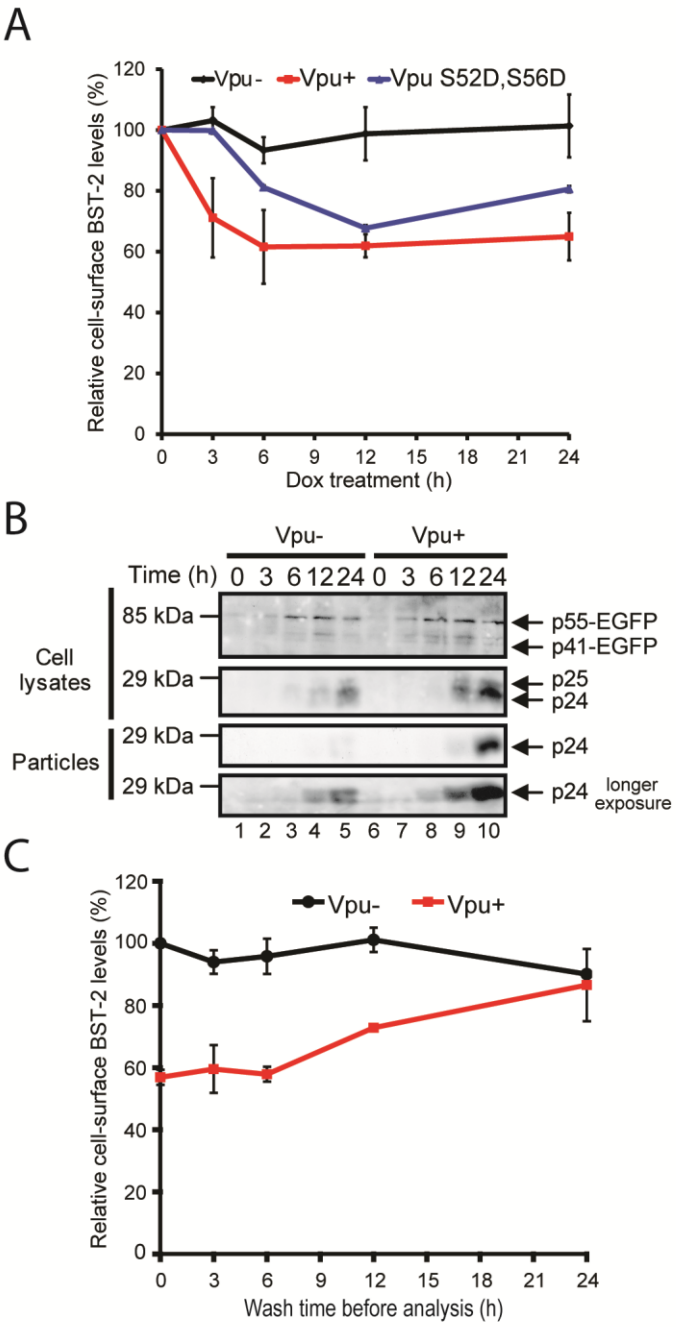
A
Vpu-
Vpu+
Vpu S52D,S56D
Relative cell-surface BST-2 levels (%)
Dox treatment (h)
B
Vpu-
Vpu+
Time (h) 0 3 6 12 24 0 3 6 12 24
85 kDa
p55-EGFP
p41-EGFP
Cell lysates
29 kDa
p25
p24
Particles
29 kDa
p24
29 kDa
p24
longer exposure
1 2 3 4 5 6 7 8 9 10
C
Vpu-
Vpu+
Relative cell-surface BST-2 levels (%)
Wash time before analysis (h)

Figure 2

Figure 3: Distribution of BST-2 at the plasma membrane of HIV-1 infected Jurkat cells.

Jurkat cells were infected with VSV-G-pseudotyped HxBH10.GFP.IRES.*nef-vpu-* or -*vpu*+ viruses. (A) Forty-eight hours post-infection, cells were stained with anti-BST-2 Abs (cyan), fixed, permeabilized and then sequentially stained with anti-p17 Abs (red) and appropriate secondary Abs. In the lower panels (longer exposure), the gain was scaled-up to obtain BST-2 and p17 signals comparable to those detected in the HIV-1(Vpu-)-infected cells from the upper panel. 3x magnifications are shown besides the panels. (B) Jurkat cells infected with VSV-G-pseudotyped HxBH10.GFP.IRES.*nef-vpu-* or -*vpu*+ viruses were stained 48h post-infection with anti-BST-2 Abs. Surface BST-2 levels were analyzed on EGFP-positive cells by flow cytometry. (C) Cells were co-stained with anti-BST-2 Abs (cyan) and anti-CD59, anti-CD81 or anti-CD63 Abs (red) 48h post-infection, and processed as described above prior to staining with appropriate secondary Abs. The gain from Vpu-expressing cells was scaled-up as described above. Nuclei were counterstained with DAPI (blue). Green: GFP. White bar = 10 µm. (D) Quantification of BST-2 co-localization with p17 or cellular markers. The values (%) represent percentages of BST-2 (cyan pixels) overlapping with each marker (red pixels). Error bars indicate the standard deviation of the mean from the quantitative analysis of at least 25 distinct cells.

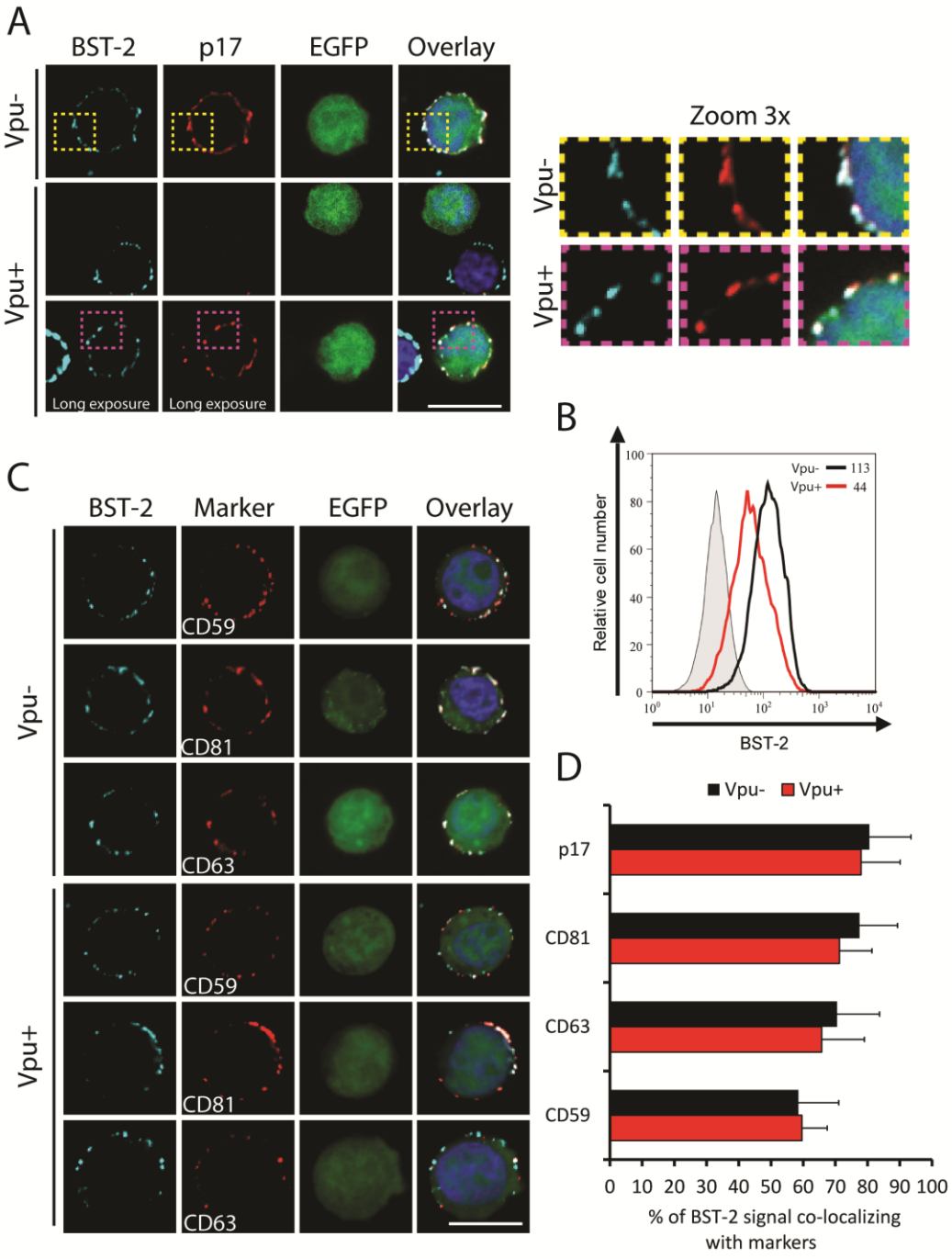
A
BST-2
p17
EGFP
Overlay
Vpu-
Vpu+
Long exposure
Long exposure
Zoom 3x
B
Relative cell number
Vpu- 113
Vpu+ 44
BST-2
C
BST-2
Marker
EGFP
Overlay
CD59
CD81
CD63
D
Vpu-
Vpu+
p17
CD81
CD63
CD59
% of BST-2 signal co-localizing with markers

Figure 3

Figure 4: Kinetics of BST-2 clearance and decay.

(A) Schematic representation of the experiment. (B-C) HeLa cells were transfected with the indicated HIV-1.rtTA.MA-EGFP proviral constructs and analyzed 48h post-transfection for surface BST-2 expression by flow cytometry. Prior to analysis, cells were incubated at 37°C for 1.5h, washed and re-incubated in presence of 1 µg/ml of Dox for the indicated period of time. Cells were then harvested and (A) surface-stained or (B) fixed, permeabilized and stained with appropriate secondary Abs as described. For the samples treated with Dox, levels of BST-2 were evaluated on EGFP-positive cells. Levels of BST-2 at the cell surface at time 0 (no Dox) were monitored on the total population. The graphs depict the surface (A) or total levels (B) of BST-2 relative to time 0. Error bars represent the standard deviation calculated from 3 independent experiments.

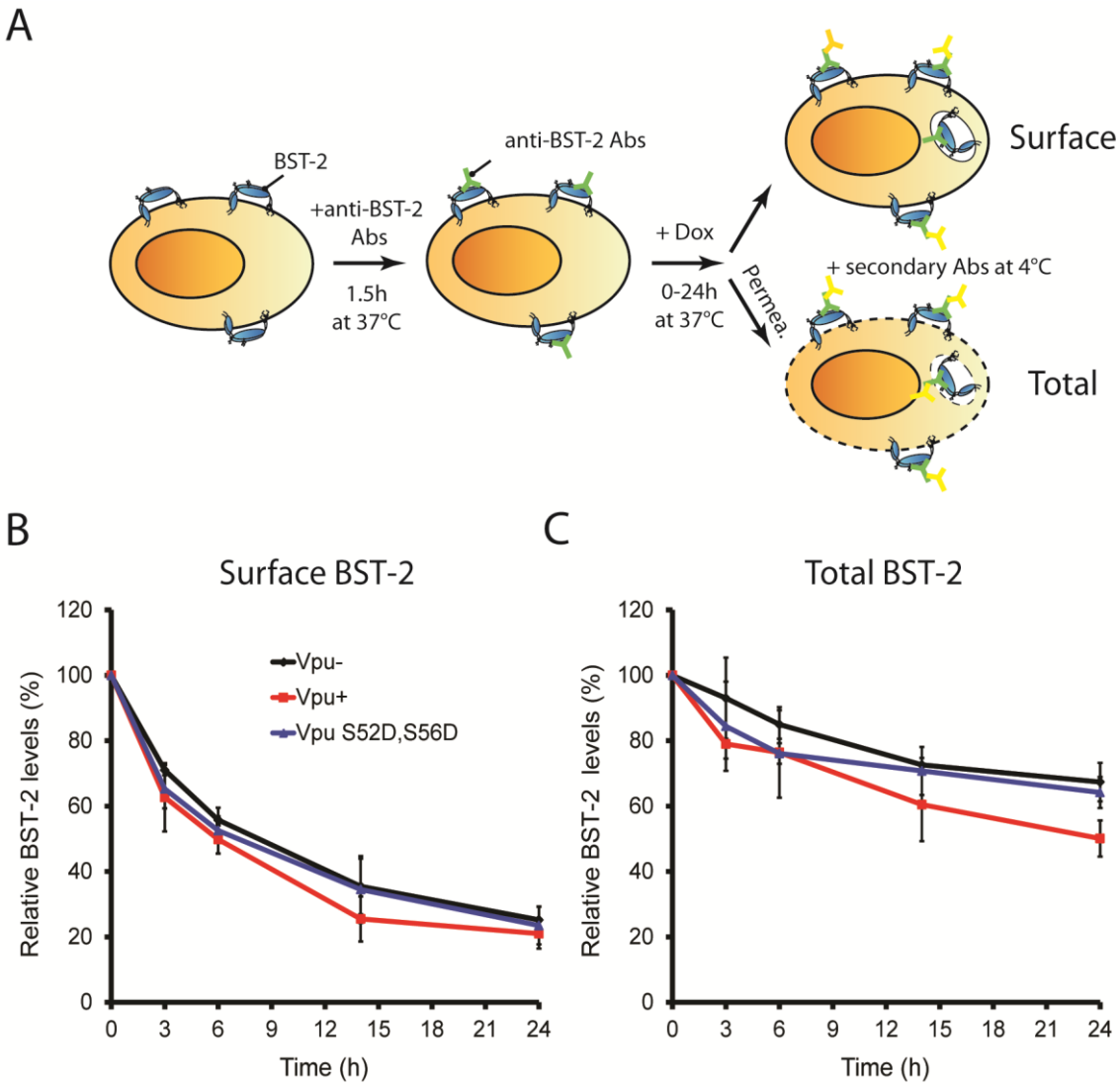
A
BST-2
+anti-BST-2 Abs
1.5h at 37°C
anti-BST-2 Abs
+ Dox
0-24h at 37°C
Permea.
Surface
+ secondary Abs at 4°C
Total
B
Surface BST-2
Relative BST-2 levels (%)
Vpu-
Vpu+
Vpu S52D,S56D
Time (h)
C
Total BST-2
Relative BST-2 levels (%)
Time (h)

Figure 4

Figure 5: Localization of internalized BST-2 molecules.

(A) HeLa cells were incubated at 37°C for 12h in presence of anti-BST-2 Abs, fixed, permeabilized and then stained for the indicated intracellular markers. Stained cells were washed and incubated with appropriate secondary Abs to detect cellular markers (green) as well as internalized BST-2 (red). Nuclei were counterstained with DAPI (blue). Cells were analyzed by confocal microscopy. White arrows highlight example of co-localization between BST-2 and specific cellular markers. White bars = 10μm. (B) Quantification of BST-2 co-localization with cellular markers. The values (%) represent the percentage of BST-2 (red pixels) overlapping with each cellular marker (green pixels). Error bars indicate the standard deviation of the mean from the quantitative analysis of at least 25 distinct cells. (C) Coverslip-seeded HeLa cells were transfected with HIV-1.rtTA.MA-EGFP *vpu*- or *vpu*+. At 36h post-transfection, cells were incubated at 37°C for 12h in presence of Dox and anti-BST-2 Abs, washed, fixed and permeabilized. Cells were then stained for the indicated intracellular makers. Stained cells were extensively washed and incubated with appropriate secondary Abs to detect cellular markers (red) as well as internalized BST-2 (cyan). Nuclei were counterstained with DAPI (blue). Cells were analyzed by confocal microscopy. White arrows highlight examples of co-localization between internalized BST-2 and cellular markers. White bars = 10μm. (D) Quantification of (C) as described in (B).

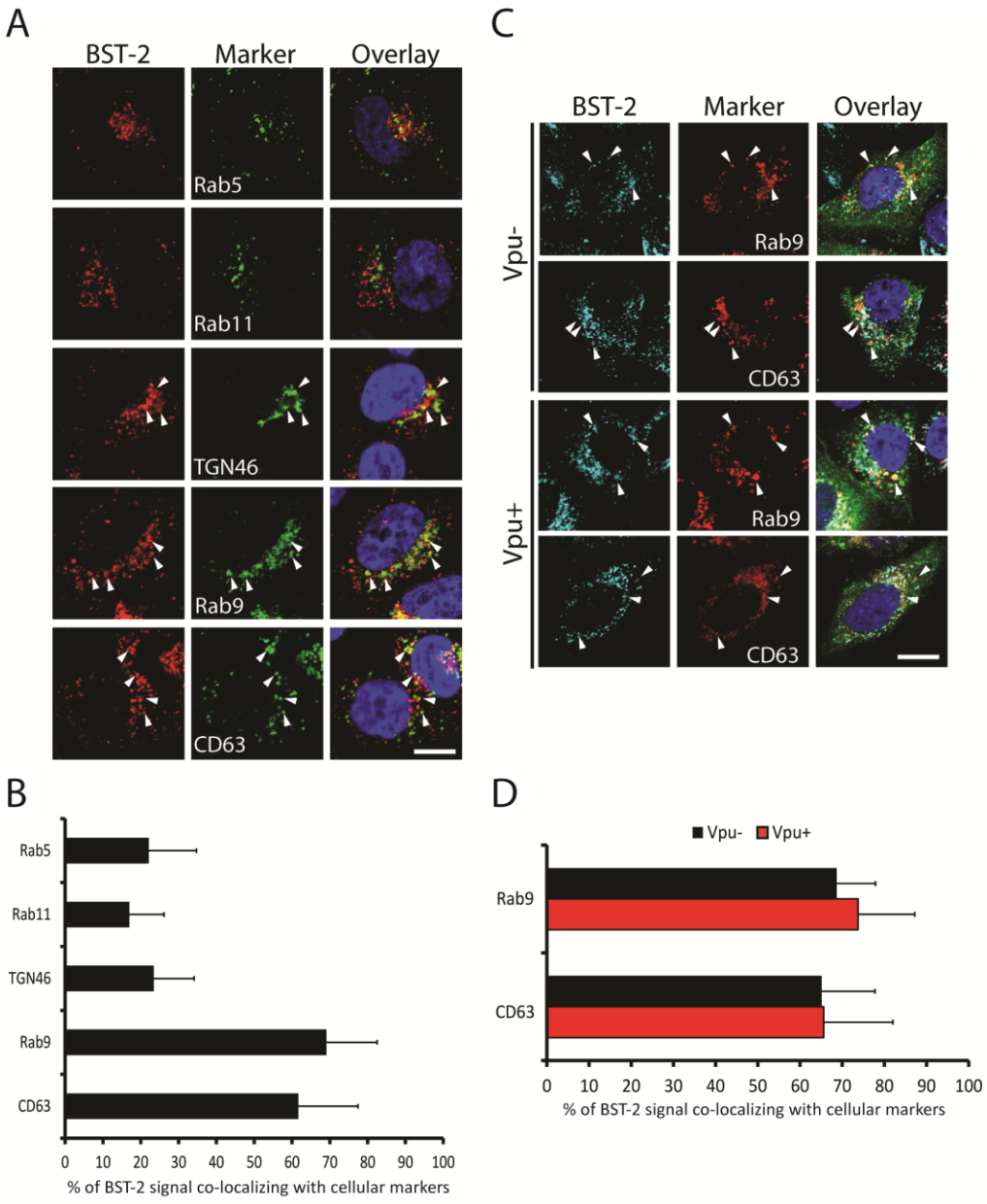
A
BST-2
Marker
Overlay
Rab5
Rab11
TGN46
Rab9
CD63
C
BST-2
Marker
Overlay
Vpu-
Vpu+
Rab9
CD63
Rab9
CD63
B
Rab5
Rab11
TGN46
Rab9
CD63
0 10 20 30 40 50 60 70 80 90 100
% of BST-2 signal co-localizing with cellular markers
D
Vpu- Vpu+
Rab9
CD63
0 10 20 30 40 50 60 70 80 90 100
% of BST-2 signal co-localizing with cellular markers

Figure 5

Figure 6: Effect of Monensin on cell-surface BST-2 expression (A-B) HeLa and (C-D) Jurkat cells were treated with 100 µM monensin for 2h at 37°C. Cell-surface LDLR (A-C) and BST-2 (B-D) levels were then monitored by flow cytometry as described.

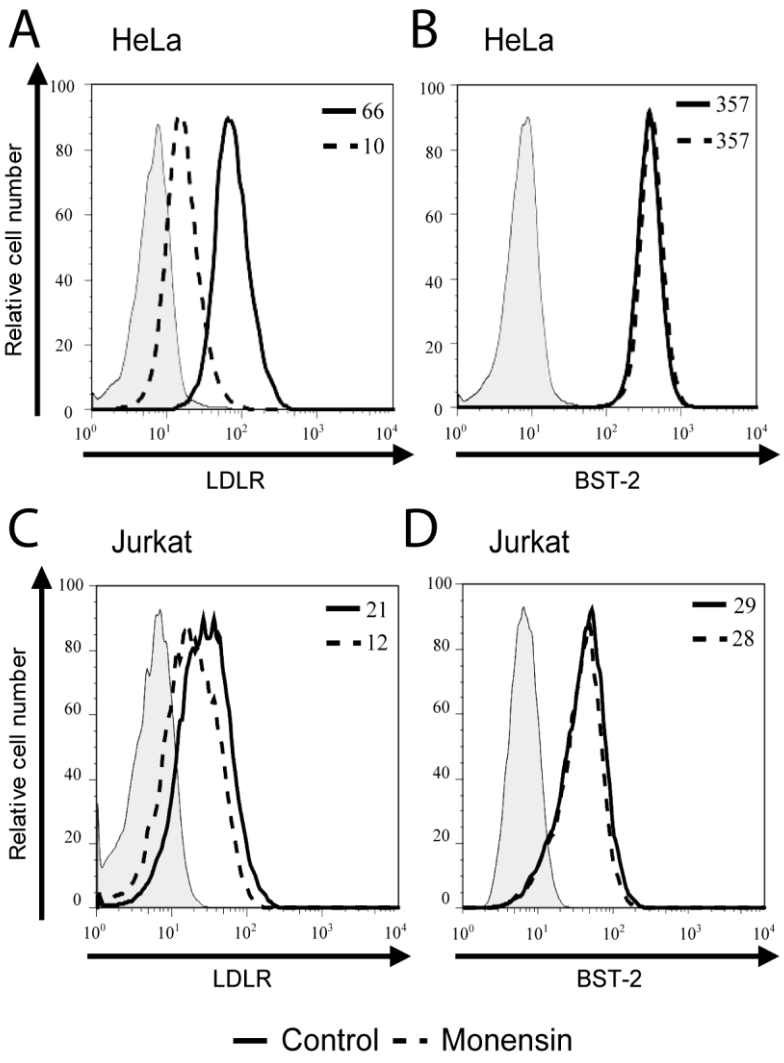
A
HeLa
B
HeLa
Relative cell number
66
10
357
357
LDLR
BST-2
C
Jurkat
D
Jurkat
21
12
29
28
LDLR
BST-2
Control
Monensin

Figure 6

Figure 7: Effect of B18R on Vpu-mediated BST-2 downregulation.

(A) Schematic representation of the experiment. (B-C) HEK293T cells were transfected with the indicated HIV-1.rtTA.MA-EGFP constructs and immediately treated with 1000 U/ml of IFN-α. Forty-two hours post-transfection, 1 µg/ml of Dox was added to the media without (B) or with 100 ng/ml of soluble B18R (C). Surface BST-2 levels were evaluated 6h later by flow cytometry. (D) Quantification of (B) and (C). The error bars represent the standard deviation calculated from 2 independent experiments. The IFN-treated Vpu-negative sample was set at 100% to illustrate the effect of B18R in presence or absence of Vpu.

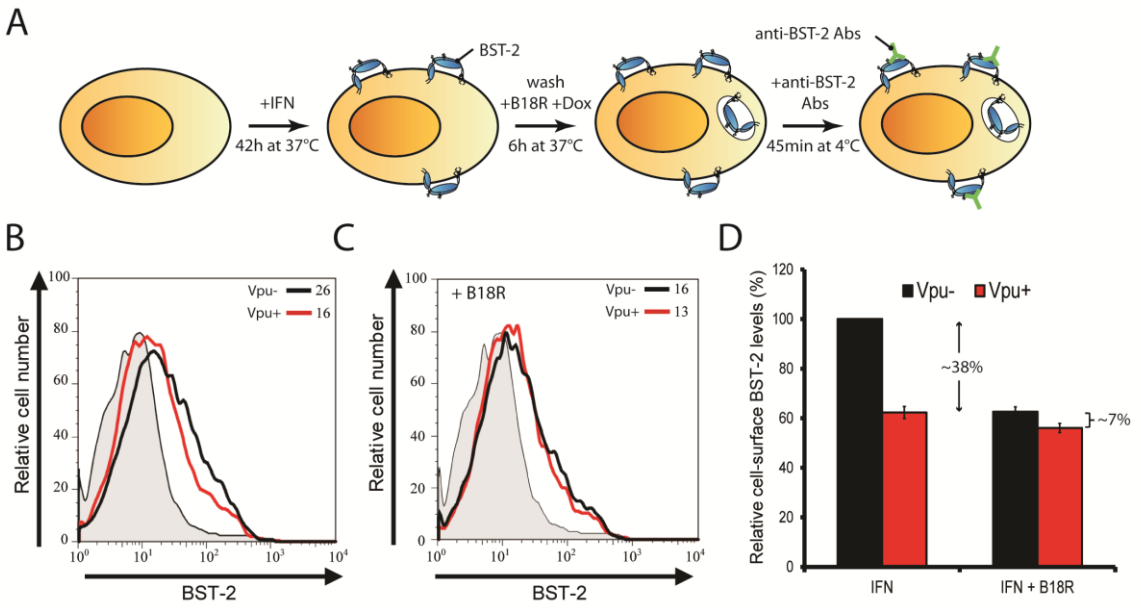
A
+IFN
42h at 37°C
BST-2
wash
+B18R +Dox
6h at 37°C
anti-BST-2 Abs
+anti-BST-2 Abs
45min at 4°C
B
Relative cell number
Vpu- 26
Vpu+ 16
BST-2
C
+ B18R
Vpu- 16
Vpu+ 13
Relative cell number
BST-2
D
Vpu-
Vpu+
Relative cell-surface BST-2 levels (%)
~38%
~7%
IFN
IFN + B18R

Figure 7

Figure 8: Effect of Vpu on the pool of newly synthesized BST-2.

(A) Schematic representation of the experiment. HeLa (B-D) and Jurkat (E-G) cells were transfected with the indicated HIV-1.rtTA.MA-EGFP constructs. Forty-one hours post-transfection, Cells were incubated at 37°C for 1h with saturating amounts of anti-BST-2 rabbit Abs. Unbound Abs were then washed away and fresh media supplemented with 1µg/ml Dox was added to cells for 6h at 37°C. Cells were then harvested and either (B and E) immediately stained with secondary anti-rabbit Abs (surface BST-2) or (C and F) incubated with anti-BST-2 mouse Abs for 45 min at 4°C, washed and stained with secondary anti-mouse Abs (neo-synthesized BST-2). In (C), a blocking control is shown (dashed line). (D and G) Quantification of (B-C) and (E-F), respectively. Vpu-negative samples were set at 100% to illustrate Vpu-mediated BST-2 downregulation for both types of staining. The error bars represent the standard deviation calculated from two distinct experiments.

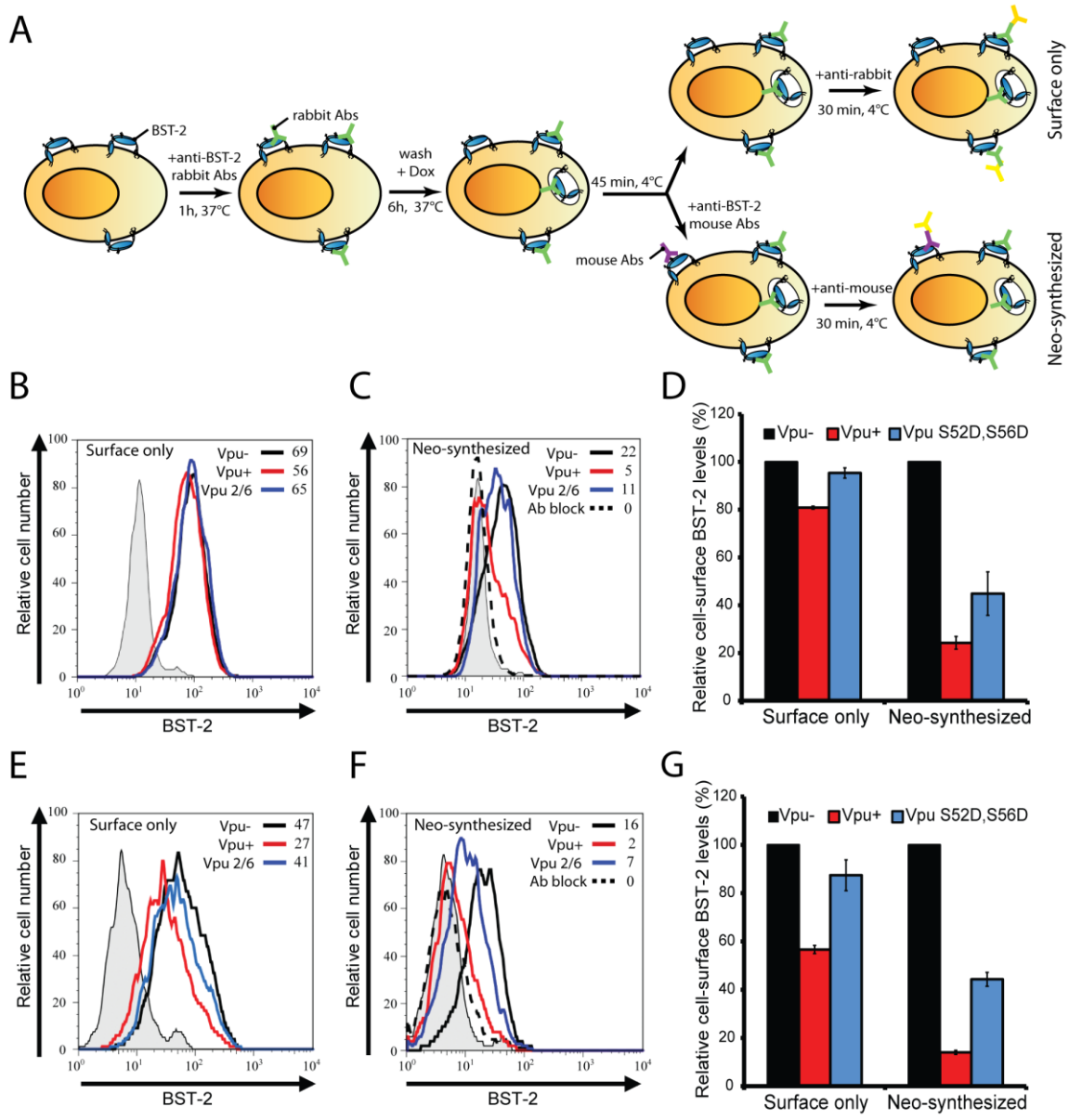
A
BST-2
+anti-BST-2
rabbit Abs
1h, 37°C
rabbit Abs
wash
+ Dox
6h, 37°C
45 min, 4°C
+anti-rabbit
30 min, 4°C
Surface only
+anti-BST-2
mouse Abs
mouse Abs
+anti-mouse
30 min, 4°C
Neo-synthesized
B
Surface only
Vpu- 69
Vpu+ 56
Vpu 2/6 65
Relative cell number
BST-2
C
Neo-synthesized
Vpu- 22
Vpu+ 5
Vpu 2/6 11
Ab block 0
Relative cell number
BST-2
D
Vpu-
Vpu+
Vpu S52D,S56D
Relative cell-surface BST-2 levels (%)
Surface only
Neo-synthesized
E
Surface only
Vpu- 47
Vpu+ 27
Vpu 2/6 41
Relative cell number
BST-2
F
Neo-synthesized
Vpu- 16
Vpu+ 2
Vpu 2/6 7
Ab block 0
Relative cell number
BST-2
G
Vpu-
Vpu+
Vpu S52D,S56D
Relative cell-surface BST-2 levels (%)
Surface only
Neo-synthesized

Figure 8

Figure S1: Recruitment of β-TrCP2 by Vpu optimizes cell-surface BST-2 downregulation.

(A) Semi-quantitative analysis of β-TrCP2 depletion in HeLa cells by RT PCR. Total RNA isolated from cell lines stably expressing the indicated shRNA was used to monitor the depletion of β-TrCP2. The cellular gene GADPH was used as a specificity and loading control. (B) Control and β-TrCP2-depleted HeLa cells were transfected with the indicated HIV-1.rtTA.MA-EGFP constructs and analyzed 48h post-transfection for surface BST-2 levels on p24-positive cells by flow cytometry. Prior to analysis, cells were treated for the indicated period of time with 1 µg/ml of Dox. Error bars represent the standard deviation calculated from three independent experiments.

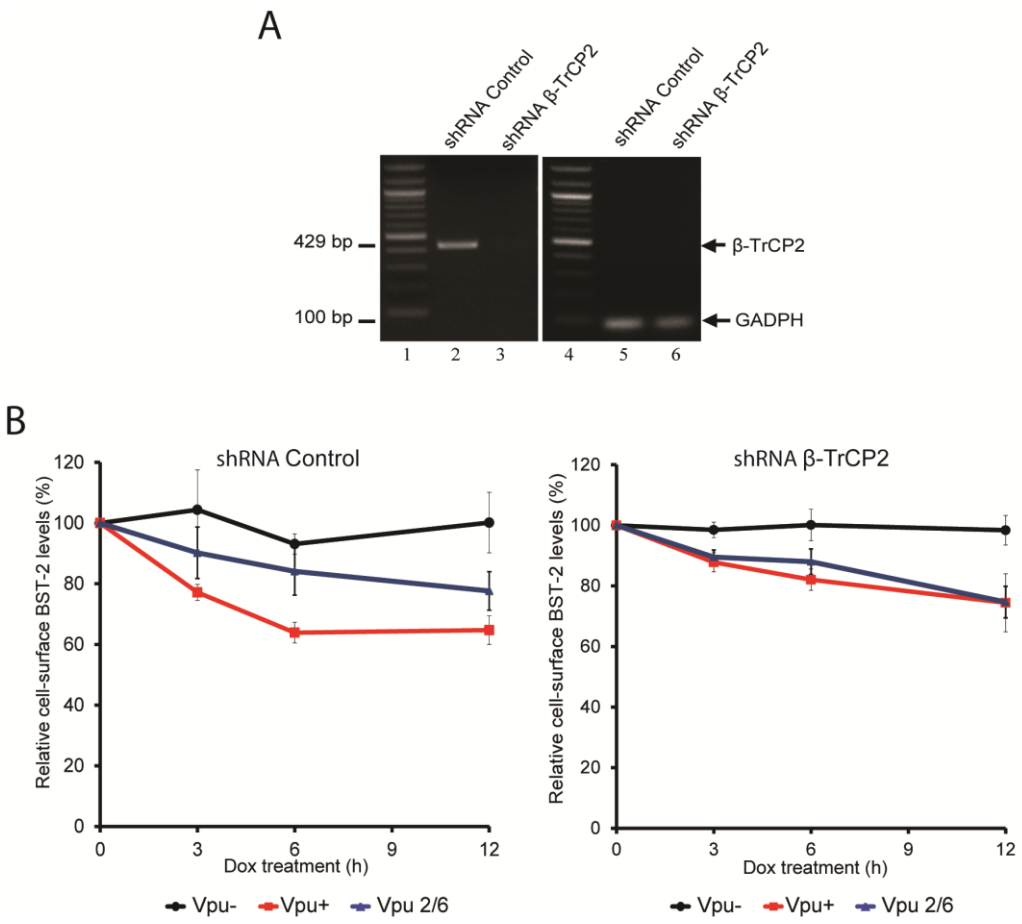
A
shRNA Control
shRNA β-TrCP2
shRNA Control
shRNA β-TrCP2
429 bp
100 bp
β-TrCP2
GADPH
1 2 3 4 5 6
B
shRNA Control
shRNA β-TrCP2
Relative cell-surface BST-2 levels (%)
Dox treatment (h)
Vpu-
Vpu+
Vpu 2/6

Figure S1

Figure S2: Analysis of BST-2 subcellulat localization in fixed cells.

HeLa cells were fixed, permeabilized, stained for intracellular BST-2 (green) and the indicated intracellular markers (red), and then incubated with appropriate secondary Abs. Nuclei were counterstained with DAPI (blue). Cells were analyzed by confocal microscopy. ConA indicate a condition in which cells were pre-treated before fixation with 50 nM of the lysosome acidification inhibitor concanamycin A. White arrows highlight examples of co-localization between BST-2 and specific cellular markers. White bars = 10μm.

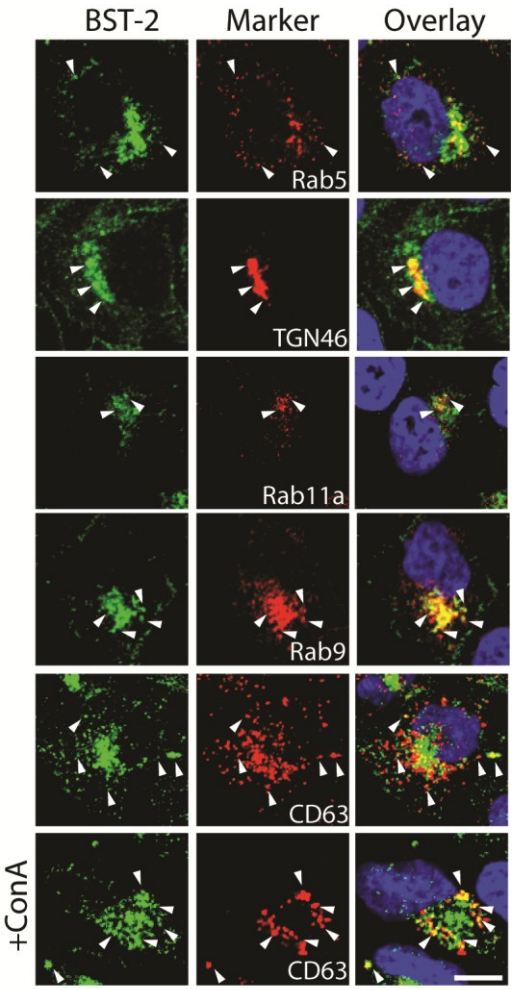

Figure S2

Figure S3: Pathway followed by internalized BST-2 molecules to reach lysosomal compartments.

(A-B) HeLa cells were incubated at 37°C for 0-6h in presence of anti-BST-2 Abs, fixed, permeabilized and then stained for (A) TGN46 or (B) CD63. Stained cells were washed and incubated with appropriate secondary Abs to detect cellular markers (red) as well as internalized BST-2 (green). Nuclei were counterstained with DAPI (blue). Cells were analyzed by confocal microscopy. White arrows highlight examples of co-localization between BST-2 and CD63. White bars = 10µm. (C) Quantification of BST-2 co-localization with cellular markers. The values (%) represent the percentage of BST-2 (green pixels) overlapping with each cellular marker (red pixels). Error bars indicate the standard deviation of the mean from the quantitative analysis of at least 25 distinct cells.

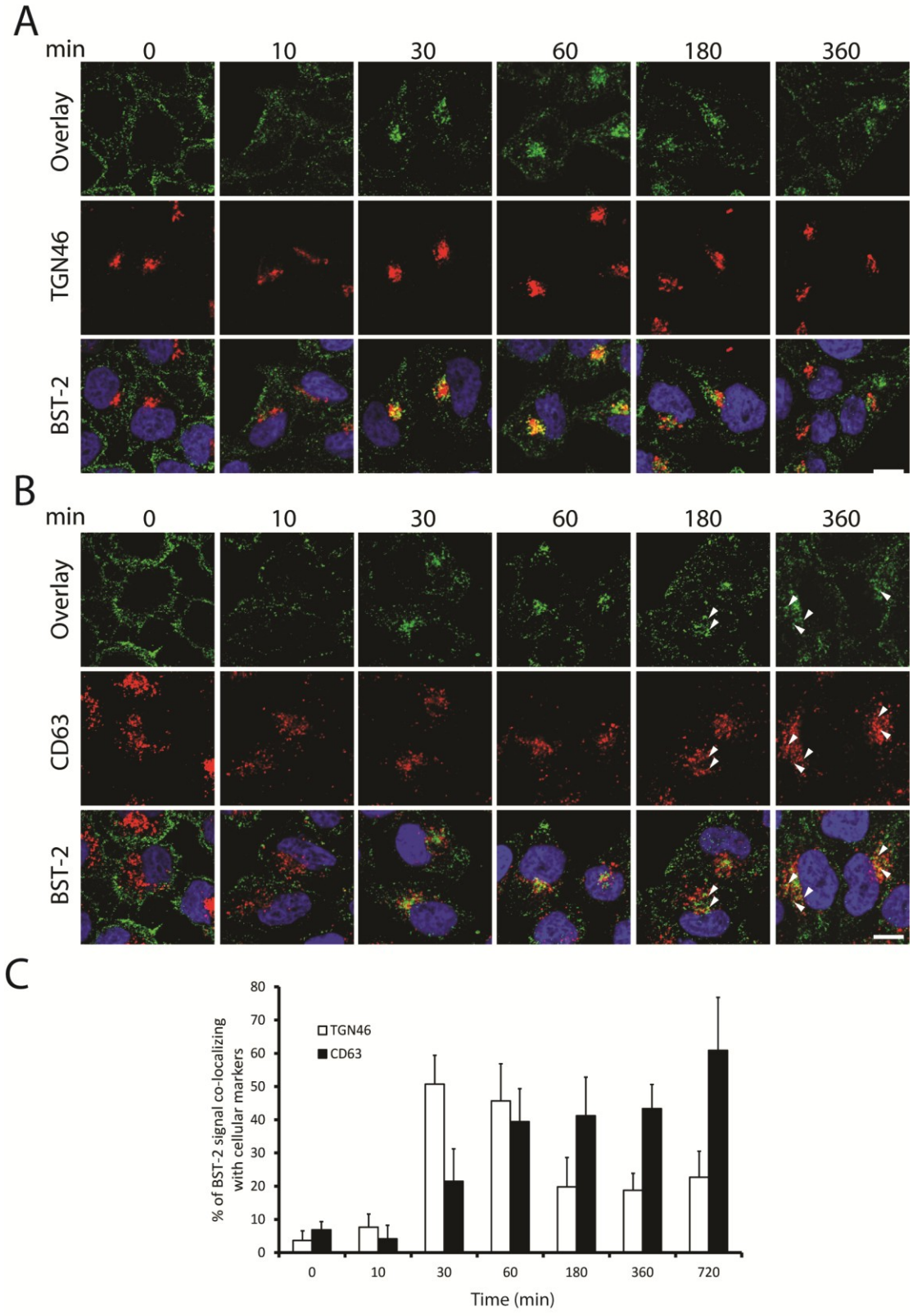
A
min
0
10
30
60
180
360
Overlay
TGN46
BST-2
B
min
0
10
30
60
180
360
Overlay
CD63
BST-2
C
% of BST-2 signal co-localizing with cellular markers
TGN46
CD63
0
10
20
30
40
50
60
70
80
0
10
30
60
180
360
720
Time (min)

Figure S3

Figure S4: Recombinant B18R prevents BST-2 expression at the surface of type 1 IFN-treated HEK293T cells.

(A) HEK293T cells were treated with 1000 U/ml of IFN-α for 1h at 37°C. Cells were then washed and re-incubated for 24h at 37°C in presence of 0-100 ng/ml of recombinant B18R. Cells were then harvested, stained with an anti-BST-2 Abs, washed, stained with an appropriate secondary Ab and analyzed by flow cytometry. MFI values for each condition are depicted within the histogram. (B) HEK-blue IFN-α/β^{TM} cells were cultured for 24h in presence of different dilution of the media collected from (A). Supernatants from HEK-blue IFN-α/β^{TM} cells were subsequently incubated in presence of QUANTI-blue to detect the levels of SEAP secreted upon exposure of HEK-blue IFN-α/β^{TM} cells to type I IFN. The graph depicts the relative light unit (RLU) detected by luminometry and is indicative of the levels of active type I IFN secreted by HEK293T cells.

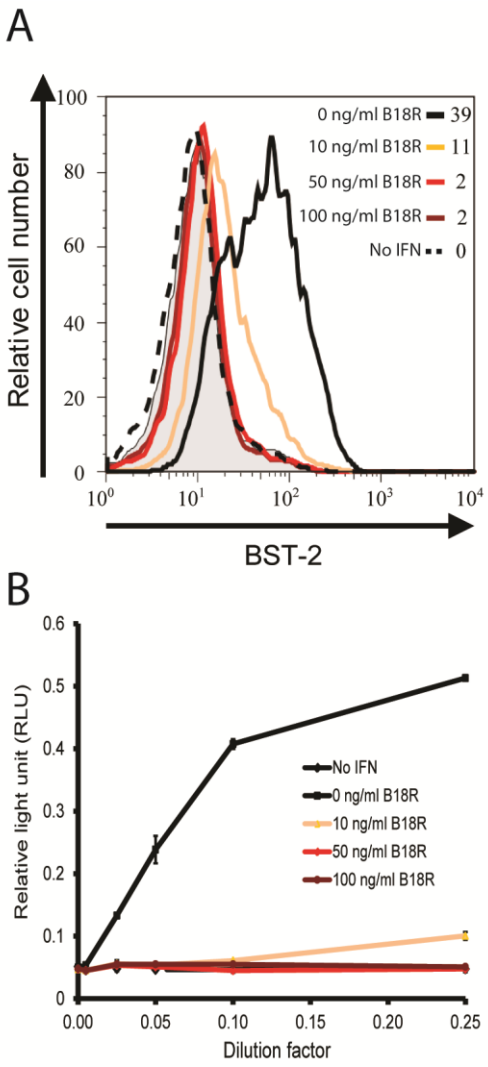
A
Relative cell number
100
80
60
40
20
0
0 ng/ml B18R 39
10 ng/ml B18R 11
50 ng/ml B18R 2
100 ng/ml B18R 2
No IFN 0
10^0
10^1
10^2
10^3
10^4
BST-2
B
Relative light unit (RLU)
0.6
0.5
0.4
0.3
0.2
0.1
0
No IFN
0 ng/ml B18R
10 ng/ml B18R
50 ng/ml B18R
100 ng/ml B18R
0.00
0.05
0.10
0.15
0.20
0.25
Dilution factor

Figure S4

DISCUSSION

1. Contributions de la thèse

Le premier chapitre de cette thèse avait principalement pour but d'évaluer les conséquences fonctionnelles du trafic cellulaire de Vpu. Nous avons situé des déterminants de sa localisation dans le RTG au niveau de sa région charnière entre le domaine transmembranaire et cytoplasmique de Vpu, ainsi qu'à la deuxième hélice cytoplasmique. Plus spécifiquement, notre étude suggère l'existence d'un motif cryptique (D/E)YXXϕ(I/L/V)L de triage vers les lysosomes potentiellement ré-activable dans la région charnière de Vpu de sous-type B. La contribution essentielle de cet article demeure néanmoins la constatation de l'importance de la distribution de Vpu de sous-type B au niveau du RTG afin de faciliter la relâche des particules virales.

Alors que le premier chapitre situait le mécanisme d'antagonisme au niveau du RTG, le deuxième chapitre a permis d'en comprendre la nature. L'invalidation du modèle de dégradation de Tetherin par Vpu via le recrutement de β-TrCP comme mécanisme principal d'antagonisme fut une contribution majeure dans un contexte où, à l'époque, il représentait le principal modèle. La démonstration de la séquestration par Vpu du facteur de restriction dans le RTG est une contribution essentielle qui permit d'établir les bases de l'actuel modèle d'antagonisme. De plus, nous avons présenté les premières évidences directes de l'importance de la liaison des domaines transmembranaires de Vpu et Tetherin pour la séquestration et l'antagonisme de cette dernière.

Le troisième chapitre nous a d'abord permis de prouver le synchronisme de la réduction du niveau de Tetherin en surface et son antagonisme, supportant ainsi l'idée que cette déplétion constitue bel et bien un processus essentiel à la neutralisation par Vpu. De plus, nous avons résolu le paradoxe chronologique de l'antagonisme rapide du facteur de restriction par une protéine virale tardive en démontrant que le blocage par Vpu du réapprovisionnement de Tetherin en surface combiné à son internalisation naturelle à partir de la membrane plasmique, légèrement accélérée en présence de la

protéine virale, peuvent suffire à l'établissement d'un nouvel équilibre favorable à la relâche des particules virales. Donc, le troisième chapitre nous a permis d'intégrer les différents mécanismes, plus ou moins efficaces selon le type cellulaire, par lesquels Vpu contre l'activité restrictive de Tetherin en un modèle unificateur.

2. Un modèle unificateur

Tel que mentionné ci-haut, l'ensemble de mon travail a permis l'élaboration d'un modèle unificateur tenant compte de tous les mécanismes précédemment proposés de neutralisation de Tetherin par Vpu (voir Figure 4). En absence de Vpu, la Tetherin de surface est internalisée et lentement triée dans des compartiments endosomaux. Cette perte en surface est compensée par l'arrivée de molécules de Tetherin nouvellement synthétisées. Essentiellement, Vpu préviendrait le réapprovisionnement du facteur de restriction en surface en interceptant au niveau du RTG les molécules néo-synthétisées en route vers la membrane plasmique. Il en résulterait l'établissement d'un nouvel équilibre en surface et ce, à temps pour l'initiation du processus de relâche des particules virales. L'accumulation de Vpu dans le RTG, assurée par les déterminants de trafic présents dans sa queue cytoplasmique, maximise probablement sa capacité à intercepter Tetherin, qui transite obligatoirement à travers cette organelle durant son transport vers la surface. Selon les cellules, l'effet variable de Vpu au niveau de la clairance de la Tetherin de surface pourrait aussi plus ou moins contribuer à l'établissement de ce nouvel équilibre.

L'interception de la Tetherin néo-synthétisée impliquerait vraisemblablement deux mécanismes distincts, soit la séquestration de Tetherin suivie de sa dégradation dans les lysosomes. La distinction entre ces deux composantes devient évidente en observant le phénotype du mutant Vpu S52D,S56D, qui est incapable de recruter β-TrCP. Son incapacité à induire la dégradation de la Tetherin contraste avec sa capacité à ralentir efficacement le transport du facteur de restriction, ce qui se traduit globalement par une neutralisation partielle du facteur de restriction. En fait, la séquestration pourrait représenter un préalable à la dégradation, qui permet probablement d'exacerber le blocage du réapprovisionnement de la Tetherin en surface. Le recrutement de β-TrCP

par Vpu pourrait permettre dans certains types de cellules d'accélérer la clairance de Tetherin à partir de la surface (Figure 4 et 8, chapitre 3).

Il est intéressant de noter que l'effet combiné de ces deux processus ne permet qu'une diminution partielle du niveau de Tetherin en surface durant l'infection, soit environ 50%, mais qui semble suffisante à l'antagonisme complet du facteur de restriction. Ce niveau de déplétion durant l'infection n'est pas comparable à ceux observés dans les cas de CD4 et CD1d, où différentes stratégies développées par le virus permettent des déplétions bien plus complètes (178, 262). Dans le cas de Tetherin, il est possible que le virus ait évolué afin de garder un certain niveau de Tetherin en surface tout en permettant la relâche virale. En effet, outre son activité antivirale, Tetherin engagerait le récepteur ILT-7 (transcrit 7 similaire aux immunoglobulines) présent à la surface des cellules dendritiques et initierait la régulation négative de la boucle d'activation de la voie d'IFN (29). De plus, Tetherin assurerait l'intégrité du réseau d'actine cortical dans les cellules épithéliales polarisées, et peut-être au niveau de certains microdomaines dans les cellules non-polarisées (202). Ainsi, la déplétion partielle de Tetherin pourrait représenter un compromis entre une relâche virale efficace d'une part, et une prévention de la sécrétion chronique d'IFN et le maintien de l'intégrité de certains sous-domaines en surface d'autre part. Il sera d'ailleurs intéressant de comparer l'effet de Vpu sur ces fonctions par rapport à une déplétion totale de l'expression de Tetherin grâce à des petits ARN d'interférence.

La résistance de la Tetherin à la monensin, qui bloque certaines voies de recyclage rapide, peut sembler surprenante (Figure 6, chapitre 3). Cependent, ce type de trafic est généralement observé dans le cas de protéines exprimées de façon endogène telle que le récepteur de transferrin, le récepteur de lipoprotéine de faible densité (LDLR) ou le récepteur du facteur de croissance épidermique (EGFR). Or, la Tetherin est surtout exprimée suivant l'induction des cellules par l'IFN et serait impliquée dans la régulation négative de cette voie (75). L'absence de recyclage de Tetherin suite à son internalisation pourrait permettre une régulation plus stricte de son expression en surface. En effet, son recyclage constitutif ralentirait probablement le rétablissement de son niveau basal suivant la disparition de l'IFN dans le milieu. Il est donc concevable

que le recyclage de Tetherin suivant son internalisation mènerait à une sécrétion exagérément durable de l'IFN. Néanmoins, nos données ne permettent pas d'exclure que Tetherin recycle par une voie différente que celle empruntée par l'EGFR, le récepteur de transferin ou le LDLR. Advenant l'existence d'un tel type de trafic, le recyclage de Tetherin pourrait expliquer la lenteur du processus de dégradation de la protéine internalisée suite à son internalisation. Il serait aussi envisageable que l'effet modéré de Vpu sur le pool de Tetherin en surface soit la conséquence de sa séquestration en cours de recyclage au niveau du RTG.

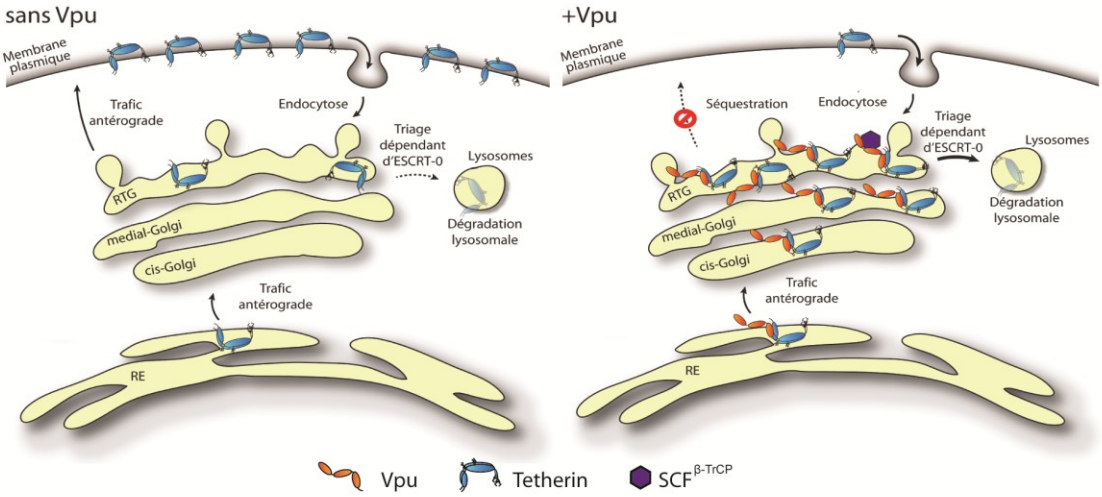

Figure 4: Modèle de la déplétion de Tetherin de surface par Vpu
Tetherin trafique vers la membrane plasmique d'où elle est éventuellement dégagée par endocytose. Leur reconnaissance par la machinerie ESCRT-0 assure leur triage vers les lysosomes. Suite à l'expression de Vpu, la clairance de Tetherin en surface est légèrement accélérée. Les molécules nouvellement synthétisées forment des complexes avec la protéine virale, deviennent bloquées dans le RTG loin des sites d'assemblage où elles restreignent la relâche des particules virales. Les molécules ainsi trappées sont probablement ubiquitinées en conséquence du recruitement de β-TrCP par Vpu. Cette Tetherin marquée devient mieux reconnue par la machinerie ESCRT-0, facilitant ainsi leur triage vers les lysosomes. Ces deux effets combinés provoquent l'établissement d'un nouvel équilibre en surface caractérisé par de plus faibles niveaux de Tetherin.

3. La contribution de β-TrCP

L'incapacité de Vpu S52D,S56D à recruter β-TrCP se traduit par une déficience fonctionnelle à deux niveaux: la dégradation de Tetherin et, dans une moindre mesure, l'accélération de sa clairance à partir de la surface. Ce cofacteur étant une sous-unité d'une E3 ligase, sa contribution à l'antagonisme de Tetherin a naturellement été reliée à l'ubiquitination de cette dernière. En effet, certaines études ont mis en évidence la poly-ubiquitination (243) et la mono-ubiquitination du facteur de restriction (190) en présence de Vpu dans différents systèmes plus ou moins physiologiques. Par contre, les implications de l'ubiquitination de Tetherin par Vpu ne sont globalement pas bien comprises. Alors qu'elle semblerait influer sur sa stabilité (86, 243), voire peut-être sur son trafic post-endocytique (173), elle ne semble pas critique à son antagonisme (86, 190, 241). Il est intriguant de noter que l'éventualité d'une régulation de l'activité de Vpu par sa propre ubiquitination n'a jamais été directement vérifiée, quoiqu'une certaine ubiquitination de cette protéine accessoire via son interaction avec β-TrCP ait déjà été rapportée (9).

Bien que le recrutement de β-TrCP semble dispensable lors de l'antagonisme de Tetherin, il donne visiblement de meilleurs résultats puisque le mutant Vpu S52D,S56D n'est pas en mesure de contrer Tetherin avec la même efficacité que Vpu de type sauvage (Figure 2, chapitre 2). Traditionnellement, cette sous-unité de la E3 ligase $SCF^{\beta\text{-}TrCP}$ est associée à une dégradation de type protéasomal (129, 159, 267). Cependant, β-TrCP peut tout aussi bien promouvoir la dégradation lysosomale, tel que démontré dans le cas du récepteur-1 d'IFN-α/β (139). La négation de l'effet de Vpu sur les niveaux de Tetherin par l'usage d'un bloqueur de la dégradation lysosomale tel que la concanamycin A (54, 173) et l'implication de la machinerie ESCRT lors de ce processus impliquent une protéolyse de type lysosomal (113). Si l'implication de β-TrCP dans la dégradation lysosomale de Tetherin ne pose pas de problème conceptuel, il en est tout autre en ce qui concerne son internalisation. Dans le cas du récepteur-1 d'IFN-α/β, son association à des chaînes d'ubiquitine reliées entre elles par des lysines en position 63 est associée à son internalisation et à son triage vers les lysosomes (139). Il pourrait en être de même pour Tetherin en présence de Vpu, surtout à la lumière de notre observation selon laquelle Vpu pourrait affecter directement le facteur de

restriction en surface, particulièrement dans les cellules Jurkats (Figures 4 et 8, Chapitre 3). Cependant, bien peu de données solides étayent l'importance de l'ubiquitine lors de l'antagonisme de Tetherin outre la contribution de β-TrCP. Il serait donc intéressant d'évaluer la potentielle contribution de l'ubiquitine et, le cas échéant, de déterminer la nature des chaînes d'ubiquitine potentiellement impliquées, les types de liaison entre les résidus d'une même chaîne étant généralement associés à des mécanismes bien précis (109). Tout de même, l'éventualité selon laquelle Vpu mène à l'ubiquitination de la Tetherin au niveau de la membrane plasmique est difficile à concilier avec l'accumulation quasi exclusive de Vpu dans le RTG et son apparente exclusion de la surface (Figure 1, Chapitre 1). Ce phénotype pourrait peut-être être expliqué par un recyclage de la Tetherin, advenant l'existence d'un tel type de processus résistant à la monensin (Figure 6, Chapitre 3). Le cas échéant, l'ubiquitination de la Tetherin internalisée par Vpu au niveau du RTG pourrait empêcher son recyclage en surface, favoriser sa ré-internalisation suivant son recyclage ou simplement promouvoir son triage vers les lysosomes. En ce sens, une meilleure compréhension des voies de trafic employées par Tetherin en présence et en absence de Vpu permettront de vérifier cette hypothèse. Une autre explication plausible serait l'expression transitoire de Vpu en surface, indétectable en microscopie confocale. Il est en effet envisageable que Vpu atteigne la membrane plasmique et y ubiquitine Tetherin avant d'être rapidement rapatriée dans le RTG. Il sera donc nécessaire de vérifier par des méthodes plus sensibles et dans différents types cellulaires si Vpu de sous-type B est en mesure d'atteindre de façon transitoire la membrane plasmique.

Bien que nous comprenions assez bien présentement comment β-TrCP contribue à la dégradation lysosomale de Tetherin induite par Vpu, son réel apport à l'antagonisme ne l'est pas. Les prochains défis quant à la mécanistique de l'augmentation de la relâche du VIH-1 par Vpu se situent d'ailleurs probablement à ce niveau. Il est possible que la dégradation permette d'éviter la saturation de Vpu dans le RTG lorsque les niveaux de Tetherin sont élevés, advenant par exemple une exposition soutenue à l'IFN. Cette idée est consistante avec une étude récente réalisée par Schindler et collègues (213). Leurs conclusions, obtenues par la comparaison de la réplication du virus dans des macrophages exprimant de hauts niveaux de Tetherin versus dans des lymphocytes T

CD4 provenant de cultures *ex vivo* de thymus qui en expriment de plus modestes, suggèrent que la nécessité de β-TrCP corrèle avec le niveau du facteur de restriction. Puisque la nécessité du cofacteur semble variable en fonction du système utilisé, l'évaluation future de la contribution de β-TrCP devra tenter de mieux comprendre les contextes cellulaires qui en nécessitent le recrutement afin de contrer Tetherin.

La nécessité de β-TrCP ne corrèle pas qu'avec les niveaux de Tetherin; elle semble aussi corréler avec les niveaux de la E-cadhérine, une protéine créant la jonction entre la β-caténine et le réseau de microfilaments nécessaire aux jonctions cellulaires étanches. Cette dernière, tout comme Tetherin, est notoirement mieux exprimée dans les macrophages adhérents que dans les lymphocytes en suspension. Il est intéressant de noter que le recrutement par Vpu de $SCF^{\beta\text{-}TrCP}$ réduirait la disponibilité de cette E3 ligase pour ses substrats naturels. En conséquence, l'expression de Vpu résulterait en la stabilisation d'IκBα, de la β-caténine, du facteur de transcription-4 (ATF4), de la protéine du cycle de division cellulaire 25A (cdc25A) et de Snail (15, 20, 62, 209). Ce dernier est un facteur de transcription qui, justement, régule négativement la E-cadhérine. Le recrutement de β-TrCP par Vpu pourrait donc avoir un effet collatéral sur la relâche virale indépendamment de l'expression de Tetherin en diminuant les niveaux de E-cadhérine, cette dernière ayant un effect négatif sur la relâche (28, 209), ce qui pourrait d'ailleurs expliquer la modeste stimulation de la relâche virale par Vpu dans des cellules confluentes n'exprimant pas la Tetherin (52). Il serait donc intéressant de mettre en perspective l'effet de la Tetherin et de la E-cadhérine dans ces cellules. Peu importe si l'apport de β-TrCP reflète un effet direct sur Tetherin ou indirect via E-cadhérine, une meilleure compréhension du rôle de β-TrCP durant l'antagonisme de Tetherin sera cruciale au progrès de nos connaissances sur Vpu. S'il s'avère que ce cofacteur revêt une réelle importance physiologique, il pourrait représenter une cible thérapeutique pluripotente afin de rétablir à la fois les niveaux cellulaires de CD4, de Tetherin et/ou de la E-cadhérine.

Le modèle proposé en Figure 4 intègre les résultats provenant de plusieurs études distinctes, mais unies par une même faiblesse, soit l'usage de lignées cellulaires. De tels outils sont utiles pour les études mécanistiques poussées, mais ne reflètent pas

nécessairement la situation prévalant *in vivo*. Par exemple, l'effet de Vpu sur le pool de Tetherin en surface semble exacerbé dans les cellules Jurkats, une lignée lymphoïde, par rapport aux cellules HeLa. Il est aussi possible que le recrutement de β-TrCP soit particulièrement crucial dans les macrophages. Il sera donc primordial de confirmer ce modèle (Figure 4) dans des systèmes physiologiques tels que des cellules primaires ou, encore mieux, directement dans un modèle animal.

4. Régulation de l'activité fonctionnelle de Vpu par sa localisation

Le défaut de Vpu S52D,S56D est généralement associé à son incapacité à recruter β-TrCP. Or, la déficience de ce mutant pourrait s'expliquer autrement. En effet, les sérines 52 et 56 font partie d'un motif très conservé parmi les protéines Vpu des différents sous-groupes du VIH-1, soit le motif ED**S**GNE**S**EG situé entre ses deux hélices-α cytoplasmiques (Figure 4). Ce motif de reconnaissance pour β-TrCP, aussi retrouvé chez ses autres substrats tels que Cdc25A, Emi1, β-caténine et IκBα (62, 116, 129, 136, 180, 221), contient aussi un motif potentiel de rapatriement des protéines membranaires vers le RTG. En effet, les sérines phosphorylées (ED**S**GNE**S**EG) précédées ou entourées de deux résidus chargés positivement sont très semblables aux motifs de rapatriement de la furine, du transporteur vésiculaire de la monoamine (VMAT)-1, de VMAT-2, de la protéine transmembranaire associée aux vésicules-4 (VAMP-4), de la carboxypeptidase (CPD), de la proprotéine convertase 6B (PC6B) et de la protéine associée à Myc (PAM) (18). Similairement à ces protéines, la modification de ces motifs potentiels dans le cas de Vpu corrèle avec sa délocalisation du RTG au profit de vésicules cytoplasmiques et de la membrane plasmique (Figure 5 du Chapitre 1). À l'instar de ce qui est observé dans le cas de Vpu R30A,K31A, cette localisation aberrante pourrait expliquer son incapacité à contrer complètement Tetherin. Il est intéressant de noter que la substitution des sérines en position 52 et 56 pour des asparagines ou des acides glutamiques, changements relativement conservateurs, semble affecter bien moindrement l'activité de la protéine que lorsqu'elles sont changées en alanines ((54, 85, 155, 173, 213, 248) et Figure 2 du Chapitre 2). Il serait intéressant de

vérifier l'effet de chacune de ces substitutions au niveau de la localisation de la protéine par microscopie confocale.

Outre la possible présence d'un motif de rapatriement entre les deux hélices-α, les données actuelles suggèrent deux principaux déterminants affectant l'accumulation de Vpu dans le RTG (Figure 4). Le premier se situe au niveau du motif superposé (D/E)YXXϕ(I/L/V)L dans la région charnière et pourrait représenter un signal cryptique à la fois d'exportation vers les endosomes et de rapatriement vers le RTG à partir de la surface. Le deuxième serait présent dans la deuxième hélice-α cytoplasmique, quoique cette dernière pourrait plutôt fournir un contexte structurel propice au recrutement d'un cofacteur reconnaissant plutôt le motif de rapatriement di-acidique mentionné ci-haut. Il est à noter que cette deuxième hélice-α comporte aussi un motif (D/E)XXXϕ(I/L/V)L qui pourrait être impliqué dans la localisation de Vpu au niveau du RTG. Ces deux régions contiennent un certain degré de polymorphisme (Figure 4); elles pourraient donc expliquer certaines variations fonctionnelles observées parmi les différents sous-types du VIH-1 (210). Il sera intéressant de vérifier si la corrélation entre la rétention de Tetherin dans le RTG et son antagonisme est aussi applicable dans les cas de ces différentes protéines Vpu polymorphiques. La comparaison des séquences de ces différentes protéines donnera de précieux indices quant à la nature des déterminants responsables de cette variation phénotypique.

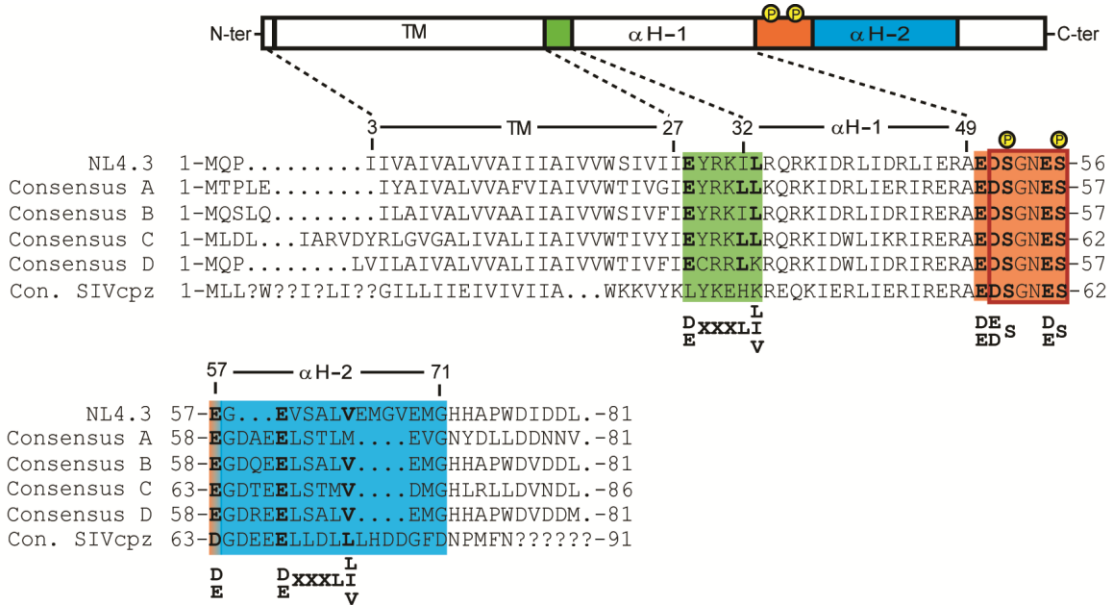

Figure 5: Délimitation des zones susceptibles de contenir un signal de localisation
Topologie et séquences consensus de Vpu du VIH-1 des sous-types A-D, du VIScpz et du virus prototype de laboratoire NL4.3 (base de données du VIH, www.hiv.lanl.gov). Les points d'interrogation soulignent les résidus qui ne font pas consensus pour un sous-type donné. La boîte rouge foncé indique le motif conservé reconnu par β-TrCP. Les rectangles de couleur (vert, rouge orangé et bleu) délimitent et situent les trois zones susceptibles de contenir un signal de localisation. Les motifs sont indiqués sous les rectangles alors que les résidus respectant le consensus de ces motifs sont dénotés par des caractères gras. Les symboles X et Φ correspondent à des résidus variables et hydrophobiques, respectivement. αH: hélice-α.

Bien que l'accumulation de Vpu de sous-type B dans le RTG soit nécessaire, il n'est pas exclu qu'un trafic dans d'autres compartiments puisse optimiser son activité antagoniste. D'ailleurs, il semblerait que l'inhibition de la fonction des endosomes de recyclage affecte l'activité de Vpu (250). Il n'est pas inconcevable que Vpu « patrouille » la voie de sécrétion afin de fournir à la Tetherin des motifs en *trans* permettant son rapatriement dans le RTG. Selon cette hypothèse, la faiblesse du signal de rapatriement de Vpu R30A,K31A, et possiblement de Vpu S52D,S56D, ne permet peut-être pas ce genre d'activité, confinant leur activité antagoniste uniquement au sein du RTG. Le criblage systématique par mutagénèse dirigée des trois régions de la queue cytoplasmique de Vpu susceptibles de contrôler son trafic permettra de mieux délimiter les motifs de triage et de décortiquer la nature des signaux qu'ils fournissent. Conjugué à des techniques de spectrométrie de masse, cet exercice permettra peut-être d'identifier des

cofacteurs cellulaires modulant son transport intracellulaire et son activité antagoniste. Il sera aussi intéressant d'évaluer l'effet de tels motifs associés à Vpu sur le trafic de Tetherin. L'inactivation de différentes protéines GTPase Rab pourra aussi identifier les différentes voies de trafic contribuant à l'antagonisme. Notons qu'en ciblant ces facteurs cellulaires, il est possible de bloquer virtuellement toutes les voies classiques du trafic des protéines en interférant, par exemple, avec les fonctions de Rab6, 9 et 31 (rapatriement à partir des endosomes tardifs vers le RTG), de Rab8,10-15,23 (RTG vers la surface des cellules polarisées), de Rab5 (endocytose), de Rab7 et 21 (vers les lysosomes) et de Rab11 (recyclage) (108).

5. La spécificité relative de Vpu

Comment l'interaction de Vpu avec Tetherin prévient le transport antérograde de cette dernière demeure obscure. Puisque ces deux protéines interagissent via leur domaine transmembranaire respectif, il est peu probable que Vpu cache des motifs de transport au niveau du domaine cytoplasmique de Tetherin. Il demeure tout de même envisageable que leur association modifie légèrement la conformation de Tetherin et en modifie l'export à partir du RTG vers la surface. Une autre possibilité est que, tel que mentionné ci-haut, Vpu fournisse des motifs de rapatriement au facteur de restriction. En fait, il n'est pas clair si cette interaction est directe ou non, et si elle est suffisante à la séquestration. La contribution d'un tiers partenaire cellulaire inconnu n'est pas à exclure. Des approches d'isolation de complexes Vpu-Tetherin conjugués à la protéomique permettront peut-être d'identifier un tel cofacteur, s'il existe.

L'importance d'identifier un(des) éventuel(s) partenaire(s) de Vpu impliqué(s) dans son activité de séquestration transcende l'étude de l'interrelation entre Tetherin et son antagoniste. En effet, il est intriguant qu'un domaine transmembranaire d'à peine 23 acides aminés puisse lier et réguler l'expression de surface de si nombreux substrats tels que Tetherin, CD4, l'antigène des cellules NK, B et T (NTB-A), CD1d et peut-être même les CMH-I et -II (57, 107, 124, 178, 223). Si le mode d'action sous-jacent à la controversée déplétion des CMH par Vpu demeure spéculatif, les mécanismes contrôlant l'expression de surface des autres substrats de Vpu sont beaucoup mieux

caractérisés. Les molécules de CD1d exposent des antigènes lipidiques aux cellules NKT à partir de cellules présentatrices d'antigènes professionnelles telles que les cellules dendritiques et les macrophages (163). Vpu préviendrait la présentation d'antigènes lipidiques aux cellules NKT en interceptant CD1d au cours de son recyclage (178). NTB-A est une molécule dont l'homo-dimérisation de deux sous-unités, une à la surface d'une cellule NK et l'autre à la surface d'une cellule cible, entraîne à la co-activation de la cellule NK, favorisant ainsi la lyse de la cellule ainsi reconnue (19, 72). Vpu réduit considérablement les niveaux de surface de cette molécule probablement par séquestration intracellulaire, où l'importance du domaine transmembranaire de Vpu et l'absence de dégradation rappellent le mécanisme d'antagonisme de Tetherin (223). Finalement, outre la dégradation de la protéine par le protéasome, Vpu serait en mesure de séquestrer CD4 par la liaison de leur domaine transmembranaire respectif, et ce, indépendamment de β-TrCP (152).

Il semble donc que Vpu ait la capacité de lier le domaine transmembranaire de tous ces récepteurs et d'en provoquer la séquestration intracellulaire. Bien que la multifonctionnalité des protéines virales accessoires ne soit plus à être démontrée, un si grand nombre de partenaires pour une si petite région est surprenante. Outre le fait qu'elles sont toutes associées aux membranes par un domaine transmembranaire, la comparaison de leur séquence primaire n'évoque aucune autre forme d'homologie. Le recrutement par Vpu d'un intermédiaire cellulaire multipotent communément impliqué dans le transport de ces protéines pourrait représenter une stratégie efficace par laquelle Vpu pourrait multiplier ses substrats grâce à un site de liaison unique. Ce genre d'intermédiaire spécifique à certains cargos est relativement commun. Par exemple, notons la chaperone Bap31 qui contrôle le transport de CD81 et de CD44 vers les lysosomes (8), les protéines associées aux membranes RING-CH (MARCH) qui contrôlent le transport endosomal de la syntaxin 6, de TGN38, du récepteur de transferin (182) et de HLA-DR (47), Rab8 et AP-1B qui permettent l'export basolatéral de LDLR et du récepteur de la transferin (6, 69, 74) et Rab14 qui régule l'exportation de l'endotubin et du peptide intestinal vasoactif/MAL au domaine apical (130). De façon alternative, Vpu pourrait entrer en compétition avec de tels facteurs cellulaires et en

prévenir le recrutement par Tetherin, interférant ainsi avec le transport normal du facteur de restriction.

Ce large éventail de substrats soulève une question cruciale : à quel point la déplétion de protéines de surface par Vpu est-elle spécifique? Il y a plusieurs années, l'éventualité que Vpu puisse avoir un effet global sur la voie de sécrétion des protéines vers la membrane plasmique fut évoquée. Cependant, cette étude n'était pas exhaustive puisqu'elle ne mesurait que la sécrétion de la gp120 soluble et l'exportation de l'enveloppe du virus de la stomatitis vésiculaire (VSV) (255). Il est intéressant de noter que les auteurs de cette étude avaient remarqué que la mutation des sites de phosphorylation en position 52 et 56 ne bloque que très partiellement cet effet sur le transport, ce qui est cohérent avec nos données obtenues dans le cas du trafic de Tetherin. Malgré le large spectre d'action de Vpu, il est désormais clair que cette protéine virale revêt une certaine spécificité, n'ayant aucun effet sur l'expression de surface du récepteur de transferin (101, 124), de CD74 (107), de la molécule d'adhésion inter-cellulaire (ICAM) (124), de CD59 et de CD71 (178), de LDLR et du polypeptide relié à la séquence A du CMH-I (MICA) (données non-publiées). De plus, un effet général de Vpu sur la voie de sécrétion n'est pas compatible avec la maturation et le transit de la protéine de l'enveloppe vers les sites d'assemblage viral. La poursuite de la quête d'identification des déterminants conférant sensibilité ou résistance à Vpu aux protéines cellulaires permettront évidemment de mieux comprendre la biologie de cet intrigant modulateur de la voie de sécrétion.

Il est intéressant de noter que, contrairement à CD4 ou à Tetherin, aucune dégradation ou accélération de l'internalisation de CD1d ou de NTB-A n'a été observée. Puisque ces molécules sont vraisemblablement co-exprimées sont dans les lymphocytes ou les macrophages, il est fort possible qu'il y ait compétition entre elles pour leur association à Vpu. Il est donc probablement avantageux pour, voire nécessaire, cette dernière de se libérer de Tetherin en la triant vers les lysosomes. Suivant ce raisonnement, l'absence de dégradation dans les cas de NTB-A et CD1d est surprenante, quoique ce ne soit pas nécessairement la dégradation en soi qui permette la libération de Vpu. Tel que mentionné précédemment, l'absence de données fiables quant à

l'implication de l'ubiquitine au cours de l'antagonisme de Tetherin ne nous permet que de spéculer sur le sujet. En effet, il existe quelques cas de protéines dont l'ubiquitination empêche leur association avec leurs partenaires respectifs. En effet, l'ubiquitination de la protéine Tax du virus T-lymphotropique humain (HTLV-1) permettrait sa dissociation d'avec des protéines contenues dans les foyers nucléaires (79) alors que l'ubiquitination du récepteur de l'hormone de croissance épidermale substrat-15 (Eps15) empêche son association à la clathrine (34). Il est intéressant de noter qu'un mutant incapable de recruter β-TrCP ne parvient pas à réduire de façon optimale les niveaux de NTB-A en surface, et ce même si aucun processus de dégradation n'est impliqué. Il est tentant de spéculer que l'ubiquitination des substrats de Vpu ont une triple utilité : 1) libérer Vpu, ce qui a pour conséquence de 2) bloquer irréversiblement leur trafic vers la membrane plasmique et dans certains cas 3) induire leur dégradation. Notons que l'implication de l'ubiquitine dans la régulation du transport de ces protéines n'est pas à exclure puisqu'une telle régulation du trafic vers la surface a déjà été décrite (1, 18, 183, 227). Contrairement à CD4 et à Tetherin, il n'est par contre pas clair si Vpu entraîne l'ubiquitination de CD1d et de NTB-A (57). Rappelons qu'étant donné le caractère dispensable de β-TrCP pour la séquestration, ce type de mécanisme ne serait que complémentaire. L'importance de la dissociation/dégradation des substrats pourrait être vérifiée en comparant l'affinité de Vpu pour Tetherin en présence de ses autres substrats, surtout dans un contexte où la dégradation du facteur de restriction est prévenue par la déplétion de β-TrCP.

L'apparente semi-sélectivité de Vpu pourrait bien être reliée à certains microdomaines à la surface des cellules. Bien que l'accumulation de Tetherin aux sites d'assemblage soit désormais claire (Figure 3 du Chapitre 3), l'affinité des autres substrats pour certains microdomaines ne l'est pas. La déstabilisation de tels microdomaines par Vpu ne serait pas particulièrement surprenante. En effet, sa première hélice cytoplasmique lui confère des propriétés amphipatiques généralement associées à la déstabilisation et à la courbature des membranes lipidiques (44, 45). Cette possibilité est d'autant plus renforcée par l'homologie de Vpu à M2 d'influenza, dont l'effet sur la courbature de la membrane virale a récemment été démontré (204). Tout comme M2, Vpu pourrait même multimériser en canaux ioniques qui déstabilisent les bicouches

lipidiques en solution, du moins *in vitro* (64), quoique l'implication de ce type de structure multimérique au cours de l'antagonisme de Tetherin soit fortement controversée (101, 133, 254). Quoiqu'il en soit, il sera intéressant de comparer l'association des substrats de Vpu aux microdomaines cellulaires. D'une part, cette analyse pourrait mener à l'identification de nouveaux substrats de Vpu et d'autre part, améliorerait considérablement notre connaissance de la biologie de cette protéine virale. Clairement, des études supplémentaires seront nécessaires à la compréhension de l'impact de Vpu sur le transport des protéines vers la surface des cellules infectées.

6. La pertinence de la séquestration/antagonisme pour la pathogénèse

Historiquement, le caractère dispensable des protéines Vpu, Nef, Vpr et Vif pour la réplication du virus dans des systèmes *in vitro* leur a valu le qualificatif « d'accessoire ». Le dogme fut longtemps qu'elles n'étaient nécessaires qu'à la propagation optimale du virus *in vivo*. Cependant, il est désormais clair que Nef, Vif ainsi que Vpr dans les macrophages, optimisent certaines étapes précoces de la réplication même, *in vitro* (42, 48, 61, 65, 66, 76, 77, 151). Le seul modèle animal rapporté à l'heure actuelle permettant d'évaluer directement l'apport de Vpu à la pathogénèse implique l'usage du virus d'immunodéficience simienne-humaine (VISH) chez le macaque (118, 230). Dans ce modèle où les gènes *tat, rev, vpu* et *env* du VISmac239 ont été substitués par leur équivalent chez le VIH-1, l'expression de Vpu s'est avérée importante à la pathogénicité du virus (229). En fait, la randomisation du domaine transmembranaire de Vpu, qui annule la séquestration et l'antagonisme de Tetherin par Vpu *in vitro*, diminuerait la pathogénicité du virus dans ce modèle (105). Or, ce constat peut difficilement être imputable à l'antagonisme de Tetherin puisque la variante simienne du facteur de restriction est résistante à Vpu (114, 147, 166, 185, 210, 266); il reflète donc probablement l'importance des effets de la protéine virale sur CD4, NTB-A et CD1d ou tout autre substrat plutôt que sur le facteur de restriction. Un bien meilleur modèle animal pour évaluer l'effet de l'antagonisme de Tetherin sur la réplication et la pathogénèse serait l'utilisation d'un modèle animal tel que la souris où le système immunitaire est préalablement humanisé par transfert adoptif (273).

Il existe tout de même plusieurs indices indirects de l'importance de la séquestration et de l'antagonisme de Tetherin par Vpu pour la pathogénèse du virus. L'identification de mutants de Vpu retrouvés spécifiquement chez des patients non-progresseurs à long terme représente un premier argument en ce sens (265). Dans cette étude, plusieurs mutations retrouvées dans des clones viraux indépendants et provoquant un arrêt prématuré de la traduction se sont avérées groupées en amont du domaine transmembranaire de Vpu, suggérant que l'absence de la capacité de séquestration de Vpu hypothèque la propagation du virus. Une autre étude *in vitro* s'intéressant à la fonctionnalité de Vpu provenant des groupes M, N et O du VIH-1 (210) a démontré que la fonction de dégradation de CD4 est conservée chez les groupes M et O alors qu'aucune des protéines Vpu du groupe O testées ne s'est avérée en mesure de contrer Tetherin. Cette observation est très intéressante du fait de la faible pathogénicité du groupe O: à ce jour, seulement quelques rares cas isolés ont été rapportés (210). La très grande conservation de l'antagonisme de Tetherin entre les différentes souches de VIH ou VIS, indépendamment de la nature de l'antagoniste s'en chargeant, laisse présager un rôle important de cette fonction (114, 143, 210, 270). Le meilleur argument en ce sens demeure probablement du gain d'une fonction antagoniste anti-Tetherin *in vivo* chez la protéine de l'enveloppe gp41 du virus VISmac239 dont le gène *nef* codant pour l'antagoniste de Tetherin simien chez ce virus avait préalablement été inactivé (222). Sans démontrer directement l'importance de Vpu à cet effet, cette donnée illustre tout de même l'importance de la présence d'au moins un tel antagoniste.

Cette augmentation de la pathogénicité du virus reliée à l'antagonisme de Tetherin pourrait intuitivement être attribuée à l'augmentation de la relâche des particules virales. En fait, l'expression de Vpu, bien qu'améliorant les titres de virus produits, n'accélère pas la cinétique de réplication du virus à proprement dit (132, 216). La découverte du mode de transmission du VIH-1 d'une cellule à une autre via une synapse virale fit émerger à l'idée selon laquelle l'accumulation de virus infectieux à la membrane plasmique en présence de la Tetherin pourrait améliorer ce type de transmission et ainsi compenser la faible efficacité de la relâche virale (162, 228). La corrélation entre l'amélioration du transfert de cellule à cellule et l'invalidation du gène *vpu* telle qu'observée chez certains clones viraux passés successivement *in vitro* ne fit

que renforcer cette supposition (92). Cependant, aucun consensus n'a émergé des trois études qui ont tenté d'évaluer l'effet de Tetherin sur ce type de transmission: dans deux d'entre elles, la transmission synaptique semblait être restreinte par Tetherin (30, 137), alors qu'elle semblait améliorée dans la troisième (120). Ce paradoxe reflète probablement des effets alternatifs dépendamment du niveau de Tetherin à la surface des cellules donatrices et des cellules cibles (137), rendant hasardeuse toute spéculation sur la contribution nette de Vpu sur la propagation virale *in vivo*.

Il est concevable que l'avantage conféré par l'augmentation de la relâche virale sur la propagation virale soit négligeable dans des zones où la concentration élevée en cellules favorise plutôt les contacts cellulaires et la transmission de cellule à cellule. Par contre, elle devient potentiellement bien plus significative dans le système circulatoire, où la turbulence pourrait interférer avec ce mode de transmission, tel qu'observé *in vitro* (228). Cet avantage permettrait peut-être aussi de multiplier chez l'hôte les foyers d'infection éloignés les uns des autres. Suivant cette logique, la grande prépondérance dans la population du groupe M, capable de surmonter la restriction imposée par la Tetherin, pourrait aussi signifier une amélioration de la transmissibilité du virus d'un individu à l'autre due à de meilleurs titres viraux dans les fluides corporels. Cette idée est compatible avec l'augmentation de l'expression de Tetherin dans le tractus vaginal du mouton par l'IFNtau, l'hormone de reconnaissance de gestation chez ce mammifère (7). En effet, Tetherin pourrait représenter une barrière à la transmission sexuelle au niveau de cette muqueuse. Il sera intéressant d'évaluer si une telle barrière existe chez les primates et d'en vérifier l'intégrité en présence d'un antagoniste de Tetherin le cas échéant.

La pertinence de Vpu durant l'infection n'est fort probablement pas restreinte à son effet sur CD4 et Tetherin. Tel que mentionné précédemment, la délétion du domaine transmembranaire de Vpu affecte la pathogénèse du virus chez le singe indépendamment de l'antagonisme de Tetherin. Il est donc probable que la séquestration des autres substrats de Vpu tels que NTB-A et CD1d contribue aussi à la pathogénèse. Bien sûr, la déplétion de NTB-A et de CD1d a certainement pour conséquence de protéger les cellules infectées de la lyse par les cellules NK et NKT (198). Cependant,

Vpu pourrait avoir des effets bien plus subtils. Certaines composantes du virus, nommément Vpr et gp41, ont la propriété d'augmenter l'expression de surface de certains ligands des cellules NK (68, 199, 253, 259). Cette augmentation des ligands entraînerait la lyse très efficace par les cellules NK si ce n'était de l'effet modérateur de Vpu via la déplétion des molécules co-activatrices NTB-A (223). Par contre, tel ne serait pas le cas dans les cellules avoisinantes non-infectées mais tout de même transduites par des particules partiellement défectives contenant Vpr (199). Il est donc envisageable que Vpu stimule indirectement la lyse des cellules non-infectées avoisinantes en stimulant la sécrétion de particules défectueuses et exacerbe ainsi la déplétion des lymphocytes T CD4, phénomène observé *in vivo* (91). Finalement, l'expression de Vpu a peut-être pour effet indirect de diminuer la présentation d'antigènes spécifiques au VIH-1. S'il n'est pas clair si Tetherin accélère véritablement l'internalisation des virus matures restreints en surface, l'expression du facteur de restriction tend clairement à augmenter l'accumulation de virus matures dans les endosomes tardifs et les lysosomes (176, 184). Puisque ces compartiments représentent les sites de chargement de peptides sur les CMH-I, Tetherin pourrait incidemment favoriser la présentation antigénique en absence de Vpu. Cette notion est aussi compatible avec notre observation que la Tetherin internalisée semble se diriger vers les endosomes tardifs plutôt que d'être recyclée en surface (Figure 5 et 6 du Chapitre 3).

7. Vpu : l'improbable cible thérapeutique?

Seules les protéines accessoires n'ont pas sérieusement été considérées par l'industrie comme cibles potentielles. Pourtant, l'idée d'utiliser les protéines accessoires comme cible thérapeutique ne date pas d'hier (171, 245). Les récentes percées sur la biologie de Vpu laissent présager un intéressant potentiel thérapeutique, d'autant plus que cette protéine agit sur la production virale, une étape négligée par les classes actuelles de médicaments. Puisque le domaine transmembranaire de Vpu semble assurer plusieurs fonctions indépendantes, une petite molécule synthétique dirigée contre ce domaine pourrait théoriquement à la fois prévenir la sécrétion de particules infectieuses ou défectives, rétablir la présentation de lipides antigéniques et stimuler la lyse des

cellules infectées par les cellules NK. La faisabilité d'une telle approche thérapeutique a déjà été démontrée, du moins en ce qui concerne l'augmentation de la relâche de particules virales. Tel que mentionné précédemment, Vpu a une certaine homologie avec la protéine M2 d'influenza. Hout et collègues ont démontré qu'une simple mutation dans le domaine transmembranaire de Vpu la rendait sensible à l'action de la rimantadine, un inhibiteur de M2 (104). L'abrogation de l'activité antagoniste de ce mutant par la présence de rimantadine a corrélé avec la réduction de la relâche du virus *in vitro*, suggérant qu'une petite molécule dirigée contre le domaine transmembrane de Vpu pourrait rétablir la restriction (104). Des tentatives de développement de dérivés d'amiloride ciblant directement le domaine transmembranaire de Vpu se sont soldées par des résultats similaires, quoique les effets de tels composés ne semblaient pas tout à fait spécifiques à Vpu (63, 127, 144, 145). Le rationnel de leur développement, qui reposait sur la formation *in vitro* de canaux ioniques par Vpu dans des bicouches lipidiques, fut cependant remis en question par de récentes données qui n'ont pas supporté la pertinence de telles structures dans des systèmes cellulaires (64, 217, 226). Il n'est pas à exclure par contre que ces composés dirigés contre le domaine transmembranaire de Vpu puisses bloquer l'association de Vpu à ses différents substrats. Il serait donc intéressant de tester leurs effets sur l'antagonisme de Tetherin, plus spécifiquement au niveau de l'interaction Tetherin-Vpu.

L'émergence de souches virales résistantes demeure un obstacle au développement d'une drogue ciblant Vpu. En effet, la pression sélective exercée sur le virus en absence d'activité de Vpu pourrait forcer un gain de fonction chez d'autres protéines virales. Puisqu'aucune souche de VIH-1 ne semble avoir développé une protéine Nef antagoniste, le coût évolutif requis pour compenser la perte de son site de reconnaissance au niveau de la Tetherin humaine est probablement trop élevé. La saturabilité de Tetherin par Gag (185) pourrait plutôt laisser présager la sélection de souches virales caractérisées par la forte expression de cette protéine. Le gain d'une fonction antagoniste dans la gp41 de VISmac239Δ*nef* suite à des passages successifs *in vitro* évoque plutôt la possibilité du gain d'une fonction antagoniste au niveau de la protéine de l'enveloppe (222). Des protéines de l'enveloppe aux propriétés neutralisantes ont d'ailleurs été identifiées chez le VIH-2 et même chez le VIH-1 AD8,

un virus CCR5-tropique (21, 215), ce qui suggère que ce type de réversion serait possible chez l'humain et probablement à un moindre coût évolutif que pour Nef. Avant d'investir des efforts pour le développement d'une thérapie ciblant Vpu, il sera donc important d'évaluer la fréquence de telles réversions et leurs conséquences sur la pathogénicité du virus.

CONCLUSION

Grâce à nos travaux, la stratégie employée par Vpu afin de faciliter la relâche des particules virales est beaucoup mieux comprise. Les contributions scientifiques de cette thèse en témoignent : elle 1) identifie des régions responsables de la localisation de Vpu; 2) met en évidence pour la première fois le mécanisme de séquestration de Tetherin dans le RTG par cette dernière lors de son antagonisme; 3) désigne la liaison entre des domaines transmembranaires de Vpu et de Tetherin comme un déterminant critique à la séquestration et donc, à l'antagonisme; 4) renforce la causalité entre la déplétion de la Tetherin en surface et l'augmentation de la relâche virale; et 5) valide l'idée que le blocage par Vpu du réapprovisionnement de Tetherin en surface suffit à sa déplétion. Cependant, son plus grand mérite aura probablement été de proposer un modèle où la plupart des mécanismes d'antagonismes suggérés à ce jour ont trouvé une pertinence.

Néanmoins, beaucoup reste à faire afin d'élucider complètement le mécanisme d'antagonisme de Tetherin par Vpu. Bien sûr, la nécessité de développer de nouvelles thérapies guidera probablement les axes de recherche sur ces deux protéines dans les années à venir. Par exemple, afin d'évaluer la possibilité de se servir de l'interaction entre β-TrCP et Vpu comme cible thérapeutique, la réelle contribution de β-TrCP selon les contextes cellulaires devra être mieux comprise. L'amélioration de nos connaissances sur le rôle revêtu par Vpu dans la modulation du système immunitaire, soit via ses effets sur CD1d, NTB-A et potentiellement Tetherin serait aussi à privilégier. Bien sûr, il sera critique d'évaluer rigoureusement la contribution de toutes les différentes fonctions de la protéine dans un modèle *in vivo*. Finalement, l'évaluation de la fréquence de souches résistantes ou de révertants dans un contexte où Vpu est inhibée démontrera s'il vaut la peine d'investir dans l'élaboration d'une telle thérapie. Il est tout de même à souhaiter que cette recherche thérapeutique n'empêchera pas la poursuite de questions plus mécanistiques et académiques qui pourraient ouvrir de tous nouveaux axes de recherche tels que la compréhension des évènements menant à l'altération par Vpu du trafic cellulaire de si nombreuses protéines et la découverte de

nouveaux substrats de Vpu. Du moins, espérons-le pour les virologistes fondamentalistes que nous sommes.

RÉFÉRENCES

1. **Acconcia, F., S. Sigismund, and S. Polo.** 2009. Ubiquitin in trafficking: the network at work. Experimental cell research **315:**1610-8.
2. **Aiken, C.** 2006. Viral and cellular factors that regulate HIV-1 uncoating. Current opinion in HIV and AIDS **1:**194-9.
3. **Alter, G., and M. Altfeld.** 2009. NK cells in HIV-1 infection: evidence for their role in the control of HIV-1 infection. Journal of internal medicine **265:**29-42.
4. **Ancuta, P., P. Monteiro, and R. P. Sekaly.** 2010. Th17 lineage commitment and HIV-1 pathogenesis. Current opinion in HIV and AIDS **5:**158-65.
5. **Andrew, A. J., E. Miyagi, and K. Strebel.** 2011. Differential Effects of Human Immunodeficiency Virus Type 1 Vpu on the Stability of BST-2/Tetherin. Journal of virology **85:**2611-9.
6. **Ang, A. L., H. Folsch, U. M. Koivisto, M. Pypaert, and I. Mellman.** 2003. The Rab8 GTPase selectively regulates AP-1B-dependent basolateral transport in polarized Madin-Darby canine kidney cells. The Journal of cell biology **163:**339-50.
7. **Arnaud, F., S. G. Black, L. Murphy, D. J. Griffiths, S. J. Neil, T. E. Spencer, and M. Palmarini.** 2010. Interplay between ovine bone marrow stromal cell antigen 2/tetherin and endogenous retroviruses. Journal of virology **84:**4415-25.
8. **Bartee, E., C. A. Eyster, K. Viswanathan, M. Mansouri, J. G. Donaldson, and K. Fruh.** 2010. Membrane-Associated RING-CH proteins associate with Bap31 and target CD81 and CD44 to lysosomes. PloS one **5:**e15132.
9. **Belaidouni, N., C. Marchal, R. Benarous, and C. Besnard-Guerin.** 2007. Involvement of the betaTrCP in the ubiquitination and stability of the HIV-1 Vpu protein. Biochemical and biophysical research communications **357:**688-93.
10. **Belzile, J. P., L. G. Abrahamyan, F. C. Gerard, N. Rougeau, and E. A. Cohen.** 2010. Formation of mobile chromatin-associated nuclear foci containing

HIV-1 Vpr and VPRBP is critical for the induction of G2 cell cycle arrest. PLoS pathogens **6:**e1001080.

11. **Belzile, J. P., G. Duisit, N. Rougeau, J. Mercier, A. Finzi, and E. A. Cohen.** 2007. HIV-1 Vpr-mediated G2 arrest involves the DDB1-CUL4AVPRBP E3 ubiquitin ligase. PLoS pathogens **3:**e85.
12. **Belzile, J. P., J. Richard, N. Rougeau, Y. Xiao, and E. A. Cohen.** 2010. HIV-1 Vpr induces the K48-linked polyubiquitination and proteasomal degradation of target cellular proteins to activate ATR and promote G2 arrest. Journal of virology **84:**3320-30.
13. **Benlahrech, A., and S. Patterson.** 2011. HIV-1 infection and induction of interferon alpha in plasmacytoid dendritic cells. Current opinion in HIV and AIDS.
14. **Bennasser, Y., S. Y. Le, M. L. Yeung, and K. T. Jeang.** 2004. HIV-1 encoded candidate micro-RNAs and their cellular targets. Retrovirology **1:**43.
15. **Besnard-Guerin, C., N. Belaidouni, I. Lassot, E. Segeral, A. Jobart, C. Marchal, and R. Benarous.** 2004. HIV-1 Vpu sequesters beta-transducin repeat-containing protein (betaTrCP) in the cytoplasm and provokes the accumulation of beta-catenin and other SCFbetaTrCP substrates. The Journal of biological chemistry **279:**788-95.
16. **Bieniasz, P. D.** 2009. The cell biology of HIV-1 virion genesis. Cell host & microbe **5:**550-8.
17. **Blagoveshchenskaya, A. D., L. Thomas, S. F. Feliciangeli, C. H. Hung, and G. Thomas.** 2002. HIV-1 Nef downregulates MHC-I by a PACS-1- and PI3K-regulated ARF6 endocytic pathway. Cell **111:**853-66.
18. **Bonifacino, J. S., and L. M. Traub.** 2003. Signals for sorting of transmembrane proteins to endosomes and lysosomes. Annual review of biochemistry **72:**395-447.
19. **Bottino, C., M. Falco, S. Parolini, E. Marcenaro, R. Augugliaro, S. Sivori, E. Landi, R. Biassoni, L. D. Notarangelo, L. Moretta, and A. Moretta.** 2001. NTB-A [correction of GNTB-A], a novel SH2D1A-associated surface molecule contributing to the inability of natural killer cells to kill Epstein-Barr virus-

infected B cells in X-linked lymphoproliferative disease. The Journal of experimental medicine **194:**235-46.

20. **Bour, S., C. Perrin, H. Akari, and K. Strebel.** 2001. The human immunodeficiency virus type 1 Vpu protein inhibits NF-kappa B activation by interfering with beta TrCP-mediated degradation of Ikappa B. The Journal of biological chemistry **276:**15920-8.
21. **Bour, S., U. Schubert, K. Peden, and K. Strebel.** 1996. The envelope glycoprotein of human immunodeficiency virus type 2 enhances viral particle release: a Vpu-like factor? Journal of virology **70:**820-9.
22. **Brass, A. L., D. M. Dykxhoorn, Y. Benita, N. Yan, A. Engelman, R. J. Xavier, J. Lieberman, and S. J. Elledge.** 2008. Identification of host proteins required for HIV infection through a functional genomic screen. Science **319:**921-6.
23. **Briggs, J. A., T. Wilk, R. Welker, H. G. Krausslich, and S. D. Fuller.** 2003. Structural organization of authentic, mature HIV-1 virions and cores. The EMBO journal **22:**1707-15.
24. **Browne, E. P., C. Allers, and N. R. Landau.** 2009. Restriction of HIV-1 by APOBEC3G is cytidine deaminase-dependent. Virology **387:**313-21.
25. **Bryant, M., and L. Ratner.** 1990. Myristoylation-dependent replication and assembly of human immunodeficiency virus 1. Proceedings of the National Academy of Sciences of the United States of America **87:**523-7.
26. **Buchbinder, S. P., D. V. Mehrotra, A. Duerr, D. W. Fitzgerald, R. Mogg, D. Li, P. B. Gilbert, J. R. Lama, M. Marmor, C. Del Rio, M. J. McElrath, D. R. Casimiro, K. M. Gottesdiener, J. A. Chodakewitz, L. Corey, and M. N. Robertson.** 2008. Efficacy assessment of a cell-mediated immunity HIV-1 vaccine (the Step Study): a double-blind, randomised, placebo-controlled, test-of-concept trial. Lancet **372:**1881-93.
27. **Campbell, E. M., R. Nunez, and T. J. Hope.** 2004. Disruption of the actin cytoskeleton can complement the ability of Nef to enhance human immunodeficiency virus type 1 infectivity. Journal of virology **78:**5745-55.

28. **Cano, A., M. A. Perez-Moreno, I. Rodrigo, A. Locascio, M. J. Blanco, M. G. del Barrio, F. Portillo, and M. A. Nieto.** 2000. The transcription factor snail controls epithelial-mesenchymal transitions by repressing E-cadherin expression. Nature cell biology **2:**76-83.

29. **Cao, W., L. Bover, M. Cho, X. Wen, S. Hanabuchi, M. Bao, D. B. Rosen, Y. H. Wang, J. L. Shaw, Q. Du, C. Li, N. Arai, Z. Yao, L. L. Lanier, and Y. J. Liu.** 2009. Regulation of TLR7/9 responses in plasmacytoid dendritic cells by BST2 and ILT7 receptor interaction. The Journal of experimental medicine **206:**1603-14.

30. **Casartelli, N., M. Sourisseau, J. Feldmann, F. Guivel-Benhassine, A. Mallet, A. G. Marcelin, J. Guatelli, and O. Schwartz.** 2010. Tetherin restricts productive HIV-1 cell-to-cell transmission. PLoS pathogens **6:**e1000955.

31. **Casey, L., X. Wen, M. Flagg, M. Nekorchuk, and C. De Noronha.** 2011. Vpr Directs Depletion of Cellular Endoribonuclease Dicer through the DCAF1-CRL4 Ubiquitin Ligase Complex. 18th Conference on Retroviruses and Oppotunistic Infections (CROI), February 28th.

32. **Chatterji, U., M. D. Bobardt, P. Gaskill, D. Sheeter, H. Fox, and P. A. Gallay.** 2006. Trim5alpha accelerates degradation of cytosolic capsid associated with productive HIV-1 entry. The Journal of biological chemistry **281:**37025-33.

33. **Chaudhuri, R., O. W. Lindwasser, W. J. Smith, J. H. Hurley, and J. S. Bonifacino.** 2007. Downregulation of CD4 by human immunodeficiency virus type 1 Nef is dependent on clathrin and involves direct interaction of Nef with the AP2 clathrin adaptor. Journal of virology **81:**3877-90.

34. **Chen, H., S. Polo, P. P. Di Fiore, and P. V. De Camilli.** 2003. Rapid Ca2+-dependent decrease of protein ubiquitination at synapses. Proceedings of the National Academy of Sciences of the United States of America **100:**14908-13.

35. **Chen, K., J. Huang, C. Zhang, S. Huang, G. Nunnari, F. X. Wang, X. Tong, L. Gao, K. Nikisher, and H. Zhang.** 2006. Alpha interferon potently enhances the anti-human immunodeficiency virus type 1 activity of APOBEC3G in resting primary CD4 T cells. Journal of virology **80:**7645-57.

36. **Chowers, M. Y., C. A. Spina, T. J. Kwoh, N. J. Fitch, D. D. Richman, and J. C. Guatelli.** 1994. Optimal infectivity in vitro of human immunodeficiency virus type 1 requires an intact nef gene. Journal of virology **68:**2906-14.

37. **Ciuffi, A., M. Llano, E. Poeschla, C. Hoffmann, J. Leipzig, P. Shinn, J. R. Ecker, and F. Bushman.** 2005. A role for LEDGF/p75 in targeting HIV DNA integration. Nature medicine **11:**1287-9.

38. **ClinicalTrials.gov.** . www.clinicaltrials.gov

39. **Cohen, E. A., E. F. Terwilliger, Y. Jalinoos, J. Proulx, J. G. Sodroski, and W. A. Haseltine.** 1990. Identification of HIV-1 vpr product and function. Journal of acquired immune deficiency syndromes **3:**11-8.

40. **Cohen, G. B., R. T. Gandhi, D. M. Davis, O. Mandelboim, B. K. Chen, J. L. Strominger, and D. Baltimore.** 1999. The selective downregulation of class I major histocompatibility complex proteins by HIV-1 protects HIV-infected cells from NK cells. Immunity **10:**661-71.

41. **Coley, W., R. Van Duyne, L. Carpio, I. Guendel, K. Kehn-Hall, S. Chevalier, A. Narayanan, T. Luu, N. Lee, Z. Klase, and F. Kashanchi.** 2010. Absence of DICER in monocytes and its regulation by HIV-1. The Journal of biological chemistry **285:**31930-43.

42. **Connor, R. I., B. K. Chen, S. Choe, and N. R. Landau.** 1995. Vpr is required for efficient replication of human immunodeficiency virus type-1 in mononuclear phagocytes. Virology **206:**935-44.

43. **Conticello, S. G., R. S. Harris, and M. S. Neuberger.** 2003. The Vif protein of HIV triggers degradation of the human antiretroviral DNA deaminase APOBEC3G. Current biology : CB **13:**2009-13.

44. **Cornell, R. B., and S. G. Taneva.** 2006. Amphipathic helices as mediators of the membrane interaction of amphitropic proteins, and as modulators of bilayer physical properties. Current protein & peptide science **7:**539-52.

45. **Cui, H., E. Lyman, and G. A. Voth.** 2011. Mechanism of membrane curvature sensing by amphipathic helix containing proteins. Biophysical journal **100:**1271-9.

46. **Darke, P. L., R. F. Nutt, S. F. Brady, V. M. Garsky, T. M. Ciccarone, C. T. Leu, P. K. Lumma, R. M. Freidinger, D. F. Veber, and I. S. Sigal.** 1988. HIV-1 protease specificity of peptide cleavage is sufficient for processing of gag and pol polyproteins. Biochemical and biophysical research communications **156:**297-303.

47. **De Gassart, A., V. Camosseto, J. Thibodeau, M. Ceppi, N. Catalan, P. Pierre, and E. Gatti.** 2008. MHC class II stabilization at the surface of human dendritic cells is the result of maturation-dependent MARCH I down-regulation. Proceedings of the National Academy of Sciences of the United States of America **105:**3491-6.

48. **Deacon, N. J., A. Tsykin, A. Solomon, K. Smith, M. Ludford-Menting, D. J. Hooker, D. A. McPhee, A. L. Greenway, A. Ellett, C. Chatfield, V. A. Lawson, S. Crowe, A. Maerz, S. Sonza, J. Learmont, J. S. Sullivan, A. Cunningham, D. Dwyer, D. Dowton, and J. Mills.** 1995. Genomic structure of an attenuated quasi species of HIV-1 from a blood transfusion donor and recipients. Science **270:**988-91.

49. **DeHart, J. L., A. Bosque, R. S. Harris, and V. Planelles.** 2008. Human immunodeficiency virus type 1 Vif induces cell cycle delay via recruitment of the same E3 ubiquitin ligase complex that targets APOBEC3 proteins for degradation. Journal of virology **82:**9265-72.

50. **DeHart, J. L., E. S. Zimmerman, O. Ardon, C. M. Monteiro-Filho, E. R. Arganaraz, and V. Planelles.** 2007. HIV-1 Vpr activates the G2 checkpoint through manipulation of the ubiquitin proteasome system. Virology journal **4:**57.

51. **Deng, H., R. Liu, W. Ellmeier, S. Choe, D. Unutmaz, M. Burkhart, P. Di Marzio, S. Marmon, R. E. Sutton, C. M. Hill, C. B. Davis, S. C. Peiper, T. J. Schall, D. R. Littman, and N. R. Landau.** 1996. Identification of a major co-receptor for primary isolates of HIV-1. Nature **381:**661-6.

52. **Deora, A., and L. Ratner.** 2001. Viral protein U (Vpu)-mediated enhancement of human immunodeficiency virus type 1 particle release depends on the rate of cellular proliferation. Journal of virology **75:**6714-8.

53. **Diaz-Griffero, F., X. Li, H. Javanbakht, B. Song, S. Welikala, M. Stremlau, and J. Sodroski.** 2006. Rapid turnover and polyubiquitylation of the retroviral restriction factor TRIM5. Virology **349:**300-15.

54. **Douglas, J. L., K. Viswanathan, M. N. McCarroll, J. K. Gustin, K. Fruh, and A. V. Moses.** 2009. Vpu directs the degradation of the human immunodeficiency virus restriction factor BST-2/Tetherin via a {beta}TrCP-dependent mechanism. Journal of virology **83:**7931-47.

55. **Douglas, J. L., K. Viswanathan, M. N. McCarroll, J. K. Gustin, K. Fruh, and A. V. Moses.** 2009. Vpu directs the degradation of the human immunodeficiency virus restriction factor BST-2/Tetherin via a {beta}TrCP-dependent mechanism. J Virol **83:**7931-47.

56. **Druillennec, S., and B. P. Roques.** 2000. HIV-1 NCp7 as a target for the design of novel antiviral agents. Drug news & perspectives **13:**337-49.

57. **Dube, M., M. G. Bego, C. Paquay, and E. A. Cohen.** 2010. Modulation of HIV-1-host interaction: role of the Vpu accessory protein. Retrovirology **7:**114.

58. **Dube, M., B. B. Roy, P. Guiot-Guillain, J. Binette, J. Mercier, A. Chiasson, and E. A. Cohen.** 2010. Antagonism of tetherin restriction of HIV-1 release by Vpu involves binding and sequestration of the restriction factor in a perinuclear compartment. PLoS Pathog **6:**e1000856.

59. **Dube, M., B. B. Roy, P. Guiot-Guillain, J. Binette, J. Mercier, A. Chiasson, and E. A. Cohen.** 2010. Antagonism of tetherin restriction of HIV-1 release by Vpu involves binding and sequestration of the restriction factor in a perinuclear compartment. PLoS pathogens **6:**e1000856.

60. **Dube, M., B. B. Roy, P. Guiot-Guillain, J. Mercier, J. Binette, G. Leung, and E. A. Cohen.** 2009. Suppression of Tetherin-restricting activity upon human immunodeficiency virus type 1 particle release correlates with localization of Vpu in the trans-Golgi network. Journal of virology **83:**4574-90.

61. **Eckstein, D. A., M. P. Sherman, M. L. Penn, P. S. Chin, C. M. De Noronha, W. C. Greene, and M. A. Goldsmith.** 2001. HIV-1 Vpr enhances viral burden by facilitating infection of tissue macrophages but not nondividing CD4+ T cells. The Journal of experimental medicine **194:**1407-19.

62. **Estrabaud, E., E. Le Rouzic, S. Lopez-Verges, M. Morel, N. Belaidouni, R. Benarous, C. Transy, C. Berlioz-Torrent, and F. Margottin-Goguet.** 2007. Regulated degradation of the HIV-1 Vpu protein through a betaTrCP-independent pathway limits the release of viral particles. PLoS pathogens **3:**e104.

63. **Ewart, G. D., K. Mills, G. B. Cox, and P. W. Gage.** 2002. Amiloride derivatives block ion channel activity and enhancement of virus-like particle budding caused by HIV-1 protein Vpu. European biophysics journal : EBJ **31:**26-35.

64. **Ewart, G. D., T. Sutherland, P. W. Gage, and G. B. Cox.** 1996. The Vpu protein of human immunodeficiency virus type 1 forms cation-selective ion channels. Journal of virology **70:**7108-15.

65. **Fackler, O. T., N. Kienzle, E. Kremmer, A. Boese, B. Schramm, T. Klimkait, C. Kucherer, and N. Mueller-Lantzsch.** 1997. Association of human immunodeficiency virus Nef protein with actin is myristoylation dependent and influences its subcellular localization. European journal of biochemistry / FEBS **247:**843-51.

66. **Fan, L., and K. Peden.** 1992. Cell-free transmission of Vif mutants of HIV-1. Virology **190:**19-29.

67. **Fausther-Bovendo, H., N. Sol-Foulon, D. Candotti, H. Agut, O. Schwartz, P. Debre, and V. Vieillard.** 2009. HIV escape from natural killer cytotoxicity: nef inhibits NKp44L expression on CD4+ T cells. AIDS **23:**1077-87.

68. **Fausther-Bovendo, H., V. Vieillard, S. Sagan, G. Bismuth, and P. Debre.** 2010. HIV gp41 engages gC1qR on CD4+ T cells to induce the expression of an NK ligand through the PIP3/H2O2 pathway. PLoS pathogens **6:**e1000975.

69. **Fields, I. C., E. Shteyn, M. Pypaert, V. Proux-Gillardeaux, R. S. Kang, T. Galli, and H. Folsch.** 2007. v-SNARE cellubrevin is required for basolateral sorting of AP-1B-dependent cargo in polarized epithelial cells. The Journal of cell biology **177:**477-88.

70. **Fisher, A. G., B. Ensoli, L. Ivanoff, M. Chamberlain, S. Petteway, L. Ratner, R. C. Gallo, and F. Wong-Staal.** 1987. The sor gene of HIV-1 is required for efficient virus transmission in vitro. Science **237:**888-93.

71. **Fitzpatrick, K., M. Skasko, T. J. Deerinck, J. Crum, M. H. Ellisman, and J. Guatelli.** 2010. Direct restriction of virus release and incorporation of the interferon-induced protein BST-2 into HIV-1 particles. PLoS pathogens **6:**e1000701.

72. **Flaig, R. M., S. Stark, and C. Watzl.** 2004. Cutting edge: NTB-A activates NK cells via homophilic interaction. Journal of immunology **172:**6524-7.

73. **Flynn, N. M., D. N. Forthal, C. D. Harro, F. N. Judson, K. H. Mayer, and M. F. Para.** 2005. Placebo-controlled phase 3 trial of a recombinant glycoprotein 120 vaccine to prevent HIV-1 infection. The Journal of infectious diseases **191:**654-65.

74. **Folsch, H., M. Pypaert, P. Schu, and I. Mellman.** 2001. Distribution and function of AP-1 clathrin adaptor complexes in polarized epithelial cells. The Journal of cell biology **152:**595-606.

75. **Fujita, T., Y. Kimura, M. Miyamoto, E. L. Barsoumian, and T. Taniguchi.** 1989. Induction of endogenous IFN-alpha and IFN-beta genes by a regulatory transcription factor, IRF-1. Nature **337:**270-2.

76. **Gabuzda, D. H., K. Lawrence, E. Langhoff, E. Terwilliger, T. Dorfman, W. A. Haseltine, and J. Sodroski.** 1992. Role of vif in replication of human immunodeficiency virus type 1 in CD4+ T lymphocytes. Journal of virology **66:**6489-95.

77. **Gabuzda, D. H., H. Li, K. Lawrence, B. S. Vasir, K. Crawford, and E. Langhoff.** 1994. Essential role of vif in establishing productive HIV-1 infection in peripheral blood T lymphocytes and monocyte/macrophages. Journal of acquired immune deficiency syndromes **7:**908-15.

78. **Garrett, E. D., L. S. Tiley, and B. R. Cullen.** 1991. Rev activates expression of the human immunodeficiency virus type 1 vif and vpr gene products. Journal of virology **65:**1653-7.

79. **Gatza, M. L., T. Dayaram, and S. J. Marriott.** 2007. Ubiquitination of HTLV-I Tax in response to DNA damage regulates nuclear complex formation and nuclear export. Retrovirology **4:**95.

80. **Geraghty, R. J., K. J. Talbot, M. Callahan, W. Harper, and A. T. Panganiban.** 1994. Cell type-dependence for Vpu function. Journal of medical primatology **23:**146-50.

81. **Ghosh, R. K., S. M. Ghosh, and S. Chawla.** 2011. Recent advances in antiretroviral drugs. Expert opinion on pharmacotherapy **12:**31-46.

82. **Giannetti, A., G. Zambruno, A. Cimarelli, A. Marconi, M. Negroni, G. Girolomoni, and U. Bertazzoni.** 1993. Direct detection of HIV-1 RNA in epidermal Langerhans cells of HIV-infected patients. Journal of acquired immune deficiency syndromes **6:**329-33.

83. **Goff, S. P.** 2007. Host factors exploited by retroviruses. Nature reviews. Microbiology **5:**253-63.

84. **Goffinet, C., I. Allespach, S. Homann, H. M. Tervo, A. Habermann, D. Rupp, L. Oberbremer, C. Kern, N. Tibroni, S. Welsch, J. Krijnse-Locker, G. Banting, H. G. Krausslich, O. T. Fackler, and O. T. Keppler.** 2009. HIV-1 antagonism of CD317 is species specific and involves Vpu-mediated proteasomal degradation of the restriction factor. Cell Host Microbe **5:**285-97.

85. **Goffinet, C., I. Allespach, S. Homann, H. M. Tervo, A. Habermann, D. Rupp, L. Oberbremer, C. Kern, N. Tibroni, S. Welsch, J. Krijnse-Locker, G. Banting, H. G. Krausslich, O. T. Fackler, and O. T. Keppler.** 2009. HIV-1 antagonism of CD317 is species specific and involves Vpu-mediated proteasomal degradation of the restriction factor. Cell host & microbe **5:**285-97.

86. **Goffinet, C., S. Homann, I. Ambiel, N. Tibroni, D. Rupp, O. T. Keppler, and O. T. Fackler.** 2010. Antagonism of CD317 restriction of human immunodeficiency virus type 1 (HIV-1) particle release and depletion of CD317 are separable activities of HIV-1 Vpu. Journal of virology **84:**4089-94.

87. **Goila-Gaur, R., and K. Strebel.** 2008. HIV-1 Vif, APOBEC, and intrinsic immunity. Retrovirology **5:**51.

88. **Gorelick, R. J., S. M. Nigida, Jr., J. W. Bess, Jr., L. O. Arthur, L. E. Henderson, and A. Rein.** 1990. Noninfectious human immunodeficiency virus type 1 mutants deficient in genomic RNA. Journal of virology **64:**3207-11.

89. **Gorry, P. R., and P. Ancuta.** 2011. Coreceptors and HIV-1 pathogenesis. Current HIV/AIDS reports **8:**45-53.

90. **Gorry, P. R., G. Bristol, J. A. Zack, K. Ritola, R. Swanstrom, C. J. Birch, J. E. Bell, N. Bannert, K. Crawford, H. Wang, D. Schols, E. De Clercq, K. Kunstman, S. M. Wolinsky, and D. Gabuzda.** 2001. Macrophage tropism of human immunodeficiency virus type 1 isolates from brain and lymphoid tissues predicts neurotropism independent of coreceptor specificity. Journal of virology **75:**10073-89.

91. **Guadalupe, M., E. Reay, S. Sankaran, T. Prindiville, J. Flamm, A. McNeil, and S. Dandekar.** 2003. Severe CD4+ T-cell depletion in gut lymphoid tissue during primary human immunodeficiency virus type 1 infection and substantial delay in restoration following highly active antiretroviral therapy. Journal of virology **77:**11708-17.

92. **Gummuluru, S., C. M. Kinsey, and M. Emerman.** 2000. An in vitro rapid-turnover assay for human immunodeficiency virus type 1 replication selects for cell-to-cell spread of virus. Journal of virology **74:**10882-91.

93. **Gupta, R. K., S. Hue, T. Schaller, E. Verschoor, D. Pillay, and G. J. Towers.** 2009. Mutation of a single residue renders human tetherin resistant to HIV-1 Vpu-mediated depletion. PLoS pathogens **5:**e1000443.

94. **Gupta, R. K., S. Hue, T. Schaller, E. Verschoor, D. Pillay, and G. J. Towers.** 2009. Mutation of a single residue renders human tetherin resistant to HIV-1 Vpu-mediated depletion. PLoS Pathog **5:**e1000443.

95. **Gupta, R. K., P. Mlcochova, A. Pelchen-Matthews, S. J. Petit, G. Mattiuzzo, D. Pillay, Y. Takeuchi, M. Marsh, and G. J. Towers.** 2009. Simian immunodeficiency virus envelope glycoprotein counteracts tetherin/BST-2/CD317 by intracellular sequestration. Proc Natl Acad Sci U S A **106:**20889-94.

96. **Gupta, R. K., P. Mlcochova, A. Pelchen-Matthews, S. J. Petit, G. Mattiuzzo, D. Pillay, Y. Takeuchi, M. Marsh, and G. J. Towers.** 2009. Simian immunodeficiency virus envelope glycoprotein counteracts tetherin/BST-2/CD317 by intracellular sequestration. Proceedings of the National Academy of Sciences of the United States of America **106:**20889-94.

97. **Habermann, A., J. Krijnse-Locker, H. Oberwinkler, M. Eckhardt, S. Homann, A. Andrew, K. Strebel, and H. G. Krausslich.** 2010. CD317/tetherin is enriched in the HIV-1 envelope and downregulated from the plasma membrane upon virus infection. Journal of virology **84:**4646-58.

98. **Hallenberger, S., V. Bosch, H. Angliker, E. Shaw, H. D. Klenk, and W. Garten.** 1992. Inhibition of furin-mediated cleavage activation of HIV-1 glycoprotein gp160. Nature **360:**358-61.

99. **Hammonds, J., J. J. Wang, H. Yi, and P. Spearman.** 2010. Immunoelectron microscopic evidence for Tetherin/BST2 as the physical bridge between HIV-1 virions and the plasma membrane. PLoS pathogens **6:**e1000749.

100. **Harris, R. S., K. N. Bishop, A. M. Sheehy, H. M. Craig, S. K. Petersen-Mahrt, I. N. Watt, M. S. Neuberger, and M. H. Malim.** 2003. DNA deamination mediates innate immunity to retroviral infection. Cell **113:**803-9.

101. **Hauser, H., L. A. Lopez, S. J. Yang, J. E. Oldenburg, C. M. Exline, J. C. Guatelli, and P. M. Cannon.** 2010. HIV-1 Vpu and HIV-2 Env counteract BST-2/tetherin by sequestration in a perinuclear compartment. Retrovirology **7:**51.

102. **Hindmarsh, P., and J. Leis.** 1999. Retroviral DNA integration. Microbiology and molecular biology reviews : MMBR **63:**836-43, table of contents.

103. **Hoshino, S., B. Sun, M. Konishi, M. Shimura, T. Segawa, Y. Hagiwara, Y. Koyanagi, A. Iwamoto, J. Mimaya, H. Terunuma, S. Kano, and Y. Ishizaka.** 2007. Vpr in plasma of HIV type 1-positive patients is correlated with the HIV type 1 RNA titers. AIDS research and human retroviruses **23:**391-7.

104. **Hout, D. R., M. L. Gomez, E. Pacyniak, L. M. Gomez, B. Fegley, E. R. Mulcahy, M. S. Hill, N. Culley, D. M. Pinson, W. Nothnick, M. F. Powers, S. W. Wong, and E. B. Stephens.** 2006. Substitution of the transmembrane

domain of Vpu in simian-human immunodeficiency virus (SHIVKU1bMC33) with that of M2 of influenza A results in a virus that is sensitive to inhibitors of the M2 ion channel and is pathogenic for pig-tailed macaques. Virology **344:**541-59.

105. **Hout, D. R., M. L. Gomez, E. Pacyniak, L. M. Gomez, S. H. Inbody, E. R. Mulcahy, N. Culley, D. M. Pinson, M. F. Powers, S. W. Wong, and E. B. Stephens.** 2005. Scrambling of the amino acids within the transmembrane domain of Vpu results in a simian-human immunodeficiency virus (SHIVTM) that is less pathogenic for pig-tailed macaques. Virology **339:**56-69.

106. **Hrecka, K., M. Gierszewska, S. Srivastava, L. Kozaczkiewicz, S. K. Swanson, L. Florens, M. P. Washburn, and J. Skowronski.** 2007. Lentiviral Vpr usurps Cul4-DDB1[VprBP] E3 ubiquitin ligase to modulate cell cycle. Proceedings of the National Academy of Sciences of the United States of America **104:**11778-83.

107. **Hussain, A., C. Wesley, M. Khalid, A. Chaudhry, and S. Jameel.** 2008. Human immunodeficiency virus type 1 Vpu protein interacts with CD74 and modulates major histocompatibility complex class II presentation. Journal of virology **82:**893-902.

108. **Hutagalung, A. H., and P. J. Novick.** 2011. Role of Rab GTPases in membrane traffic and cell physiology. Physiological reviews **91:**119-49.

109. **Ikeda, F., and I. Dikic.** 2008. Atypical ubiquitin chains: new molecular signals. 'Protein Modifications: Beyond the Usual Suspects' review series. EMBO reports **9:**536-42.

110. **Iwabu, Y., H. Fujita, M. Kinomoto, K. Kaneko, Y. Ishizaka, Y. Tanaka, T. Sata, and K. Tokunaga.** 2009. HIV-1 accessory protein Vpu internalizes cell-surface BST-2/tetherin through transmembrane interactions leading to lysosomes. The Journal of biological chemistry **284:**35060-72.

111. **Iwamoto, A., N. Hosoya, and A. Kawana-Tachikawa.** 2010. HIV-1 tropism. Protein & cell **1:**510-3.

112. **Izquierdo-Useros, N., M. Naranjo-Gomez, I. Erkizia, M. C. Puertas, F. E. Borras, J. Blanco, and J. Martinez-Picado.** 2010. HIV and mature dendritic cells: Trojan exosomes riding the Trojan horse? PLoS pathogens **6:**e1000740.

113. **Janvier, K., A. Pelchen-Matthews, J. B. Renaud, M. Caillet, M. Marsh, and C. Berlioz-Torrent.** 2011. The ESCRT-0 component HRS is required for HIV-1 Vpu-mediated BST-2/tetherin down-regulation. PLoS pathogens **7:**e1001265.

114. **Jia, B., R. Serra-Moreno, W. Neidermyer, A. Rahmberg, J. Mackey, I. B. Fofana, W. E. Johnson, S. Westmoreland, and D. T. Evans.** 2009. Species-specific activity of SIV Nef and HIV-1 Vpu in overcoming restriction by tetherin/BST2. PLoS pathogens **5:**e1000429.

115. **Jia, B., R. Serra-Moreno, W. Neidermyer, A. Rahmberg, J. Mackey, I. B. Fofana, W. E. Johnson, S. Westmoreland, and D. T. Evans.** 2009. Species-specific activity of SIV Nef and HIV-1 Vpu in overcoming restriction by tetherin/BST2. PLoS Pathog **5:**e1000429.

116. **Jin, J., T. Shirogane, L. Xu, G. Nalepa, J. Qin, S. J. Elledge, and J. W. Harper.** 2003. SCFbeta-TRCP links Chk1 signaling to degradation of the Cdc25A protein phosphatase. Genes & development **17:**3062-74.

117. **Jin, Y. J., C. Y. Cai, X. Zhang, H. T. Zhang, J. A. Hirst, and S. J. Burakoff.** 2005. HIV Nef-mediated CD4 down-regulation is adaptor protein complex 2 dependent. Journal of immunology **175:**3157-64.

118. **Joag, S. V., Z. Li, C. Wang, F. Jia, L. Foresman, I. Adany, D. M. Pinson, E. B. Stephens, and O. Narayan.** 1998. Chimeric SHIV that causes CD4+ T cell loss and AIDS in rhesus macaques. Journal of medical primatology **27:**59-64.

119. **Jolly, C.** 2011. Cell-to-cell transmission of retroviruses: Innate immunity and interferon-induced restriction factors. Virology **411:**251-9.

120. **Jolly, C., N. J. Booth, and S. J. Neil.** 2010. Cell-cell spread of human immunodeficiency virus type 1 overcomes tetherin/BST-2-mediated restriction in T cells. Journal of virology **84:**12185-99.

121. **Kaletsky, R. L., J. R. Francica, C. Agrawal-Gamse, and P. Bates.** 2009. Tetherin-mediated restriction of filovirus budding is antagonized by the Ebola glycoprotein. Proc Natl Acad Sci U S A **106:**2886-91.

122. **Kao, S. Y., A. F. Calman, P. A. Luciw, and B. M. Peterlin.** 1987. Anti-termination of transcription within the long terminal repeat of HIV-1 by tat gene product. Nature **330:**489-93.

123. **Katzmann, D. J., S. Sarkar, T. Chu, A. Audhya, and S. D. Emr.** 2004. Multivesicular body sorting: ubiquitin ligase Rsp5 is required for the modification and sorting of carboxypeptidase S. Molecular biology of the cell **15:**468-80.

124. **Kerkau, T., I. Bacik, J. R. Bennink, J. W. Yewdell, T. Hunig, A. Schimpl, and U. Schubert.** 1997. The human immunodeficiency virus type 1 (HIV-1) Vpu protein interferes with an early step in the biosynthesis of major histocompatibility complex (MHC) class I molecules. The Journal of experimental medicine **185:**1295-305.

125. **Khan, M. A., R. Goila-Gaur, S. Opi, E. Miyagi, H. Takeuchi, S. Kao, and K. Strebel.** 2007. Analysis of the contribution of cellular and viral RNA to the packaging of APOBEC3G into HIV-1 virions. Retrovirology **4:**48.

126. **Khan, M. A., S. Kao, E. Miyagi, H. Takeuchi, R. Goila-Gaur, S. Opi, C. L. Gipson, T. G. Parslow, H. Ly, and K. Strebel.** 2005. Viral RNA is required for the association of APOBEC3G with human immunodeficiency virus type 1 nucleoprotein complexes. Journal of virology **79:**5870-4.

127. **Khoury, G., G. Ewart, C. Luscombe, M. Miller, and J. Wilkinson.** 2010. Antiviral efficacy of the novel compound BIT225 against HIV-1 release from human macrophages. Antimicrobial agents and chemotherapy **54:**835-45.

128. **Kirchhoff, F.** 2010. Immune evasion and counteraction of restriction factors by HIV-1 and other primate lentiviruses. Cell host & microbe **8:**55-67.

129. **Kitagawa, M., S. Hatakeyama, M. Shirane, M. Matsumoto, N. Ishida, K. Hattori, I. Nakamichi, A. Kikuchi, and K. Nakayama.** 1999. An F-box protein, FWD1, mediates ubiquitin-dependent proteolysis of beta-catenin. The EMBO journal **18:**2401-10.

130. **Kitt, K. N., D. Hernandez-Deviez, S. D. Ballantyne, E. T. Spiliotis, J. E. Casanova, and J. M. Wilson.** 2008. Rab14 regulates apical targeting in polarized epithelial cells. Traffic **9:**1218-31.

131. **Klatzmann, D., E. Champagne, S. Chamaret, J. Gruest, D. Guetard, T. Hercend, J. C. Gluckman, and L. Montagnier.** 1984. T-lymphocyte T4 molecule behaves as the receptor for human retrovirus LAV. Nature **312:**767-8.

132. **Klimkait, T., K. Strebel, M. D. Hoggan, M. A. Martin, and J. M. Orenstein.** 1990. The human immunodeficiency virus type 1-specific protein vpu is required for efficient virus maturation and release. Journal of virology **64:**621-9.

133. **Kobayashi, T., H. Ode, T. Yoshida, K. Sato, P. Gee, S. P. Yamamoto, H. Ebina, K. Strebel, H. Sato, and Y. Koyanagi.** 2011. Identification of amino acids in the human tetherin transmembrane domain responsible for HIV-1 Vpu interaction and susceptibility. Journal of virology **85:**932-45.

134. **Krausslich, H. G., H. Schneider, G. Zybarth, C. A. Carter, and E. Wimmer.** 1988. Processing of in vitro-synthesized gag precursor proteins of human immunodeficiency virus (HIV) type 1 by HIV proteinase generated in Escherichia coli. Journal of virology **62:**4393-7.

135. **Krementsov, D. N., P. Rassam, E. Margeat, N. H. Roy, J. Schneider-Schaulies, P. E. Milhiet, and M. Thali.** 2010. HIV-1 assembly differentially alters dynamics and partitioning of tetraspanins and raft components. Traffic **11:**1401-14.

136. **Kroll, M., F. Margottin, A. Kohl, P. Renard, H. Durand, J. P. Concordet, F. Bachelerie, F. Arenzana-Seisdedos, and R. Benarous.** 1999. Inducible degradation of IkappaBalpha by the proteasome requires interaction with the F-box protein h-betaTrCP. The Journal of biological chemistry **274:**7941-5.

137. **Kuhl, B. D., R. D. Sloan, D. A. Donahue, T. Bar-Magen, C. Liang, and M. A. Wainberg.** 2010. Tetherin restricts direct cell-to-cell infection of HIV-1. Retrovirology **7:**115.

138. **Kuhl, B. D., R. D. Sloan, D. A. Donahue, C. Liang, and M. A. Wainberg.** 2011. Vpu-mediated tetherin antagonism of ongoing HIV-1 infection in CD4(+) T-cells is not directly related to the extent of tetherin cell surface downmodulation. Virology.

139. **Kumar, K. G., J. J. Krolewski, and S. Y. Fuchs.** 2004. Phosphorylation and specific ubiquitin acceptor sites are required for ubiquitination and degradation

of the IFNAR1 subunit of type I interferon receptor. The Journal of biological chemistry **279:**46614-20.

140. **Lama, J., A. Mangasarian, and D. Trono.** 1999. Cell-surface expression of CD4 reduces HIV-1 infectivity by blocking Env incorporation in a Nef- and Vpu-inhibitable manner. Current biology : CB **9:**622-31.

141. **Le Rouzic, E., N. Belaidouni, E. Estrabaud, M. Morel, J. C. Rain, C. Transy, and F. Margottin-Goguet.** 2007. HIV1 Vpr arrests the cell cycle by recruiting DCAF1/VprBP, a receptor of the Cul4-DDB1 ubiquitin ligase. Cell cycle **6:**182-8.

142. **Le Tortorec, A., and S. J. Neil.** 2009. Antagonism to and intracellular sequestration of human tetherin by the human immunodeficiency virus type 2 envelope glycoprotein. J Virol **83:**11966-78.

143. **Le Tortorec, A., and S. J. Neil.** 2009. Antagonism to and intracellular sequestration of human tetherin by the human immunodeficiency virus type 2 envelope glycoprotein. Journal of virology **83:**11966-78.

144. **Lemaitre, V., R. Ali, C. G. Kim, A. Watts, and W. B. Fischer.** 2004. Interaction of amiloride and one of its derivatives with Vpu from HIV-1: a molecular dynamics simulation. FEBS letters **563:**75-81.

145. **Lemaitre, V., D. Willbold, A. Watts, and W. B. Fischer.** 2006. Full length Vpu from HIV-1: combining molecular dynamics simulations with NMR spectroscopy. Journal of biomolecular structure & dynamics **23:**485-96.

146. **Levy, D. N., Y. Refaeli, R. R. MacGregor, and D. B. Weiner.** 1994. Serum Vpr regulates productive infection and latency of human immunodeficiency virus type 1. Proceedings of the National Academy of Sciences of the United States of America **91:**10873-7.

147. **Lim, E. S., H. S. Malik, and M. Emerman.** 2010. Ancient adaptive evolution of tetherin shaped the functions of Vpu and Nef in human immunodeficiency virus and primate lentiviruses. Journal of virology **84:**7124-34.

148. **Lopez-Verges, S., G. Camus, G. Blot, R. Beauvoir, R. Benarous, and C. Berlioz-Torrent.** 2006. Tail-interacting protein TIP47 is a connector between Gag and Env and is required for Env incorporation into HIV-1 virions.

Proceedings of the National Academy of Sciences of the United States of America **103:**14947-52.

149. **Lopez, L. A., S. J. Yang, H. Hauser, C. M. Exline, K. G. Haworth, J. Oldenburg, and P. M. Cannon.** 2010. Ebola virus glycoprotein counteracts BST-2/Tetherin restriction in a sequence-independent manner that does not require tetherin surface removal. J Virol **84:**7243-55.

150. **Lu, Y. L., R. P. Bennett, J. W. Wills, R. Gorelick, and L. Ratner.** 1995. A leucine triplet repeat sequence (LXX)4 in p6gag is important for Vpr incorporation into human immunodeficiency virus type 1 particles. Journal of virology **69:**6873-9.

151. **Lundquist, C. A., M. Tobiume, J. Zhou, D. Unutmaz, and C. Aiken.** 2002. Nef-mediated downregulation of CD4 enhances human immunodeficiency virus type 1 replication in primary T lymphocytes. Journal of virology **76:**4625-33.

152. **Magadan, J. G., F. J. Perez-Victoria, R. Sougrat, Y. Ye, K. Strebel, and J. S. Bonifacino.** 2010. Multilayered mechanism of CD4 downregulation by HIV-1 Vpu involving distinct ER retention and ERAD targeting steps. PLoS pathogens **6:**e1000869.

153. **Majumder, B., N. J. Venkatachari, S. O'Leary, and V. Ayyavoo.** 2008. Infection with Vpr-positive human immunodeficiency virus type 1 impairs NK cell function indirectly through cytokine dysregulation of infected target cells. Journal of virology **82:**7189-200.

154. **Majumder, B., N. J. Venkatachari, E. A. Schafer, M. L. Janket, and V. Ayyavoo.** 2007. Dendritic cells infected with vpr-positive human immunodeficiency virus type 1 induce CD8+ T-cell apoptosis via upregulation of tumor necrosis factor alpha. Journal of virology **81:**7388-99.

155. **Mangeat, B., G. Gers-Huber, M. Lehmann, M. Zufferey, J. Luban, and V. Piguet.** 2009. HIV-1 Vpu neutralizes the antiviral factor Tetherin/BST-2 by binding it and directing its beta-TrCP2-dependent degradation. PLoS pathogens **5:**e1000574.

156. **Mangeat, B., G. Gers-Huber, M. Lehmann, M. Zufferey, J. Luban, and V. Piguet.** 2009. HIV-1 Vpu neutralizes the antiviral factor Tetherin/BST-2 by

binding it and directing its beta-TrCP2-dependent degradation. PLoS Pathog **5:**e1000574.

157. **Mangeat, B., P. Turelli, G. Caron, M. Friedli, L. Perrin, and D. Trono.** 2003. Broad antiretroviral defence by human APOBEC3G through lethal editing of nascent reverse transcripts. Nature **424:**99-103.

158. **Mansouri, M., K. Viswanathan, J. L. Douglas, J. Hines, J. Gustin, A. V. Moses, and K. Fruh.** 2009. Molecular mechanism of BST2/tetherin downregulation by K5/MIR2 of Kaposi's sarcoma-associated herpesvirus. J Virol **83:**9672-81.

159. **Margottin, F., S. P. Bour, H. Durand, L. Selig, S. Benichou, V. Richard, D. Thomas, K. Strebel, and R. Benarous.** 1998. A novel human WD protein, h-beta TrCp, that interacts with HIV-1 Vpu connects CD4 to the ER degradation pathway through an F-box motif. Molecular cell **1:**565-74.

160. **Mariani, R., D. Chen, B. Schrofelbauer, F. Navarro, R. Konig, B. Bollman, C. Munk, H. Nymark-McMahon, and N. R. Landau.** 2003. Species-specific exclusion of APOBEC3G from HIV-1 virions by Vif. Cell **114:**21-31.

161. **Marin, M., K. M. Rose, S. L. Kozak, and D. Kabat.** 2003. HIV-1 Vif protein binds the editing enzyme APOBEC3G and induces its degradation. Nature medicine **9:**1398-403.

162. **Martin, N., and Q. Sattentau.** 2009. Cell-to-cell HIV-1 spread and its implications for immune evasion. Current opinion in HIV and AIDS **4:**143-9.

163. **Mattner, J., K. L. Debord, N. Ismail, R. D. Goff, C. Cantu, 3rd, D. Zhou, P. Saint-Mezard, V. Wang, Y. Gao, N. Yin, K. Hoebe, O. Schneewind, D. Walker, B. Beutler, L. Teyton, P. B. Savage, and A. Bendelac.** 2005. Exogenous and endogenous glycolipid antigens activate NKT cells during microbial infections. Nature **434:**525-9.

164. **McCune, J. M., L. B. Rabin, M. B. Feinberg, M. Lieberman, J. C. Kosek, G. R. Reyes, and I. L. Weissman.** 1988. Endoproteolytic cleavage of gp160 is required for the activation of human immunodeficiency virus. Cell **53:**55-67.

165. **McDonald, D., M. A. Vodicka, G. Lucero, T. M. Svitkina, G. G. Borisy, M. Emerman, and T. J. Hope.** 2002. Visualization of the intracellular behavior of HIV in living cells. The Journal of cell biology **159:**441-52.

166. **McNatt, M. W., T. Zang, T. Hatziioannou, M. Bartlett, I. B. Fofana, W. E. Johnson, S. J. Neil, and P. D. Bieniasz.** 2009. Species-specific activity of HIV-1 Vpu and positive selection of tetherin transmembrane domain variants. PLoS pathogens **5:**e1000300.

167. **Mehle, A., B. Strack, P. Ancuta, C. Zhang, M. McPike, and D. Gabuzda.** 2004. Vif overcomes the innate antiviral activity of APOBEC3G by promoting its degradation in the ubiquitin-proteasome pathway. The Journal of biological chemistry **279:**7792-8.

168. **Melikyan, G. B., R. M. Markosyan, H. Hemmati, M. K. Delmedico, D. M. Lambert, and F. S. Cohen.** 2000. Evidence that the transition of HIV-1 gp41 into a six-helix bundle, not the bundle configuration, induces membrane fusion. The Journal of cell biology **151:**413-23.

169. **Mervis, R. J., N. Ahmad, E. P. Lillehoj, M. G. Raum, F. H. Salazar, H. W. Chan, and S. Venkatesan.** 1988. The gag gene products of human immunodeficiency virus type 1: alignment within the gag open reading frame, identification of posttranslational modifications, and evidence for alternative gag precursors. Journal of virology **62:**3993-4002.

170. **Miller, M. D., M. T. Warmerdam, I. Gaston, W. C. Greene, and M. B. Feinberg.** 1994. The human immunodeficiency virus-1 nef gene product: a positive factor for viral infection and replication in primary lymphocytes and macrophages. The Journal of experimental medicine **179:**101-13.

171. **Miller, R. H., and N. Sarver.** 1995. HIV accessory proteins: emerging therapeutic targets. Molecular medicine **1:**479-85.

172. **Mitchell, R. S., C. Katsura, M. A. Skasko, K. Fitzpatrick, D. Lau, A. Ruiz, E. B. Stephens, F. Margottin-Goguet, R. Benarous, and J. C. Guatelli.** 2009. Vpu antagonizes BST-2-mediated restriction of HIV-1 release via beta-TrCP and endo-lysosomal trafficking. PLoS Pathog **5:**e1000450.

173. **Mitchell, R. S., C. Katsura, M. A. Skasko, K. Fitzpatrick, D. Lau, A. Ruiz, E. B. Stephens, F. Margottin-Goguet, R. Benarous, and J. C. Guatelli.** 2009. Vpu antagonizes BST-2-mediated restriction of HIV-1 release via beta-TrCP and endo-lysosomal trafficking. PLoS pathogens **5:**e1000450.

174. **Miyagi, E., A. J. Andrew, S. Kao, and K. Strebel.** 2009. Vpu enhances HIV-1 virus release in the absence of Bst-2 cell surface down-modulation and intracellular depletion. Proceedings of the National Academy of Sciences of the United States of America **106:**2868-73.

175. **Miyagi, E., S. Opi, H. Takeuchi, M. Khan, R. Goila-Gaur, S. Kao, and K. Strebel.** 2007. Enzymatically active APOBEC3G is required for efficient inhibition of human immunodeficiency virus type 1. Journal of virology **81:**13346-53.

176. **Miyakawa, K., A. Ryo, T. Murakami, K. Ohba, S. Yamaoka, M. Fukuda, J. Guatelli, and N. Yamamoto.** 2009. BCA2/Rabring7 promotes tetherin-dependent HIV-1 restriction. PLoS pathogens **5:**e1000700.

177. **Miyauchi, K., Y. Kim, O. Latinovic, V. Morozov, and G. B. Melikyan.** 2009. HIV enters cells via endocytosis and dynamin-dependent fusion with endosomes. Cell **137:**433-44.

178. **Moll, M., S. K. Andersson, A. Smed-Sorensen, and J. K. Sandberg.** 2010. Inhibition of lipid antigen presentation in dendritic cells by HIV-1 Vpu interference with CD1d recycling from endosomal compartments. Blood **116:**1876-84.

179. **Morita, E., V. Sandrin, J. McCullough, A. Katsuyama, I. Baci Hamilton, and W. I. Sundquist.** 2011. ESCRT-III Protein Requirements for HIV-1 Budding. Cell host & microbe **9:**235-42.

180. **Moshe, Y., J. Boulaire, M. Pagano, and A. Hershko.** 2004. Role of Polo-like kinase in the degradation of early mitotic inhibitor 1, a regulator of the anaphase promoting complex/cyclosome. Proceedings of the National Academy of Sciences of the United States of America **101:**7937-42.

181. **Munier, C. M., C. R. Andersen, and A. D. Kelleher.** 2011. HIV vaccines: progress to date. Drugs **71:**387-414.

182. **Nakamura, N., H. Fukuda, A. Kato, and S. Hirose.** 2005. MARCH-II is a syntaxin-6-binding protein involved in endosomal trafficking. Molecular biology of the cell **16:**1696-710.

183. **Nathan, J. A., and P. J. Lehner.** 2009. The trafficking and regulation of membrane receptors by the RING-CH ubiquitin E3 ligases. Experimental cell research **315:**1593-600.

184. **Neil, S. J., S. W. Eastman, N. Jouvenet, and P. D. Bieniasz.** 2006. HIV-1 Vpu promotes release and prevents endocytosis of nascent retrovirus particles from the plasma membrane. PLoS pathogens **2:**e39.

185. **Neil, S. J., T. Zang, and P. D. Bieniasz.** 2008. Tetherin inhibits retrovirus release and is antagonized by HIV-1 Vpu. Nature **451:**425-30.

186. **Omoto, S., M. Ito, Y. Tsutsumi, Y. Ichikawa, H. Okuyama, E. A. Brisibe, N. K. Saksena, and Y. R. Fujii.** 2004. HIV-1 nef suppression by virally encoded microRNA. Retrovirology **1:**44.

187. **Ono, A., S. D. Ablan, S. J. Lockett, K. Nagashima, and E. O. Freed.** 2004. Phosphatidylinositol (4,5) bisphosphate regulates HIV-1 Gag targeting to the plasma membrane. Proceedings of the National Academy of Sciences of the United States of America **101:**14889-94.

188. **Pacyniak, E., M. L. Gomez, L. M. Gomez, E. R. Mulcahy, M. Jackson, D. R. Hout, B. J. Wisdom, and E. B. Stephens.** 2005. Identification of a region within the cytoplasmic domain of the subtype B Vpu protein of human immunodeficiency virus type 1 (HIV-1) that is responsible for retention in the golgi complex and its absence in the Vpu protein from a subtype C HIV-1. AIDS research and human retroviruses **21:**379-94.

189. **Pal, R., M. S. Reitz, Jr., E. Tschachler, R. C. Gallo, M. G. Sarngadharan, and F. D. Veronese.** 1990. Myristoylation of gag proteins of HIV-1 plays an important role in virus assembly. AIDS research and human retroviruses **6:**721-30.

190. **Pardieu, C., R. Vigan, S. J. Wilson, A. Calvi, T. Zang, P. Bieniasz, P. Kellam, G. J. Towers, and S. J. Neil.** 2010. The RING-CH ligase K5 antagonizes restriction of KSHV and HIV-1 particle release by mediating

ubiquitin-dependent endosomal degradation of tetherin. PLoS pathogens **6:**e1000843.

191. **Pardieu, C., R. Vigan, S. J. Wilson, A. Calvi, T. Zang, P. Bieniasz, P. Kellam, G. J. Towers, and S. J. Neil.** 2010. The RING-CH ligase K5 antagonizes restriction of KSHV and HIV-1 particle release by mediating ubiquitin-dependent endosomal degradation of tetherin. PLoS Pathog **6:**e1000843.

192. **Peng, G., K. J. Lei, W. Jin, T. Greenwell-Wild, and S. M. Wahl.** 2006. Induction of APOBEC3 family proteins, a defensive maneuver underlying interferon-induced anti-HIV-1 activity. The Journal of experimental medicine **203:**41-6.

193. **Perez-Caballero, D., T. Zang, A. Ebrahimi, M. W. McNatt, D. A. Gregory, M. C. Johnson, and P. D. Bieniasz.** 2009. Tetherin inhibits HIV-1 release by directly tethering virions to cells. Cell **139:**499-511.

194. **Pitisuttithum, P., P. Gilbert, M. Gurwith, W. Heyward, M. Martin, F. van Griensven, D. Hu, J. W. Tappero, and K. Choopanya.** 2006. Randomized, double-blind, placebo-controlled efficacy trial of a bivalent recombinant glycoprotein 120 HIV-1 vaccine among injection drug users in Bangkok, Thailand. The Journal of infectious diseases **194:**1661-71.

195. **Pizzato, M., A. Helander, E. Popova, A. Calistri, A. Zamborlini, G. Palu, and H. G. Gottlinger.** 2007. Dynamin 2 is required for the enhancement of HIV-1 infectivity by Nef. Proceedings of the National Academy of Sciences of the United States of America **104:**6812-7.

196. **Planelles, V., J. B. Jowett, Q. X. Li, Y. Xie, B. Hahn, and I. S. Chen.** 1996. Vpr-induced cell cycle arrest is conserved among primate lentiviruses. Journal of virology **70:**2516-24.

197. **Rice, A. P., and M. B. Mathews.** 1988. Transcriptional but not translational regulation of HIV-1 by the tat gene product. Nature **332:**551-3.

198. **Richard, J., and E. A. Cohen.** 2010. HIV-1 Vpu disarms natural killer cells. Cell host & microbe **8:**389-91.

199. **Richard, J., S. Sindhu, T. N. Pham, J. P. Belzile, and E. A. Cohen.** 2010. HIV-1 Vpr up-regulates expression of ligands for the activating NKG2D receptor and promotes NK cell-mediated killing. Blood **115:**1354-63.

200. **Rizzuto, C. D., R. Wyatt, N. Hernandez-Ramos, Y. Sun, P. D. Kwong, W. A. Hendrickson, and J. Sodroski.** 1998. A conserved HIV gp120 glycoprotein structure involved in chemokine receptor binding. Science **280:**1949-53.

201. **Roeth, J. F., M. Williams, M. R. Kasper, T. M. Filzen, and K. L. Collins.** 2004. HIV-1 Nef disrupts MHC-I trafficking by recruiting AP-1 to the MHC-I cytoplasmic tail. The Journal of cell biology **167:**903-13.

202. **Rollason, R., V. Korolchuk, C. Hamilton, M. Jepson, and G. Banting.** 2009. A CD317/tetherin-RICH2 complex plays a critical role in the organization of the subapical actin cytoskeleton in polarized epithelial cells. The Journal of cell biology **184:**721-36.

203. **Ross, T. M., A. E. Oran, and B. R. Cullen.** 1999. Inhibition of HIV-1 progeny virion release by cell-surface CD4 is relieved by expression of the viral Nef protein. Current biology : CB **9:**613-21.

204. **Rossman, J. S., X. Jing, G. P. Leser, and R. A. Lamb.** 2010. Influenza virus M2 protein mediates ESCRT-independent membrane scission. Cell **142:**902-13.

205. **Sakaguchi, K., N. Zambrano, E. T. Baldwin, B. A. Shapiro, J. W. Erickson, J. G. Omichinski, G. M. Clore, A. M. Gronenborn, and E. Appella.** 1993. Identification of a binding site for the human immunodeficiency virus type 1 nucleocapsid protein. Proceedings of the National Academy of Sciences of the United States of America **90:**5219-23.

206. **Sakai, H., K. Tokunaga, M. Kawamura, and A. Adachi.** 1995. Function of human immunodeficiency virus type 1 Vpu protein in various cell types. The Journal of general virology **76 (Pt 11):**2717-22.

207. **Sakai, K., J. Dimas, and M. J. Lenardo.** 2006. The Vif and Vpr accessory proteins independently cause HIV-1-induced T cell cytopathicity and cell cycle arrest. Proceedings of the National Academy of Sciences of the United States of America **103:**3369-74.

208. **Sakuma, R., A. A. Mael, and Y. Ikeda.** 2007. Alpha interferon enhances TRIM5alpha-mediated antiviral activities in human and rhesus monkey cells. Journal of virology **81:**10201-6.

209. **Salim, A., and L. Ratner.** 2008. Modulation of beta-catenin and E-cadherin interaction by Vpu increases human immunodeficiency virus type 1 particle release. Journal of virology **82:**3932-8.

210. **Sauter, D., M. Schindler, A. Specht, W. N. Landford, J. Munch, K. A. Kim, J. Votteler, U. Schubert, F. Bibollet-Ruche, B. F. Keele, J. Takehisa, Y. Ogando, C. Ochsenbauer, J. C. Kappes, A. Ayouba, M. Peeters, G. H. Learn, G. Shaw, P. M. Sharp, P. Bieniasz, B. H. Hahn, T. Hatziioannou, and F. Kirchhoff.** 2009. Tetherin-driven adaptation of Vpu and Nef function and the evolution of pandemic and nonpandemic HIV-1 strains. Cell host & microbe **6:**409-21.

211. **Sauter, D., M. Schindler, A. Specht, W. N. Landford, J. Munch, K. A. Kim, J. Votteler, U. Schubert, F. Bibollet-Ruche, B. F. Keele, J. Takehisa, Y. Ogando, C. Ochsenbauer, J. C. Kappes, A. Ayouba, M. Peeters, G. H. Learn, G. Shaw, P. M. Sharp, P. Bieniasz, B. H. Hahn, T. Hatziioannou, and F. Kirchhoff.** 2009. Tetherin-driven adaptation of Vpu and Nef function and the evolution of pandemic and nonpandemic HIV-1 strains. Cell Host Microbe **6:**409-21.

212. **Sayah, D. M., E. Sokolskaja, L. Berthoux, and J. Luban.** 2004. Cyclophilin A retrotransposition into TRIM5 explains owl monkey resistance to HIV-1. Nature **430:**569-73.

213. **Schindler, M., D. Rajan, C. Banning, P. Wimmer, H. Koppensteiner, A. Iwanski, A. Specht, D. Sauter, T. Dobner, and F. Kirchhoff.** 2010. Vpu serine 52 dependent counteraction of tetherin is required for HIV-1 replication in macrophages, but not in ex vivo human lymphoid tissue. Retrovirology **7:**1.

214. **Schrofelbauer, B., Y. Hakata, and N. R. Landau.** 2007. HIV-1 Vpr function is mediated by interaction with the damage-specific DNA-binding protein DDB1. Proceedings of the National Academy of Sciences of the United States of America **104:**4130-5.

215. **Schubert, U., S. Bour, R. L. Willey, and K. Strebel.** 1999. Regulation of virus release by the macrophage-tropic human immunodeficiency virus type 1 AD8 isolate is redundant and can be controlled by either Vpu or Env. Journal of virology **73:**887-96.

216. **Schubert, U., K. A. Clouse, and K. Strebel.** 1995. Augmentation of virus secretion by the human immunodeficiency virus type 1 Vpu protein is cell type independent and occurs in cultured human primary macrophages and lymphocytes. Journal of virology **69:**7699-711.

217. **Schubert, U., A. V. Ferrer-Montiel, M. Oblatt-Montal, P. Henklein, K. Strebel, and M. Montal.** 1996. Identification of an ion channel activity of the Vpu transmembrane domain and its involvement in the regulation of virus release from HIV-1-infected cells. FEBS letters **398:**12-8.

218. **Schubert, U., and K. Strebel.** 1994. Differential activities of the human immunodeficiency virus type 1-encoded Vpu protein are regulated by phosphorylation and occur in different cellular compartments. Journal of virology **68:**2260-71.

219. **Schumacher, A. J., G. Hache, D. A. Macduff, W. L. Brown, and R. S. Harris.** 2008. The DNA deaminase activity of human APOBEC3G is required for Ty1, MusD, and human immunodeficiency virus type 1 restriction. Journal of virology **82:**2652-60.

220. **Schwartz, O., A. Dautry-Varsat, B. Goud, V. Marechal, A. Subtil, J. M. Heard, and O. Danos.** 1995. Human immunodeficiency virus type 1 Nef induces accumulation of CD4 in early endosomes. Journal of virology **69:**528-33.

221. **Semple, J. I., V. A. Smits, J. R. Fernaud, I. Mamely, and R. Freire.** 2007. Cleavage and degradation of Claspin during apoptosis by caspases and the proteasome. Cell death and differentiation **14:**1433-42.

222. **Serra-Moreno, R., B. Jia, M. Breed, X. Alvarez, and D. T. Evans.** 2011. Compensatory changes in the cytoplasmic tail of gp41 confer resistance to tetherin/BST-2 in a pathogenic nef-deleted SIV. Cell host & microbe **9:**46-57.

223. **Shah, A. H., B. Sowrirajan, Z. B. Davis, J. P. Ward, E. M. Campbell, V. Planelles, and E. Barker.** 2010. Degranulation of natural killer cells following interaction with HIV-1-infected cells is hindered by downmodulation of NTB-A by Vpu. Cell host & microbe **8:**397-409.

224. **Sharova, N., Y. Wu, X. Zhu, R. Stranska, R. Kaushik, M. Sharkey, and M. Stevenson.** 2008. Primate lentiviral Vpx commandeers DDB1 to counteract a macrophage restriction. PLoS pathogens **4:**e1000057.

225. **Siliciano, R. F.** 2010. What do we need to do to cure HIV infection. Topics in HIV medicine : a publication of the International AIDS Society, USA **18:**104-8.

226. **Skasko, M., A. Tokarev, C. C. Chen, W. B. Fischer, S. K. Pillai, and J. Guatelli.** 2011. BST-2 is rapidly down-regulated from the cell surface by the HIV-1 protein Vpu: evidence for a post-ER mechanism of Vpu-action. Virology **411:**65-77.

227. **Sorkin, A., and L. K. Goh.** 2009. Endocytosis and intracellular trafficking of ErbBs. Experimental cell research **315:**683-96.

228. **Sourisseau, M., N. Sol-Foulon, F. Porrot, F. Blanchet, and O. Schwartz.** 2007. Inefficient human immunodeficiency virus replication in mobile lymphocytes. Journal of virology **81:**1000-12.

229. **Stephens, E. B., S. V. Joag, B. Atkinson, M. Sahni, Z. Li, L. Foresman, I. Adany, and O. Narayan.** 1997. Infected macaques that controlled replication of SIVmac or nonpathogenic SHIV developed sterilizing resistance against pathogenic SHIV(KU-1). Virology **234:**328-39.

230. **Stephens, E. B., C. McCormick, E. Pacyniak, D. Griffin, D. M. Pinson, F. Sun, W. Nothnick, S. W. Wong, R. Gunderson, N. E. Berman, and D. K. Singh.** 2002. Deletion of the vpu sequences prior to the env in a simian-human immunodeficiency virus results in enhanced Env precursor synthesis but is less pathogenic for pig-tailed macaques. Virology **293:**252-61.

231. **Stivahtis, G. L., M. A. Soares, M. A. Vodicka, B. H. Hahn, and M. Emerman.** 1997. Conservation and host specificity of Vpr-mediated cell cycle arrest suggest a fundamental role in primate lentivirus evolution and biology. Journal of virology **71:**4331-8.

232. **Stopak, K., C. de Noronha, W. Yonemoto, and W. C. Greene.** 2003. HIV-1 Vif blocks the antiviral activity of APOBEC3G by impairing both its translation and intracellular stability. Molecular cell **12:**591-601.

233. **Strauss, J. H., and E. G. Strauss.** 2000. Viruses and human diseases. Academic Press**:**Chapitre 5.

234. **Strebel, K., D. Daugherty, K. Clouse, D. Cohen, T. Folks, and M. A. Martin.** 1987. The HIV 'A' (sor) gene product is essential for virus infectivity. Nature **328:**728-30.

235. **Strebel, K., T. Klimkait, F. Maldarelli, and M. A. Martin.** 1989. Molecular and biochemical analyses of human immunodeficiency virus type 1 vpu protein. Journal of virology **63:**3784-91.

236. **Stremlau, M., C. M. Owens, M. J. Perron, M. Kiessling, P. Autissier, and J. Sodroski.** 2004. The cytoplasmic body component TRIM5alpha restricts HIV-1 infection in Old World monkeys. Nature **427:**848-53.

237. **Stremlau, M., M. Perron, M. Lee, Y. Li, B. Song, H. Javanbakht, F. Diaz-Griffero, D. J. Anderson, W. I. Sundquist, and J. Sodroski.** 2006. Specific recognition and accelerated uncoating of retroviral capsids by the TRIM5alpha restriction factor. Proceedings of the National Academy of Sciences of the United States of America **103:**5514-9.

238. **Stuchell-Brereton, M. D., J. J. Skalicky, C. Kieffer, M. A. Karren, S. Ghaffarian, and W. I. Sundquist.** 2007. ESCRT-III recognition by VPS4 ATPases. Nature **449:**740-4.

239. **Stumptner-Cuvelette, P., S. Morchoisne, M. Dugast, S. Le Gall, G. Raposo, O. Schwartz, and P. Benaroch.** 2001. HIV-1 Nef impairs MHC class II antigen presentation and surface expression. Proceedings of the National Academy of Sciences of the United States of America **98:**12144-9.

240. **Suzuki, Y., and R. Craigie.** 2007. The road to chromatin - nuclear entry of retroviruses. Nature reviews. Microbiology **5:**187-96.

241. **Tervo, H. M., S. Homann, I. Ambiel, J. V. Fritz, O. T. Fackler, and O. T. Keppler.** 2011. beta-TrCP is dispensable for Vpu's ability to overcome the CD317/Tetherin-imposed restriction to HIV-1 release. Retrovirology **8:**9.

242. **Terwilliger, E. F., E. A. Cohen, Y. C. Lu, J. G. Sodroski, and W. A. Haseltine.** 1989. Functional role of human immunodeficiency virus type 1 vpu. Proceedings of the National Academy of Sciences of the United States of America **86:**5163-7.

243. **Tokarev, A. A., J. Munguia, and J. C. Guatelli.** 2011. Serine-threonine ubiquitination mediates downregulation of BST-2/tetherin and relief of restricted virion release by HIV-1 Vpu. Journal of virology **85:**51-63.

244. **Towers, G. J., T. Hatziioannou, S. Cowan, S. P. Goff, J. Luban, and P. D. Bieniasz.** 2003. Cyclophilin A modulates the sensitivity of HIV-1 to host restriction factors. Nature medicine **9:**1138-43.

245. **Trono, D.** 1995. HIV accessory proteins: leading roles for the supporting cast. Cell **82:**189-92.

246. **Tsibris, A. M., and M. S. Hirsch.** 2010. Antiretroviral therapy in the clinic. Journal of virology **84:**5458-64.

247. **UNAIDS.** 2010. UNAIDS report on the global AIDS epidemic.

248. **Van Damme, N., D. Goff, C. Katsura, R. L. Jorgenson, R. Mitchell, M. C. Johnson, E. B. Stephens, and J. Guatelli.** 2008. The interferon-induced protein BST-2 restricts HIV-1 release and is downregulated from the cell surface by the viral Vpu protein. Cell host & microbe **3:**245-52.

249. **Varthakavi, V., R. M. Smith, S. P. Bour, K. Strebel, and P. Spearman.** 2003. Viral protein U counteracts a human host cell restriction that inhibits HIV-1 particle production. Proceedings of the National Academy of Sciences of the United States of America **100:**15154-9.

250. **Varthakavi, V., R. M. Smith, K. L. Martin, A. Derdowski, L. A. Lapierre, J. R. Goldenring, and P. Spearman.** 2006. The pericentriolar recycling endosome plays a key role in Vpu-mediated enhancement of HIV-1 particle release. Traffic **7:**298-307.

251. **Venkatachari, N. J., B. Majumder, and V. Ayyavoo.** 2007. Human immunodeficiency virus (HIV) type 1 Vpr induces differential regulation of T cell costimulatory molecules: direct effect of Vpr on T cell activation and immune function. Virology **358:**347-56.

252. **VerPlank, L., F. Bouamr, T. J. LaGrassa, B. Agresta, A. Kikonyogo, J. Leis, and C. A. Carter.** 2001. Tsg101, a homologue of ubiquitin-conjugating (E2) enzymes, binds the L domain in HIV type 1 Pr55(Gag). Proceedings of the National Academy of Sciences of the United States of America **98:**7724-9.

253. **Vieillard, V., J. L. Strominger, and P. Debre.** 2005. NK cytotoxicity against CD4+ T cells during HIV-1 infection: a gp41 peptide induces the expression of an NKp44 ligand. Proceedings of the National Academy of Sciences of the United States of America **102:**10981-6.

254. **Vigan, R., and S. J. Neil.** 2010. Determinants of tetherin antagonism in the transmembrane domain of the human immunodeficiency virus type 1 Vpu protein. Journal of virology **84:**12958-70.

255. **Vincent, M. J., and M. Abdul Jabbar.** 1995. The human immunodeficiency virus type 1 Vpu protein: a potential regulator of proteolysis and protein transport in the mammalian secretory pathway. Virology **213:**639-49.

256. **Wang, J., E. L. Reuschel, J. M. Shackelford, L. Jeang, D. K. Shivers, J. A. Diehl, X. F. Yu, and T. H. Finkel.** 2011. HIV-1 Vif promotes the G- to S-phase cell-cycle transition. Blood **117:**1260-9.

257. **Wang, J., J. M. Shackelford, C. R. Casella, D. K. Shivers, E. L. Rapaport, B. Liu, X. F. Yu, and T. H. Finkel.** 2007. The Vif accessory protein alters the cell cycle of human immunodeficiency virus type 1 infected cells. Virology **359:**243-52.

258. **Wang, T., C. Tian, W. Zhang, K. Luo, P. T. Sarkis, L. Yu, B. Liu, Y. Yu, and X. F. Yu.** 2007. 7SL RNA mediates virion packaging of the antiviral cytidine deaminase APOBEC3G. Journal of virology **81:**13112-24.

259. **Ward, J., Z. Davis, J. DeHart, E. Zimmerman, A. Bosque, E. Brunetta, D. Mavilio, V. Planelles, and E. Barker.** 2009. HIV-1 Vpr triggers natural killer cell-mediated lysis of infected cells through activation of the ATR-mediated DNA damage response. PLoS pathogens **5:**e1000613.

260. **Warrilow, D., G. Tachedjian, and D. Harrich.** 2009. Maturation of the HIV reverse transcription complex: putting the jigsaw together. Reviews in medical virology **19:**324-37.

261. **Wei, P., M. E. Garber, S. M. Fang, W. H. Fischer, and K. A. Jones.** 1998. A novel CDK9-associated C-type cyclin interacts directly with HIV-1 Tat and mediates its high-affinity, loop-specific binding to TAR RNA. Cell **92:**451-62.

262. **Wildum, S., M. Schindler, J. Munch, and F. Kirchhoff.** 2006. Contribution of Vpu, Env, and Nef to CD4 down-modulation and resistance of human immunodeficiency virus type 1-infected T cells to superinfection. Journal of virology **80:**8047-59.

263. **Williams, M., J. F. Roeth, M. R. Kasper, R. I. Fleis, C. G. Przybycin, and K. L. Collins.** 2002. Direct binding of human immunodeficiency virus type 1 Nef to the major histocompatibility complex class I (MHC-I) cytoplasmic tail disrupts MHC-I trafficking. Journal of virology **76:**12173-84.

264. **Xiao, Y., G. Chen, J. Richard, N. Rougeau, H. Li, N. G. Seidah, and E. A. Cohen.** 2008. Cell-surface processing of extracellular human immunodeficiency virus type 1 Vpr by proprotein convertases. Virology **372:**384-97.

265. **Yamada, T., and A. Iwamoto.** 2000. Comparison of proviral accessory genes between long-term nonprogressors and progressors of human immunodeficiency virus type 1 infection. Archives of virology **145:**1021-7.

266. **Yang, S. J., L. A. Lopez, H. Hauser, C. M. Exline, K. G. Haworth, and P. M. Cannon.** 2010. Anti-tetherin activities in Vpu-expressing primate lentiviruses. Retrovirology **7:**13.

267. **Yaron, A., A. Hatzubai, M. Davis, I. Lavon, S. Amit, A. M. Manning, J. S. Andersen, M. Mann, F. Mercurio, and Y. Ben-Neriah.** 1998. Identification of the receptor component of the IkappaBalpha-ubiquitin ligase. Nature **396:**590-4.

268. **Yondola, M. A., F. Fernandes, A. Belicha-Villanueva, M. Uccelini, Q. Gao, C. Carter, and P. Palese.** 2011. Budding capability of the influenza virus neuraminidase can be modulated by tetherin. Journal of virology **85:**2480-91.

269. **Zamborlini, A., Y. Usami, S. R. Radoshitzky, E. Popova, G. Palu, and H. Gottlinger.** 2006. Release of autoinhibition converts ESCRT-III components into potent inhibitors of HIV-1 budding. Proceedings of the National Academy of Sciences of the United States of America **103:**19140-5.

270. **Zhang, F., S. J. Wilson, W. C. Landford, B. Virgen, D. Gregory, M. C. Johnson, J. Munch, F. Kirchhoff, P. D. Bieniasz, and T. Hatziioannou.** 2009. Nef proteins from simian immunodeficiency viruses are tetherin antagonists. Cell host & microbe **6:**54-67.

271. **Zhang, F., S. J. Wilson, W. C. Landford, B. Virgen, D. Gregory, M. C. Johnson, J. Munch, F. Kirchhoff, P. D. Bieniasz, and T. Hatziioannou.** 2009. Nef proteins from simian immunodeficiency viruses are tetherin antagonists. Cell Host Microbe **6:**54-67.

272. **Zhang, J., and C. Liang.** 2010. BST-2 diminishes HIV-1 infectivity. Journal of virology **84:**12336-43.

273. **Zhang, L., G. I. Kovalev, and L. Su.** 2007. HIV-1 infection and pathogenesis in a novel humanized mouse model. Blood **109:**2978-81.

274. **Zhou, H., M. Xu, Q. Huang, A. T. Gates, X. D. Zhang, J. C. Castle, E. Stec, M. Ferrer, B. Strulovici, D. J. Hazuda, and A. S. Espeseth.** 2008. Genome-scale RNAi screen for host factors required for HIV replication. Cell host & microbe **4:**495-504.

275. **Zhou, Q., D. Chen, E. Pierstorff, and K. Luo.** 1998. Transcription elongation factor P-TEFb mediates Tat activation of HIV-1 transcription at multiple stages. The EMBO journal **17:**3681-91.